

**GREEN SYNTHESIS OF 1,2,3-TRIAZOLES AND APPLICATION  
OF THEIR PALLADIUM *N*-HETEROCYCLIC CARBENE  
COMPLEXES AS CATALYST AND ANTICANCER AGENTS**

Thesis  
submitted to  
University of Calicut  
in partial fulfillment of the requirements  
for the award of the Degree of

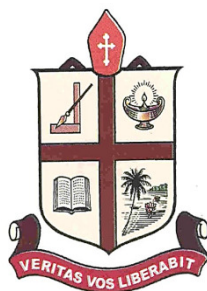
**Doctor of Philosophy in  
Chemistry**

By

**DRISHYA SASIDHARAN**

Under the guidance of

**Dr. PAULSON MATHEW**



**RESEARCH AND POSTGRADUATE DEPARTMENT OF CHEMISTRY**

**ST. THOMAS' COLLEGE (AUTONOMOUS)**

**(UNIVERSITY OF CALICUT)**

**THRISSUR, KERALA-680001**



RESEARCH AND POSTGRADUATE DEPARTMENT OF CHEMISTRY  
ST. THOMAS' COLLEGE (AUTONOMOUS) THRISSUR, KERALA-68000

Phone: 0487 2338883

(Affiliated to University of Calicut and Nationally accredited at 'A' level by NAAC)

---

Dr. Paulson Mathew, M.Phil., MBA, Ph.D  
Associate Professor

25-10-2019

## CERTIFICATE

I hereby certify that, this is the revised version of the thesis entitled "*Green synthesis of 1,2,3-triazoles and application of their Palladium N-heterocyclic carbene complexes as catalyst and anticancer agents*" submitted by Ms. **Drishya Sasidharan** under my guidance after incorporating the necessary corrections/suggestions made by the adjudicators.

.....  
**Dr. Paulson Mathew**  
(Supervising Teacher)



**RESEARCH AND POSTGRADUATE DEPARTMENT OF CHEMISTRY  
ST. THOMAS' COLLEGE (AUTONOMOUS) THRISSUR, KERALA-68000**

**Phone: 0487 2338883**

*(Affiliated to University of Calicut and Nationally accredited at 'A' level by NAAC)*

---

**Dr. Paulson Mathew, M.Phil., MBA, Ph.D**  
**Associate Professor**

18-02-2019

## **CERTIFICATE**

This is to certify that the thesis entitled "*Green synthesis of 1,2,3-triazoles and application of their Palladium N-heterocyclic carbene complexes as catalyst and anticancer agents*" is an authentic record of research work carried out by Ms. Drishya Sasidharan under my supervision in partial fulfillment of the requirements for the degree of Doctor of Philosophy in Chemistry of University of Calicut and further that no part thereof has been presented before for any other degree

.....  
**Dr. Paulson Mathew**  
**(Supervising Teacher)**

## **ACKNOWLEDGEMENT**

First and foremost, I thank Almighty God who is with me throughout my life.

I am extremely happy to acknowledge my sincere gratitude to my supervising guide **Dr. Paulson Mathew**, Associate Professor, Dept. of Chemistry, St. Thomas' College for teaching, training and inspiring me to excel. His expertise, skilled guidance, patience and whole-hearted support have helped me tremendously throughout my research. I express my heartfelt thanks for his enlightened discussions on both theoretical and experimental aspects of the research work. I would not have reached to this point without his generous assistance. I have been the fortunate beneficiary of extensive supervision by such as experienced and talented person his innovative ideas, inevitable suggestions and timely advice have made this work worth its luster. I take this opportunity to extend my overwhelming thanks to my guide for his creative and constructive feedback.

I am highly obliged to **Dr. Ignatius Antony**, Principal, St.Thomas' College, former Principal **Dr. P.O. Jenson** and the management for permitting me to carry out my research work in this esteemed institution.

I am grateful to **Dr. Joby Thomas. K**, Head of the department of Chemistry, St.Thomas' College for his scholarly comments and constant encouragement which have been of immense help to me in maintaining the excellence of my work. I express my genuine gratitude for his care and support.

I convey my sincere thanks to **Dr. K.L Joy, Dr. C.L. Joshy, Dr. Sunil Jose. T, Dr. Jency Thomas, Dr. Jinish Antony. M, Ms. Reeja Johnson, Dr. Joseph Joly V. L, Mr. Aji. C. V and Sr. Jisha Joseph**, professors of Dept of Chemistry for the help and support extended to me during my work.

A special word of thanks to all my friends especially **Research scholars** who were always willing to help and give their best suggestions throughout the study.

I also express my sincere gratitude to **STIC-CUSAT, IIRBS-M.G UNIVERSITY, SAIF-IIT BOMBAY, XRD UNIT-ST.THOMAS' COLLEGE, THRISSUR** for providing analytical data.



## *Acknowledgement*

---

I express my sincere gratitude to ***Dr. Ramadasan Kuttan, Research Director, Amala Cancer Research Centre*** for providing facilities to conduct cytotoxicity studies and ***Dr. C.R Meera, Assistant professor*** and ***Head, Department of Microbiology, St. Marys' College, Thrissur*** for conducting antibacterial and antifungal studies.

I sincerely acknowledge the help rendered by all the ***Non-teaching staffs*** of Department of Chemistry, St.Thomas' College

Finally, I am forever indebted to my ***Family*** for their understanding, support and encouragement when it was most required.

I consider it my privilege to acknowledge and shall remain indebted to each and every one by their rich and varied contribution has enabled my study in every little way, however small or big contribution may be.

***With heartfelt gratitude***

***Drishya Sasidharan***

## **DECLARATION**

I hereby declare that the thesis entitled “**Green synthesis of 1,2,3-triazoles and application of their palladium *N*- heterocyclic carbene complexes as catalyst and anticancer agents**” is the outcome of original research work undertaken and carried out by me at St. Thomas College, Thrissur, Kerala, under the guidance of **Dr. Paulson Mathew**, Associate Professor, St. Thomas’ College. I also declare that the material presented in this thesis is original and does not form the basis for the award of any other degree, diploma or other similar titles of any other university.

Drishya Sasidharan

## TABLE OF CONTENT

CHAPTER NUMBER	CONTENT	PAGE NUMBER
	<b>Acknowledgement</b>	i-ii
	<b>Table of content</b>	iii-vi
	<b>List of Tables</b>	vii
	<b>List of Figures</b>	viii-ix
<b>1</b>	<b>Introduction</b>	1-4
<b>2</b>	<b>Literature review</b>	5-24
	<i>References</i>	25-31
<b>3</b>	<b>Synthesis of 1,4-disubstituted 1,2,3-triazoles using Cu(I) stabilized on N,N'-methylene bis-acrylamide crosslinked polyvinyl pyrrolidone</b>	
<b>3.1</b>	<i>Introduction</i>	32
<b>3.2</b>	<i>Review of Literature</i>	33-43
<b>3.3.1</b>	<i>Reagents and Materials</i>	44
<b>3.3.2</b>	<i>Instruments</i>	44
<b>3.4</b>	<b>Result and Discussion</b>	45
<b>3.4.1</b>	<i>Infrared spectral studies of copolymer and CuPVPNNMBA</i>	45-46
<b>3.4.2</b>	<i>Morphological and elemental composition studies</i>	47-48
<b>3.4.3</b>	<i>Powder X-ray diffraction</i>	49
<b>3.4.4</b>	<i>X-ray photoelectron spectroscopy</i>	50-51
<b>3.4.5</b>	<i>Thermogravimetric analysis</i>	52
<b>3.5</b>	<b>Synthesis of 1,4-disubstitued 1,2,3-triazole using CuPVPNNMBA as heterogeneous catalyst</b>	53-59

CHAPTER NUMBER	CONTENT	PAGE NUMBER
3.6	<i>Characterization of 1,4-disubstituted 1,2,3-triazole</i>	60-63
3.7	<i>Spectral data of 1,4-disubstituted 1,2,3-triazole</i>	64-67
3.8	<b>Experimental details</b>	68-69
3.9	<b>Conclusion</b>	69
	<i>References</i>	70-77
4	<b>Plant extract mediated synthesis of copper oxide and silver nanoparticles : Application in catalysis and biological studies</b>	
4.1	<i>Introduction</i>	78
4.2	<i>Synthesis and application of nanoparticles: A Review</i>	79-90
4.3.1	<i>Reagents and Materials</i>	91
4.3.2	<i>Instruments</i>	91
4.4	<b>Results and Discussion</b>	92
4.4.1	<i>Preparation of plant extract</i>	93
4.4.2	<i>Visual inspection</i>	93
4.4.3	<i>UV-Visible spectroscopy analysis</i>	94
4.4.4	<i>Infrared Spectral analysis</i>	94-95
4.4.5	<i>Powder X-ray diffraction analysis</i>	95-96
4.4.6	<i>FEG-SEM and EDX analysis</i>	97-98
4.4.7	<i>HR-TEM analysis</i>	98-99
4.4.8	<b>Catalytic activity of the synthesized copper oxide(CuO) nanopartilce in CuAAC reaction</b>	100-104

CHAPTER NUMBER	CONTENT	PAGE NUMBER
4.4.9	<i>Characterization of 1,4-disubstituted 1,2,3-triazole</i>	105-108
4.5	<i>Spectral data of 1,4-disubstituted 1,2,3-triazoles</i>	109-112
4.6	<b>Sunlight induced synthesis of silver nanoparticles</b>	
4.6.1	<i>Visual inspection of Silver nanoparticle</i>	113
4.6.2	<i>UV-Visible spectral studies of silver nanoparticles</i>	113-114
4.6.3	<i>Infrared spectral analysis</i>	114
4.6.4	<i>Powder X-ray Diffraction analysis</i>	115
4.6.5	<i>EDS analysis</i>	116
4.6.6	<i>HR-TEM analysis</i>	116-117
4.6.7	<b>Catalytic activity of the synthesized silver nanoparticle in Azide-Alkyne cycloaddition reaction</b>	118
4.6.8	<i>Antibacterial studies of silver nanoparticle</i>	119-120
4.7	<b>Experimental details</b>	121-122
4.8	<b>Conclusion</b>	122
	<i>References</i>	123-135
5	<b>Synthesis of 1,2,3-triazolyldene palladium complexes: Application as catalyst for Suzuki-Miyaura coupling reaction and Cytotoxic studies</b>	
5.1	<i>Introduction</i>	136-139
5.2	<i>Review of Literature</i>	140-154
5.3.1	<i>Reagents and Materials</i>	155

---

<b>CHAPTER NUMBER</b>	<b>CONTENT</b>	<b>PAGE NUMBER</b>
<b>5.3.2</b>	<i>Instruments</i>	155
<b>5.4</b>	<b>Results and Discussion</b>	
<b>5.4.1</b>	<i>Synthesis of complexes</i>	156-174
<b>5.4.2</b>	<i>Catalytic study of palladium N-heterocyclic carbene complex</i>	175-178
<b>5.4.3</b>	<i>Cytotoxicity studies of palladium carbene complexes</i>	179-181
<b>5.5</b>	<i>Spectral data of compounds</i>	182-185
<b>5.6</b>	<b>Experimental details</b>	186-192
<b>5.7</b>	<b>Conclusion</b>	192
	<i>References</i>	193-200
<b>6</b>	<b>Summary &amp; Conclusions</b>	201-203

---

*One child, one teacher, one pen and  
one book can change the world*

*Malala Yousafzai*

*To*  
*My Husband*



## List of Figures

Figure No	Title	Page No
<b>Chapter 3</b>		
1	FTIR of PVPNNMBA and CuPVPNNMBA	46
2	Schematic representation of incorporation of metal ion in the polymer matrix	47
3	SEM images of PVPNNMBA and CuPVPNNMBA	47
4	EDX Spectra of CuPVPNNMBA	48
5	XRD pattern of CuPVPNNMBA	49
6.1	Cu2p XPS core level spectra of CuPVPNNMBA	50
6.2	O1s XPS spectra of CuPVPNNMBA	51
6.3	C1s XPS spectra of CuPVPNNMBA	51
7	TG and DTA curve of CuPVPNNMBA	52
8	Reusability of the catalyst	58
9	SEM images of CuPVPNNMBA and reused catalyst	58-59
10	EDS spectrum of reused catalyst	59
11	FTIR spectra of 1-benzyl-4-phenyl-1H-1,2,3-triazole	60
12	<sup>1</sup> H NMR spectra of 1-benzyl-4-phenyl-1H-1,2,3-triazole	61
13	<sup>13</sup> C NMR spectra of 1-benzyl-4-phenyl-1H-1,2,3-triazole	62
14	Mass spectra of 1-benzyl-4-phenyl-1H-1,2,3-triazole	63
<b>Chapter 4</b>		
1	Photographs of fruit extract, copper acetate solution and reaction mixture CuO nanoparticle obtained after microwave irradiation	93
2	UV-Visible spectra of CuO nanoparticles	94
3	FTIR spectra of CuO nanoparticle	95
4	XRD pattern of synthesized CuO nanoparticle - <i>Myristica fragrans</i> fruit extract	96
5	FEG SEM images of CuO nanoparticle synthesized using <i>Myristica fragrans</i> fruit extract	97
6	Particle size distribution histogram of CuO nanoparticles	97
7	EDS spectra of CuO nanoparticle - <i>Myristica fragrans</i>	98
8	HR-TEM images of CuO NPs at different magnification and SAED pattern	98
9	Reusability of CuONPs in CuAAC reaction	104
10	FTIR spectra of 1-(2,4-dichlorobenzyl)-4-phenyl-1H-1,2,3-triazole	105
11	<sup>1</sup> H NMR spectra of 1-(2,4-dichlorobenzyl)-4-phenyl-1H-1,2,3-triazole	106
12	<sup>13</sup> C NMR spectra of 1-(2,4-dichlorobenzyl)-4-phenyl-1H-1,2,3-triazole	107
13	Mass spectra of 1-(2,4-dichlorobenzyl)-4-phenyl-1H-1,2,3-triazole	108

14	Photographs of fruit extract, silver nitrate solution and reaction mixture containing Ag NPs	113
15	UV-Visible spectrum of Ag NPs	114
16	FTIR spectra of AgNPs- <i>Myristica fragrans</i>	114
17	XRD pattern of Ag NPs	115
18	EDS spectrum of Silver nanoparticles	116
19	HR-TEM images of silver nanoparticles at different magnification and SAED pattern	117
20	Antimicrobial activity of Ag-NPs-- <i>Myristica fragrans</i> against various human pathogen microorganism	120
<b>Chapter 5</b>		
7.1	<sup>1</sup> H NMR of compound <b>95</b>	157
7.2	<sup>13</sup> C NMR of compound <b>95</b>	158
8.1	<sup>1</sup> H NMR of compound <b>96</b>	160
8.2	<sup>13</sup> C NMR of compound <b>96</b>	160
9.1	<sup>1</sup> H NMR of compound <b>97</b>	161
9.2	<sup>13</sup> C NMR of compound <b>97</b>	162
10.1	<sup>1</sup> H NMR of compound <b>98</b>	164
10.2	<sup>13</sup> C NMR of compound <b>98</b>	165
11.1	<sup>1</sup> H NMR of compound <b>100</b>	166
11.2	<sup>13</sup> C NMR of compound <b>100</b>	167
12.1	<sup>1</sup> H NMR of compound <b>99</b>	168
12.2	<sup>13</sup> C NMR of compound <b>99</b>	169
13	ORTEP diagram of the palladium complex <b>99</b>	170
14.1	<sup>1</sup> H NMR of compound <b>102d</b>	173
14.2	<sup>13</sup> C NMR of compound <b>102d</b>	174
15	Cytotoxicity activities of complexes <b>99,100, 102d-f</b>	181
16.1	<sup>1</sup> H NMR of compound <b>biphenyl</b>	182
16.2	<sup>13</sup> C NMR of compound <b>biphenyl</b>	183

## List of Tables

Table No.	Title	Page No
<b>Chapter 3</b>		
1	FTIR absorption bands of PVPNNMBA and CuPVPNNMBA	46
2	Optimization of reaction conditions for the reaction of benzyl chloride, sodium azide and phenylacetylene	53-54
3	Synthesis of 1,4-disubstituted 1,2,3-triazole with different halides and alkynes	55-56
4	Reusability of CuPVPNNMBA	57
<b>Chapter 4</b>		
1	Optimization of the CuAAC reaction in terms of catalyst loading, solvent, temperature and time using benzyl chloride, sodium azide, phenyl acetylene and CuO NPs	101
2	Synthesis of 1,4-disubstituted 1,2,3-triazole using alkyl/aryl halides and alkyne	102-103
3	Reusability of CuO nanoparticle	104
4	Optimization of solvent system for AgAAC reaction	118
5	Zone of inhibition of silver nanoparticle against bacterial strains	119
<b>Chapter 5</b>		
1	Crystallographic data of complex <b>99</b>	170
2	N-Pd-N complexes	172
3	Optimization of base used for the $C_{tzi}$ -Pd- $N_{tzi}$ complex <b>99</b> catalyzed Suzuki coupling of bromobenzene with phenyl boronic acid	176
4	Suzuki-Miyaura coupling of reaction of aryl halides and boronic acids at room temperature	176-177
5	Cytotoxicity results of complexes <b>99, 100</b>	180
6	Cytotoxicity results of complexes <b>102 d-f</b>	180

# Chapter 1

## Introduction

In 1836 Berzelius introduced the term catalyst; according to him catalyst is a substance which enhances the rate of reaction without being consumed. Catalysis plays an important role in production of bulk chemicals and fuels. They are important in the economic and environmental perspective. Main advantage of using catalyst in a chemical reaction is selectivity. Currently there are technologies available for the design and development of catalyst mainly by the discovery of atom scale measurements, and high resolution spectroscopic techniques. Catalysts are divided into three types; homogeneous, heterogeneous and enzymatic, each employed with a single aim to enhance the rate of chemical reaction.

Environmental concern encourages the chemical community to search for more environmentally benign processes for chemical synthesis. Two important issues in this regard are development of recyclable heterogeneous catalysts and use of less toxic solvents and reagents. “Green chemistry” is a common word having twelve distinct principles which explores the use of no solvent or green solvent and green catalyst for synthetic purpose. The weakness of using non-green solvent and catalyst made the researchers to think about the “green” strategy. Water is taken as the commonly used “green solvent”. A catalyst should be cost effective, environment friendly, highly active, easily recyclable, and easy to recover from reaction medium. Heterogeneous catalysis became more relevant as it satisfies the crucial objectives of “green chemistry” minimizing waste and optimizing the use of resources thereby leading to sustainability. Now a days, merging of two fields like catalysis and organic synthesis became more prominent due to economic and environmental reasons.

One of the objectives of the present research work is the development of efficient, cost effective and green catalytic system for the synthesis of 1,2,3-triazole *via* click reaction. For this we developed two catalytic systems, one using copper supported polymer which can be prepared by suspension polymerization followed by complexation with copper and the second one by using nanoparticles prepared using

*Myristica fragrans* fruit extract. Our next aim was to develop a simple but efficient synthesis of *N*-heterocyclic carbene complex starting from 1,2,3-triazole and its application in catalysis as well as biological activity.

The thesis is divided into 6 chapters. A review on the CuAAC synthesis of 1,4-disubstituted 1,2,3-triazole are highlighted in chapter 2. In the review, more priority has been given to the importance of heterogeneous catalysts in triazole synthesis.

1,2,3-triazoles are important class of heterocyclic compounds because of their wide range of biological activities and applications in industry. Huisgen's 1,3-dipolar cycloaddition commonly called click reaction is used to assemble this scaffold. Click reactions are mainly of two types, copper catalyzed azide-alkyne cycloaddition (CuAAC) reaction and thiol-ene reaction. CuAAC leads to the formation of 1,4-disubstituted 1,2,3-triazoles by the reaction between terminal alkyne and azide in the presence of copper(II). The uncatalyzed reaction requires high temperature and lacks regioselectivity in products. Heterogeneously catalyzed click reaction takes more benefits compared to the homogeneous one including simplicity in product isolation, recyclability and reducing environmental concerns.

Chapter 3 describes the synthesis of *N,N'*-methylene bis-acrylamide cross linked *N*-vinyl-2-pyrrolidone (PVPNNMBA). The polymer matrix can reduce Cu(II) to Cu(I) and can stabilise the later within the polymer matrix, preventing further reduction. Techniques like FTIR, XRD, EDS, SEM, XPS, ICP-AES, TGA-DTA etc. were used to characterize the polymer. The copper supported polymer catalyst was used for the efficient synthesis of 1,4-disubstituted 1,2,3-triazole and optimization of catalyst was carried out in terms of solvent, temperature and catalyst loading. The catalyst performs well in water as solvent with minimum catalyst loading. The products were characterized using <sup>1</sup>H NMR, <sup>13</sup>C NMR, GC-MS. The study demonstrated that copper supported polymer material is an excellent heterogeneous catalyst for the azide-alkyne click reaction.

Chapter 4 explains the preparation and characterization of copper oxide and silver nanoparticles from *Myristica fragrans* fruit extract. Hydrothermal method was adopted for the preparation of the fruit extract. Bioreduction of copper acetate produces copper oxide nanoparticless. Phytoconstituents present in the fruit extract are responsible for the metal reduction. Light induced reduction of silver nanoparticle

was carried out in presence of *Myristica fragrans* fruit extract. Color change observed during the reaction indicates the formation of silver nanoparticles and the same was confirmed by UV-visible absorption spectroscopy. FTIR provides an indication of the functional groups present in the phytoconstituents. Powder X-ray diffraction studies were used for phase identification and size of copper oxide nanoparticles. Nano size of the copper oxide was confirmed using FEG-SEM, and HR-TEM. EDS was used to find out the elemental composition of the nanoparticles entrapped in phytoconstituents. Copper oxide and silver nanoparticles have been tested for its potential as a heterogeneous catalyst for CuAAC click reaction in water.

Catalytic activity of silver nanoparticle was also investigated for azide-alkyne cycloaddition reaction (AgAAC). Silver nanoparticles were not suitable for the regioselective synthesis of 1,4-disubstituted triazoles. As the metallic silver is known to possess biological activities, antibacterial properties of synthesized silver nanoparticles were studied. The antibacterial activity largely depends on the size and shape of the nanoparticle and its influence on the activity was also studied.

In organometallic catalysts a central metal is bonded to organic ligands. Properties of the catalyst are determined by both the central metal atom and the coordinated ligands. The success of organometallic catalysts depends on the relative ease of catalyst modification by changing the ligand environment. Simply by changing the ligands around the metal centre, one can tune its catalytic properties.

Over the last two decades, *N*-heterocyclic carbenes (NHCs) have emerged as ligands for a variety of transition metals. After the isolation of the first “bottleable” NHC by Arduengo in 1991, a large variety of NHCs have been synthesized. Among these, imidazolylidene and triazolylidene have become more popular. Initially, NHCs were considered as phosphine mimics, the difference between phosphine and NHCs becomes more apparent now. *N*-heterocyclic carbene complexes have application in several fields. In Medicinal field they have application as antimicrobial and antitumor agents. It can be used as a homogeneous catalyst for a variety of chemical reactions like transfer hydrogenation, C-C bond forming cross coupling reactions like Heck, Suzuki-Miyaura and Sonogashira reactions.

Chapter 5 describes the synthesis of 1,2,3-triazoles and their palladium *N*-heterocyclic carbene complexes. We have synthesized palladium triazole/triazolylidene complexes

with different bonding pattern. These complexes were characterized by  $^1\text{H}$  NMR,  $^{13}\text{C}$  NMR, and SXRD. The catalytic efficiency of the palladium *N*-heterocyclic complexes containing C-Pd-N bonding pattern shows better catalytic activity towards Suzuki-Miyaura cross coupling reaction in water and compared to its activity with other synthesized complexes. The Cytotoxicity of these complexes has been studied and the carbene complex with C-Pd-N bonding pattern was found to have good activity compared to other palladium complexes. A summary and conclusion of the work is presented in Chapter 6.

## Chapter 2

### Literature Review

In 1893 Michael A first reported the synthesis of 1,2,3-triazole from phenyl azide and diethyl acetylene dicarboxylate in the absence of catalyst.<sup>1</sup> After seven decades Husigen studied the thermal reaction<sup>2</sup> and found that the reaction is largely exothermic. Its low reaction rate at elevated temperature indicates its high activation barrier. Major drawback of this reaction is the thermodynamic instability, the formation of undesired alkyne- alkyne coupling product and lack of regioselectivity. In 2002, Sharpless and Meldal independently made a mile stone in Husigen 1, 3-dipolar cycloaddition reaction by introducing Cu (I) catalyst by the *in situ* reduction of Cu (II) salt with sodium ascorbate which improves the regioselectivity, rate of the reaction and provides high yield under mild reaction condition.<sup>3,4</sup> Synthesis of 1,4-disubstituted 1,2,3-triazole from terminal alkyne and an aliphatic azide in presence of copper was termed as Copper catalyzed azide- alkyne cycloaddition reaction (abbreviated to CuAAC). This method provides good functional group tolerance and can be carried out in aqueous media as well as in aqueous with organic co-solvents. Azides which are 1,3-dipolar compound represented by zwitterionic all-octet resonance structures are ambivalent in the 1- and 3-positions, thus displaying electrophilic as well as nucleophilic activity. The dipolarophile can be any double or triple bond (**Fig 1**).

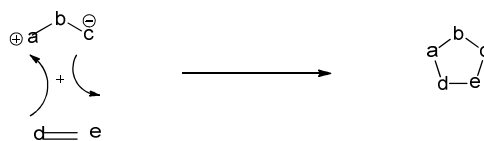
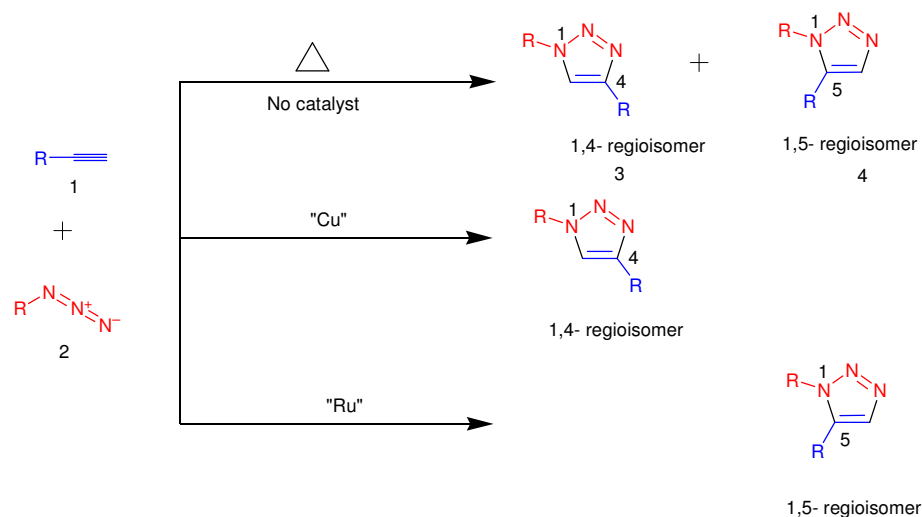


Fig 1

Introducing transition metal provides regioselectivity; copper provides 1,4-disubstituted 1,2,3- triazole where as ruthenium gives 1,5- disubstituted 1,2,3-triazole.<sup>5,6</sup> (**Scheme 1**) Similarly transition metals like Silver,<sup>7-13</sup> Gold,<sup>14,15</sup> Iridium,<sup>16-18</sup> Nickel,<sup>19</sup> Zinc,<sup>20-22</sup> and Lanthanides<sup>23,24</sup> also catalyze the cycloaddition reaction.





Scheme 1

Triazole compounds have made its role in different field like synthetic, pharmaceutical and biological.<sup>25</sup> Triazole ring system have attractive features which attracts both coordination and organometallic researchers (**Fig.2**).

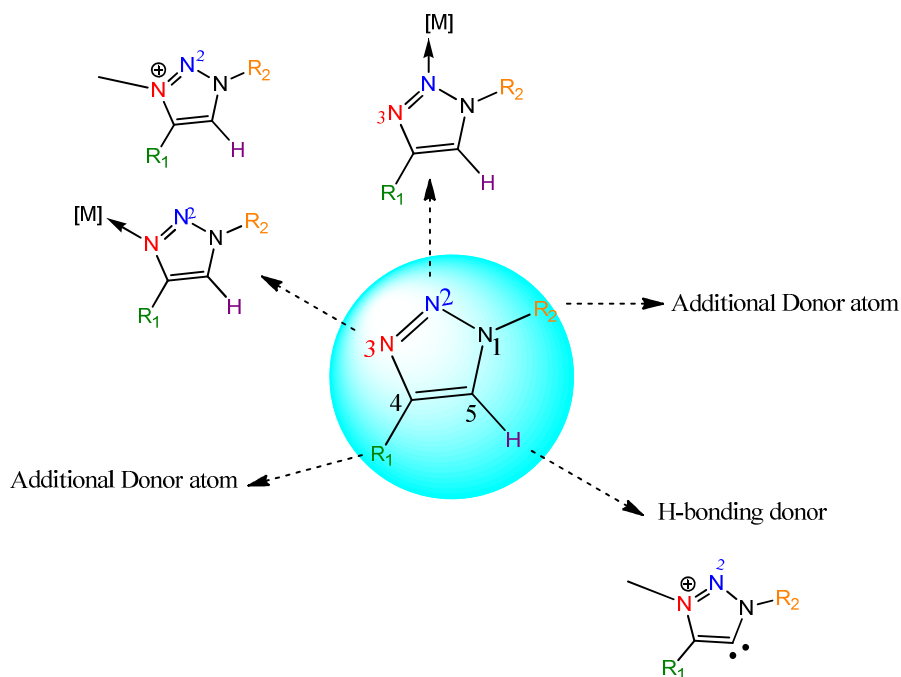


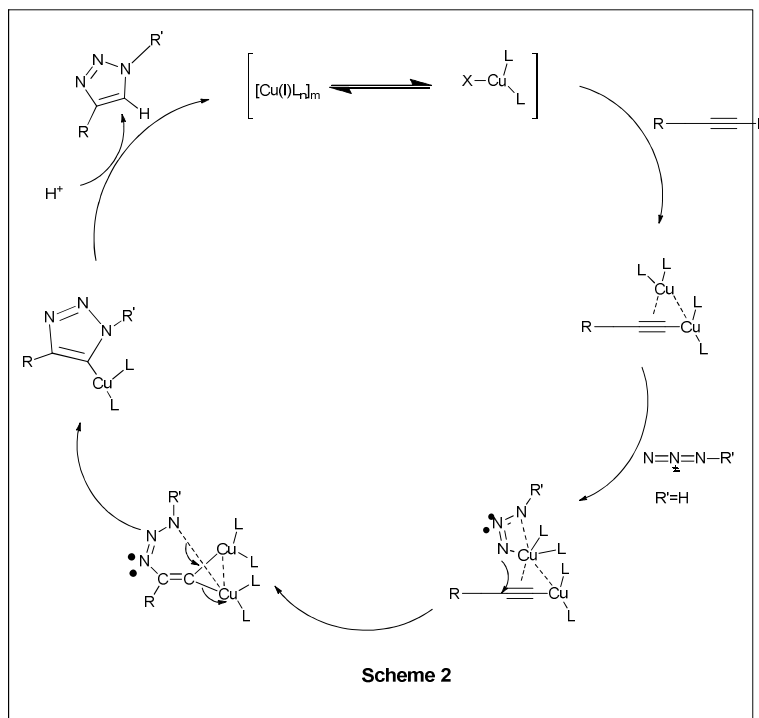
**Fig 2** Attractive features of triazole ring system

In the triazole system, N3 is the basic donor atom through which it can act as monodentate ligand. The presence of additional donor groups made the system as a

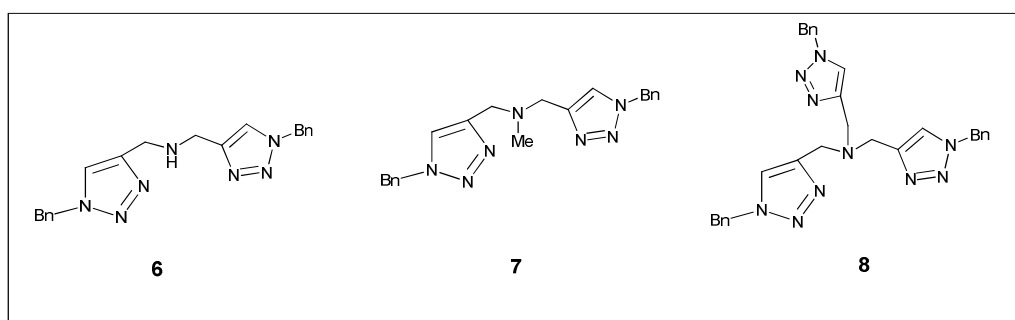
chelate ligand which allows the incorporation of multi triazole ligands within the backbone and thereby generating multi-dentate triazole ligand systems. The alkylation of N3 followed by the deprotonation of triazole C-H leads to the generation of 1,2,3-triazol-5-ylidene which belongs to abnormal *N*-heterocyclic carbene ligand. The deprotonation of ring hydrogen results the formation of carbanion which also allows the triazole system to act as monodentate ligand. The presence of substituent at N1 which contain donor atom compel the metal to bind through N2 rather than N3 because of the chelate effect.

### Mechanism

CuAAC proceeds through a step-wise mechanism which includes i) abstraction of a proton to form highly polarized acetylene to yield Cu(I)-acetylide complex, ii) interaction of Cu(I) acetylide with azide and activate it for the nucleophilic addition of acetylide carbon to the 'end' nitrogen of the azide forming copper(III) metallacycle, iii) ring contraction of metallacycle to a triazolyl- copper derivative followed by protonation yields triazole (**Scheme 2**).

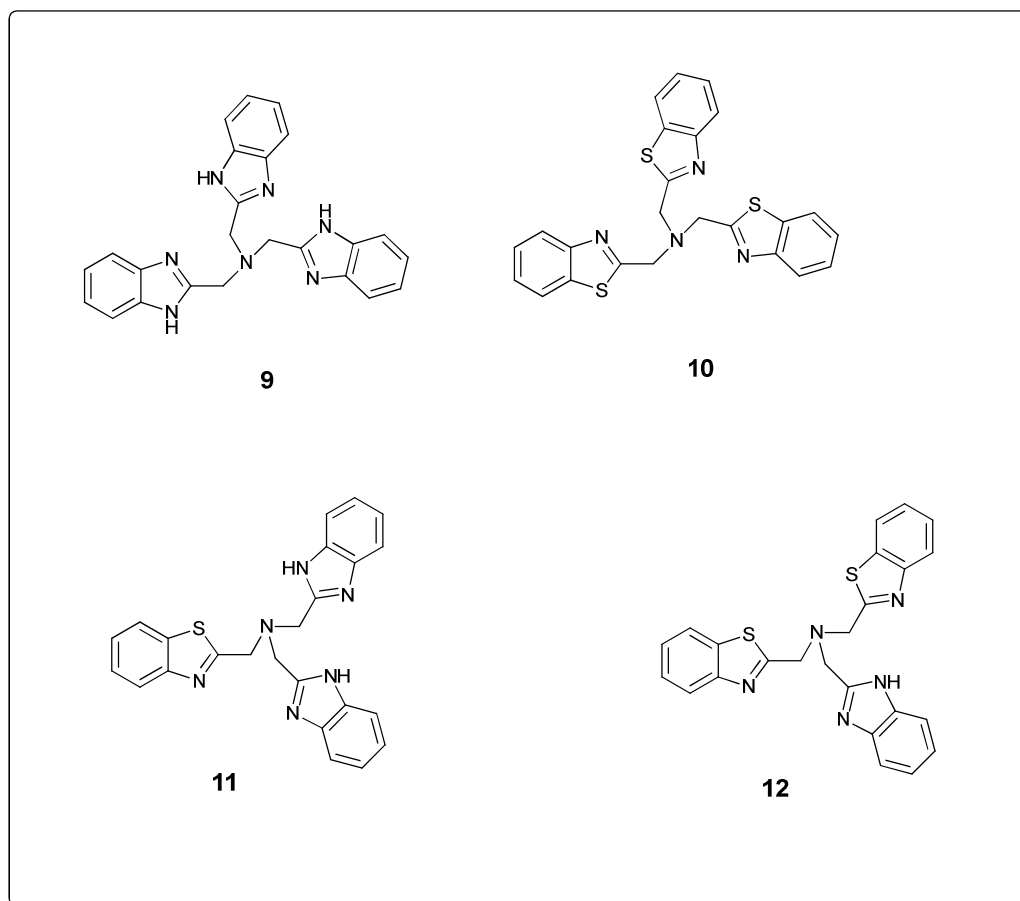


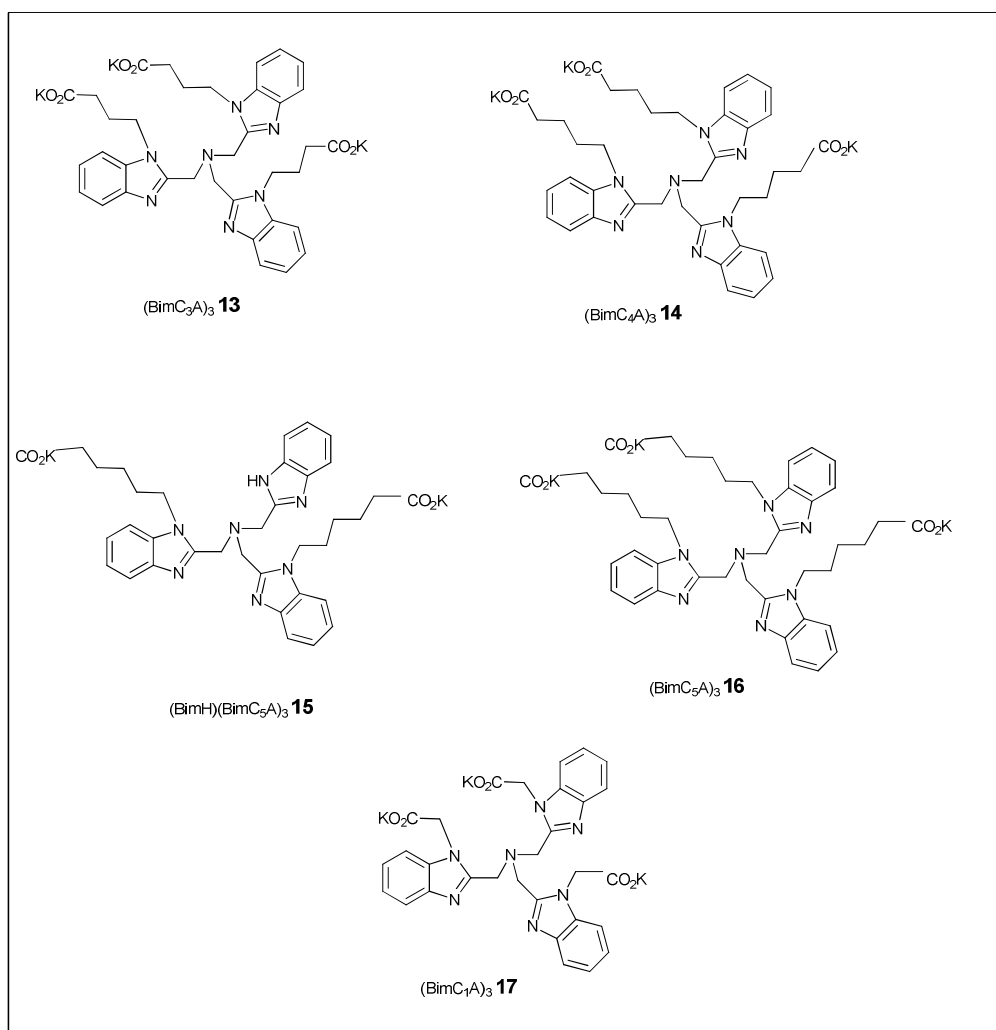
Here copper (I) is the actual catalyst for this cycloaddition reaction. In order to maintain its concentration copper (II) source and a reducing agent is required. Sharpless and Fokin developed a catalytic system of  $\text{CuSO}_4$  with sodium ascorbate in water/alcohol mixture.<sup>26</sup> Polytriazoles was found to be good ligands which will protect Cu(I) under aerobic and aqueous conditions. They tightly bound to the metal to maintain the oxidation state. Bistriazoles **6** and **7** gives excellent performance of about 94% and 98% yield with  $[\text{Cu}(\text{CH}_3\text{CN})_4] \text{PF}_6$  when compared to tris-triazole TBTA **8** with 84% yield. But when reducing the amount of copper catalyst to 0.25 mol% bistriazoles are not as potent in protecting Cu(I) oxidation state whereas TBTA withstands all conditions.<sup>27</sup>



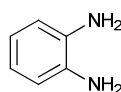
Highly nitrogenated ligands tend to accelerate the reaction by stabilizing and protecting copper(I) species from further oxidation.<sup>28</sup>

Acceleration of catalyst in the presence of ligand was studied by Finn and coworkers in 2007.<sup>29</sup> They synthesized a central tertiary amine surrounded by three benzimidazole heterocycles **9-12** and its derivatives **13-17**. The reaction rate depends on the nature of heterocycle and the substituents on the benzimidazole ring. The catalytic efficiency will remain as such when there is one benzimidazole side arm is present. The rate of CuAAC increases in the order  $(\text{Bth})_3 \ll (\text{Bth})(\text{BimH})_2 < (\text{BimH})_3 \ll (\text{Bth})_2(\text{BimH})$ . Carboxylic acid or ester group attached to the benzimidazole rings via  $(\text{CH}_2)_4$  and  $(\text{CH}_2)_5$  were found to be an excellent catalyst. On the other hand,  $(\text{BimC}_1\text{A})_3$  **17** produced one of the worst performing catalysts as the acid group is directly attached to the benzimidazole by a  $\text{CH}_2$ -linker.



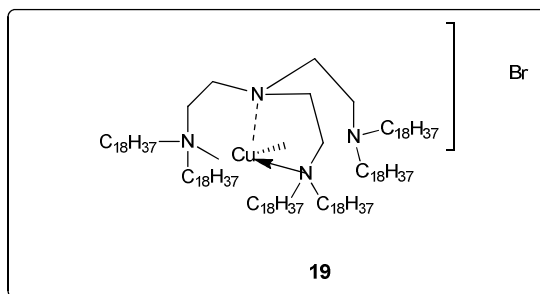


Cycloaddition of different alkynes with glucosyl azide was done in water by using CuSO<sub>4</sub> and sodium ascorbate in presence of *o*-phenylenediamine **18**.<sup>30</sup>

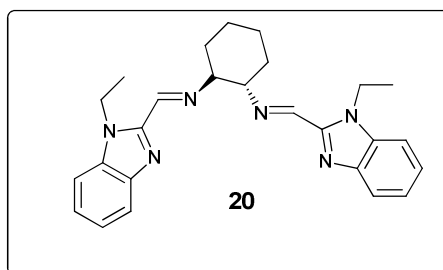


**18**

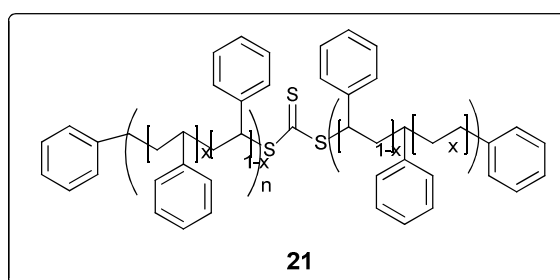
The use of complex **19** as catalyst effectively protects copper from oxidation. Less polar nature of the catalyst allows its separation from hydrocarbon solvents by simple filtration and can be reused two times with no decrease in the yield of triazole.<sup>31</sup>



Nitrogen tetradentate ligand **20** was also reported for CuAAC reaction.<sup>32</sup> The reaction proceeds at room temperature using 2mol% Cu(I) salt for 10h. The reaction was successful using different substrates having electron rich, electron poor, and hindered alkyl halides in acetonitrile-water solvent mixture.



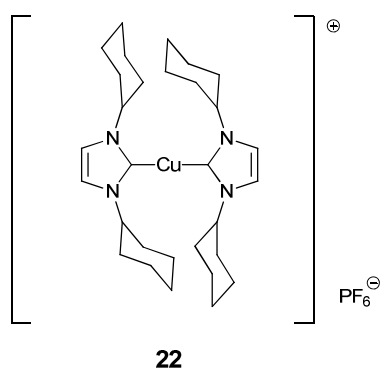
In 2010 Prez and coworkers developed TBTA functionalized styrenic monomer which on RAFT copolymerization with styrene followed by complexation with copper fabricate a good catalyst **21** for CuAAC. The catalyst can be reused 6 times, with minimum loss of activity.<sup>33</sup>



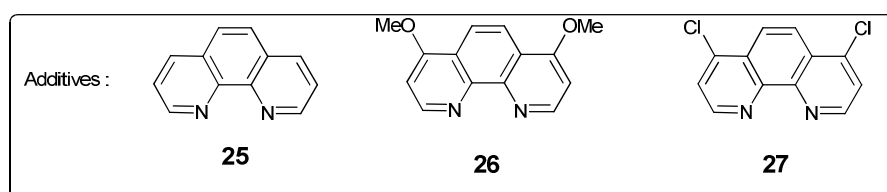
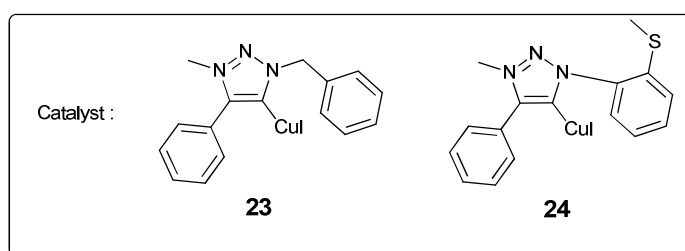
Nolan *et al* reported the catalytic activity of *N*-Heterocyclic carbene complex in CuAAC. They tested the catalytic efficiency of [(IPr)CuCl] and [SIMesCuBr].<sup>34</sup> Latter only gives better yield while the former led to partial conversion. It is to be noted that the yield became high and also the reaction time get reduced using water as solvent. They also tested its activity with internal alkynes; the reaction of benzyl

azide, 3-hexyne in presence of catalyst and under copper free condition. Yield of product found to be >5% under copper free condition.

In 2008 Nolen *et al.* again reported the catalytic activity of 2mol% of [(NHC)<sub>2</sub>Cu]X at room temperature using water as solvent.<sup>35</sup> The catalytic activities of different complexes were studied in which **24** was found to give better result within 90min. Using **24** optimization of solvents was done. The reaction could be better using acetonitrile as solvent as well as in neat condition. Surprisingly, catalyst loading can be reduced to 0.5mol% under neat condition.



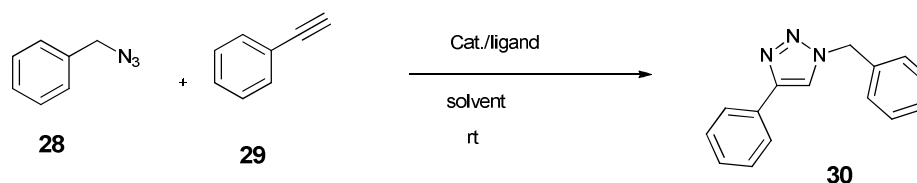
Gautier and Sarkar reported Cu(I) mesoionic carbene with nitrogen additives can be used for cycloaddition reaction.<sup>36</sup> The nitrogen additives tend to increase the solubility of catalyst, while decrease in the bond strength of Copper-chlorine bond, thereby hydrolysis leads to catalytically active species.



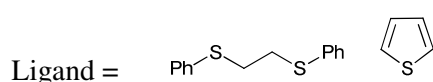
Without the use of additives, catalysts only give 20% and 5% yields respectively even after 24 h. The reaction time was reduced by adding additives and good yield of the product was observed. Additive containing electron donating methoxy group tends to

the oxidation of copper as identified by the color change from yellow orange to green due to the formation of copper(I) additive. Electron withdrawing chloride ion also facilitates the reaction.

Sulfur base ligands for CuAAC reaction was first reported by Fu and coworkers in 2008.<sup>37</sup> They developed cycloaddition reaction of water insoluble substrates at room temperature. They used inexpensive chemicals like CuBr/PhSMe. However, they attempted different sulfur containing compounds in cycloaddition reaction like thioanisole, dimethyl sulfoxide, thiophene etc. Among the copper salts they used CuBr because of weak dissolving power of CuI in water. They initially tested using simple reaction of benzyl azide with phenylacetylene (**Scheme 3**). Mixed solvents had given better results and pointed to the choice of water as solvent. They varied the amount of copper as well as ligands, the use of more copper and ligand provided not only the best result but also shortened the reaction time. On increasing ligand concentration from 30 to 50 mol% and catalyst concentration from 5 to 10%, they observed an increase in the yield from 93 to 98 % within 5min reaction time.



Scheme 3



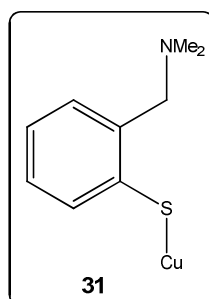
MeSMe, PhSMe, DMSO

They also carried out cycloaddition of aliphatic and aryl azides with alkynes. Substrates having good solubility in water had given higher reaction rate than one having low solubility. There is no significant difference in reactivity when using electron rich, electron deficient and sterically demanding substrates etc. They summarized that CuBr/thioanisole catalytic system was highly efficient in the cycloaddition reaction.

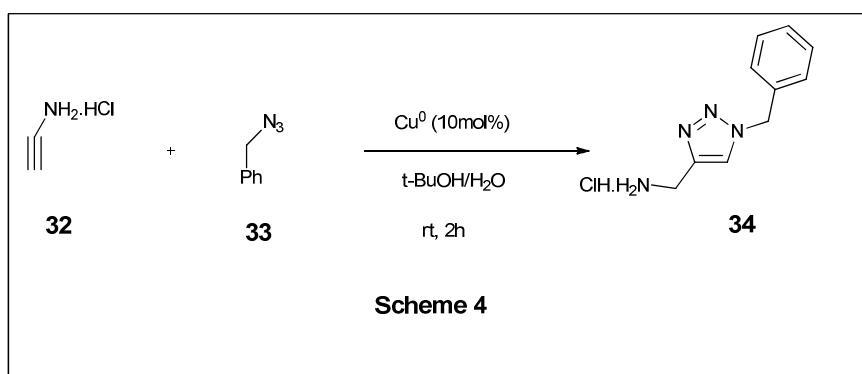
Catalytic efficiency of (2-aminoarenethiolato)copper(I) was tested in 2009.<sup>38</sup> Efficiency was tested by using in three different azide using classical catalyst and by



{[2-(Dimethylamino)methyl]thiophenolato}copper(I) complex **31**. Both acetonitrile and dichloromethane were suitable for the reaction.

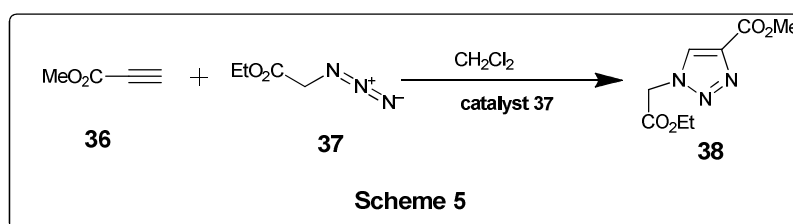
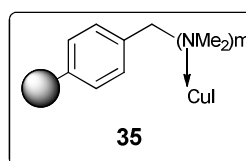


Orgueira *et al.* developed an effective protocol for CuAAC cycloaddition reaction.<sup>39</sup> They assumed that the presence of an amine hydrochloride salt would lead to produce catalytically active Cu(I) species from Cu(0) nanosize activated powder, which have large surface area that could enhance acetylide copper complex formation followed by cycloaddition reaction (**Scheme 4**). They got high yield in each reaction by using 10mol% Cu(0) and 1 eqv amine hydrochloride salt in *t*-BuOH/H<sub>2</sub>O mixture for 2 h room temperature stirring.

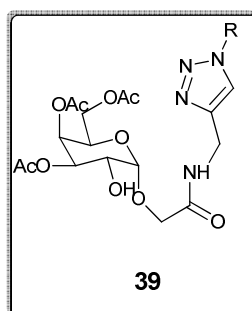


## Heterogeneous Catalyst for CuAAC

Girard and coworkers used polymer supported copper iodide as catalyst.<sup>40</sup> Amberlyst A-21 containing dimethyl-aminomethyl functionality which acts as both base and chelating agent was taken as polymer support in acetonitrile as solvent. This copper immobilized catalyst **35**, AAC reaction provide 1,4-disubstituted triazole **38** in excellent yields. Recyclability and stability of the catalyst was studied using the click reaction between propiolic acid methyl ester **36** and ethyl azidoacetate **37** (Scheme 5). The catalyst can be reused for 4 times without any loss in catalytic activity.



Complex glycoside molecules **39** with antimicrobial activity synthesized by CuAAC reaction using copper(I) iodide supported on Amberlyst A-21 resin and dichloromethane as solvent.<sup>41</sup>

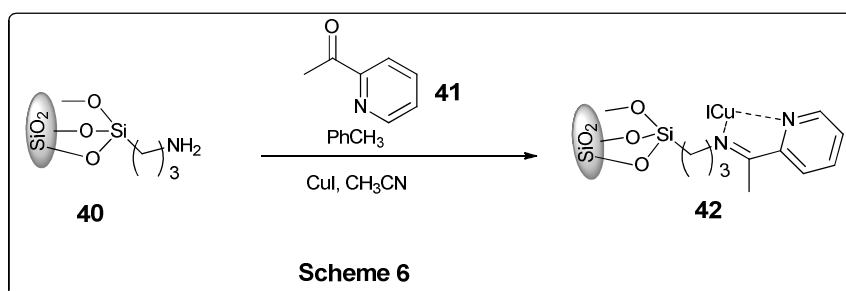


Impregnation of activated wood charcoal with aqueous solution of copper nitrate under sonication was reported by Lipshutz.<sup>42</sup> Using 10 mol% catalyst, a model reaction was carried out by using benzyl azide and phenylacetylene in dioxane at room temperature for 10 h. Addition of triethylamine or heating the reaction mixture will reduce the reaction time. The catalyst can be reused 3 times.

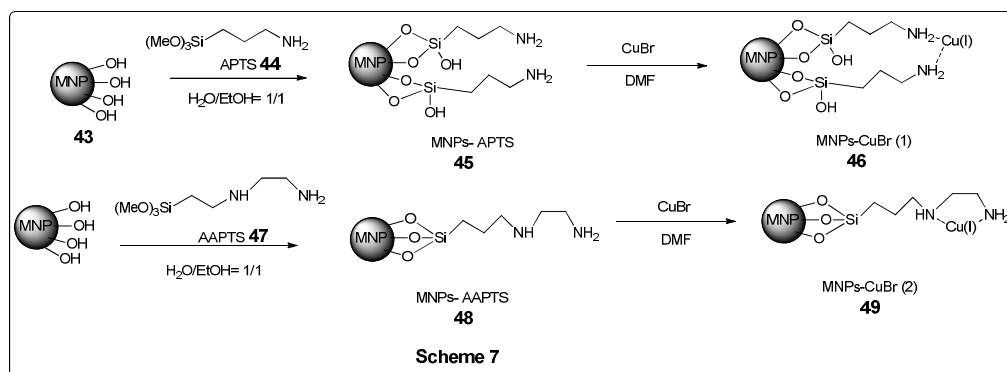
Cuprous oxide immobilized on charcoal with 0.89wt% of copper catalyzes CuAAC reaction.<sup>43</sup> The catalyst was found to be effective in aqueous isopropyl alcohol with 5% catalyst loading in the presence of triethylamine as base.

Xiong reported the CuAAC reaction catalyzed by CuBr supported on graphene oxide (GO)/Fe<sub>3</sub>O<sub>4</sub>.<sup>44</sup> The catalyst was prepared by two step process; i) coprecipitation method in which GO/Fe<sub>3</sub>O<sub>4</sub> was prepared from graphene oxide. ii) refluxing GO/Fe<sub>3</sub>O<sub>4</sub> in ethanolic solution of CuBr under nitrogen atmosphere. The CuAAC reaction was carried out in water either using conventional heating or under microwave irradiation using model reaction of sodium azide, phenylacetylene and benzyl chloride. The catalyst GO/Fe<sub>3</sub>O<sub>4</sub>-CuBr provides excellent result compared to copper acetate. Using optimized reaction conditions CuAAC reaction of different halide and alkynes were conducted in water using 5 mol% of catalyst at 80°C.

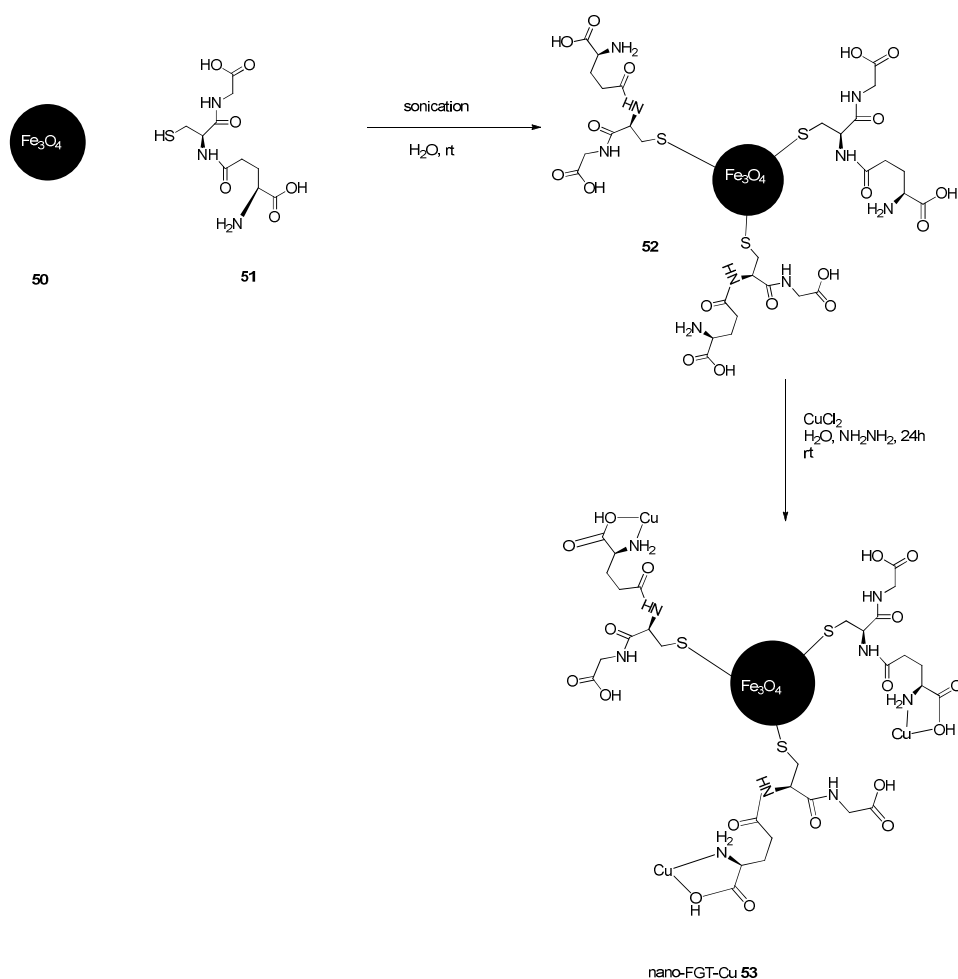
Imine functionalized silica was prepared by Paul in 2010<sup>45</sup> by refluxing 3-aminopropyl silica with 2-acetylpyridine in toluene (**Scheme 6**). Impregnation of Cu (I) was done at room temperature by stirring imine grafted silica with CuI in acetonitrile. Copper linked silica was found to be a good catalyst for Huisgen cycloaddition reaction between benzyl halide and allyl chlorides with 5 mol% Cu loading. The catalytic efficiency remains unaltered even after seven cycles.



Amino modified magnetic nanoparticles containing copper was synthesized by Xiong in 2013.<sup>46</sup> Magnetic nanoparticles were prepared conventional procedure, which was modified either with 3-aminopropyltrimethoxysilane (APTS) or [3-(2-aminoethylamino)propyl]trimethoxysilane (AAPTS) by using with a molar ratio of 2:1 in ethanol: water system (v/v = 1/1). The obtained MNP's were treated with CuBr in DMF at room temperature for 6 h. TEM analysis revealed that average diameter around 10-20 nm with quasi spherical shape.



Varma reported the synthesis and catalytic activity of copper nano particles on glutathione functionalized nano ferrite particles (**nano-FGT-Cu**).<sup>47</sup> Initially they functionalized the nano ferrite particles by sonicating nano ferrite with glutathione in water for 2 h. Copper was incorporated into the NP's by the addition of copper chloride  $\text{CuCl}_2 \cdot 2\text{H}_2\text{O}$  in alkaline medium. TEM results confirm the size which is in the range of 10-25 nm. Weight percentage of copper in catalyst was found out using ICP-AES analysis [1.57%]. Optimization of the reaction conditions were carried out using benzyl azide and phenyl acetylene using microwave irradiation at 120 °C in water as medium. They studied the catalytic activity of **nano-FGT-Cu 53** by performing the reaction between benzyl azide and different alkynes. They didn't observe 1,5- regioisomer in the product. The recovery of the catalyst can be carried out by magnetic separation.



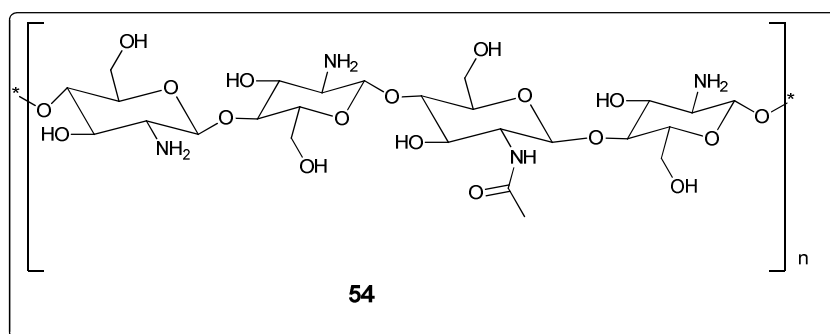
Scheme 8

Alumina supported copper nanoparticles were prepared by Kantham in 2006 using aerogel method.<sup>48</sup> For this, copper(II) acetylacetonate in methanol was mixed with toluene and then aluminium isopropoxide was added followed by stirring for 2 h. To the above mixture stoichiometric amount of deionized water was added and stirring continued for 18h, followed by autoclaving at 10 kg/cm<sup>2</sup> and 265 °C for 10 min. Drying of the aerogel material at 120 °C gives a fine powder of Cu-Al<sub>2</sub>O<sub>3</sub> nanoparticle. The XRD pattern reveals the presence of both metallic copper and cuprous oxide nanoparticles. Presence of cuprous oxide is due to the oxidation of copper during drying of nanoparticles at 120 °C. The surface area of nanoparticle was found to be 250 m<sup>2</sup>/g with an average pore diameter of 64.2 Å. From the optimization studies, water was found to be the best solvent to obtain higher yield. One pot synthesis of 1,2,3-triazoles from sodium azide, terminal alkynes and alkyl/allyl halides in water was effectively catalyzed by Cu-Al<sub>2</sub>O<sub>3</sub> nanoparticles. The products were recovered by simple extraction with ethyl acetate. The catalyst could be reused

for 3 times without any loss in catalytic activity. Using ICP AES analysis copper content of recovered catalyst after fourth cycle, was found to be the same as fresh.

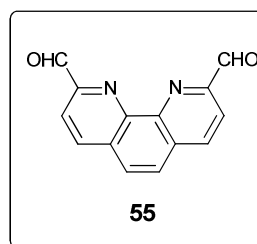
1,2,3-triazole derivatives obtained by the click reaction catalyzed by Cu/Al<sub>2</sub>O<sub>3</sub> under ball milling without using any solvent and additives was studied by Ranu *et. al.*<sup>49</sup> Catalyst was prepared by adding alumina to aqueous solution of CuSO<sub>4</sub> aged for 2h at 25°C. The product obtained is having a copper content of 18.8 mg/g. Triazole derivatives were obtained with excellent yields within 1h.

Biopolymers have gained enormous importance for various applications. Chitosan, a polysaccharide which is derived from chitin have gained much attention in catalysis due to its insolubility in organic solvents, the presence of amino group which anchor transition metal ion or it can be converted to Schiff base which act as ligand.



When Chitosan microspheres dried in supercritical CO<sub>2</sub>, it provides stable aerogel porous support with large surface area having pore size >10nm and using this technique amine groups makes more visible towards reactants.<sup>50,51</sup>

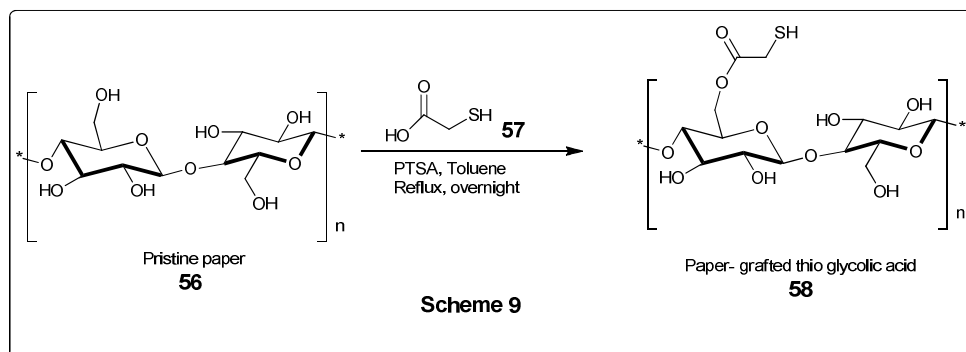
Copper was loaded to the chitosan aerogels in acetonitrile aqueous solution of copper triflate and sodium ascorbate at room temperature with repeated washing followed by metal loading at different concentrations from 0.5 to 2.1 mmol of Cu(I) per gram of catalyst.<sup>52</sup> For the synthesis of Schiff base, they selected both mono and dialdehydes which forms cross linking throughout the chitosan network. Among these, 2,9-diformylphenanthroline **57** was found to be the best ligand. Optimization of reaction conditions were carried out and most polar solvents provides better result. Using the catalyst, cycloaddition reaction was carried out in EtOH at 70 °C which converts the reactants to 1,4-triazole after 12 h. Reusability of the catalyst was checked using the model reaction between phenylacetylene and benzyl azide and the catalyst could be reused for four times without copper leaching.



Copper immobilized on chitosan was prepared by Varma<sup>53</sup> which was done by suspending Chitosan in an aqueous solution of copper sulfate for 3 h. The product was centrifuged and dried under vacuum. Amount of copper in catalyst found to be 5.1 wt% using ICP-AES. Initially the cycloaddition reaction was carried out to optimize the reaction condition in water at room temperature which provides excellent result within 4h. Expected triazole product obtained in excellent yield (93-99%) within 4-12 h. Reusability of the catalyst was studied using benzyl azide and phenylacetylene and the product was extracted using ethyl acetate. The catalyst was recovered by decanting and dried at 50 °C which can be further used for 5 cycles. Copper leaching was studied using ICP- AES. Before the reaction copper content was 5.1wt % and after 5<sup>th</sup> cycle copper content was found to be 5.02%.

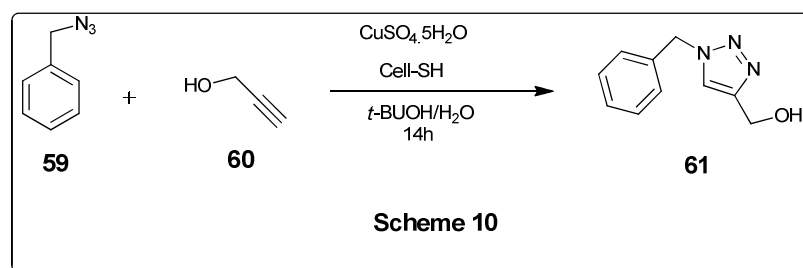
Agarose supported copper catalyst was reported by Gholinejad<sup>54</sup> in which catalyst was prepared by mixing CuBr solution in water with agarose hydrogel suspension followed by the addition of NaBH<sub>4</sub> to reduce copper(I) to copper nanoparticle which was indicated by the color change from gray to dark green. After cooling to room temperature the reaction mixture was centrifuged and dried in oven at 80 °C for 24 h. They conducted different CuAAC reactions by introducing arenediazonium salt from aniline. For the catalytic studies 0.05 mol% of the catalyst was added to a mixture of alkyl halide, sodium azide and an alkyne in water and stirring at 40 °C for 8 h leads to the formation of products. The catalyst can be reused for other 5 successive runs.

Felgin *et.al* reported a low cost and simple method for the reduction of Cu(II) to Cu(I) using functionalized cellulose paper.<sup>55</sup> To break the hydrogen bonds pristine cellulose paper was soaked in aqueous solution of 10% NaOH at 25 °C for 24 h which also enhance reactivity of hydroxyl group, followed by the esterification using *p*-toluene sulfonic acid (PTSA) and they assumed that functionalization mainly took place on the primary hydroxyl functional groups (**Scheme 9**).



The paper cell-SH **60** can act as a sensor and detect the presence of Cu(II) by producing colorimetric change which can be identified using naked eyes. As the concentration of Cu(II) decreases the color of paper strip changes from black to pale brownish. They recorded UV diffuse reflectance spectrum of paper strip dipped in both copper free water sample and aqueous solution of Cu(II) with different concentration. In copper free sample they observed absorbance at 257 nm corresponds to carbonyl groups of ester function whereas the samples containing copper ions shows two  $S \rightarrow Cu$  charge transfer bands at 506 and 665 nm respectively. They assumed that there is a thiol-mediated reduction of Cu(II) to Cu(I) which results in the formation of Cu(I)-SCH<sub>2</sub>R complexes and leads to  $S \rightarrow Cu$  charge transfer. This was confirmed by dipping the paper strip into an aqueous solution of CuCl<sub>2</sub> which turns black within seconds and the paper was characterized using SEM and XPS which confirms the presence of copper thiol complexes. Using this paper strip based reduction of Cu(II) to Cu(I) they investigated its catalytic efficiency in CuAAC reaction.<sup>56</sup> Initially they carried out a model reaction using propargyl alcohol and benzyl azide in presence of CuSO<sub>4</sub> · 5H<sub>2</sub>O using *t*-BuOH/H<sub>2</sub>O (1:1) solvent for 14 h at different temperature (**Scheme 10**). At room temperature with 16 mol% SH loading provides sluggish results. As temperature increases with 16 mol% SH loading and 2 mol% Cu loading provides better results. The scope of the catalyst was studied using various azides and alkynes.





They investigated the reusability of the catalyst using the same model reaction. The catalyst provides a comparatively normal yield in the second cycle without further addition of copper whereas a sharp decrease in yield was observed in third cycle.

Cellulose supported CuI nanoparticle was reported as heterogeneous catalyst for 1,2,3-triazole synthesis by Desai.<sup>57</sup> The catalyst was prepared by adding microcrystalline cellulose to a suspension of CuI in methanol which was then stirred overnight. Residue obtained by filtration which was washed with methanol and acetone and dried under vacuum at 50 °C. For the catalytic studies, they carried out model reaction using benzyl bromide, phenyl acetylene and sodium azide under neat condition at room temperature but the result obtained was not good. Then they tried different solvents, reaction temperature and amount of catalyst optimizing the reaction conditions to 100 mg of Cell-CuI catalyst in aqueous medium at 70 °C. The catalyst can be recovered by filtration followed by washing with ethyl acetate followed by acetone dried in air. This can be reused for 5 successive runs without any loss in catalytic activity. They investigated the reusability of the catalyst using the same model reaction. The catalyst provides a comparatively normal yield in the second cycle without further addition of copper whereas a sharp decrease in yield was observed in the third cycle.

Copper nanoparticles were generated by the chemical reduction of copper (II) acetate monohydrate using hydrazine hydrate in ionic liquid in which PVP was added as a stabilizing agent. Using the above generated copper nanoparticle Salunkhe developed a new catalyst for CuAAC reaction.<sup>58</sup> The model reaction was carried out by using phenyl azide and phenyl acetylene afforded solid product within 20 min. Cycloadduct from other reaction was separated by extraction using diethyl ether followed by evaporation resulted in good yield of the product. They also tested the recyclability of catalyst, the brown color of solution indicates the presence of Cu(0) even after running five consecutive run.

Using copper wire as catalyst and supercritical carbon dioxide ( $\text{scCO}_2$ ) as organic media Xu and coworkers proposed a reusable and effective catalyst for CuAAC reaction.<sup>59</sup> The reactions were carried out at different temperatures, in the presence and absence of metallic copper. Higher yield obtained in the presence of catalyst at high temperature. For a model reaction they used copper wire of length 10 cm, as the length increases catalytic efficiency increased. The recovered catalyst can be reused further.

Phase transfer catalyst  $\beta$ -cyclodextrin discovered >100 years ago are cyclic oligosaccharides having the ability to form complex using their lipophilic inner cavities and hydrophilic outer surfaces. They contain  $\alpha$ -D glucopyranose linked by  $\alpha$ -(1,4) glycosidic bonds.<sup>60</sup> This phase transfer catalyst was found to be effective catalyst for CuAAC reaction.<sup>61</sup> The relevance of using cyclodextrin as catalyst lies under the fact that it can include water-insoluble organic materials into the cavity in aqueous solution. Model reaction was carried out using benzyl azide and phenylacetylene with different mol% of cyclodextrin in water. Using 1 mol% of catalyst, the reaction was completed within 30 min with 97% isolated yield. Scope of the reaction was studied using various azides and alkynes, providing excellent yield of 1,4-disubstituted triazoles.

Oyster shell powder supported copper(I) used as catalyst for cycloaddition reaction.<sup>62</sup> OSPs-supported CuBr proved as effective catalyst under microwave irradiation using water as solvent within short time of 15 min. The catalyst could be reused without any loss in activity even after eight cycles.

Xiong reported Cu-FBP (fish bone powder) catalyzed synthesis of 1,2,3-triazole by one pot three component coupling reaction using propargyl bromide, organic azide and organic amine under microwave irradiation using water as a solvent.<sup>63</sup> For this they cleaned fish bones under ultrasonic irradiation using hot deionised water which was then kept in ethanol to soak and dried. Crushed into powder and sieved to 100 mesh. Introduction of copper was done by adding CuBr into FBPs in DMF under  $\text{N}_2$  atmosphere. Solvent was evaporated under vacuum, the solid product was then washed using distilled water. The presence of copper in FBPs was identified using absorption decrease in FTIR peaks due to metal-ligand bond formation. Comparison of XRD peaks indicates the presence of copper in FBPs. The catalyst was stable up to

250 °C. XPS spectrum of Cu-FBP displays characteristic peaks at 932.4 and 952.6 eV correspond to Cu2p<sub>3/2</sub> and Cu2p<sub>1/2</sub>, respectively. The scope of the catalyst was studied using various organic amines, propargyl bromide and benzyl azide in water triethyl amine mixture and stirred at 80 °C under microwave irradiation providing excellent yield of 1,2,3- triazole. The catalyst separated by filtration from the reaction mixture was reused and provide almost 79% yield even after 7 cycles of experiment. The copper percentage in the catalyst after 7<sup>th</sup> cycle was determined by ICP-AES and found out to be 0.71wt% which was lesser compared to fresh catalyst.

Cuttlebone@CuCl<sub>2</sub> was reported as heterogeneous catalyst for 1,2,3-triazole synthesis via three component reaction between terminal alkynes, organic bromides and sodium azide.<sup>64</sup> For the preparation of catalyst cuttlebone was powdered washed and dried at 100 °C which was then stirred with CuCl<sub>2</sub> in deionized water at room temperature for 10 h. In order to remove excess copper the catalyst washed with ethanol and dried at 50 °C for 12 h. For the catalytic application, the catalyst was added to a solution of phenyl acetylene, benzyl bromide and sodium azide in water which was then stirred at 40 °C. The total conversion of reactants to product, monitored by TLC, the catalyst was filtered by simple filtration and the reaction mixture was extracted using ethyl acetate and dried under vacuum.

CuAAC reaction became very popular because of its easiness in handling, wide application in different fields and good functional group tolerance. The reaction can be carried out by any Cu(I) source and in solvents including aqueous. Heterogenisation of CuAAC reaction is well accepted by grafting or depositing active copper(I) species on polymers, carbon based materials, silica etc.

## References

- (1) Michael, A. Ueber Die Einwirkung von Diazobenzolimid Anf Herrn S t o e h r Zur Erwidernng ; 94–95.
- (2) Huisgen, R. 1,3-Dipolar Cycloadditions. Past and Future. *Angew. Chem. Int. Ed.* **1963**, 2 (10), 565–598.
- (3) Kolb, H. C.; Finn, M. G.; Sharpless, K. B. Click Chemistry: Diverse Chemical Function from a Few Good Reactions. *Angew. Chemie - Int. Ed.* **2001**, 40 (11), 2004–2021.
- (4) Tornøe, C. W.; Christensen, C.; Meldal, M. Peptidotriazoles on Solid Phase : [1,2,3]-Triazoles by Regiospecific Copper ( I ) -Catalyzed 1,3-Dipolar Cycloadditions of Terminal Alkynes to Azides. *J. Org. Chem.* **2002**, 67, 3057–3064.
- (5) Rasmussen, L. K.; Boren, B. C.; Fokin, V. V. Ruthenium-Catalyzed Cycloaddition of Aryl Azides and Alkynes. *Org. Lett.* **2007**, 9 (4), 5–7.
- (6) Johansson, J. R.; Beke-Somfai, T.; Said Stålsmeden, A.; Kann, N. Ruthenium-Catalyzed Azide Alkyne Cycloaddition Reaction: Scope, Mechanism, and Applications. *Chem. Rev.* **2016**, 116 (23), 14726–14768.
- (7) McNulty, J.; Keskar, K.; Vemula, R. The First Well-Defined Silver(I)-Complex-Catalyzed Cycloaddition of Azides onto Terminal Alkynes at Room Temperature. *Chem. - A Eur. J.* **2011**, 17 (52), 14727–14730.
- (8) McNulty, J.; Keskar, K. Discovery of a Robust and Efficient Homogeneous Silver(I) Catalyst for the Cycloaddition of Azides onto Terminal Alkynes. *European J. Org. Chem.* **2012**, No. 28, 5462–5470.
- (9) Ortega-Arizmendi, A. I.; Aldeco-Pérez, E.; Cuevas-Yañez, E. Alkyne-Azide Cycloaddition Catalyzed by Silver Chloride and “Abnormal” Silver N-Heterocyclic Carbene Complex. *Sci. World J.* **2013**, 2013.
- (10) Salam, N.; Sinha, A.; Roy, A. S.; Mondal, P.; Jana, N. R.; Islam, S. M. Synthesis of Silver-Graphene Nanocomposite and Its Catalytic Application for the One-Pot Three-Component Coupling Reaction and One-Pot Synthesis of 1,4-Disubstituted 1,2,3-Triazoles in Water. *RSC Adv.* **2014**, 4 (20), 10001–10012.
- (11) Ali, A. A.; Chetia, M.; Saikia, B.; Saikia, P. J.; Sarma, D. AgN(CN)<sub>2</sub>/DIPEA/H<sub>2</sub>O-EG: A Highly Efficient Catalytic System for

- Synthesis of 1,4-Disubstituted-1,2,3 Triazoles at Room Temperature. *Tetrahedron Lett.* **2015**, *56* (43), 5892–5895.
- (12) Ferretti, A. M.; Ponti, A.; Molteni, G. Silver(I) Oxide Nanoparticles as a Catalyst in the Azide-Alkyne Cycloaddition. *Tetrahedron Lett.* **2015**, *56* (42), 5727–5730.
- (13) Connell, T. U.; Schieber, C.; Silvestri, I. P.; White, J. M.; Williams, S. J.; Donnelly, P. S. Copper and Silver Complexes of Tris(Triazole)Amine and Tris(Benzimidazole) Amine Ligands: Evidence That Catalysis of an Azide-Alkyne Cycloaddition (“click”) Reaction by a Silver Tris(Triazole)Amine Complex Arises from Copper Impurities. *Inorg. Chem.* **2014**, *53* (13), 6503–6511.
- (14) Boominathan, M.; Pugazhenthiran, N.; Nagaraj, M.; Muthusubramanian, S.; Murugesan, S.; Bhuvanesh, N. Nanoporous Titania-Supported Gold Nanoparticle-Catalyzed Green Synthesis of 1,2,3-Triazoles in Aqueous Medium. *ACS Sustain. Chem. Eng.* **2013**, *1* (11), 1405–1411.
- (15) Díaz Arado, O.; Mönig, H.; Wagner, H.; Franke, J. H.; Langewisch, G.; Held, P. A.; Studer, A.; Fuchs, H. On-Surface Azide-Alkyne Cycloaddition on Au(111). *ACS Nano* **2013**, *7* (10), 8509–8515.
- (16) Rasolofonjatovo, E.; Theeramunkong, S.; Bouriaud, A.; Kolodych, S.; Chaumontet, M.; Chimie, S. De; Yvette, F.-G. Iridium-Catalyzed Cycloaddition of Azides and 1 - Bromoalkynes at Room Temperature. *Org. Lett.* **2013**, *15*, 4698–4701.
- (17) Luo, Q.; Jia, G.; Sun, J.; Lin, Z. Theoretical Studies on the Regioselectivity of Iridium-Catalyzed 1,3 - Dipolar Azide – Alkyne Cycloaddition Reactions. *J. Org. Chem.* **2014**, *79*, 11970–11980.
- (18) Ding, S.; Jia, G.; Sun, J. Iridium-Catalyzed Intermolecular Azide-Alkyne Cycloaddition of Internal Thioalkynes under Mild Conditions. *Angew. Chemie - Int. Ed.* **2014**, *126*, 1908–1911.
- (19) Surya Prakash Rao, H.; Chakibanda, G. Raney Ni Catalyzed Azide-Alkyne Cycloaddition Reaction. *RSC Adv.* **2014**, *4* (86), 46040–46048.
- (20) Meng, X.; Xu, X.; Gao, T.; Chen, B. Zn / C-Catalyzed Cycloaddition of Azides and Aryl Alkynes. **2010**, 5409–5414.
- (21) Li, Y.; Qi, X.; Lei, Y.; Lan, Y. Mechanism and Selectivity for Zinc-Mediated

- Cycloaddition of Azides with Alkynes: A Computational Study. *RSC Adv.* **2015**, 5 (61), 49802–49808.
- (22) Smith, C. D.; Greaney, M. F. Zinc Mediated Azide-Alkyne Ligation to 1,5- and 1,4,5-Substituted 1,2,3-Triazoles. *Org. Lett.* **2013**, 15 (18), 4826–4829.
- (23) Hong, L.; Lin, W.; Zhang, F.; Liu, R.; Zhou, X. Ln[N(SiMe<sub>3</sub>)<sub>2</sub>]<sub>3</sub>-Catalyzed Cycloaddition of Terminal Alkynes to Azides Leading to 1,5-Disubstituted 1,2,3-Triazoles: New Mechanistic Features. *Chem. Commun.* **2013**, 49 (49), 5589–5591.
- (24) Wang, J. M.; Yu, S. B.; Li, Z. M.; Wang, Q. R.; Li, Z. T. Mechanism of Samarium-Catalyzed 1,5-Regioselective Azide-Alkyne [3 + 2]-Cycloaddition: A Quantum Mechanical Investigation. *J. Phys. Chem. A* **2015**, 119 (8), 1359–1368.
- (25) Lauria, A.; Delisi, R.; Mingoia, F.; Terenzi, A.; Martorana, A.; Barone, G.; Almerico, A. M. 1,2,3-Triazole in Heterocyclic Compounds, Endowed With Biological Activity, Through 1,3-Dipolar Cycloadditions. *European J. Org. Chem.* **2014**, 16, 3289–3306.
- (26) Rostovtsev, V. V.; Green, L. G.; Fokin, V. V.; Sharpless, K. B. A Stepwise Huisgen Cycloaddition Process: Copper ( I ) -Catalyzed Regioselective “ Ligation” of Azides and Terminal Alkynes. *Angew. Chem. Int. Ed.* **2002**, 41, 2596–2599.
- (27) Chan, T. R.; Hilgraf, R.; Sharpless, K. B.; Fokin, V. V. Polytriazoles as Copper ( I ) -Stabilizing Ligands in Catalysis. *Org. Lett.* **2004**, 6, 2853–2855.
- (28) Yan, Z.; Zhao, Y.; Fan, M.; Liu, W.; Liang, Y. General Synthesis of ( 1-Substituted-1 H -1 , 2 , 3-Triazol-4- Ylmethyl ) -Dialkylamines via a Copper ( I ) -Catalyzed Three-Component Reaction in Water. *Tetrahedron* **2005**, 61, 9331–9337.
- (29) Rodionov, V. O.; Presolski, S. I.; Gardinier, S.; Lim, Y. H.; Finn, M. G. Benzimidazole and Related Ligands for Cu-Catalyzed Azide-Alkyne Cycloaddition. *J. Am. Chem. Soc.* **2007**, 129, 12696–12704.
- (30) Aurelie Baron, Yves Bleriot, M. S. and B. V. Phenylenediamine Catalysis of " Click Glycosylations " in Water : Practical and Direct Access to Unprotected Neoglycoconjugates Phenylenediamine Catalysis of “ Click Glycosylations ” in Water : Practical and Direct Access to Unprotected Neoglycoconjugates. *Org.*

- Biomol. Chem.* **2008**, *6*, 1898–1901.
- (31) Candelon, N.; Laste, D.; Diallo, A. K.; Aranzaes, J. R.; Astruc, D.; Vincent, J. A Highly Active and Reusable Copper ( I )-Tren Catalyst for the “ Click ” 1 , 3-Dipolar Cycloaddition of Azides and Alkynes { . *Chem. Commun.* **2008**, 741–743.
- (32) N-arylation, C. I.; Cycloaddition, A. A.; Li, F.; Hor, T. S. A. Facile Synthesis of Nitrogen Tetradentate Ligands and Their Applications in Cu(I) -Catalyzed N-Arylation and Azide–Alkyne Cycloaddition. *Chem. - A Eur. J.* **2009**, *15*, 10585–10592.
- (33) Du, F.; Lammens, M.; Skey, J.; Wallyn, S.; Reilly, O.; Du, F. Polymeric Ligands as Homogeneous , Reusable Catalyst Systems for Copper Assisted Click Chemistry W. *Chem. Commun.* **2010**, *46*, 8719–8721.
- (34) Díez-González Silvia, Correa Andrea , Cavallo Luigi, N. S. P. (NHC)Copper(I)-Catalyzed [3+2] Cycloaddition of Azides and Mono- or Disubstituted Alkynes. *Chem. - A Eur. J.* **2006**, *12*, 7558–7564.
- (35) Díez-gonzález, S.; Stevens, D.; Nolan, S. P. A [( NHC ) CuCl ] Complex as Latent Click Catalyst. *Chem. Commun.* **2008**, 4747–4749.
- (36) Hohloch, S.; Sarkar, B.; Nauton, L.; Cisnetti, F.; Gautier, A.; Hohloch, S.; Sarkar, B.; Nauton, L.; Cisnetti, F.; Gautier, A. Are Cu ( I)– Mesoionic NHC Carbenes Associated with Nitrogen Additives the Best Cu – Carbene Catalysts for the Azide – Alkyne Click Reaction in Solution? A Case Study . *Tetrahedron Lett.* **2013**, *54* (1808–1812).
- (37) Wang, F.; Fu, H.; Zhao, Y. Quick and Highly Efficient Copper-Catalyzed Cycloaddition of Aliphatic and Aryl Azides with Terminal Alkynes “ on Water .” *Green Chem.* **2008**, *10*, 452–456.
- (38) Fabbrizzi, P.; Cicchi, S.; Brandi, A.; Sperotto, E.; Kotten, G. Van. An Efficient ( 2-Aminoarenethiolato ) Copper ( I ) Complex for the Copper-Catalysed Huisgen Reaction ( CuAAC ). *Eur. J. Org. Chem. Chem.* **2009**, 5423–5430.
- (39) Orgueira, A.; Fokas, D.; Isome, Y.; Chan, P. C.; Baldino, C. M. Regioselective Synthesis of [1,2,3]-Triazoles Catalyzed ByCu ( I ) Generated in Situ from Cu ( 0 ) Nanosize Activated Powder and Amine Hydrochloride Salts. *Tetrahedron Lett.* **2005**, *46*, 2911–2914.
- (40) Girard, C.; Önen, E.; Aufort, M.; Beauvière, S.; Samson, E.; Herscovici, J.

- Reusable Polymer-Supported Catalyst for the [3+2] Huisgen Cycloaddition in Automation Protocols. *Org. Lett.* **2006**, *8*, 1689–1692.
- (41) Xavier, N. M.; Goulart, M.; Neves, A.; Justino, J.; Chambert, S.; Rauter, A. P.; Queneau, Y. Synthesis of Sugars Embodying Conjugated Carbonyl Systems and Related Triazole Derivatives from Carboxymethyl Glycoside Lactones. Evaluation of Their Antimicrobial Activity and Toxicity. *Bioorganic Med. Chem.* **2011**, *19*, 926–938.
- (42) Lipshutz, B. H.; Taft, B. R. Heterogeneous Copper-in-Charcoal-Catalyzed Click Chemistry. *Angew. Chem. Int. Ed.* **2006**, *118*, 8415–8418.
- (43) Rojas-lima, S.; Santillan, R.; Universitaria, C. Cuprous Oxide on Charcoal-Catalyzed Ligand-Free Synthesis of 1,4-Disubstituted 1,2,3-Triazoles via Click Chemistry. *ARKIVOC* **2013**, No. iii, 139–164.
- (44) Xiong, X.; Chen, H.; Tang, Z.; Jiang, Y. Supported CuBr on Graphene Oxide/Fe<sub>3</sub>O<sub>4</sub>: A Highly Efficient, Magnetically Separable Catalyst for the Multi-Gram Scale Synthesis of 1,2,3-Triazoles. *RSC Adv.* **2014**, *4*, 9830–9837.
- (45) Shamim, T.; Paul, S. Silica Functionalized Cu(I) as a Green and Recyclable Heterogeneous Catalyst for the Huisgen 1,3-Dipolar Cycloaddition in Water at Room Temperature. *Catal. Letters* **2010**, *136*, 260–265.
- (46) Xiong, X.; Cai, L. Application of Magnetic Nanoparticle-Supported CuBr: A Highly Efficient and Reusable Catalyst for the One-Pot and Scale-up Synthesis of 1,2,3-Triazoles under Microwave-Assisted Conditions. *Catal. Sci. Technol.* **2013**, *3*, 1301–1307.
- (47) R. B. Nasir Baig, R. S. V. A Highly Active Magnetically Recoverable Nano Ferrite-Glutathione-Copper (Nano-FGT-Cu) Catalyst for Huisgen 1,3-Dipolar Cycloadditions. *Green Chem.* **2012**, *14*, 625–632.
- (48) Kantam, M. L.; Jaya, V. S.; Sreedhar, B.; Rao, M. M.; Choudary, B. M. Preparation of Alumina Supported Copper Nanoparticles and Their Application in the Synthesis of 1,2,3-Triazoles. *J. Mol. Catal. A Chem.* **2006**, *256*, 273–277.
- (49) Mukherjee, N.; Ahammed, S.; Bhadra, S.; Ranu, B. C. Solvent-Free One-Pot Synthesis of 1,2,3-Triazole Derivatives by the “Click” Reaction of Alkyl Halides or Aryl Boronic Acids, Sodium Azide and Terminal Alkynes over a Cu/Al<sub>2</sub>O<sub>3</sub> Surface under Ball-Milling. *Green Chem.* **2013**, *15*, 389–397.
- (50) Valentin, R.; Bonelli, B.; Garrone, E.; Di Renzo, F.; Quidnard, F. Accessibility



- of the Functional Group of Chitosan Aerogel Probed by FT-IR-Monitored Deuteration. *Biomacromolecules* **2007**, *8*, 3646–3650.
- (51) Valentin, R.; Molvinger, K.; Viton, C.; Domard, A.; Quignard, F. From Hydrocolloids to High Specific Surface Area Porous Supports for Catalysis. *Biomacromolecules* **2005**, *6*, 2785–2792.
- (52) Chtchigrovsky, M.; Primo, A.; Gonzalez, P.; Molvinger, K.; Robitzer, M.; Quignard, F.; Taran, F. *Zuschriften Functionalized Chitosan as a Green , Recyclable , Biopolymer-*. **2009**, 6030–6034.
- (53) Baig, R. B. N.; Varma, R. S. Copper on Chitosan: A Recyclable Heterogeneous Catalyst for Azide-Alkyne Cycloaddition Reactions in Water. *Green Chem.* **2013**, *15* (7), 1839–1843.
- (54) Gholinejad, M.; Jeddi, N. Copper Nanoparticles Supported on Agarose as a Bioorganic and Degradable Polymer for Multicomponent Click Synthesis of 1,2,3-Triazoles under Low Copper Loading in Water. *ACS Sustain. Chem. Eng.* **2014**, *2*, 2658–2665.
- (55) Rull-Barrull, J.; D'Halluin, M.; Le Grogneq, E.; Felpin, F. X. A Paper-Based Biomimetic Device for the Reduction of Cu(II) to Cu(i)-Application to the Sensing of Cu(II). *Chem. Commun.* **2016**, *52* (39), 6569–6572.
- (56) Rull-Barrull, J.; d'Halluin, M.; Le Grogneq, E.; Felpin, F. X. Harnessing the Dual Properties of Thiol-Grafted Cellulose Paper for Click Reactions: A Powerful Reducing Agent and Adsorbent for Cu. *Angew. Chemie - Int. Ed.* **2016**, *55* (43), 13549–13552.
- (57) Chavan, P. V.; Pandit, K. S.; Desai, U. V.; Kulkarni, M. A.; Wadgaonkar, P. P. Cellulose Supported Cuprous Iodide Nanoparticles (Cell-CuI NPs): A New Heterogeneous and Recyclable Catalyst for the One Pot Synthesis of 1,4-Disubstituted-1,2,3-Triazoles in Water. *RSC Adv.* **2014**, *4* (79), 42137–42146.
- (58) Raut, D.; Wankhede, K.; Vaidya, V.; Bhilare, S.; Darwatkar, N. Copper Nanoparticles in Ionic Liquids : Recyclable and Efficient Catalytic System for 1 , 3-Dipolar Cycloaddition Reaction. *Catal. Commun.* **2009**, *10*, 1240–1243.
- (59) He, X.; Li, X.; Guo, N.; Zhao, Y.; Xu, G.; Li, W. Metallic Copper Wire-A Simple, Clear and Reusable Catalyst for the CuAAC Reaction in Supercritical Carbon Dioxide. *RSC Adv.* **2015**, *5*, 73340–73345.
- (60) Loftsson, T.; Brewster, M. E. Pharmaceutical Applications of Cyclodextrins:

- Drug Solubilisation and Stabilization. *J. Pharm. Sci.* **1996**, 85 (11), 1017–1025.
- (61) Shin, J.-A.; Lim, Y.-G.; Lee, K.-H. Copper-Catalyzed Azide–Alkyne Cycloaddition Reaction in Water Using Cyclodextrin as a Phase Transfer Catalyst. *J. Org. Chem.* **2012**, 77 (8), 4117–4122.
- (62) Xiong, X.; Cai, L.; Jiang, Y.; Han, Q. Eco-Efficient, Green, and Scalable Synthesis of 1,2,3-Triazoles Catalyzed by Cu(I) Catalyst on Waste Oyster Shell Powders. *ACS Sustain. Chem. Eng.* **2014**, 2 (4), 765–771.
- (63) Xiong, X.; Tang, Z.; Sun, Z.; Meng, X.; Song, S.; Quan, Z. Supported Copper (I) Catalyst from Fish Bone Waste: An Efficient, Green and Reusable Catalyst for the Click Reaction toward *N*-Substituted 1,2,3-TRIAZOLES. *Appl. Organomet. Chem.* **2018**, 32 (1), e3946.
- (64) Ghodsinia, S. S. E.; Akhlaghinia, B.; Jahanshahi, R. Direct Access to Stabilized CuI using Cuttlebone as a Natural-Reducing Support for Efficient CuAAC Click Reactions in Water. *RSC Adv.* **2016**, 6 (68), 63613–63623.

## Chapter 3

### Synthesis of 1,4-disubstituted 1,2,3-triazoles using Cu(I) stabilized on N,N'-methylene bis-acrylamide cross linked polyvinylpyrrolidone

#### 3.1 Introduction

Polymer supported metal complexes are a class of compounds in which metal precursors are implanted over a polymer support. It binds the metal ions through coordinate bond using heteroatoms like oxygen or nitrogen and stabilized on the polymer matrix. Microenvironment of the ligand is an important factor that affects the complexation. During metalation, changes occur in both polymer and metal precursor. One of the important applications of polymer-metal complexes is in catalysis which coalesce the advantages of both homogenous and heterogeneous catalysts. Copper(I) catalyzed azide-alkyne cycloaddition (CuAAC) reaction was independently introduced by Sharpless<sup>1</sup> and Meldal.<sup>2</sup> Various methods have been developed in order to increase the efficiency of the reaction which includes the introduction of different catalytic systems like homogeneous, heterogeneous and magnetic heterogeneous catalysts,<sup>3-5</sup> nanoparticles,<sup>6-8</sup> one pot procedures<sup>9</sup> and using water as reaction media.<sup>10,11</sup> The copper catalyzed version of click reaction is the most commonly used one for the regioselective synthesis of 1,4-disubstituted 1,2,3-triazoles.<sup>12,13</sup> Nitrogen containing ligands are known to stabilize the Cu(I) active species in reaction media even in water.<sup>14</sup> It was observed that CuAAC accelerated by the ligands such as tris(2-aminoethyl)amine derivatives, acryl amide can minimize the amount of Cu(I) catalyst to an order less than 1%.<sup>15,16</sup> Poly(*N*-vinyl-2-pyrrolidone) (PVP) is widely used as reducing agent, stabilizer and growth modifier in nanoparticle synthesis.<sup>17-20</sup> These nanoparticles are also used as catalysts for 1,3-dipolar cycloaddition reactions for the synthesis of 1,2,3-triazoles.<sup>21</sup>

### **3.2 Review of literature**

In recent years, polymer supported metal complexes have achieved great attention due to their wide application in bioinorganic and synthetic chemistry. Merrifield in 1963 introduced “solid phase technique” for the synthesis of peptides using insoluble cross linked macromolecules as supports. Such functionalized polymers were used as catalysts and protecting groups in the synthesis of pharmaceuticals, agricultural, dyes etc. Application of functional polymers depends on the chemical modification made, such that the polymers have characteristic physical properties of polymer and chemical reactivities of the incorporated functional groups. Functionalized polymers found out their application as reducing agents,<sup>22</sup> to understand biological reactions of macromolecules,<sup>23</sup> photoconductive polymers<sup>24</sup> and polymeric surfactants.<sup>25</sup> Polymer metal complexes belong to coordination compounds in which the central metal atom or ion is attached with molecules or ions. They have application in diverse fields like organic synthesis,<sup>26,27</sup> waste water treatment,<sup>28</sup> hydrometallurgy,<sup>29</sup> polymer drug grafts,<sup>30</sup> environmental protection<sup>31</sup> and nuclear chemistry.<sup>32</sup> The polymer – metal complexes possess characteristic structure in which the central metal ions are surrounded by a giant polymer chain bound to metal ion through coordinate bonds. Here the polymer chain is obtained by the polymerization of monomer units containing coordinating atoms like N, O and S. Polymer supported metal complexes have various advantages like easy recovery by simple filtration, recyclability etc. Therefore, it can be reused and hence economic.

Polymeric metal complexes are classified depending on the preparation methods

1. Complexation of polymeric ligand with metal ion; which is again subdivided into
  - 1.1 Pendent polymer metal complexes and
  - 1.2 Inter/ intra molecular bridged polymer complex
2. Complexation of metal ions with multifunctional polymer ligands
3. Polymerization of metal containing monomer units.

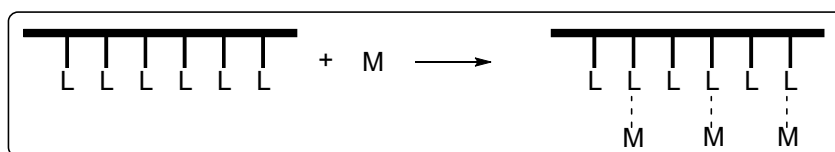
Complexation of polymeric ligands with metal ion results in different types of coordination structures which are divided into Pendent and Inter and/or Intramolecular bridged polymers.

## 1.1 Pendent Polymer metal complexes

In this type, the metal ion is attached to the polymer ligand through the functional group which is tagged on the polymer chain. Pendent complexes are classified as monodentate and polydentate depending on the chelating abilities of the ligands.

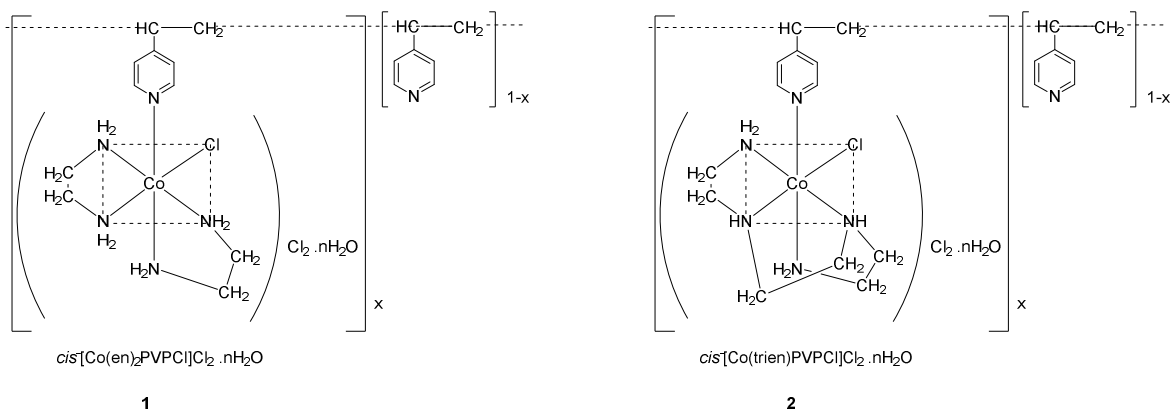
## 1.1.1. Monodentate pendent polymer complexes

Here metal ion or metal complex is attached to the one labile ligand which is substituted by the polymeric ligand (**Scheme 1**)



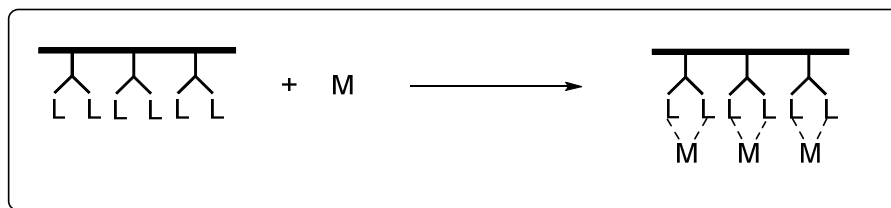
Scheme 1

Kurimura<sup>33</sup> and Tsuchide<sup>34</sup> reported the synthesis of poly-4-vinylpyridine complexes (**1** and **2**) with various metal chelates belonging to monodentate type.



## 1.1.2. Polydentate pendent polymer complexes

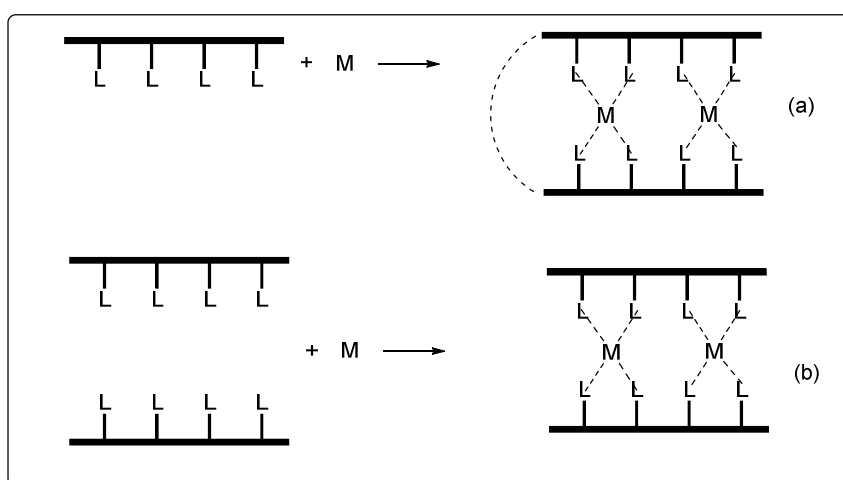
Polydentate ligand on complexation results in the formation of bridged structures (**Scheme 2**)



Scheme 2

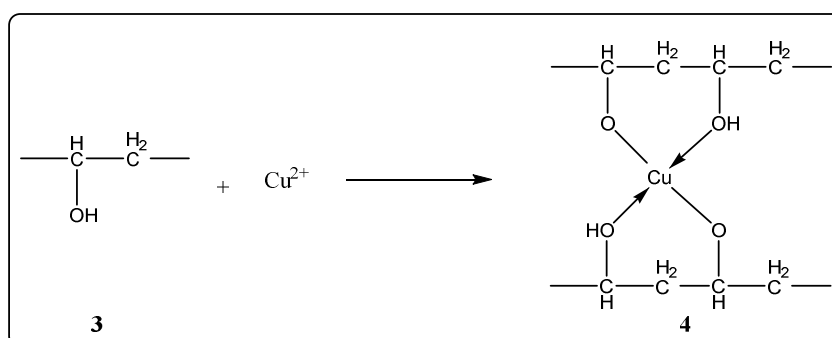
## 1.2. Inter and/or intra molecularly bridged polymer metal complexes

This type of complexes results after the reaction of metal ion with polymeric ligand that has four or six coordinating bonding hands (**Scheme 3**).



Scheme 3 M= metal ion, a) intra polydentate b) inter polydentate

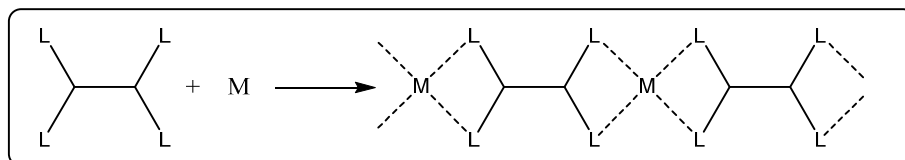
Poly(vinyl alcohol)(PVA) copper(II) complex is the simplest example belonging to the above category<sup>35</sup> (**Scheme 4**).



Scheme 4

## 2. Complexation of metal ions with multifunctional polymer ligand

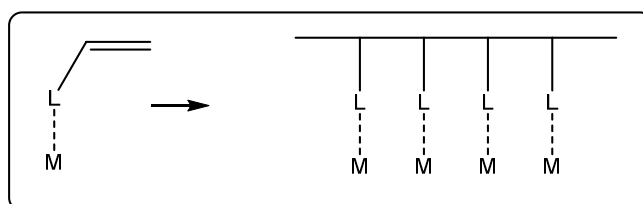
Polymer chain in this type is composed of coordinate bonds and ligands that act as bridging unit. Multidentate ligands tend to form this type of polymer metal complex (Scheme 5).



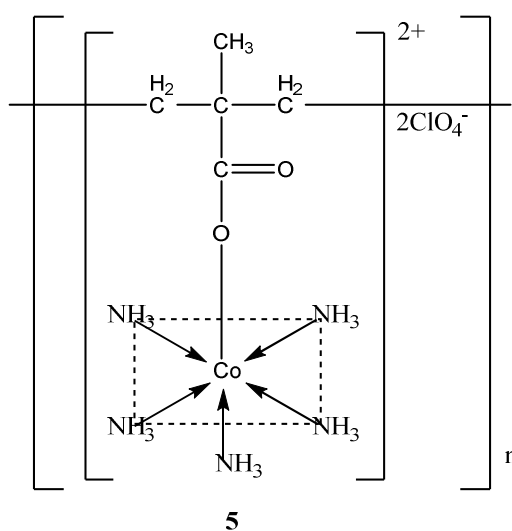
Scheme 5

## 3. Polymerization of metal containing monomer unit

This type of polymer metal complex is formed by the polymerization of functionalized ligand units. Most studied example of this type complex is vinyl complexes which polymerize through radical polymerization of vinyl monomer containing transition metal ions (Scheme 6).



Scheme 6



5

**Application of Polymer-metal complexes as catalysts**

Catalysts are the substances that increase the rate of a chemical reaction by providing an alternative pathway with a lower energy of activation compared to uncatalyzed reaction. Reactions can be catalyzed homogeneously and heterogeneously. In homogeneous catalysis, both reactants and catalyst are in the same phase whereas in heterogeneous reactions they are in different phases. Heterogeneous catalysts gained more attention in organic synthesis because of their good thermal stability, good selectivity, and they are insoluble in reaction media facilitating easy recovery of catalyst by filtration or centrifugation. The advantages of homogeneous catalysts are better reproducibility, selectivity and requirement of less drastic conditions. But the major disadvantage was the difficulty in recovery of the catalyst from the reaction media which can be avoided by binding homogeneous catalyst to inorganic carrier or organic polymer. Therefore, when incorporating a transition metal ion or complex into polymer support, we get a polymer supported catalyst and the recovery and recyclability of the catalyst became easy because of the insoluble support. Such catalysts can be renamed as “Heterogeneously homogeneous” catalyst. The catalytic activity of polymer metal complexes is affected by

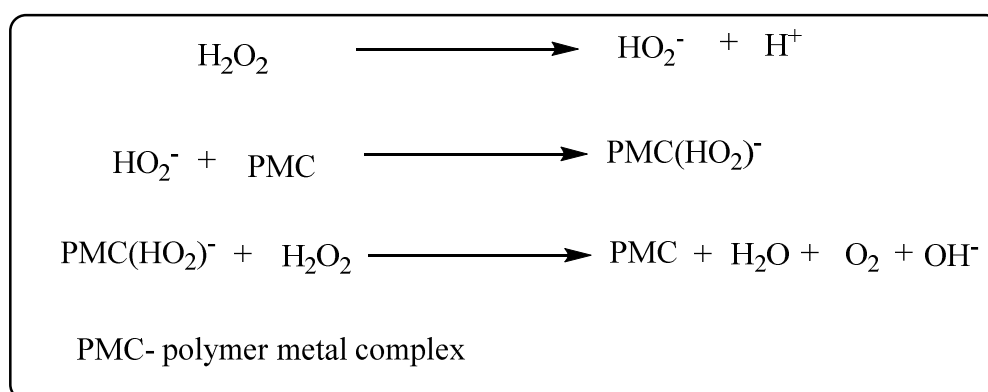
- i. Porosity and surface area
- ii. Nature of polymer support and extent of cross linking
- iii. Spacer effect
- iv. Swelling and solvation of polymer matrix

The pore size and surface area is largely affected by the nature and degree of cross linking. Greater the porosity, greater will be the solvent flow and higher will be the catalytic activity. To increase the reaction rate, the catalyst must be highly porous and the active species should be largely distributed over the interior of the catalyst. Cross linked polymer support offers better stability to metal complex compared to the linear one. Nature and extent of cross linking in polymer matrix strongly affect the complexation process; as the degree of cross linking increases, lesser will be the metal ion intake which lowers the stability of polymer metal complex as the polymer became more rigid.



Varghese *et.al* reported the effect of molecular interaction on the structure of polymer metal complex.<sup>36</sup> Length of the pendent chain largely affects the amount of metal complexed and the structure of metal complex. Steric hindrance of functional groups arises due to the shorter distance which decreases the efficiency of complex formation. The reactivity of functional groups will be less because of steric hindrance occurred by the interference of polymer chains. To increase the reactivity of functional groups there must be a separation between from the active site and polymer matrix.<sup>37</sup>  $\alpha,\omega$ -Dibromoalkanes,<sup>38</sup>  $\omega$ -bromoalkane,<sup>39</sup> triethylamine<sup>40</sup> are commonly used spacers. The degree of cross linking has major effect on swelling nature of the polymer back bone. As the degree of cross linking increases the extent of swelling decreases. Different factors that made difficulties in the swelling nature are length of polymer chain, chain entanglement, efficiency of cross link formation, nature and proportion of monomer to diluent ratio used during the polymer matrix synthesis. Gel type polymer supports with microporous nature and lesser cross linking are widely used as polymer support and catalyst. Upon swelling the gel supports exposes the reactive site towards the reactants.

Polymer supported catalysts can catalyze different types of reactions. For example, poly( $\beta$ -diketone)Cu(II)<sup>41</sup> in the oxidation of L-ascorbic acid, poly(vinylalcohol)<sup>42</sup> and NNMBA cross linked polyacrylamides with glycine functionalities<sup>43</sup> exhibit catalytic activity towards the decomposition of  $H_2O_2$ (Scheme 7).

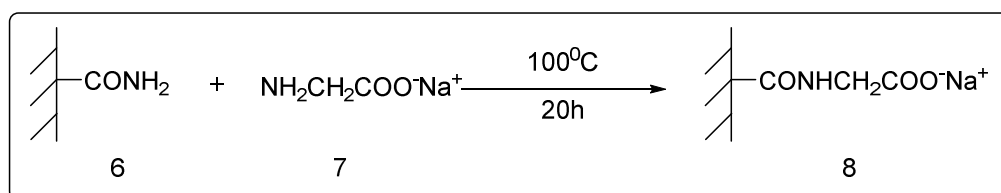


Scheme 7

Cobalt containing polyvinyl pyrrolidone complexes was synthesized by Musin in 1988.<sup>44</sup> Alcoholic solution of  $CoCl_2$  was added to PVP solution. Stirred for half an

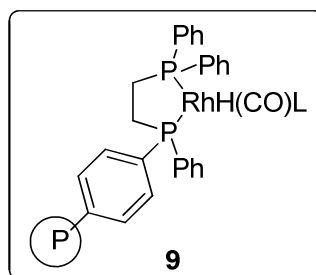
hour, solvent evaporated by rotary evaporator and dried in vacuum oven at 60-80°C. Cobalt containing coordination compounds have biological relevance, like vitamin B<sub>12</sub>. They investigated the biological action of Cobalt-PVP complex. The cobalt complex reduces the cardiotoxic action, which was due to the known nature of PVP in improving the blood flow. Metal complexation of cross linked polyacrylamide supported dithiocarbamates was reported in 1992 by Pillai.<sup>45</sup> Kannan and coworkers reported the oxidation of cyclohexanol to cyclohexanone was done by poly(2-hydroxy-4-acryloyloxybenzaldehyde)-Cu(II)/Ni(II) complexes.<sup>46</sup>

Hydrolytic dehydrogenation of ammonia borane was catalyzed by PVP stabilized Ni(II) catalyst.<sup>47</sup> Later in 1998 B. Mathew reported the synthesis of NNMBA cross linked polyacrylamide supported glycine.<sup>48</sup> Cross links were introduced by free radical polymerization using potassium persulfate as initiator. Glycine functions were incorporated by transamidation using excess sodium salt of glycine at 100°C for 24h (Scheme 8).

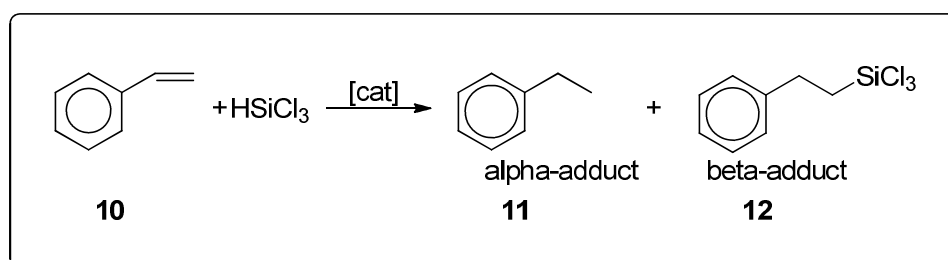


Scheme 8

Seguel reported the synthesis and characterization of Cu(II), Co(II), Ni(II) and Zn(II) complexes of poly(maleic acid).<sup>49</sup> Hydrogenation of olefins catalyzed by poly(acrylic acid) Ru(II) complexes was reported by Hirai in 1974.<sup>50</sup> Using polymer supported Rh(I) catalyst, Grubbs reported the rate of hydrogenation of olefins.<sup>51</sup> Hydrogenation of alkenes and alkynes were catalyzed by poly(styryl)bipyridinePd(II) acetate.<sup>52</sup> Catalyst reduces more crowded or sterically hindered alkenes rather than less hindered ones. Nayak reported the reduction of alkenes and alkynes under mild conditions using polystyrene supported Pd(II) species.<sup>53</sup> The rate of hydroformylation reaction was found to be increased when the catalyst was bound to a polymer matrix. The hydroformylation reaction of 1-pentene was carried out using polymer anchored rhodium complex **9**.<sup>54</sup>

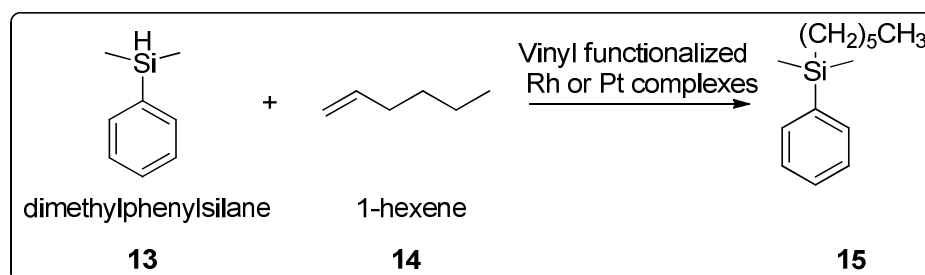


Hydrosilylation of phenylacetylene was catalyzed by polyamide supported metal complexes.<sup>55</sup> Polymer supported ferrocene derivatives of platinum and palladium complexes shows excellent catalytic activity for the hydrosilylation of olefins by trichlorosilane. The catalyst can be reused without any significant loss in catalytic activity<sup>56</sup> (**Scheme 9**).



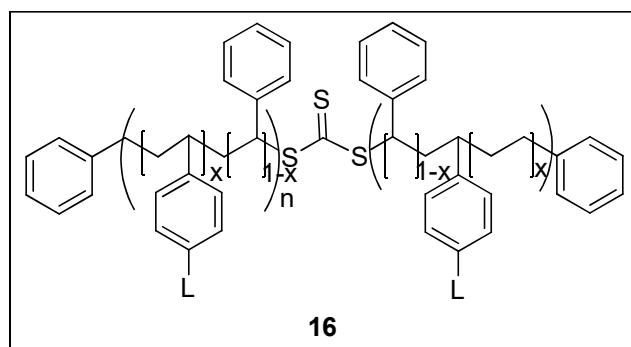
Scheme 9

Tetraamineplatinum(II) chloride on silica supported polyethylene glycol is an example of supported liquid-phase catalyst (SLPC)<sup>57</sup> in which the catalyst component dissolved in a liquid phase and coated over a porous material. The catalyst shows high activity towards the hydrosilylation of phenylacetylene and found to be stable under all the reaction conditions they had studied. Hydrosilylation of terminal olefins catalyzed by both rhodium and platinum complexes of vinyl functionalized polysiloxanes was reported by Michalska in 2004<sup>58</sup> (**Scheme 10**).



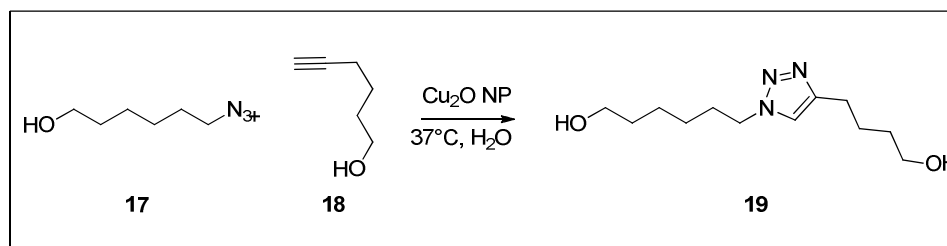
Scheme 10

Jiang reported the synthesis and catalytic activity of poly- $\gamma$ -mercaptopropylsiloxane-platinum complex in the hydrosilylation of 1-hexene and acetylene.<sup>59</sup> Addition of triethoxysilane to 1-hexene at 80°C or at room temperature using the catalyst provides n-hexyltriethoxysilane only whereas the addition towards acetylene provides vinyltriethoxysilane and bis(triethoxysilyl) ethane in good yields. Epoxidation of cyclohexene has been studied by Tempesti in 1987<sup>60</sup> in which molybdenum-boron mixed oxo derivatives were immobilized on to the polymeric support and carried out the epoxidation using t-butyl or ethylbenzenhydroperoxide. The catalyst provides a comparable result with that of bimetallic boron-molybdenum catalyst. They concluded that the grafting on the polymer support didn't negatively affect the reaction. Similar work was done by Stamenova<sup>60</sup> and Sherrington<sup>61</sup> using polymer supported molybdenum and vanadium catalyst with different polymer supports. Polymer matrices containing Mn(III) salen complexes were synthesized and the catalytic activity in epoxidation has been studied by Sivaram.<sup>62</sup> Catalytic oxidation of phenol using PVP or chitosan stabilized copper catalyst<sup>63</sup> provided 80% phenol conversions compared to commercially available CuO/ $\gamma$ -Al<sub>2</sub>O<sub>3</sub> under similar reaction conditions. Prez *et.al* reported the synthesis and catalytic activity of styrene functionalized TBTA (Tris((1-benzyl-4-triazolyl)methylamine) monomer which copolymerized via RAFT (Reversible addition-fragmentation chain-transfer) polymerization to afford the catalyst support **16**. This was used for the complexation with copper(I) source providing a reusable catalyst<sup>64</sup> for the click synthesis of 1,2,3-triazoles. They checked the reusability of the catalyst and it can be reused for 6 times without any loss in the catalytic activity.



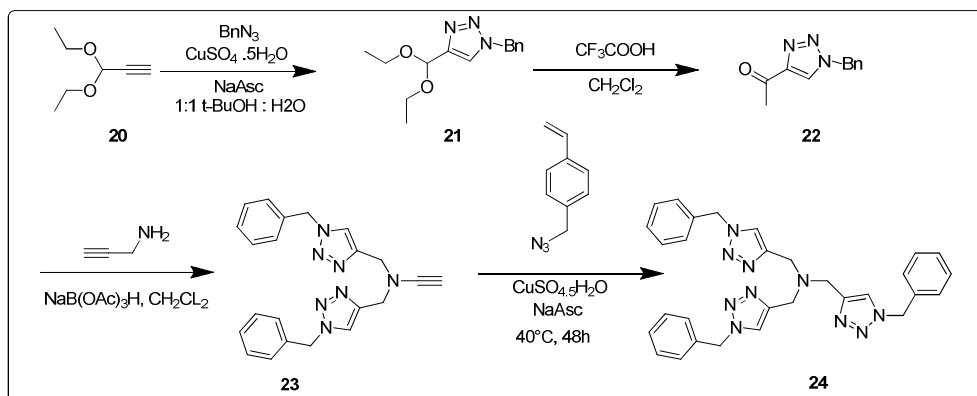
Suzuka reported the synthesis of polymer supported 2,2'-biarylpyridine copper complexes for cycloaddition reaction.<sup>65</sup> Chen reported the synthesis of PVP coated

$\text{Cu}_2\text{O}$  catalyst which shows good catalytic activity for azide-alkyne click reaction in water<sup>66</sup>(Scheme 11).



Scheme 11

Prez and coworkers first synthesized TBTA based monomer **23**(Scheme 12) in a method developed by Fokin *et.al.*<sup>67</sup> They used CuAAC scheme for the monomer preparation and RAFT instead of ATRP because the transition metal ion used as the catalyst will react with TBTA monomer and leads to uncontrollable polymerization. Using TBTA/Cu polymer they conducted model reaction of CuAAC using benzyl chloride and phenyl acetylene.



Scheme 12

Magnetic poly(imidazole/imidazolium)-supported  $\text{Cu(II)}$  complex were prepared and its catalytic activity for CuAAC was studied by Pourjavadi.<sup>68</sup> After the synthesis of MNPs it was further functionalized using 3-(trimethoxysilyl)propylmethacrylate. Monomer ([EVim][ $\text{BF}_4$ ]) was obtained by heating 1-vinylimidazole and ethyl bromide in methanol at  $60^\circ\text{C}$  for 20 h and the solid was separated by simple decantation and dried in vacuum. Copper was introduced to the catalyst using  $\text{CuSO}_4$  in water by vigorous stirring continuously for 3 days at  $70^\circ\text{C}$ .  $\text{Cu(I)}$ -poly(2-aminobenzoic acid) ( $\text{Cu(I)}$ -pABA) was prepared by dissolving 2-aminobenzoic acid in Milli-Q water at 60

°C,  $\text{CuSO}_4 \cdot 5\text{H}_2\text{O}$  dissolved in DMF was added to the above solution with continuous stirring. This catalyst was used for click reaction in aqueous media.<sup>69</sup>

### **Scope of the present work**

There are a number of reports on CuAAC reactions catalyzed by heterogeneous catalyst having various advantages like easy recovery, simple product isolation etc. Most of the heterogeneous system uses copper(I) as the metal precursor which is the catalytically active species in CuAAC reaction. Polymer metal complexes with application in CuAAC reaction using copper(I) source were found to be less. Herein, we have developed a catalytic system containing catalytically active copper(I) species stabilized within the polymeric matrix for the CuAAC reaction.

### **3.3.1 Reagents and Materials**

- Anhydrous sodium sulphate, glacial acetic acid, copper sulfate and sodium dihydrogen phosphate, N,N'-methylene bisacrylamide, phenyl acetylene and 4-ethynyl toluene were purchased from Sigma Aldrich, Bangalore.
- N-vinyl pyrrolidone, benzyl chloride, 4-chlorobenzyl chloride, 2,4-dichlorobenzyl chloride, 4-nitro benzyl bromide, N-butyl bromide, allyl bromide, 1-chloromethyl naphthalene, cyclopentyl bromide and 2-bromoethyl benzene were purchased from Spectrochem, Mumbai
- Sodium azide from Nice chemicals, Kochi
- Ethanol, Distilled water

### **3.3.2 Instruments**

- IR spectra was recorded on a Shimadzu IR Affinity- 1 Spectrometer using KBr pellets
- SEM performed on JEOL Model JSM-7600F along with identification of chemical composition of sample using energy dispersive X-ray spectroscopy.
- Powder X-ray diffraction pattern was recorded on Bruker AXS, D8 Advance. operating at 20kV using Cu-K $\alpha$  radiation( $\lambda = 0.1542\text{nm}$ )
- TG-DTA results obtained from Perkin Elmer, Diamond TG/DTA
- X-ray photoelectron Spectroscopy (XPS): Kratos Analytical U K Model Axis Ultra AL K alpha
- NMR – Bruker Avance III, 400MHz
- GC-MS – Thermo Fisher Scientific
- Buchi Rotavapour
- Mechanical overhead rotator

### **3.4 Results and Discussion**

N,N'-methylene bisacrylamide (NNMBA) cross linked polyvinylpyrrolidone copolymer(PVPNNMBA) was synthesized by suspension polymerization of N-vinyl pyrrolidone using NNMBA as cross linking agent and AIBN used as radical initiator. To maintain the optimum rigidity and swelling properties, the degree of cross linking was maintained to 4%. Immobilization of copper ions into the polymer matrix (CuPVPNNMBA) was done by swelling the polymer in glacial acetic acid followed by heating the polymer with copper(II) sulphate in glacial acetic acid.

Reduction of copper(II) to copper(I) takes place in the presence of polyvinyl pyrrolidone(PVP) which can act as a mild reducing agent.<sup>70,71</sup> This reducing power of PVP was attributed by the presence of end hydroxyl group.<sup>72</sup> NNMBA plays a dual role as cross linking agent and the amide moiety can facilitate coordination to copper.<sup>73</sup> Further reduction of copper(I) to copper(0) was prevented by the coordination of copper(I) with the oxygen atom of pyrrolidone and nitrogen atom of NNMBA which stabilize Cu(I) in the polymer matrix. These observations were affirmed by different characterization techniques.

#### **3.4.1 Infrared spectral studies of PVPNNMBA and CuPVPNNMBA**

Comparison of the FTIR spectrum of PVPNNMBA and CuPVPNNMBA helps to differentiate them and can be used as the primary evidence for the incorporation of copper into the polymer matrix (**Table 1 & Fig 1**). The free N-vinyl pyrrolidone exhibited  $\nu_{\text{CH}_2}$  wagging of vinyl bond around  $850\text{cm}^{-1}$ ,  $\nu_{\text{C=C}}$  at  $1630\text{cm}^{-1}$  and  $1426\text{cm}^{-1}$  corresponds to vinyl scissoring. These peaks were absent in PVPNNMBA and CuPVPNNMBA spectrum. This confirms the formation of PVPNNMBA and CuPVPNNMBA sacrificing the vinylic bond. Peak at  $629\text{cm}^{-1}$  is characteristic of  $\text{Cu}_2\text{O}$ . Due to the interaction with copper ions in the polymer, the characteristic peak of carbonyl shifted from  $1656\text{cm}^{-1}$  to  $1614\text{cm}^{-1}$ (**Fig 1**). Similar shifting of peaks were noticed at  $1446\text{cm}^{-1}$  to  $1438\text{cm}^{-1}$ ,  $3360\text{cm}^{-1}$  and  $3110\text{cm}^{-1}$  to  $3376\text{cm}^{-1}$  and  $3273\text{cm}^{-1}$ ,  $1547\text{cm}^{-1}$  to  $1558\text{cm}^{-1}$  corresponding to C-N-C stretching, secondary amide, N-H bending vibrations respectively.



Table 1. FTIR absorption bands

FTIR absorption ( $\text{cm}^{-1}$ )						
Sample	Vinyl Scissoring & $=\text{CH}_2$ wagging	Amide	N-H Bend	N-H Str	C-H Str	M-O
PVPNNMBA	Absent	1655	1547	3441	2882	Absent
CuPVPNNMBA		1626	1516	3429	2883	683

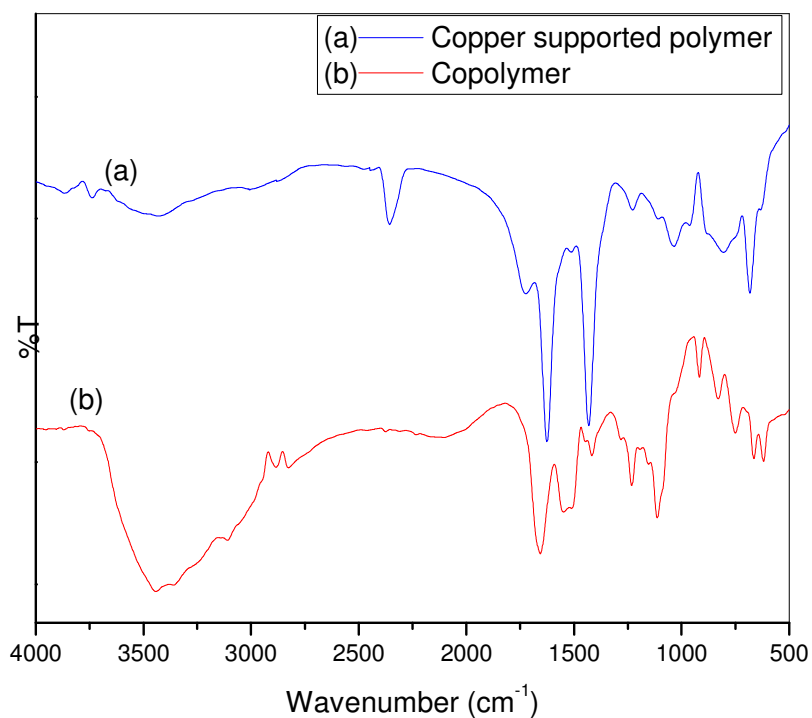
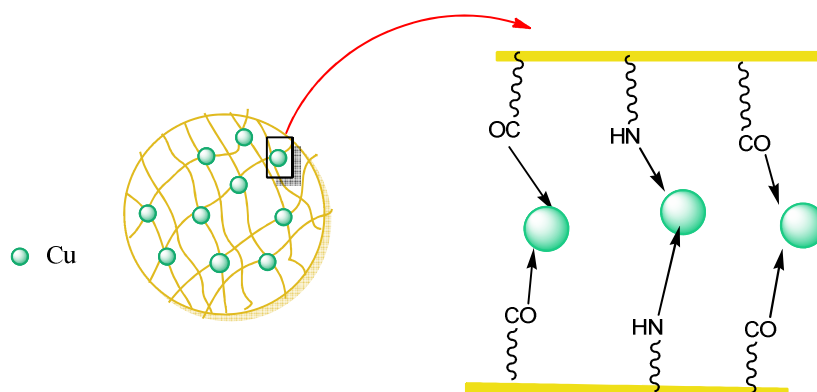


Fig.1 FTIR of Copolymer and CuPVPNNMBA



**Fig .2** Schematic representation of incorporation of metal ion in the polymer matrix

### **3.4.2 Morphological and elemental composition studies**

Scanning electron micrographs provides information about nature of the surface and size of particles. An X-ray beam emitted from the sample during SEM analysis makes use for the elemental analysis termed as energy dispersive X-ray spectroscopy (EDX). The emitted X-ray beam will be a characteristic of each element present in the sample. The changes occurred in the surface morphology of the copolymer during the metal complexation can be identified using this technique. In the present work, we have studied the morphological features of 4mol% NNMBA cross linked polyvinyl pyrrolidone and its copper complex. The SEM image of the cross linked polymer and copper complex are given (**Fig. 3**). Compared to pure polymer, copper added polymer adopts particle nature after complexation.

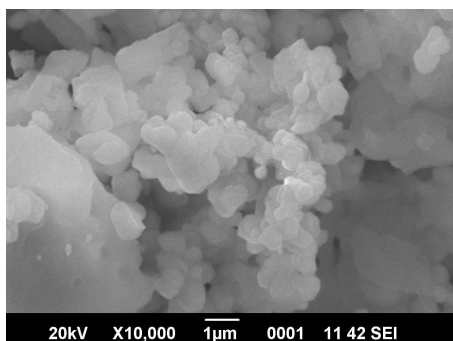
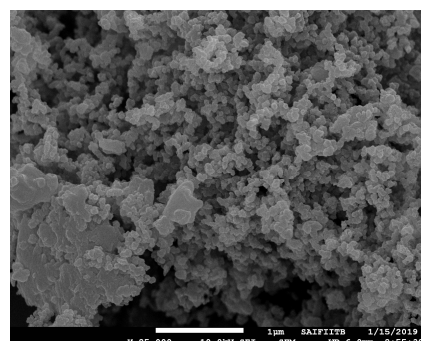


**Fig:3 I** SEM image of PVPNNMBA



**II.** SEM image of CuPVPNNMBA

Elemental composition of the polymer metal complex (CuPVPNNMBA) can be studied using EDS spectra (**Fig.4**). It confirms the presence of copper providing its characteristic peaks at 0.94 and 8.1keV corresponds to CuL $\alpha$  and CuK $\alpha$  respectively. Peak at 2.34keV indicate the presence of sulphur whereas the presence of oxygen was confirmed by the peak at 0.52keV corresponds to CuK $\alpha$  and presence of carbon provides peak at 0.28keV of CuK $\alpha$ . Peak at 0.39keV corresponds to nitrogen.

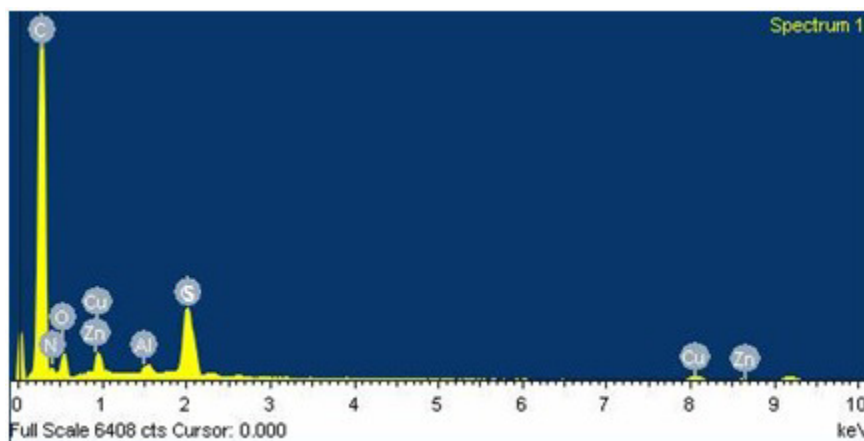


**Fig.4** EDS Spectra of CuPVPNNMBA

Inductively coupled Atomic Emission Spectroscopy (ICP-AES) also supports the EDX result which substantiates that the 1.23wt% of copper impregnated on the polymer support.

### 3.4.3 Powder X-ray diffraction

The X-ray diffraction pattern provides information about the phases, unit cell dimensions, orientation and chemical composition of the sample. X-ray diffraction is a non-destructive analytical technique, which produces monochromatic X-rays as a result of bombardment of accelerated electron with heavy metals like Cu. XRD pattern of CuPVPNNMBA given in **Fig.5**. The XRD pattern confirms the presence of copper in both oxidation state +1 and +2 in the polymer and its existence as  $\text{Cu}_2\text{O}$  and  $\text{CuSO}_4$ , supporting the EDX result. The major peaks at  $28.8^\circ$ ,  $38.4^\circ$ ,  $42.1^\circ$ ,  $61.8^\circ$  and  $73.6^\circ$  are related to the corresponding (110), (111), (200), (220) and (311) planes of  $\text{Cu}_2\text{O}$  (Cubic, JCPDS Card No. 05-0667). Peaks at  $2\theta = 18.9$ , 23, 25.4, 27.9, 32, 33.7, 48.7, 54.4 and  $59.3$  can be assigned to (-111), (021), (0-21), (031), (-221), (-140), (-312), (202) and (321) phases of  $\text{CuSO}_4$  respectively (triclinic, JCPDS File No. 77-1900).

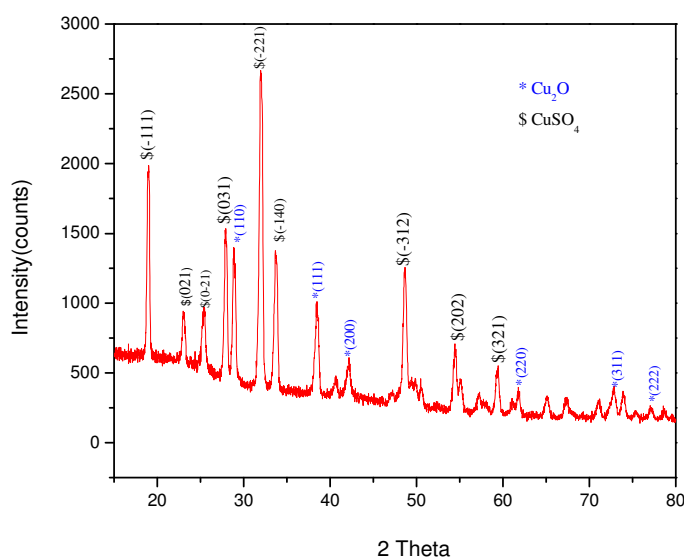


**Fig.5** XRD pattern of CuPVPNNMBA

### 3.4.4 X-ray photoelectron spectroscopy

X-ray photoelectron spectroscopy can be used for the detection and quantification of elements present in a sample. When the sample surface was irradiated with beam of X-rays commonly Al K $\alpha$  or Mg K $\alpha$ , core level electrons absorb the energy and get ejected. The outer electron fills the vacancy created by the core electron. During this process energy is emitted and the instrument measures this energy. In the present study the sample was characterized by XPS technique and confirms the presence of both Cu<sup>+</sup> and Cu<sup>2+</sup>. **Fig.6.1** XPS spectra of Cu 2p core level spectra of CuPVPNNMBA. Spin orbit doublet of Cu 2p core level produces two states 2p<sub>3/2</sub> and 2p<sub>1/2</sub>. Following conclusions have been made:

- The Cu (2p<sub>3/2</sub>) analysis reveals the presence of peak at 934.3eV which arises due to the ligand to metal charge transfer during the photoemission process and accompanying with weak satellite peaks at 940.4, 941.8, 943.1 eV due to 3d<sup>9</sup>L configuration,<sup>74</sup> confirms the presence of Cu<sup>2+</sup>. Peak at 953eV corresponds to Cu (2p<sub>1/2</sub>) level.
- The satellite peaks are found to be 6-10eV greater than the core level peak.
- The main Cu 2p<sub>3/2</sub> peak at 932.5 eV and its corresponding weak satellite peak at 948.9 eV indicate the presence of Cu<sup>+</sup>. The presence of such weak satellite peak was explained by Harmer that it could be from the minor contributions from Cu d<sup>9</sup> initial state configuration<sup>75</sup>.
- Area under the curve indicates that Cu(I) and Cu(II) are present in approximate ratio 1:2

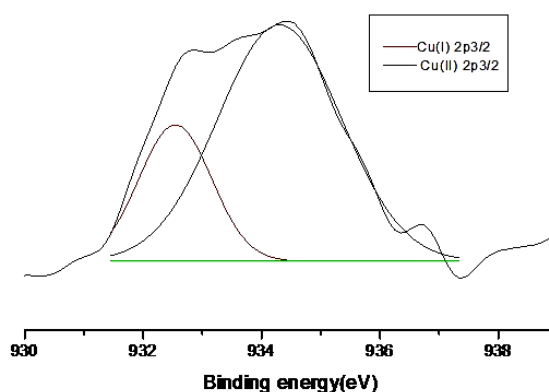


**Fig 6.1** Cu2p core level spectra of CuPVPNNMBA

- O1s Peak at 531.3 eV in XPS spectra confirms the presence of  $\text{Cu}_2\text{O}$  (Fig.6.2).

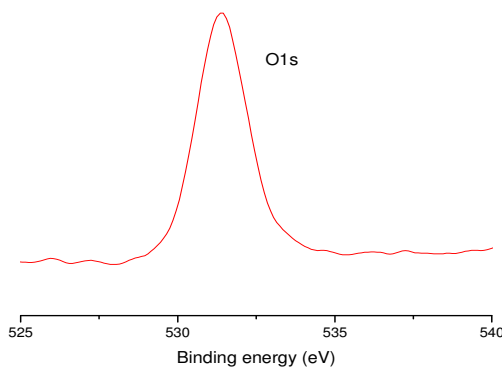


**Fig 6.2** O1s XPS spectra of CuPVPNNMBA

- The C1s spectra contains two major peaks; one at 284.6eV corresponds to polymeric hydrocarbons whereas the second one at 287.1eV belongs to C-OH<sup>76</sup> (Fig 6.3).

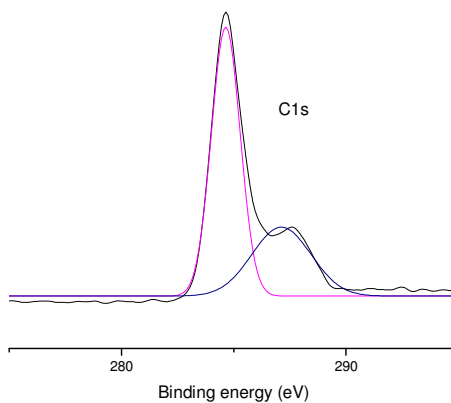


**Fig 6.3** C1s XPS spectra of CuPVPNNMBA

### 3.4.5 Thermogravimetric analysis

Thermal stability and decomposition pattern of cross linked polymers were studied using thermogravimetric analysis. The TG and DTA curve of 4mol% NNMBA cross-linked polyvinylpyrrolidone was examined and shown in Fig 7. It shows that the sample is stable up to 232°C. Initial weight loss at 121°C represents loss of water, solvent etc.

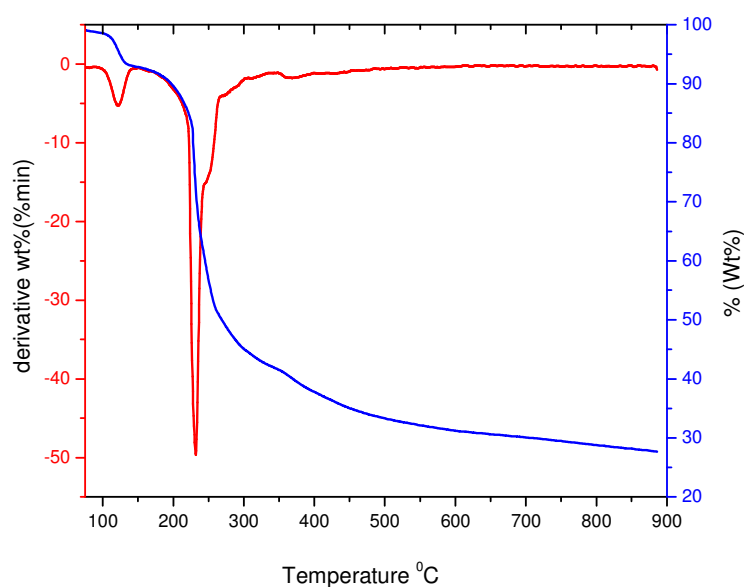


**Fig.7** TG and DTA curve of CuPVPNNMBA

The first stage of decomposition occurs from 100°C to 138°C with a weight loss of 5.18% due to the extrusion of absorbed and coordinated water molecules. The second stage starts at 185°C and continued up to 265°C. In this region, 49.4% weight loss occurs due to the rupture of polymer copper coordination bonds. Rupture of cross linking and polymeric linkages occurs from 337°C to 396°C with a weight loss of 1.73%.

### 3.5 Synthesis of 1,4-disubstituted 1,2,3-triazole using CuPVPNNMA as heterogeneous catalyst

Heterogeneous catalysts gained more attention in catalysis chemistry because of easiness in handling, reusability and recyclability. Girard and coworkers were the first to report the heterogeneous version of copper catalyzed azide-alkyne cycloaddition.<sup>77</sup> They used CuI immobilized on Amberlyst A-21 with dimethyl-aminomethyl functionality which can act as both chelating agent as well as base. To date there were enormous heterogeneous copper catalysts reported for the click reaction including those supported over biomaterials, dendrimers, mesoporous silica, magnetite etc.

Here, the catalytic activity of prepared CuPVPNNMBA was investigated in CuAAC using alkyl/ aryl halides, alkynes and sodium azide. Optimization of reaction conditions like temperature, catalyst loading, and solvent were studied by carrying out the reaction between benzyl chloride, sodium azide and phenyl acetylene (Scheme 13). Table 2 shown below represents the solvent, catalyst amount and temperature optimization studies.

**Table 2.** Optimization of the reaction conditions for the reaction of benzyl chloride, sodium azide and phenyl acetylene



**Scheme 13**

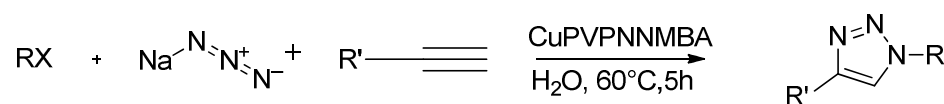
Entry	Catalyst loading	Solvent	Temperature	Yield %
1	10mg	<sup>t</sup> BuOH	rt	70
2	10mg	Ethanol	rt	65
3	10mg	THF	rt	84
4	10mg	THF/H <sub>2</sub> O	rt	92
5	10mg	H <sub>2</sub> O	rt	92



<b>6</b>	10mg	H <sub>2</sub> O	60°C	97
<b>7</b>	20mg	H <sub>2</sub> O	60°C	98
<b>8</b>	5mg	H <sub>2</sub> O	60°C	88
<b>9</b>	No catalyst	H <sub>2</sub> O	60°C	Nil
<b>10</b>	10mg	CH <sub>3</sub> CN	rt	78
<b>11</b>	10mg	DCM	rt	75
<b>12</b>	10mg	DMF	rt	60

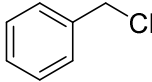
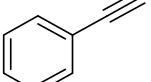
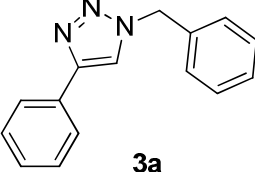
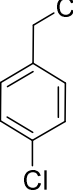
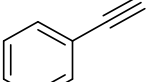
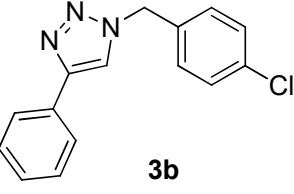
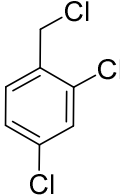
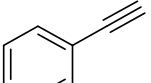
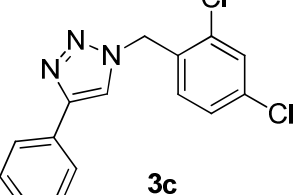
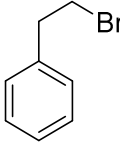
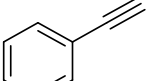
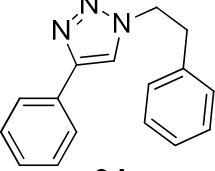
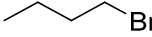
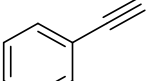
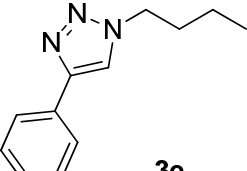
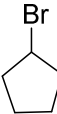
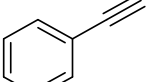
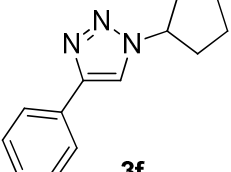
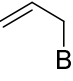
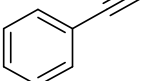
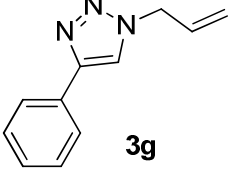
Reagents used: benzyl chloride(1 mmol), NaN<sub>3</sub> (1.5 mmol), phenyl acetylene (1.5 mmol) and solvent (5 ml)

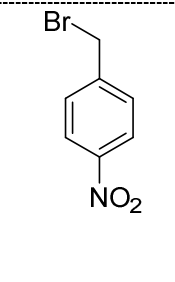
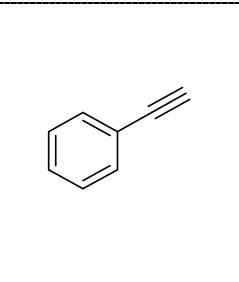
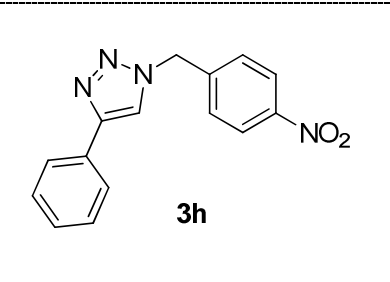
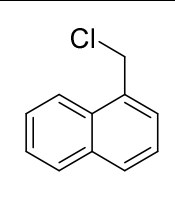
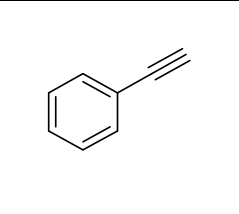
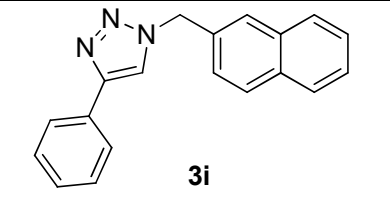
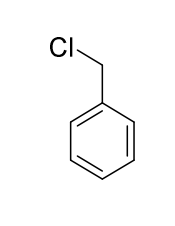
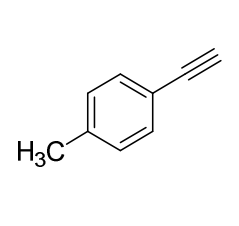
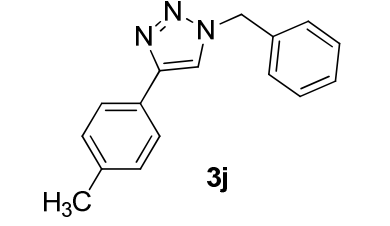
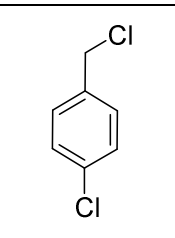
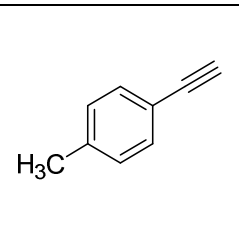
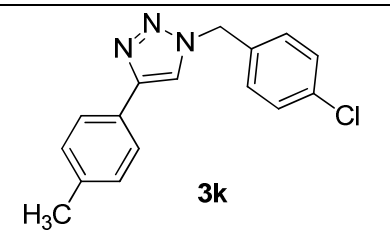
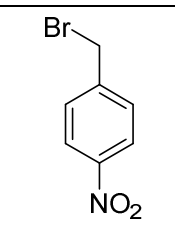
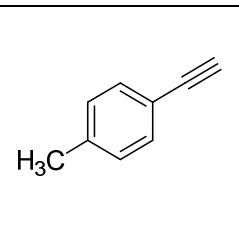
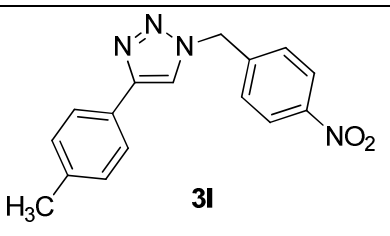
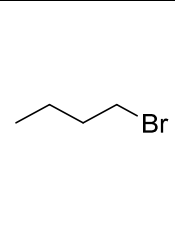
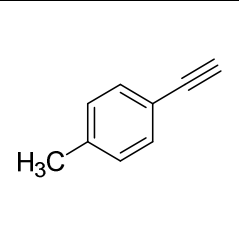
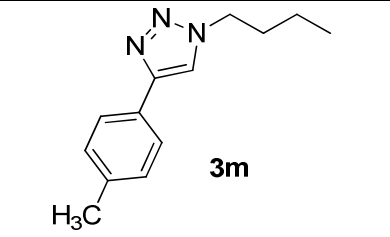
To explore the effect of catalyst amount on the conversion yield, the catalyst loading was increased from 5 to 20 mg. At room temperature, using 10mg of the catalyst in different solvents such as DMF, acetonitrile, DCM, THF, ethanol, *t*-butanol afforded low yield of the product compared to water. By increasing the reaction temperature to 60 °C in water provides better yield. Thus, an optimum condition of 10 mg of catalyst loading in water as solvent at 60 °C, the triazole was obtained in 97% yield (**Table 2, entry 6**). Increasing the amount of catalyst to 20 mg doesn't make any significant improvement while decreasing the catalyst amount to 5 mg reduced the yield of products (**Table 2, entry 7& 8**). In the absence of catalyst there was no sign of formation of the product 1-benzyl-4-phenyl-1H-1,2,3-triazole. Having the optimized reaction conditions in hand, the scope of this catalyst in triazole synthesis was studied using different alkyl/aryl halides with sodium azide and phenyl/*p*-tolylacetylene in water at 60 °C (**Table 3**). The product was extracted using ethyl acetate, dried using Na<sub>2</sub>SO<sub>4</sub>. Solvent was removed under vacuum and the product was further purified by simple recrystallization from ethanol.



**Scheme 14**

**Table 3.** Synthesis of 1,4-disubstituted 1,2,3-triazoles with different halides and alkynes\*

Sl No.	RX	R'	Product	Yield(%)
1			 <b>3a</b>	97
2			 <b>3b</b>	94
3			 <b>3c</b>	92
4			 <b>3d</b>	97
5			 <b>3e</b>	88
6			 <b>3f</b>	82
7			 <b>3g</b>	92

8			 <b>3h</b>	96
9			 <b>3i</b>	90
10			 <b>3j</b>	93
11			 <b>3k</b>	95
12			 <b>3l</b>	93
13			 <b>3m</b>	88

Reagents and conditions: organic halide(1 mmol),  $\text{NaN}_3$  (1.5 mmol), alkyne (1.5 mmol) and CuPVPNNMBA (10 mg) in water (5 ml) temperature  $60^\circ\text{C}$ , time 5h

In 2010, Hein and Fokin reported the generation of organic azide by an *in situ*  $\text{S}_\text{N}^2$  reaction between organic halide and sodium azide which was immediately used in the cycloaddition reaction with copper acetylide to yield triazole.<sup>78</sup> Presence of substituents in both organic azide and alkyne may influence the yield of product to

some extent. Electron withdrawing group slightly reduces the yield in which chlorine displays more compared to nitro group (**Table 3, entry 2,3 & 8**). Alkyl azides are less reactive compared to aryl azides (**Table 3, entry 5 & 6**). Similarly, substituent on alkyne can also affects the yield of the reaction. Electron donating methyl group in *p*-tolylacetylene diminishes the yield compared to phenylacetylene (**Table 3, entry 10, 11 & 12**).

Recent reports have demonstrated the catalytic activity of mixed valence dinuclear copper catalyst in azide alkyne cycloaddition reaction.<sup>79,80</sup> During the catalytic process Cu(I) is oxidized to Cu(II) which in turn is reduced to Cu(I) by the PVP backbone and the catalytic cycle goes on.

The benefit of heterogeneous catalyst over homogeneous is the recyclability of the catalyst. This was examined using phenyl acetylene, benzyl chloride and sodium azide as model reactants under the same reaction conditions discussed above. After the 1<sup>st</sup> run the catalyst in the aqueous layer recovered by simple filtration and washed with ethanol and acetone and then dried in vacuum oven at 70 °C for 3 h before reuse. The residual catalyst was reused for five times (**Table 4**) and found no significant dampening in catalytic activity (**Fig. 8**).

**Table 4.** Reusability of CuPVPNNMBA

Cycle	Yield (%)
Native	97
1	95
2	94
3	93
4	91
5	91

Reaction conditions: benzyl chloride(1 mmol), NaN<sub>3</sub> (1.5 mmol), phenyl acetylene (1.5 mmol) and CuPVPNNMBA (10 mg) in water (5 ml) at 60 °C for 5h

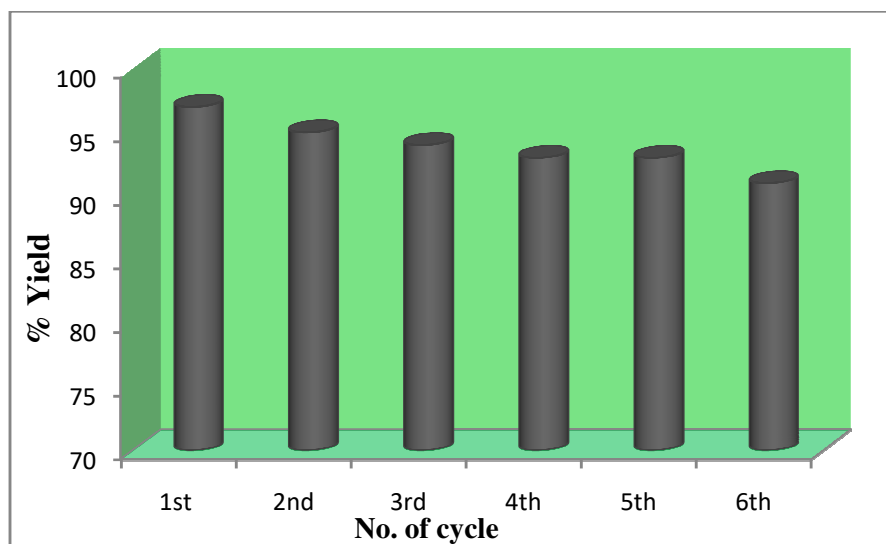


**Fig. 8** Reusability of the catalyst

To get more insight into the reused catalyst it was subjected to SEM and EDX characterization after 5<sup>th</sup> run. SEM image of the reused catalyst showed only slight change in morphology and composition relative to the original catalyst. (**Fig 9**)

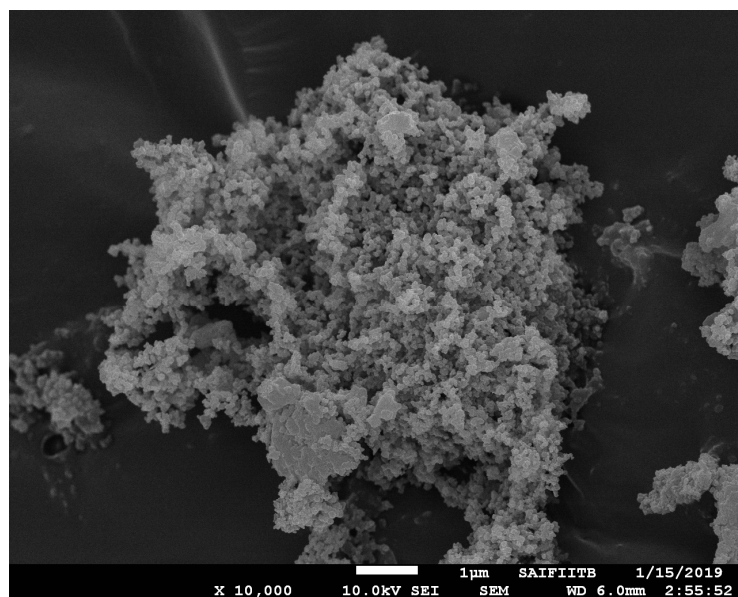


**Fig. 9** I SEM image of CuPVPNNMBA

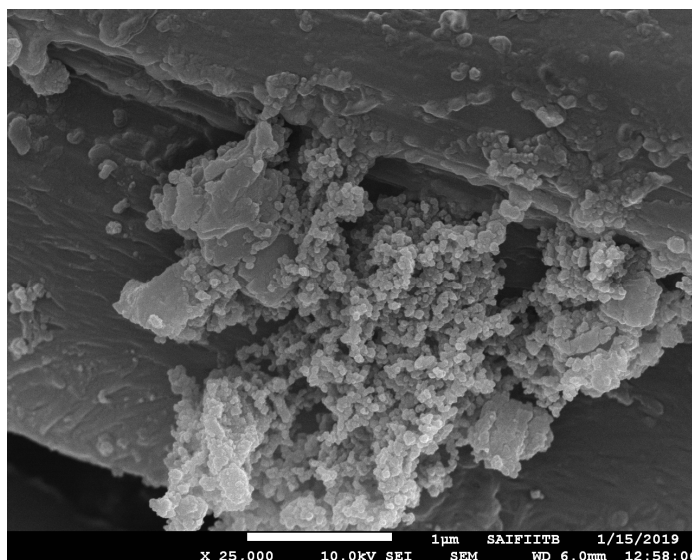


**Fig 9** II SEM image of reused catalyst

Copper in the original catalyst was found to be 1.23 wt% (**Fig 4**) while that in the reused one was found to be 1.22 wt% (**Fig 10**). This implies that there is any significant loss in the copper content after reuse.

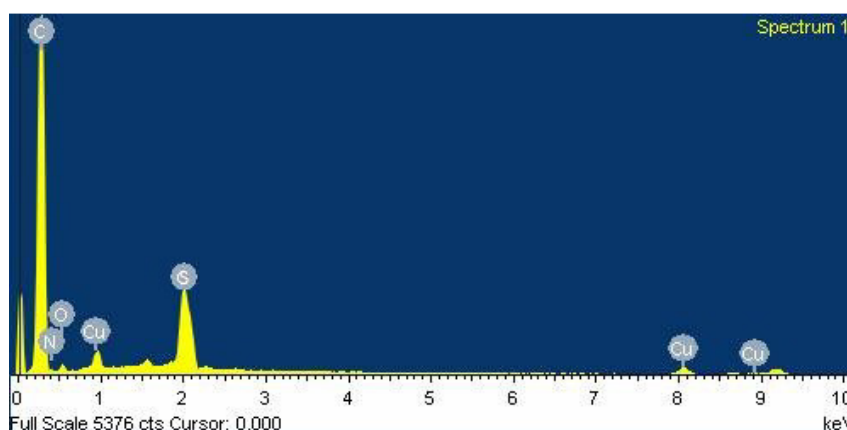
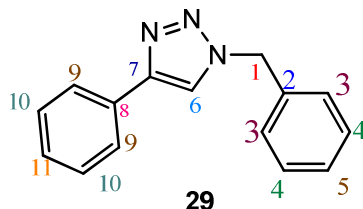


**Fig. 10** EDS spectrum of reused catalyst

The scaling up of the reaction was carried out by increasing the amount of reactants by ten-fold keeping the same reaction conditions like temperature, solvent and catalyst loading. Using 10 mg of catalyst the 97% yield of product obtained only after 7 h whereas by increasing the catalyst loading to 20 mg can reduce the reaction time to 5 h to get same yield of the product.

### 3.6 Characterization of 1,4-disubstituted 1,2,3-triazoles

**1-Benzyl-4-phenyl-1H-1,2,3-triazole (29)** was taken as a representative molecule for the general discussion.



The FT-IR spectrum of the triazole gives major absorptions at 1467, 1217, 806  $\text{cm}^{-1}$  corresponds to  $-\text{CH}_2$ ,  $\text{N}=\text{N}=\text{N}$ - and  $=\text{C}-\text{H}$  of the triazole ring (**Fig 11**).

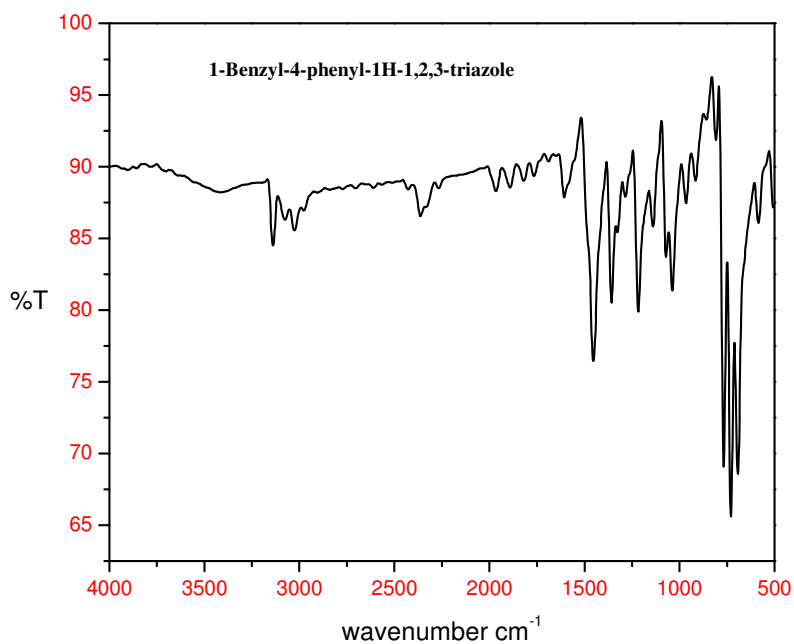


**Fig11** FT-IR spectrum of 1-benzyl-4-phenyl-1H-1,2,3-triazole

The structure of triazole was confirmed by  $^1\text{H}$  NMR spectrum (**Fig. 12**). The  $-\text{CH}_2$  proton of benzyl is observed as two proton singlet at  $\delta$  5.57. Protons at positions C3 and C5 provide multiplet at  $\delta$  7.25-7.32. The characteristic  $=\text{C}-\text{H}$  proton provides peak at  $\delta$  7.66. C4, C10 & C11 gives peak at  $\delta$  7.36-7.41 and C9 protons gives doublet at  $\delta$  7.79.

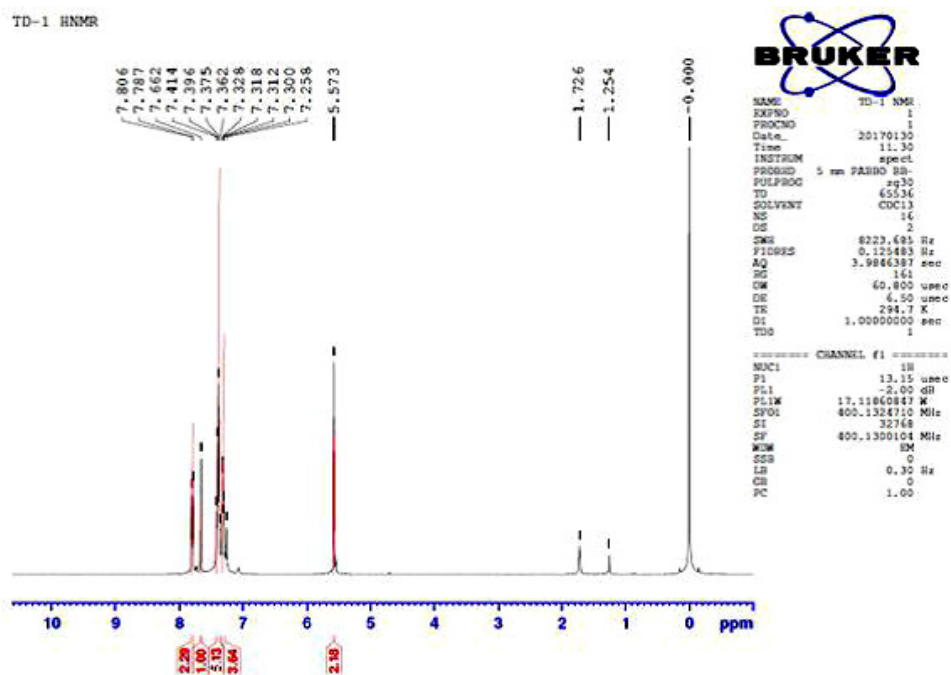
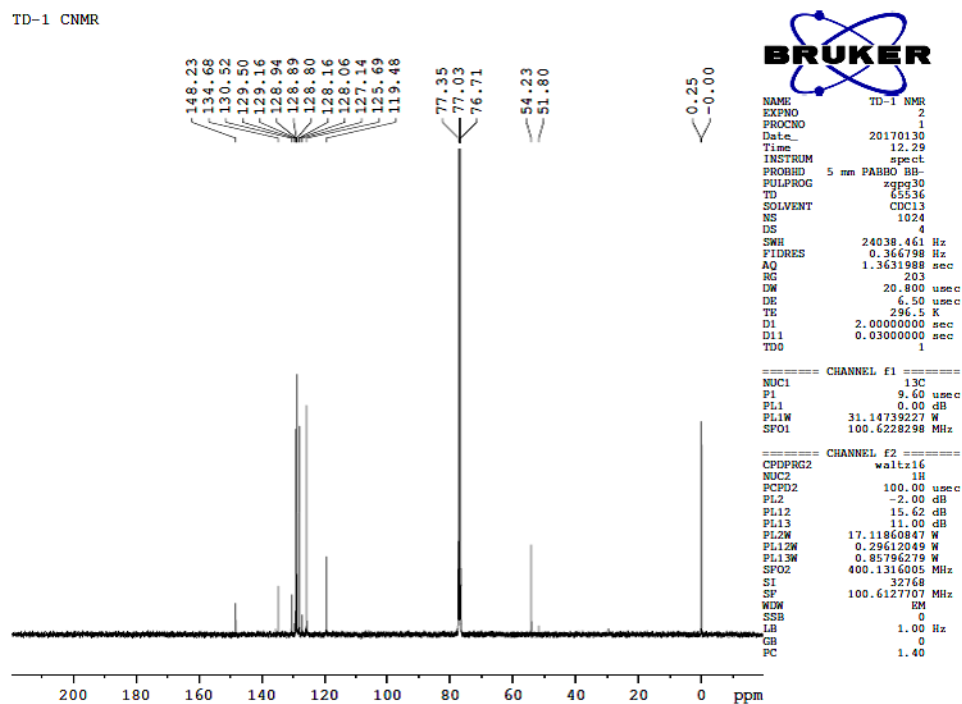


Fig 12  $^1\text{H}$  NMR spectrum of 1-benzyl-4-phenyl-1H-1,2,3-triazole

The  $^{13}\text{C}$  NMR spectrum (Fig. 13) spectrum is in agreement with both  $^1\text{H}$  NMR and FT-IR data. The downfield peak at  $\delta$  148.2 is due to the carbon at the position C7. The characteristic peak of triazole carbon (C6) that is directly bonded to hydrogen was observed at  $\delta$ 119.4 confirming the formation 1,4-disubstituted triazoles.<sup>81</sup> The benzylic carbon C1 gives peak at  $\delta$ 54.2 and the values at 134.6, 127.1, 128.1, and 128.9 attributed to the benzyl carbons C2, C3, C4 and C5 carbons. The signal at 130.5 corresponds to the phenyl carbon C8 that is connected to the triazole ring. Other peaks at 125.6, 129.1 and 129.5 belong to ortho, meta and para carbons of phenyl ring.





**Fig 13**  $^{13}\text{C}$  NMR spectrum of 1-benzyl-4-phenyl-1H-1,2,3-triazole

The structure of the compound was further confirmed by mass spectral analysis. In the mass spectrum, the molecular ion peak ( $M^+$ ) was observed at  $m/z$  235.08 (**Fig. 14**). The signal at  $m/z$  corresponds to  $M-N_2$  and the base peak at  $m/z$  116 & 91 belongs to  $M-C_8H_7N_2$  and  $M-C_8H_6N_3$  respectively.

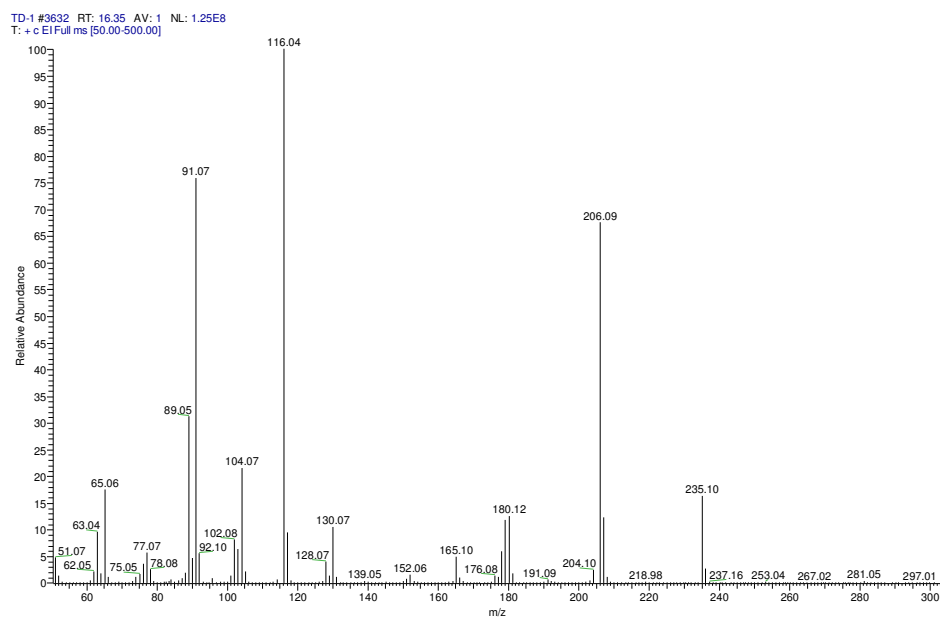
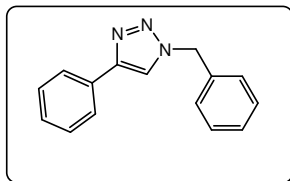


**Fig. 14** Mass spectrum of 1-benzyl-4-phenyl-1H-1,2,3-triazole

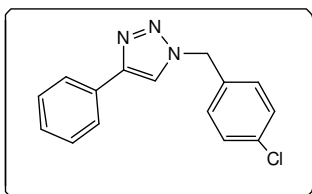
### 3.7 Spectral data of the triazoles synthesized

#### 1. 1-benzyl-4-phenyl-1*H*-1,2,3-triazole (3a)



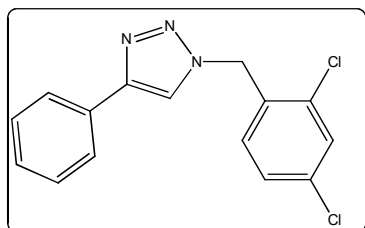
$^1\text{H}$  NMR (400 MHz,  $\text{CDCl}_3$ ):  $\delta$  5.57(s,2H), 7.30-7.32 (m, 4H), 7.36-7.41 (m, 3H), 7.66(s, 1H), 7.79 (d, 2H,  $J=7.6\text{Hz}$ ).  $^{13}\text{C}$  NMR (100.6 MHz,  $\text{CDCl}_3$ ):  $\delta$  54.2, 119.4, 125.6, 127.1, 128.1, 128.9, 129.1, 129.5, 130.5, 134.6, 148.2. Mass  $m/z$  (%): 235 ( $\text{M}^+$ , 20), 116 (100), 91 (75), 206 (70). FTIR (KBr): 3139, 3024, 2362, 1606, 1452, 1216, 1037, 767, 727, 691, 584  $\text{cm}^{-1}$

#### 2. 1-(4-chlorobenzyl)-4-phenyl-1*H*-1,2,3-triazole (3b)



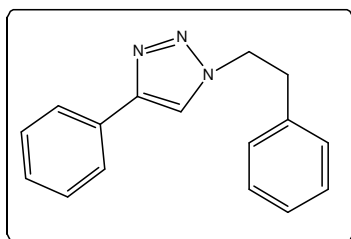
$^1\text{H}$  NMR (400 MHz,  $\text{CDCl}_3$ ):  $\delta$  5.53(s,2H), 7.23(d,3H,  $J=7.2\text{Hz}$ ), 7.41-7.34(m,6H), 7.88(s,1H).  $^{13}\text{C}$  NMR (100.6 MHz,  $\text{CDCl}_3$ ):  $\delta$  53.4, 119.4, 125.7, 128.2, 128.8, 129.3, 130.3, 132, 133.2, 134.8, 148.4. Mass  $m/z$  (%): 269 ( $\text{M}^+$ , 10), 271 ( $\text{M}^{++2}$ , 4), 116 (100), 125(44). FTIR (KBr): 3107, 3082, 3064, 3034, 2933, 1492, 1462, 1411, 1350, 1220, 1143, 1091, 1080, 1016, 975, 819, 804, 763, 688, 495  $\text{cm}^{-1}$

#### 3. 1-(2,4-dichlorobenzyl)-4-phenyl-1*H*-1,2,3-triazole (3c)



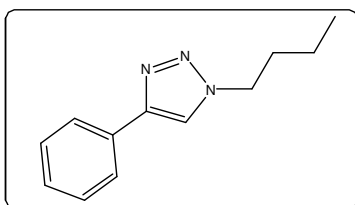
$^1\text{H}$  NMR (400MHz,  $\text{CDCl}_3$ )  $\delta$ : 5.67 (s 2H), 7.16 (s, 1H), 7.25–7.46 (m, 4H), 7.88 (s, 3H).  $^{13}\text{C}$  NMR (100.6MHz,  $\text{CDCl}_3$ )  $\delta$ : 50.8, 119.8, 125.7, 127.9, 128.2, 128.8, 129.7, 130.3, 131, 131.3, 134.1, 135.5, 148.2; Mass  $m/z$  (%): 303 ( $\text{M}^+$ , 5), 305 ( $\text{M}^{++2}$ , 3), 240, 158, 116 (100).

## 4. 4-phenyl-1-(2-phenylethyl)-1H-1,2,3-triazole (3d)



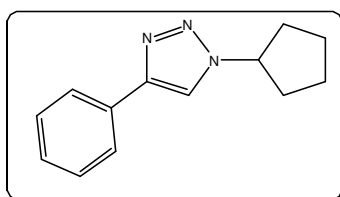
$^1\text{H}$  NMR (400 MHz,  $\text{CDCl}_3$ ):  $\delta$  3.24 (t, 2H,  $J = 7.2\text{Hz}$ ), 4.62 (t, 2H,  $J = 7.6\text{Hz}$ ), 7.13 (d, 1H,  $J=6.8$ ), 7.25–7.30 (m, 3H), 7.39 (t, 2H,  $J = 7.2\text{Hz}$ ), 7.48 (s, 1H), 7.76 (d, 2H,  $J = 6.8\text{Hz}$ ).  $^{13}\text{C}$  NMR (100.6 MHz,  $\text{CDCl}_3$ )  $\delta$ : 51.7, 36.8, 119.8, 120.0, 125.7, 127.1, 128.1, 128.7, 128.8, 130.7, 137.1, 147.5. Mass  $m/z$  (%): 249 ( $\text{M}^+$ , 35), 220 (18), 193 (13), 179 (8), 130 (34), 118 (71), 105 (100), 77 (42), 51 (8). FTIR (KBr): 3107, 3028, 1683, 1483, 1450, 1365, 1220, 1080, 1043, 94, 910, 844, 734, 690  $\text{cm}^{-1}$

## 5. 1-Butyl-4-phenyl-1H-1,2,3-triazole (3e)



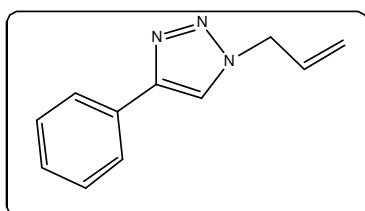
$^1\text{H}$  NMR (400 MHz,  $\text{CDCl}_3$ ):  $\delta$  0.96 (t, 3H,  $J = 7.2\text{Hz}$ ), 1.36–1.41 (m, 2H), 1.90–1.94 (m, 2H), 4.39 (t, 2H,  $J = 7.2\text{Hz}$ ), 7.33 (d, 1H,  $J=7.2\text{Hz}$ ), 7.41 (t, 2H,  $J=7.2\text{Hz}$ ), 7.74 (s, 1H), 7.83 (d, 2H,  $J=7.2\text{Hz}$ ).  $^{13}\text{C}$  NMR (100.6 MHz,  $\text{CDCl}_3$ ):  $\delta$  13.4, 19.7, 32.3, 50.1, 119.4, 125.6, 128.0, 128.8, 130.7, 147.8. Mass  $m/z$  (%): 201 ( $\text{M}^+$ , 33), 145 (16), 117 (100), 90 (24). FTIR (KBr): 3062, 2947, 2870, 1460, 1367, 1215, 1066, 761, 692  $\text{cm}^{-1}$

## 6. 1-Cyclopentyl-4-phenyl-1H-1,2,3-triazole (3f)



$^1\text{H}$  NMR (400 MHz,  $\text{CDCl}_3$ ):  $\delta$  1.76–1.8 (m, 2H), 1.91–1.95 (m, 2H), 2.05–2.12 (m, 2H), 2.26–2.31 (m, 2H), 4.94–5.01 (m, 1H), 7.31 (t, 1H,  $J = 7.2\text{Hz}$ ), 7.39 (m, 2H), 7.82 (s, 1H), 7.83 (dd, 2H,  $J=7.7, 1.55$ ).  $^{13}\text{C}$  NMR (100.6 MHz,  $\text{CDCl}_3$ ):  $\delta$  24.1, 33.4, 61.8, 118.0, 125.6, 128.0, 128.7, 130.8, 147.5. Mass  $m/z$  (%): 213 ( $\text{M}^+$  33), 184, 156, 117 (100).

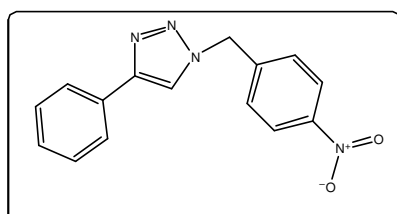
## 7. 1-Allyl-4-phenyl-1H-1,2,3-triazole (3g)



$^1\text{H}$  NMR (400 MHz,  $\text{CDCl}_3$ ):  $\delta$  5.02 (dd, 1H,  $J = 16.4\text{Hz}$ ), 5.36 (dd, 1H,  $J= 10\text{Hz}$ ), 6.01–6.11 (m, 1H),

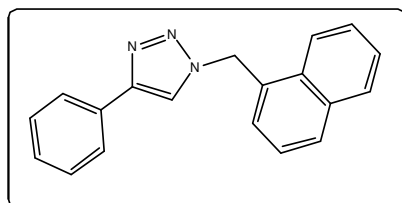
7.31–7.44 (m, 3H), 7.76 (s, 1H), 7.83(d, 2H,  $J = 7.6\text{Hz}$ ).  $^{13}\text{C}$  NMR(100.6MHz,  $\text{CDCl}_3$ ):  $\delta$  52.7, 119.4, 120.2, 125.7, 128.1, 128.8, 130.5, 131.3, 148.0. Mass  $m/z(\%)$ : 185( $\text{M}^+$ , 19), 116(100). FTIR (KBr): 3120, 3088, 2934, 2854, 1645, 1608, 1460, 1334, 1219, 1166, 1049. 985, 914, 825, 765, 690, 509  $\text{cm}^{-1}$

#### 8. 1-(4-Nitrobenzyl)-4-phenyl-1H-1,2,3-triazole (3h)



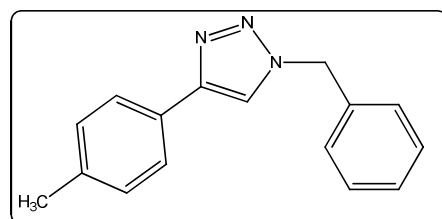
$^1\text{H}$ NMR (400 MHz,  $\text{CDCl}_3$ ):  $\delta$  5.69 (s, 2H), 7.34–7.45(m,5H), 7.76(s, 1H), 7.80(d, 2H,  $J = 7.6\text{Hz}$ ), 8.22(d, 2H,  $J = 8\text{Hz}$ ).  $^{13}\text{C}$  NMR (100.6MHz, $\text{CDCl}_3$ ):  $\delta$  53.1, 119.7, 124.3, 125.7, 128.5, 129.2,129.9, 130.0, 141.7, 148.07,148.7. Mass, $m/z$  (%): 281 ( $\text{M}^+$ , 19), 207 (44), 116 (100), 106 (24), 89 (43). FTIR (KBr): 3118, 3080, 2939, 2857, 1600, 1517, 1429, 1346, 1209, 1107, 1074, 1305, 844, 815, 761, 729, 686  $\text{cm}^{-1}$

#### 9. 1-(Naphthyl)-4-phenyl-1H-1,2,3-triazole (3i)



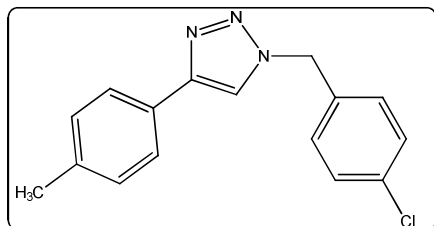
$^1\text{H}$ NMR (400 MHz,  $\text{CDCl}_3$ ):  $\delta$  5.91(s, 2H), 7.37–7.44 (m, 5H), 7.65 (m, 2H),7.81 (m, 2H), 7.90 (m, 3H) 7.91 (s, 1H).  $^{13}\text{C}$  NMR (100.6MHz,  $\text{CDCl}_3$ ):  $\delta$  52.5,119.7, 122.9, 125.4, 125.7, 126.4, 126.7, 127.9, 128.2, 129.2, 129.7, 130.1, 130.2, 131.2,131.94, 133.96. Mass  $m/z$  (%): 284 ( $\text{M}^+$ , 5), 253 (10), 207 (98), 115 (90), 84(100). FTIR (KBr); 3115, 2924, 2848, 1454, 1431, 1344, 1307, 1211, 114, 1080, 1037, 974, 912, 842, 771, 688  $\text{cm}^{-1}$

#### 10. 1-(Benzyl)-4(p-tolyl)-1H-1,2,3-triazole (3j)



$^1\text{H}$ NMR (400 MHz,  $\text{CDCl}_3$ ):  $\delta$  2.38 (s, 3H), 5.58 (s, 2H), 7.22 (d, 2H,  $J = 7.6\text{Hz}$ ), 7.32–7.41(m, 5H), 7.66 (1H, s), 7.71 (d, 2H,  $J = 8.4\text{Hz}$ ).  $^{13}\text{C}$  NMR (100.6MHz,  $\text{CDCl}_3$ ):  $\delta$  148.14, 138.18, 134.62,129.52, 129.17, 128.82, 128.1, 127.41, 125.68, 54.33, 21.33. Mass  $m/z$  (%): 249( $\text{M}^+$ , 15),220(63), 130(100), 91(72), 77(18) FTIR (KBr): 3138, 3008, 2902, 1446, 1342, 1213, 1122, 1045, 968, 788, 713, 584, 512  $\text{cm}^{-1}$

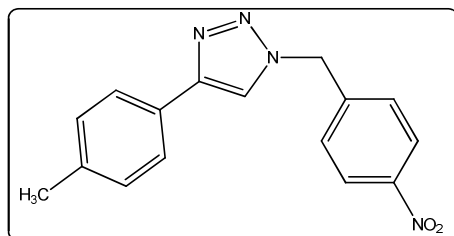
## 11. 1-(4-Chlorobenzyl)-4-(p-tolyl)-1H-1,2,3-triazole (3k)



$^1\text{H}$ NMR (400 MHz,  $\text{CDCl}_3$ ):  $\delta$  2.38 (s, 3H), 5.55 (s, 2H), 7.22-7.28(m,3H) 7.37(d,2H,  $J= 8.4\text{Hz}$ ), 7.67 (s, 1H), 7.71 (d, 2H,  $J=8\text{Hz}$ ) $^{13}\text{C}$  NMR (100.6MHz,

$\text{CDCl}_3$ ):  $\delta$  21.3, 53.5, 125.68, 127.2,129.3, 129.4, 129.5, 133.1, 134.8, 138.3, 148.3. Mass  $m/z$  (%): 283 ( $\text{M}^+$ , 12), 254 (35), 130(100). FTIR (KBr): 3113, 3012, 2953,1485, 1436, 1334, 1207, 1080, 1033, 808, 750, 507  $\text{cm}^{-1}$

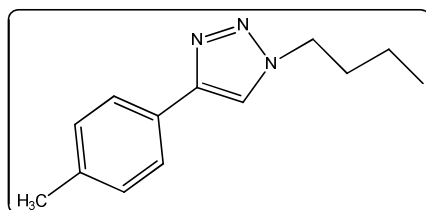
## 12. 1-(4-Nitrobenzyl)-4-(p-tolyl)-1H-1,2,3-triazole (3l)



$^1\text{H}$ NMR (400 MHz,  $\text{CDCl}_3$ ):  $\delta$  2.39 (s, 3H), 5.71 (s, 2H), 7.24 (d, 2H,  $J = 7.6\text{Hz}$ ), 7.46 (d,2H,  $J = 8.4\text{Hz}$ ), 7.72 (d, 2H,  $J = 8\text{Hz}$ ), 7.77 (s, 1H) 8.24 (d, 2H,  $J$

$= 8.4\text{Hz}$ ).  $^{13}\text{C}$  NMR(100.6MHz,  $\text{CDCl}_3$ ):  $\delta$  21.3, 53.2, 124.3, 125.74, 126.9, 128.6, 129.64, 138.6, 141.6, 148.1. Mass  $m/z$  (%): 294( $\text{M}^+$  9), 281 (25), 207 (70), 130 (100). FTIR (KBr): 3088, 3034. 2924, 2856, 1602, 1516, 1444, 1344, 1213, 1101, 1039, 972, 810, 723, 513  $\text{cm}^{-1}$

## 13. 1-Butyl-4-(p-tolyl)-1H-1,2,3-triazole (3m)



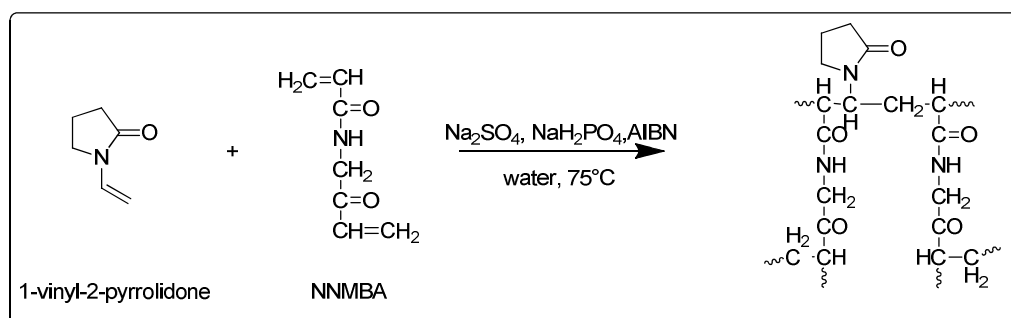
$^1\text{H}$ NMR (400 MHz,  $\text{CDCl}_3$ ):  $\delta$  0.89 (t, 3H,  $J= 7.2\text{Hz}$ ), 1.29-1.34 (m, 2H), 1.87 (m,2H), 2.30 (t, 3H,  $J=6.4\text{Hz}$ ), 4.34

(s,3H),7.06-7.18(m, 3H), 7.33 (m,2H), 7.73(s,1H). $^{13}\text{C}$  NMR (100.6MHz,  $\text{CDCl}_3$ ):  $\delta$  13.4, 19.7,21.3, 32.2, 50.62, 118.7, 125.6, 127.5, 129.2, 132.3, 138.2. Mass  $m/z$  (%): 215 ( $\text{M}^+$ , 40), 159(30), 144 (35), 131(100).

### 3.8 Experimental details

#### 3.8.1 Synthesis of 4mol% NNMBA crosslinked polyvinylpyrrolidone (PVPNNMBA)

A solution of  $\text{NaH}_2\text{PO}_4$  (0.43 g) and  $\text{Na}_2\text{SO}_4$  (20 g) in 120 ml water was heated to 70 °C with stirring for 15 min. Nitrogen gas was purged through the solution for 10 min followed by the addition of monomer pyrrolidone (5.4 g), NNMBA (0.752 g) and initiator AIBN(100 mg). Heating and stirring was continued for 5 h at 75 °C (**Scheme 15**). The reaction mixture was then cooled to room temperature and the product was filtered, washed with water and acetone dried in vacuum oven at 60 °C to afford the polymer beads. They were further purified by soxhlet extraction using acetone: methanol (1:1) mixture and sieved to 120-200 mesh size.



**Scheme 15** Synthesis of NNMBA crosslinked polyvinyl pyrrolidone

#### 3.8.2 Incorporation of copper into the polymer matrix

The cross linked polymer(1 g) was kept for swelling in glacial acetic acid (20 ml) for 5 h. Copper sulphate pentahydrate (1 g) dissolved in glacial acetic acid (15 ml) was added to the above mixture and heated at 80 °C for 1 h followed by refluxing for 4 h. The reaction mixture was cooled to room temperature and filtered, washed with water, ethanol and dried in vacuum oven at 60 °C.

### **3.8.3 General procedure for Azide-Alkyne Cycloaddition**

For the copper catalyzed azide alkyne cycloaddition reaction, organic halide(1 mmol), alkyne (1.5 mmol) and sodium azide (1.5 mmol) were taken in a 50 ml round bottom flask. To this water (5 ml) and the catalyst CuPVPNNMBA (10 mg) were added. The resulting reaction mixture was heated at 60 °C for 5 h and then cooled to room temperature. The product was extracted with ethyl acetate, dried and the solvent was removed under vacuum. Recrystallization from ethanol to afford 1,4-disubstituted 1,2,3-triazoles in excellent yields. These triazoles were characterized using <sup>1</sup>H NMR, <sup>13</sup>C NMR and GCMS analysis.

### **3.9 Conclusion**

We have synthesized NNMBA cross linked polyvinyl pyrrolidone by suspension polymerization of monomers *N*-vinyl pyrrolidone and NNMBA. The copolymer was then loaded with copper by treating with copper sulphate. Both the copolymer and its copper supported material have been fully characterized. From analysis, we observed that the polymer matrix contain both Cu(I) and Cu(II) in 1:2 ratio. The copper ions are *in situ* reduced by the PVP back bone which in turn is stabilized on the polymer matrix. The copper supported polymer material was found to be a good catalyst for one pot, multicomponent strategy towards the click reaction between azide, alkyne and halides to afford 1,4-disubstituted 1,2,3-triazoles in a regioselective manner and in excellent yields. The robustness of the catalyst includes (a) high catalytic activity, (b) cheapness, (c) easily recoverable and recyclability, (d) low catalyst loading and (e) resistance to oxidation on air and water.



## References

- (1) Rostovtsev, V. V.; Green, L. G.; Fokin, V. V.; Sharpless, K. B. “ A Stepwise Huisgen Cycloaddition Process Catalyzed by Copper ( I ): Regioselective Ligation of Azides and Terminal Alkynes .” *Angew. Chem. Int. Ed.* **2002**, *41*, 2596–2599.
- (2) Tornøe, C. W.; Christensen, C.; Meldal, M. Peptidotriazoles on Solid Phase : [1,2,3]-Triazoles by Regiospecific Copper ( I ) -Catalyzed 1,3-Dipolar Cycloadditions of Terminal Alkynes to Azides. *J. Org. Chem.* **2002**, *67*, 3057–3064.
- (3) Hudson, R.; Li, C. J.; Moores, A. Magnetic Copper-Iron Nanoparticles as Simple Heterogeneous Catalysts for the Azide-Alkyne Click Reaction in Water. *Green Chem.* **2012**, *14* (3), 622–624.
- (4) Hudson, R.; Rivière, A.; Cirtiu, C. M.; Luska, K. L.; Moores, A. Iron-Iron Oxide Core-Shell Nanoparticles Are Active and Magnetically Recyclable Olefin and Alkyne Hydrogenation Catalysts in Protic and Aqueous Media. *Chem. Commun.* **2012**, *48*, 3360–3362.
- (5) Xiong, X.; Cai, L. Application of Magnetic Nanoparticle-Supported CuBr: A Highly Efficient and Reusable Catalyst for the One-Pot and Scale-up Synthesis of 1,2,3-Triazoles under Microwave-Assisted Conditions. *Catal. Sci. Technol.* **2013**, *3*, 1301–1307.
- (6) Gholinejad, M.; Jeedi, N. Copper Nanoparticles Supported on Agarose as a Bioorganic and Degradable Polymer for Multicomponent Click Synthesis of 1,2,3-Triazoles under Low Copper Loading in Water. *ACS Sustain. Chem. Eng.* **2014**, *2*, 2658–2665.
- (7) Huang, L.; Liu, W.; Wu, J.; Fu, Y.; Wang, K.; Huo, C.; Du, Z. Nano-Copper Catalyzed Three-Component Reaction to Construct. *Tetrahedron Lett.* **2014**, *55*, 2312–2316.
- (8) Gang, F.; Dong, T.; Xu, G.; Fu, Y.; Du, Z. Nano Copper Catalyzed Three-Component Tandem Cycloaddition and N-Alkylation Reaction from Aminophenylacetylenes, Sodium Azide and Alkyl Halides. *Heterocycles* **2015**, *91*, 1964–1971.
- (9) Roy, S.; Chatterjee, T.; Islam, S. M. Polymer Anchored Cu(II) Complex: An Efficient and Recyclable Catalytic System for the One-Pot Synthesis of 1,4-

- Disubstituted 1,2,3-Triazoles Starting from Anilines in Water. *Green Chem.* **2013**, *15*, 2532–2539.
- (10) Chanda, A.; Fokin, V. V. Organic Synthesis “ On Water .” *Chem. Rev.* **2009**, *109*, 725–748.
- (11) Butler, R. N.; Coyne, A. G. Water : Nature ’ s Reaction Enforcer s Comparative Effects for Organic Synthesis “ In-Water ” and “ On-Water .” *Chem. Rev.* **2010**, *110*, 6302–6337.
- (12) Thirumurugan, P.; Matosiuk, D.; Jozwiak, K. Click Chemistry for Drug Development and Diverse Chemical – Biology Applications. *Chem. Rev.* **2013**, *13*, 4905–4979.
- (13) Meldal, M. P.; Meldal, M.; Tornøe, C. W. Cu-Catalyzed Azide – Alkyne Cycloaddition Cu-Catalyzed Azide - Alkyne Cycloaddition. *Chem. Rev.* **2017**, *108*, 2952–3015.
- (14) Yan, Z.; Zhao, Y.; Fan, M.; Liu, W.; Liang, Y. General Synthesis of ( 1-Substituted-1 H -1 , 2 , 3-Triazol-4- Ylmethyl ) -Dialkylamines via a Copper ( I ) -Catalyzed Three-Component Reaction in Water. *Tetrahedron* **2005**, *61*, 9331–9337.
- (15) Candelon, N.; Lastécouères, D.; Khadri, A.; Aranzaes, J. R.; Astruc, D. A Highly Active and Reusable Copper ( I ) -Tren Catalyst for the “ Click ” 1 , 3-Dipolar Cycloaddition of Azides and Alkynes. *Chem. Commun.* **2008**, *6*, 741–743.
- (16) Golas, P. L.; Tsarevsky, N. V; Sumerlin, B. S.; Matyjaszewski, K.; Pennsylv, V.; July, R. V. Catalyst Performance in “ Click ” Coupling Reactions of Polymers Prepared by ATRP : Ligand and Metal Effects. *Macromolecules* **2006**, *39*, 6451–6457.
- (17) Koczur, K. M.; Mourdikoudis, S.; Polavarapu, L.; Skrabalak, S. E. Polyvinylpyrrolidone (PVP) in Nanoparticle Synthesis. *Dalt. Trans.* **2015**, *44*, 17883–17905.
- (18) Deivaraj, T. C.; Lala, N. L.; Yang, J. Solvent-Induced Shape Evolution of PVP Protected Spherical Silver Nanoparticles into Triangular Nanoplates and Nanorods. *J. Colloid Interface Sci.* **2005**, *289*, 402–409.
- (19) Carotenuto, G.; Nicolais, L. Synthesis and Characterization of Gold-Based Mesoscopic Additives for Polymers. *Polym. Int.* **2004**, *53*, 2009–2014.
- (20) Umar, A. A.; Oyama, M.; Salleh, M. M. Formation of High-Yield Gold

- Nanoplates on the Surface : Effective Two-Dimensional Crystal Growth of Nanoseed in the Presence of Poly ( Vinylpyrrolidone ) and Cetyltrimethylammonium Bromide & DESIGN 2009. *Cryst. growth Des.* **2009**, *9*, 2835–2840.
- (21) Sarkar, A.; Mukherjee, T.; Kapoor, S. PVP-Stabilized Copper Nanoparticles : A Reusable Catalyst for “ Click ” Reaction between Terminal Alkynes and Azides in Nonaqueous Solvents. *J. Phys. Chem.* **2008**, *112*, 3334–3340.
- (22) Rajasree, K.; Devaky, K. S. Polymer-Bound Ethylenediamine – Borane Reagent : A New Class of Polymeric Reducing Agent. *J. Appl. Polym. Sci.* **2001**, *82*, 593–600.
- (23) Rebek, J. The Mechanistic Studies of Solid Supports-The Three Phase Test. *Tetrahedron* **1978**, *35*, 723–731.
- (24) Pearson, J. M. Photoconductive Polymers. *Pure Appl. Chem.* **1977**, *49*, 463–477.
- (25) Fendler, J. H. Polymerized Surfactants Veicles: Novel Membrane Mimetic Systems. *Science.* **2008**, *223*, 888–894.
- (26) Isied, S. S.; Christa .G Kuhen; M, L. J.; Merrifield, R. B. Specific Peptide Sequences for Metal Ion Coordination. Solid-Phase Synthesis of Cyclo -(Gly-His)<sub>3</sub>. *J. Am. Chem. Soc.* **1982**, *104*, 2632–2634.
- (27) Mathur, N. K.; Narang, C. K.; Williams, R. E. Polymers as Aids in Organic Chemistry. *New York Acad. Press* **1980**.
- (28) B.A Bolto. Pure and Applied Chemistry Novel Water Treatment Processes Which Utilize Polymers. *J. Macromol. Sci. Part A - Chem.* **1980**, *14*, 107–120.
- (29) Vernon, F. Some Aspects of Ion Exchange in Copper Hydrometallurgy. *Hydrometallurgy* **1979**, *4*, 147–157.
- (30) Ramirez, R. S.; Andrade, J. D. Polymer-Drug Grafts for Iron Chelation. *J. Macromol. Sci. Part A - Chem.* **1976**, *10*, 309–365.
- (31) Geckeler, K. E. Polymer – Metal Complexes for Environmental Protection . Chemoremediation in the Aqueous Homogeneous Phase. *Pure Appl. Chem.* **2001**, *73*, 129–136.
- (32) Schmuckler, G. Chelating Resins-Their Analytical Properties and Applications. *Talanta* **1965**, *12*, 281–290.
- (33) Kurimura, Y.; Tsuchida, E.; Kaneko, M. Preparations and Properties of Some Water-Soluble Cobalt ( III ) -Poly-4-Vinylpyridine Complexes. *J. Polym. Sci.*

*Part A-1 Polym. Chem. banner* **1971**, 9, 3511–3519.

- (34) Tsuchida, E.; Nishide, H.; Takeshita, M. Steric and Electrostatic Factors on the Formation and the Structure of Polymeric Cobalt ( III ) Complexes. *Macromol. Chem. Phys.* **1973**, 175, 2293–2306.
- (35) Suzuki, T.; Shirai, H.; Tokutake, S.; Hojo, N. Kinetics of Ligand Exchange Reaction of Cu(I)-Ammine Complex with Poly(Vinyl Alcohol) in Aqueous Solution. *Polymer (Guildf)*. **1983**, 24, 335–338.
- (36) Varghese, S.; Lele, A. K.; Srinivas, D.; Mashelkar, R. A. Role of Hydrophobicity on Structure of Polymer - Metal Complexes. *J. Phys. Chem. B* **2001**, 105, 5368–5373.
- (37) Janović, Z.; Jukić, A.; Vogl, O. Spacer Groups in Macromolecular Structures Razmakne Skupine u Strukturi Makromolekula. *Polimeri* **2010**, 31, 14–21.
- (38) Percec, V.; Zuber., M. Synthesis and Determination of the Virtual Mesophases of Polyethers Based on L-(4-Hydroxyphenyl)-2-(2-Methyl-4-Hydroxyphenyl)Ethane and *a,w*-Dibromoalkanes Containing from 17 to 20 Methylene Units. *Polym. Prepr.* **1991**, 32, 259–260.
- (39) Tomoi, M.; Kori, N.; Kakiuchi, H. A Novel One-Pot Synthesis of Spacer-Modified Polymer Supports and Phase-Transfer Catalytic Activity of Phosphonium Salts Bound to the Polymer Supports. *React. Polym.* **1985**, 3, 341–349.
- (40) Tomoi, M.; Goto, M.; Kakiuchi, H. Linalool with Acetic Anhydride Using Dialkylaminopyridines Attached by Spacer Chains to Polystyrene Resins. *J. Polym. Sci. Part A-1 Polym. Chem.* **1987**, 25, 77–86.
- (41) Nose, Y.; Hatano, M.; Kambara, S. H. U. Syntheses of New Chelate-Polymers and Its Catalytic Activities. *Die Makromol. Chemie* **1966**, 98 (2179), 136–147.
- (42) Hojo, N.; Shirai, H.; Chujo, Y. Catalytic Activity of Cu ( II ) -Poly ( Vinyl Alcohol ) Complex for Decomposition of Hydrogen Peroxide. *J. Polym. Sci. Polym. Chem. Ed. banner* **1978**, 16, 447–455.
- (43) Vinodkumar, G. S.; Mathew, B. Polymer Metal Complexes of Glycine Functions Supported on N,N'-Methylenebisacrylamide (NNMBA)-Crosslinked Polyacrylamides: Synthesis, Characterisation and Catalytic Activity. *Eur. Polym. J.* **1998**, 34, 1185–1190.
- (44) Musin, R. I.; Li, V. A.; Tulyaganov, R. T.; Kalugina, G. N.; Rashidova S. Sh. Synthesis and Biological Activity of Cobalt-Containing Polyvinylpyrrolidone

- Complexes. *Pharm. Chem. J.* **1989**, *23*, 375–378.
- (45) Mathew, B.; Pillai, V. N. R. Metal Complexation of Crosslinked Polyacrylamide-Supported Dithiocarbamates: Effect of the Molecular Character and Extent of Crosslinking on Complexation. In *Proceedings of the Indian Academy of Sciences - Chemical Sciences*; 1992; pp 43–56.
- (46) Kaliyappan, T.; Swaminathan, C. S.; Kannan, P. Synthesis and Characterization of a New Metal Chelating Polymer and Derived Ni (II) and Cu (II) Polymer Complexes. *Polymer (Guildf)*. **1996**, *37*, 2865–2869.
- (47) Umegaki, T.; Yan, J.; Zhang, X.; Shioyama, H.; Kuriyama, N.; Xu, Q. Preparation and Catalysis of Poly ( N-Vinyl-2-Pyrrolidone ) ( PVP ) Stabilized Nickel Catalyst for Hydrolytic Dehydrogenation of Ammonia Borane. *Int. J. Hydrogen Energy* **2009**, *34*, 3816–3822.
- (48) George, B.; Pillai, V. N. R.; Mathew, B. Polymer-Metal Complexes of N , N ' - Crosslinked Polyacrylamide-Supported Glycines : Effect of the Degree of Crosslinking On Metal Ion Complexatlon and Concentration. *J. Macromol. Sci. Part A >Pure Appl. Chem.* **1998**, *35*, 495–510.
- (49) Rivas, B. L.; Seguel, G. V; Ancatripai, C. Polymer-Metal Complexes : Synthesis , Characterization , and Properties of Poly ( Maleic Acid ) Metal Complexes with Cu(II), Co(II), Ni(II), and Zn(II). *Polym. Bull.* **2000**, *44*, 445–452.
- (50) Nakamura, Y.; Hirai, H. Homogeneous Hydrogenation of Alkenes by the Complex of Polyacrylic Acid with Ru(II). *Chem. Lett.* **1974**, *3*, 645–650.
- (51) Kanarek, L.; Linder, P. W.; Bryan, W. P. Catalytic Reduction of Olefins with a Polymer-Supported Rhodium(1) Catalyst. *J. Am. Chem. Soc.* **1971**, *93*, 3062–3063.
- (52) Card, R. J.; Douglas C. Neckers. Poly(Styryl)Bipyridine: Synthesis and Formation of Transition-Metal Complexes and Some of Their Physical, Chemical, and Catalytic Properties. *Inorg. Chem.* **1978**, *17*, 2345–2349.
- (53) Nayak, S. D.; Mahadevan, V.; Srinivasan, M. Hydrogenation of Alkenes and Alkynes Catalyzed by Polymer-Bound Palladium ( LI ) Complexes. *J. Catal.* **1985**, *92*, 327–339.
- (54) Pittman, C. U.; Hirao, A. Hydroformylation Catalyzed by Cis-Chelated Rhodium Complexes. Extension to Polymer-Anchored Cis-Chelated Rhodium Catalysts. *J. Org. Chem.* **1978**, *43*, 640–646.

- (55) Michalska, Z. M.; Strzelec, K.; Sobczak, J. W. Hydrosilylation of Phenylacetylene Catalyzed by Metal Complex Catalysts Supported on Polyamides Containing a Pyridine Moiety. *J. Mol. Catal. A Chem.* **2000**, *156*, 91–102.
- (56) Cullen, W. R.; Han, N. F. Polymer Supported Ferrocene Derivatives . Catalytic Hydrosilylation of Olefins by Supported Palladium and Platinum Complexes. *J. Organomet. Chem.* **1987**, *333*, 269–280.
- (57) Okamoto, M.; Kiya, H.; Suzuki, E. A Novel Catalyst Containing a Platinum Complex in Polyethylene Glycol Medium Supported on Silica Gel for Vapor-Phase Hydrosilylation of Acetylene with Trichlorosilane or Trimethoxysilane. *Chem. Commun.* **2002**, 1634–1635.
- (58) Michalska, Z. M.; Rogalski, Ł.; Różga-wijas, K.; Chojnowski, J. Synthesis and Catalytic Activity of the Transition Metal Complex Catalysts Supported on the Branched Functionalized Polysiloxanes Grafted on Silica. *J. Mol. Catal. A Chem.* **2004**, *208*, 187–194.
- (59) Wang, L.-Z.; Jiang Ying-Yan. An Active and Stable Hydrosilylation Catalyst: A Silica Supported Poly - $\gamma$ - Mercaptopropylsiloxane Platinum Complex. *J. Organomet. Chem.* **1983**, *251*, 39–44.
- (60) Tempesti, E.; Renzo, F. D. I.; Mazzocchia, C.; Modica, G. Heterogenized Boron(III)- Molybdenum(VI) Mixed Oxo Derivatives as New Bimetallic Catalysts for Cyclo- Hexene Liquid-Phase Epoxidation. *J. Mol. Catal. A Chem.* **1988**, *45*, 255–261.
- (61) Sherrington, D. .; Simpson, S. Polymer-Supported Mo and V Cyclohexene Epoxidation Catalysts: Activation, Activity, and Stability. *J. Catal.* **1991**, *131*, 115–126.
- (62) Binod B. De, Braj B. Lohray, S. S.; Dhal’J, P. K. Synthesis of Catalytically Active Polymer-Bound Transition Metal Complexes for Selective Epoxidation of Olefins? *Macromolecules* **1994**, *27* (6), 1291–1296.
- (63) Castro, I. U.; Stüber, F.; Fabregat, A.; Font, J.; Fortuny, A.; Bengoa, C. Supported Cu (II) Polymer Catalysts for Aqueous Phenol Oxidation. *J. Hazard. Mater.* **2009**, *163*, 809–815.
- (64) Du, F.; Lammens, M.; Skey, J.; Wallyn, S.; Reilly, O.; Du, F. Polymeric Ligands as Homogeneous , Reusable Catalyst Systems for Copper Assisted Click Chemistry W. *Chem. Commun.* **2010**, *46*, 8719–8721.

- (65) Suzuka, T.; Kawahara, Y.; Ooshiro, K.; Nagamine, T.; Ogihara, K.; Higa, M. Reusable Polymer Supported 2,2'-Biarylpyridine-Copper Complexes for Huisgen [3+2] Cycloaddition in Water. *Heterocycles* **2012**, *85* (3), 615–626.
- (66) Zhang, Z.; Dong, C.; Yang, C.; Hu, D.; Long, J.; Wang, L.; Li, H.; Chen, Y.; Kong, D. Stabilized Copper(I) Oxide Nanoparticles Catalyze Azide-Alkyne Click Reactions in Water. *Adv. Synth. Catal.* **2010**, *352*, 1600–1604.
- (67) Chan, T. R.; Fokin, V. V. Polymer-Supported Copper (I) Catalysts for the Experimentally Simplified Azide – Alkyne Cycloaddition. *QSAR Comb. Sci.* **2007**, *26*, 1274–1279.
- (68) Pourjavadi, A.; Hosseini, H.; Zohreh, N.; Bennett, C. Magnetic Nanoparticle Entrapped into the Cross-Linked Poly(Imidazole/Imidazolium) Immobilized Cu(II): An Effective Heterogeneous Copper Catalyst. *RSC Adv.* **2014**, *4*, 46418–46426.
- (69) Islam, R. U.; Taher, A.; Choudhary, M.; Witcomb, M. J.; Mallick, K. A Polymer Supported Cu(I) Catalyst for the ‘Click Reaction’ in Aqueous Media. *Dalt. Trans.* **2015**, *44*, 1341–1349.
- (70) Xiong, Y.; Washio, I.; Chen, J.; Cai, H.; Li, Z.; Xia, Y. Poly ( Vinyl Pyrrolidone ): A Dual Functional Reductant and Stabilizer for the Facile Synthesis of Noble Metal Nanoplates in Aqueous Solutions. *Langmuir* **2006**, *22*, 8563–8570.
- (71) Ayyappan, S.; Gopalan, R. S.; Subbanna, G. N.; Rao, C. N. R. Nanoparticles of Ag, Au, Pd and Cu Produced by Alcohol. *J. Mater. Res.* **1997**, *12*, 398–401.
- (72) Lim, B. B.; Jiang, M.; Tao, J.; Camargo, P. H. C.; Zhu, Y.; Xia, Y. Shape-Controlled Synthesis of Pd Nanocrystals in Aqueous Solutions. *Adv. Funct. Mater.* **2009**, *19*, 189–200.
- (73) George, B.; Pillai, V. N. R.; Mathew, B. Effect of the Nature of the Crosslinking Agent on the Metal- Ion Complexation Characteristics of 4 Mol % DVB- and NNMBA-Crosslinked Polyacrylamide- Supported Glycines. *J. Appl. Polym.* **1999**, *74*, 3432–3444.
- (74) Martin, L.; Martinez, H.; Poinot, D.; Pecquenard, B.; Cras, F. Le. Comprehensive X - Ray Photoelectron Spectroscopy Study of the Conversion Reaction Mechanism of CuO in Lithiated Thin Film Electrodes. *J. Phys. Chem. C* **2013**, *117*, 4421–4430.

- (75) Harmer, S. L.; Skinner, W. M.; Buckley, A. N.; Fan, L. Surface Science Species Formed at Cuprite Fracture Surfaces ; Observation of O 1 s Surface Core Level Shift. *Surf. Sci.* **2009**, *603*, 537–545.
- (76) Barr, T. L.; Seal, S. Nature of the Use of Adventitious Carbon as a Binding Energy Standard. *J. Vac. Sci. Technol. A* **1995**, *13*, 1239–1246.
- (77) Girard, C.; Önen, E.; Aufort, M.; Beauvière, S.; Samson, E.; Herscovici, J. Reusable Polymer-Supported Catalyst for the [3+2] Huisgen Cycloaddition in Automation Protocols. *Org. Lett.* **2006**, *8*, 1689–1692.
- (78) Hein, J. E.; Fokin, V. V. Copper-Catalyzed Azide-Alkyne Cycloaddition (CuAAC) and beyond: New Reactivity of Copper(I) Acetylides. *Chem. Soc. Rev.* **2010**, *39*, 1302–1315.
- (79) Ziegler, M. S.; Lakshmi, K. V; Tilley, T. D. Dicopper Cu(I)Cu(I) and Cu(I)Cu(II) Complexes in Copper-Catalyzed Azide – Alkyne Cycloaddition. *J. Am. Chem. Soc.* **2016**, *139*, 5378–5386.
- (80) El, M. M.; Saleh, T. S.; Bogami, A. S. Al. Ultrasound Assisted High-Throughput Synthesis of 1, 2, 3-Triazoles Libraries : A New Strategy for “ Click ” Copper-Catalyzed Azide-Alkyne Cycloaddition Using Copper ( I / II ) as a Catalyst. *Catal. Letters* **2018**, 1–14.
- (81) Creary, X.; Anderson, A.; Brophy, C.; Crowell, F.; Funk, Z. Method for Assigning Structure of 1,2,3-Triazoles. *J. Org. Chem.* **2012**, *77*, 8756–8761.



## Chapter 4

### **Plant mediated synthesis of Copper oxide and Silver nanoparticles: Application in catalysis and biological studies**

#### **4.1 Introduction**

Nanotechnology and natural science mutually depend on each other. Nanotechnology provides tool for the development of biological systems whereas natural science provides bio assembled components to nanotechnology. The synthesis of nanoparticles were carried out by different methods; physical, chemical and biological. Biosynthetic methods offers greener, eco-friendly and economical procedures for the synthesis of nanoparticles using microorganisms and enzymes. Plant or plant parts are also used for the fabrication of nanoparticles as they contain antioxidant as secondary metabolites.

Silver nanoparticles are known to possess unique electrical, optical and biological properties. In addition they find application in catalysis, drug delivery, sensing field etc. As a consequence of possessing antimicrobial<sup>1</sup> and antibacterial<sup>2</sup> activity silver gains more attention than other metals. Copper based compounds can promote various reactions while they can exhibit different oxidation state such as  $\text{Cu}^0$ ,  $\text{Cu}^I$ ,  $\text{Cu}^{II}$ ,  $\text{Cu}^{III}$ . They find application in various field like nanotechnology, electrocatalysis and catalyst in organic transformations.<sup>3-5</sup> Now a days, biosynthesis of nanoparticle have gained much attention due to

- i) Use of aqueous solvent
- ii) Simple procedure
- iii) Phytoconstituents act as both reducing and stabilizing agent
- iv) Eco-friendly
- v) Easy availability

## **4.2 Synthesis and Application of nanoparticles- A Review**

Recently, nanotechnology is an emerging field in chemistry which come up with wide variety of applications because of the geometry, shape and morphology of nanoscale materials.<sup>6</sup> Nanoscale material may be nanorods, nanotubes, nanoparticle and nanowires etc. The specific features of nanoparticles such as small size, high surface-volume ratio etc gave them more priority than the bulk materials in many applications. Metallic nanoparticle found out its application in various fields like cosmetics, electronics, biotechnology, coatings, therapeutic, biomedical field etc. Traditional procedure for the synthesis of nanoparticle involves wet chemical method, microemulsion, photocatalytic etc. Wet chemical method is recently upgraded as sol-gel method which produces uniform nanostructured materials with high purity even at low temperature. However the use of toxic solvents and the generated by-products in this method are hazardous to environment and health. Therefore, synthesis of nanoparticles by this method is much less in the developing world.<sup>7,8</sup> In order to avoid the drawbacks and to make the reaction green, the biosynthesis of nanoparticle came into existence. Here bio stands for the varieties of available biological sources in nature like plants, plant parts, yeast, fungi, algae, bacteria and virus. A brief discussion on different methods commonly used for the synthesis of nanoparticle is given below.

### ***Chemical reduction***

For the bulk synthesis of nanoparticle, chemical reduction of metal salt can be used.<sup>9</sup> This method is also known as wet method as it occurs in liquid medium. The reaction requires the presence of three major components

- i) Metal precursor
- ii) Reducing agent and
- iii) Stabilizing agent

The reduction of metal precursor using suitable reducing agent and in presence of a stabilizing agent can prevent the aggregation of synthesized nanoparticles. According to LaMer-Dinegar model<sup>10</sup> during the period of nucleation a number of colloidal particles will be formed and remain unchanged. Further growth of the particles will take place by the reduction of metal ion on the surface of clusters formed during the

nucleation period. Nucleation and growth of nuclei can be controlled by adjusting the reaction parameters like pH, temperature, metal precursor, reducing as well as stabilizing agent. By controlling the nucleation and growth, one can synthesize monodispersed nanoparticles i.e. the nanoparticles with uniform size distribution. Since nanoparticles possess large surface area, they have the tendency to form clusters and large particles. To prevent aggregation usually organic compounds like surfactants, organic polymer, dendrimers, stabilizing agents etc are used.<sup>11-15</sup> Chemical reduction method again is subdivided into six types according to the reducing agent used for the nanoparticle synthesis; i) citrate reduction method,<sup>16-23</sup> ii) reduction using  $\text{NaBH}_4$ ,<sup>24-26</sup> iii) polyol reduction method,<sup>27-29</sup> iv) reduction using ascorbic acid,<sup>30-35</sup> v) reduction using DMF<sup>36,37</sup> and vi) hydroxyl amine reducing agent.<sup>38</sup> Like every other procedures, chemical reduction method also had some advantages and disadvantages. The major advantages are faster reaction rate, no need of special experimental setup, large scale synthesis. By controlling the reaction conditions like temperature, pressure, pH etc one can synthesize nanoparticles in desired size, shape whereas the use of toxic chemicals produce both environmental and health hazards.

#### ***Microemulsion Method***

A microemulsion consists of ternary systems such as water, oil which is an immiscible liquids and surfactant or quaternary mixture which contains an additional reagent which acts as co-surfactant. Here the surfactant molecules form a monolayer at the interface between water and oil where hydrophobic tail dissolved in oil and hydrophilic heads in aqueous phase. In this method, both nucleation and growth of nanoparticles take place within the aqueous phase. By adjusting the water-to-surfactant ratio the droplet dimensions can be maintained. Agglomeration of nanoparticle can be controlled by the surfactant molecule by adsorbing on to the nanoparticle surface. Surfactants are classified into anionic, cationic and nonionic depending on the charges of polar head group. Anionic surfactant produces nanoparticles with smaller and narrow size distribution. Commonly used anionic surfactant are bis(2-ethylhexyl) sulfosuccinate (AOT), sodium dodecyl benzene sulfonate (SDBS) and sodium lauryl sulfate (SLS). CTAB (cetyltrimethylammonium bromide) is used as cationic surfactant whereas Triton X-100 is used as nonionic

surfactant. Major advantages of this method is the uniform size and morphology of the synthesized nanoparticle.<sup>39</sup> Drawback include the difficulty in the removal and separation of solvent from the nanoparticle

### ***Sonochemical method***

Introducing ultrasound in nanoparticle synthesis has the effect of producing very small and stable nanoparticles. The ultrasound energy can cause the rupture of chemical bonds thereby forming radicals which act as reducing agent. For examples, when the synthesis was carried out in aqueous medium, water molecules split into hydrogen and hydroxyl radicals which act as reducing agent for metal ion.<sup>40</sup> Gadanken reported the synthesis of copper nanoparticle using both thermal and sonochemical method<sup>41</sup> in which copper(II) hydrazine carboxylate was used as precursor. Thermal reduction yields pure metallic copper as product whereas both copper and copper(I) oxide are produced in sonochemical reduction. This may be attributed by the *in situ* oxidation of copper by H<sub>2</sub>O<sub>2</sub> which is generated under sonochemical conditions. Thermally derived nanoparticles shows the presence of irregularly shaped copper nanoparticle whereas sonochemical method produces a porous aggregate of irregular shaped nanoparticles. Gadanken again reported the synthesis of amorphous copper and nanocrystalline copper oxide embedded in polyaniline matrix using sonochemical reduction method.<sup>42</sup> Salkar reported the synthesis of silver nanoparticle by sonochemical reduction of silver nitrate for 1h sonication.<sup>43</sup>

### ***Photochemical method***

This method produces metal nanoparticle either by the direct photoreduction of metal precursor or by the reduction of photochemically generated intermediates like radicals. The photochemical synthesis of copper nanoparticle incorporated in poly(vinyl pyrrolidone) which act as protecting agent and bis(2,4-pentandionato)copper(II) complex used as metal precursor.<sup>44</sup> Advantages of such synthesis are clean synthesis, controllable generation of reducing agents, versatility etc.

The above methods have the drawbacks like use of toxic chemicals, nonpolar organic solvents and the use of stabilizing and capping agents. To avoid these problems,

researchers developed green synthesis of nanoparticles using biomaterials which are eco-friendly and provide clean procedure .

### ***Biosynthesis of nanoparticle***

For the eco-friendly synthesis of nanoparticles biological method was developed. The major sources for the synthesis of nanoparticle are bacteria, fungi and plant extracts. The biosynthesis is generally a bottom up approach involving the reduction and oxidation reactions.

### **Synthesis of nanoparticle from bacteria**

For the first time, synthesis of silver nanoparticle was reported from *Pseudomonas stutzeri*.<sup>45</sup> The bacteria were grown in Lennox L broth containing 50 mM AgNO<sub>3</sub> at 30 °C for 48 h in dark. The formation of silver nanoparticle was confirmed by TEM and EDX analysis. Reduction of silver ions by *Klebsiella pneumonia*, *E. coli*, and *Enterobacter cloacae* (*Enterobacteriaceae*) were reported.<sup>46</sup>

Polydispersed silver nanoparticles were synthesized from *Geobacillus stearothermophilus* by Fayaz.<sup>47</sup> High stability of this nanoparticle is attributed to the secretion of capping agent produced by the bacterium. Kalishwarala reported the synthesis of nanoparticle using *Brevibacterium casei* from dairy waste.<sup>48</sup> Wet *B. casei* along with silver nitrate incubated in an incubator was stirred at 37 °C for 24 h. The SPR of silver nanoparticle was observed at 420 nm with average particle size of 10-50 nm. *Bacillus* strain CS-11 obtained from industrial area was used for the production of silver nanoparticles.<sup>49</sup> The formation of nanoparticle at room temperature within 24 h was confirmed by UV-vis absorption at 450 nm. TEM analysis suggested that the nanoparticle is having an average size between 42-92 nm.

### **Synthesis of nanoparticle from fungus**

Due to the secretion of large amounts of enzymes by fungi than bacteria, fungus can be used for the synthesis of nanoparticles. Possible steps for the synthesis of nanoparticle includes: trapping of silver ions at the surface of fungal cells followed by the subsequent reduction of silver ions by the enzymes present in fungus. Extracellular enzymes naphthaquiniones and anthraquinones are responsible for such reduction process. Synthesis of silver nanoparticle was reported using fungus

*Verticillium*<sup>50</sup> by the intracellular reduction of silver ions to silver nanoparticle with an average dimension of 25±12 nm. Ahmad *et.al* reported the extracellular synthesis of silver nanoparticle using fungus *Fusarium oxysporum*. The synthesized nanoparticle were stabilized by the proteins secreted by fungus.<sup>51</sup> Using nitrate reductase enzyme from *Fusarium oxysporum* silver nanoparticle was synthesized in presence of a co-factor NADPH.<sup>52</sup> The synthesis involves the incubation of silver nitrate, phytochelatin, 4-hydroxyquinoline and NADPH at 25 °C for 5 h under anaerobic conditions. *Penicillium fellutanum* mediated synthesis of silver nanoparticle was reported by Kathiresan where the silver ions mixed with cell filtrate and agitated at 25 °C under dark conditions.<sup>53</sup>

### **Biosynthesis of nanoparticle using Plant**

Bio fabrication of nanoparticle using plant can be easily understood by dividing it into two categories i) intracellular synthesis and ii) extracellular synthesis. In intracellular synthesis aqueous solution of metal salt was treated with living plant or plant biomass producing metal nanoparticle and the recovery of nanoparticle was done by cell rupture. Extracellular synthesis involves the treatment of aqueous solution of metal salt with aqueous plant extract and the nanoparticles can be collected by centrifugation from the resultant colloidal solution. Treatment of individual phytoconstituent with aqueous metal salt solution results in metal ion reduction and purification of nanoparticle was done by ion exchange chromatography. There are few reports available which shows the isolation of particular phytoconstituents and used for the synthesis of nanoparticles.<sup>54-59</sup>

#### ***Living Plant Mediated Synthesis (Intracellular synthesis)***

The living plant contains heavy metal accumulation and this strategy can be used for synthesis. Yacaman reported the synthesis of silver nanoparticle from *Alfalfa sprouts*<sup>60</sup> using silver nitrate as precursor. In 2008 Harris studied the extent of metal ion formation and uptake in *Brassica juncea* and *M. sativa*.<sup>61</sup> Similarly gold nanoparticles were synthesized from plant biomass.<sup>62,63</sup> Main disadvantage of the procedure is the tedious recovery step of nanoparticle and the availability of reducing and stabilizing bioorganic compounds which varies according to different parts. The size and morphology variation of nanoparticle being observed in such cases is

attributed to the difficulties associated with the separation and purification procedures.

***Plant Extract Mediated synthesis of nanoparticle (Extracellular synthesis)***

Plant contains variety of phytoconstituents which are responsible for the reduction of metal ions. In extracellular process these phytoconstituents are extracted and exploited directly for the synthesis of metallic nanoparticles. It is very rare to produce nanoparticles with monodispersity and definite morphology as a result of variation of the phytoconstituents in plants and presence of impurities. Plant extract mediated synthesis supports the formation of spherically shaped and highly reactive nanoparticle. By controlling the reaction conditions in plant extract mediated synthesis one can produce nanoparticle for commercial application. It has been reported by many academics that high polydispersity index of such synthesis is due to the variation of phytoconstituents.

Ibrahim reported the synthesis of silver nanoparticle from banana peel extract in 2015.<sup>64</sup> Banana peel extract [BPE] act as reducing as well as capping agent. He studied different factors like optimum concentration, pH and incubation time. Metal salt concentration as well as BPE concentration influences the synthesis of nanoparticle which could be understood from the observation of color change from light reddish brown color to dark reddish brown color. The reddish brown color is attributed to the Surface Plasmon Resonance (SPR) with characteristic SPR band at  $\lambda$  433 nm. Other conditions such as at pH 2, reduction of silver ions doesn't take place which is confirmed by the absence of SPR band. Similarly at low temperature reduction occurs slowly that the development of reddish brown color appears only after 10min. Synthesized silver nanoparticle revealed good antimicrobial activity.

Lee *et.al* developed an efficient method for the synthesis of silver nanoparticle from *Myrsitica fragrans* seed extract, and found to have an excellent antimicrobial activity.<sup>65</sup> The characteristic surface plasmon resonance was observed at 410 nm corresponds to the reduction of silver ions to silver nanoparticles. The size of the Ag nanoparticle was found out using TEM and it was in the range of 7-20 nm size. The XRD patterns suggest the formation of metallic silver which has FCC structure. Antimicrobial activity of silver nanoparticles against both gram negative and gram-

positive bacteria was found to be concentration dependent, as the concentration of nanoparticle increases microbial growth decreases.

Biogenic synthesis and characterization of silver nanoparticle using *Memecylon edule* leaf extract were done by Elavazhagan and Arunachalam under dark condition.<sup>66</sup> They observed UV absorption peak at 475 nm. SEM results showed the silver nanoparticles have an average diameter of 50-90 nm. At room temperature synthesis of silver nanoparticle was carried out using *Argemone Mexicana*<sup>67</sup> within 4 h. They observed characteristic UV absorption peak at 440 nm. The XRD pattern shows that the silver nanoparticle contains both cubic and hexagonal structures. The silver nanoparticles produced were found to be toxic against the bacteria *Escherichia coli*, *Pseudomonas syringae* and the fungi *Aspergillus flavus*.

*Carica papaya* fruit extract was used for silver nanoparticle synthesis by Kothari.<sup>68</sup> Room temperature reduction of silver ions was carried out by Papaya fruit extract within 5 h and they got SPR band at 450 nm with broadening indicating the polydispersity of silver nanoparticles. Formation of silver nanoparticles was further confirmed by XRD measurements which produces characteristic peaks of metallic silver having both cubic and hexagonal structures. IR spectrum of both plant extract and silver nanoparticles confirms the role of polyols in the reduction of silver ions. Characteristic -C-O group peak of polyols was found to be absent after the bioreduction and they concluded that such polyols will be responsible for the reduction of silver ions. At a concentration of 50 ppm, silver nanoparticles exhibit anti bacterial activity against *E. coli* and *Pseudomonas aeruginosa*.

Yugandhar P. reported the synthesis of silver nanoparticle from fruit extract of *Syzygium alternifolium*.<sup>69</sup> Here formation of silver nanoparticles was confirmed by observing the color change from brown to grey. The SPR band of UV-Visible spectrum at 442 nm again confirms the formation of silver nanoparticles. This band corresponds to primary amines and proteins that are interacted with silver NPs and act as reducing agent. Surface topology of nanoparticle was studied by AFM analysis, which shows a spherical shape for silver NPs and the size is in the range of 32-68 nm as confirmed by SEM analysis. TEM analysis identifies the polydispersity nature of the silver nanoparticles without any agglomeration.



*Ocimum sanctum* (Lakshmi tulasi) which had medicinal values being a principal herb of ayurveda and used as reducing agent for the bioreduction of silver nanoparticle.<sup>70</sup> AgNO<sub>3</sub>(5ml) solution was added to the leaf extract (1ml) and stirred at room temperature for 10 min develops reddish yellow color which is due to the formation of silver nanoparticles. UV absorption peak at 406 nm confirms the presence of silver NPs. The involvement of carbonyl group in the reduction of silver ion can be understood from IR spectral data. SEM results shows the polydispersity of nanoparticles and the strong EDX signal again confirms the presence of silver NPs along with oxygen, carbon peaks which may be due to the presence of terpenoids in the plant extract

Aqueous leaf extracts of *Azadirachta indica* was used for the synthesis of silver nanoparticle by Ikra.<sup>71</sup> Optimization was carried out by varying concentration of both plant extract and silver ion concentration. Color change from yellowish to reddish brown due to the Surface Plasmon Resonance of silver particles and SPR were obtained at around 446nm. Spherical nature of silver nanoparticle was found out by TEM analysis and they also observed that there are some nanoparticles having irregular shape. Silver nanoparticle shows antibacterial activity against *E. coli* and *S. aureus*.

*Arachis hypogaea* peel extract was used for the synthesis of silver nanoparticles after 60min incubation at 28 °C.<sup>72</sup> SPR appears at 450 nm and the increase in SPR accredited by increasing the incubation time. XRD pattern confirms the formation of fcc structured metallic silver. The nanoclusters are formed by the aggregation of nanoparticle which is evident from SEM images. The spherical nature of nanoparticle was identified from TEM images. Larvicidal activity of both extract and nanoparticle was studied against two important vector mosquitoes *A. stephensi* and *A. aegypti*. The synthesized silver nanoparticle was found to be better larvicidal agent compared to the extract.

Biosynthesis of silver nanoparticle was also carried out using palm date extract.<sup>73</sup> The reaction mixture was initially colorless and became yellow which then turns to bright brown on heating. Formation of silver nanoparticle was identified by SPR band at 425 nm. The nanoparticle forms a cluster by the aggregation of smaller silver nanoparticles. Palm date fruit extract derived silver nanoparticle shows better

antimicrobial activity compared to fruit extract alone. Catalytic activity of silver nanoparticle was studied for the reduction of 4-nitrophenol and observed that as the reaction time increases reduction efficiency increases.

Lemon peel extract was used for the reduction of silver ions to metallic silver at room temperature for 5 h.<sup>74</sup> The characteristic SPR band occurred at 420 nm and SEM analysis observed some spherical as well as irregularly shaped nanoparticle. Application of the biosynthesized nanoparticle was done against dermatophytes. They show better activity against *C. albicans* and *T. mentagrophytes*.

Silver nanoparticle with cubic shape was synthesized by the bioreduction of metal precursor using garlic clove extract and showed absorption at 408 nm. From XRD data the average size of nanoparticle was found to be  $12 \pm 2.3$  nm which is in agreement with TEM results.<sup>75</sup> SEM images show the spherical nature of particles whereas EDX confirms the presence of silver. Cytotoxicity was studied against human lung epithelial (A549) and found that it not at all toxic at a concentration of 50  $\mu\text{g/ml}$ .

Copper nanoparticles were synthesized from *Citrus medica* Linn using  $\text{CuSO}_4 \cdot 5\text{H}_2\text{O}$  by Rai and coworkers.<sup>76</sup> Addition of citron fruit extract to  $\text{CuSO}_4 \cdot 5\text{H}_2\text{O}$  followed by heating in the temperature range of 60-100 °C produces a visible color change from blue to pale yellow followed by deposition of reddish brown colored precipitates indicating the formation of copper NPs. This was collected and made a colloidal solution using liquid ammonia. SPR peak was observed at 631 nm. Size of the NPs was determined by NTA (Nanoparticle Tracking Analysis) based on the Brownian movement of the particles in the sample and the average range size was found to be 33 nm. XRD analysis proved that the copper has an fcc phase. They conducted *in vitro* antimicrobial activity against *E. coli*, *P. acne*, *K. pneumoniae*, *S. typhi*, and *P. aeruginosa* and three plant pathogenic fungi viz. *F. oxysporum*, *F. graminearum* and *F. culmorum*. The nanoparticles had higher activity against *E. coli*. Liquid ammonia or copper sulfate alone doesn't have any significant activity towards these organisms. Hudlikar reported a room temperature synthesis of copper nanoparticle from *Calotropis procera*.<sup>77</sup> Size of nanoparticle was determined using HR-TEM and found out to be in the range of 5-30 nm. The XRD pattern suggests an fcc structure for

copper nanoparticle. EDAX analysis gives elemental signals at 1.00, 1.50, 2.70 and 8.00 keV corresponds to copper. FTIR spectrum consists of amide II, amide III, secondary amine, carboxylic acid, alcohol bands. Cytotoxicity of the latex stabilized nanoparticle was done and showed excellent activity.

Kim *et.al* synthesized copper nanoparticle from *Mangolia kobus* leaves.<sup>78</sup> The effect of temperature and leaf broth concentration was studied. UV-Visible analysis shows absorption maximum at 560 nm. At 25 °C the conversion was about 70% whereas after 24 h this gradually increased to 100% at 90 °C. The particle size decreases from 110 nm obtained at 25 °C to 45 nm at 95 °C. As the reaction temperature increases the rate of the reaction as well as conversion of copper ion to copper nanoparticle increases. Influence of leaf broth concentration was investigated and the results showed that rate of reaction found to be highest at 20% concentration. The average particle size was found be decreased to 15% of leaf broth concentration and then increased. Both EDS and XPS results confirm the presence of copper nanoparticle. They compared the antibacterial activity of both biosynthesized copper nanoparticles with chemically synthesized one and found to be higher in the case of biosynthesized copper nanoparticles.

Catalytic application of copper nanoparticle derived from *Ginkgo biloba* leaf extract was reported by Nasrollahzadeh.<sup>79</sup> Nanoparticle were synthesized by mixing aqueous extract of leaves with  $\text{CuCl}_2 \cdot 2\text{H}_2\text{O}$  solution followed by heating at 80 °C. The nanoparticles were collected by centrifugation followed by washing with n-hexane and ethanol. UV-visible spectrum shows absorption maxima in the range of 560-580 nm indicating the formation of copper nanoparticles. The average particle size was about 15-20 nm specified by TEM analysis. The catalytic activity of the synthesized copper nanoparticle was studied in azide-alkyne cycloaddition reaction. Optimization studies were carried out using benzyl chloride and phenyl acetylene. Ethanol was found to be good solvent and the use of 10 mol% of copper catalyst loading provides good result without any need of additional ligand or additives. Scope of the catalyst was studied using different alkynes and halides in ethanol at room temperature and good result were obtained. The product was recovered using centrifugation and washed with ethanol. The catalyst could be used as heterogeneous catalyst and reused four times without any significant loss in catalytic activity.

Nasrollahzadeh studied the Ullmann coupling reaction catalyzed by copper nanoparticle derived from leaf extract of *Euphorbia esula L.*<sup>80</sup> The SPR band observed at 580 nm corresponds to the surface Plasmon resonance which occurs due to the formation of copper nanoparticle. XRD diffraction pattern supports the formation of copper nanoparticles with fcc structure. Spherical shape of nanoparticle was identified by TEM analysis and it also shows the aggregation of smaller particle resulting in the formation of clusters. Reduction of 4-nitrophenol to 4-aminophenol was tested using the copper nanoparticle at room temperature in aqueous medium. The conversion to 4-aminophenol was monitored by UV-visible spectroscopy. To an aqueous solution of 4-nitrophenol NaBH<sub>4</sub> was added which produces 4-nitrophenolate ion having absorption at 403 nm. After the addition of copper nanoparticles, the phenolate absorption band disappeared and a new band formed at 300 nm which is the characteristic peak of 4-aminophenol. In order to optimize the reaction conditions, the reaction was carried out using different solvent and base. The best result was obtained when DMF used as solvent, Cs<sub>2</sub>CO<sub>3</sub> as base and 1 ml of CuNP.

Copper nanoparticle was synthesized and stabilized using *Quisqualis indica* extract and evaluated its cytotoxic activity and apoptosis in B16F10 melanoma cells.<sup>81</sup> Copper acetate was used as metal precursor and the addition of extract leads to the formation of copper nanoparticles. Synthesized copper nanoparticle was characterized by UV-vis spectroscopy which shows maximum absorption at 309 nm. Monodispersive and spherical nature of particles was observed by TEM analysis. The two theta values obtained corresponds to metallic copper further confirms the formation of copper nanoparticles.

Biosynthesis and application of copper nanoparticles in photocatalytic activity was studied by Bibi.<sup>82</sup> Copper chloride on treatment with *P. grantam* seed extract at 70 °C was reduced to copper nanoparticle as indicated by the color change from dull bluish brown to dark green suspension. The precipitate was washed using water followed by ethanol and dried in a vacuum oven. Plasmon resonance was observed at 553nm. XRD pattern indexed to fcc structure of copper nanoparticles and EDX analysis confirms the presence of copper. The size of copper nanoparticles was found to be in 40-80 nm range. The copper nanoparticle shows excellent photocatalytic activity towards the methylene blue dye degradation.

Copper oxide nanoparticles were synthesized from *Punicagranatum* peels extract. To a solution of copper acetate the extract was added and stirred at room temperature.<sup>83</sup> Formation of copper oxide nanoparticle was indicated by the color change from blue to green color and its formation of brown suspension. SPR of copper oxide was observed at 282 nm and the formation was further confirmed by XRD analysis. The particle appears to be spherical in nature from SEM analysis .

*Tabernaemontana divaricate* mediated synthesis of copper oxide nanoparticles were reported by Sivaraj.<sup>84</sup> Aqueous solution of copper sulphate pentahydrate was treated with 50% leaf extract followed by stirring at 100 °C for 7-8 h resulted in a brownish black solid product. The antibacterial activity of copper oxide nanoparticle was studied using urinary tract pathogen and the highest zone of inhibition observed for *Escherichia coli*.

Application of biosynthesized copper nanoparticle towards the cyanation of aldehydes using  $K_4Fe(CN)_6$  was studied by Nasrollahzadeh.<sup>85</sup> Reaction of  $CuCl_2 \cdot 2H_2O$  with aqueous plant extract at 80 °C induces a color change which was the initial identification copper nanoparticle formation. The TEM image confirms the formation of nanosized copper particles in the range of 7-35 nm. The cyanation of aldehyde in the presence of copper nanoparticle afforded benzonitrile in 93% yield.

### **Scope of the work**

Synthesis of nanoparticles using chemical or other methods stand with major drawback related to its separation from solvent and reaction mixture. “Green method” which uses natural source for the synthesis of nanoparticle reduces the use of toxic solvent and made the separation easier. Mace and seed of *Myrsitica fragrans* contains antioxidants, micronutrients and polyphenols which made it precious in medicinal field. The literature reports suggested the presence of phenyl propanoid ethers like eugenol in pericarp along with the same phytoconstituents found in the mace and seed. Pericarp of *myrsitica fragrans* doesn't gain much attention due to lack of knowledge about the medicinal values present in it. The fruit (pericarp) extract of *Myristica fragrans* alone can act as reducing as well as stabilizing agent in nanoparticle synthesis. Using the extract we had synthesized copper oxide nanoparticles and silver nanoparticle and investigated its catalytic and biological activities.

### **4.3.1 Reagents and Materials**

- *Myrsitica fragrans* ripped fruit
- Copper acetate- Merck
- Silver Nitrate- Sigma Aldrich
- Benzyl chloride, 4-chlorobenzyl chloride, 2,4-dichlorobenzyl chloride, 4-nitro benzyl bromide, N-butyl bromide, allyl bromide, 1-chloromethyl naphthalene, cyclopentyl bromide and 2-bromoethyl benzene -Spectrochem Mumbai
- Sodium azide from Nice Chemicals
- Distilled water

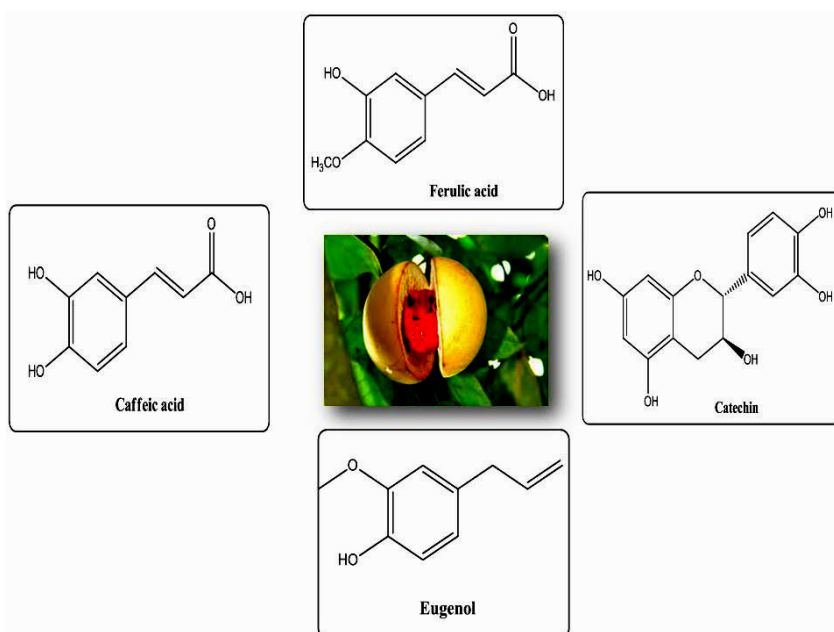
### **4.3.2 Instruments**

- IR spectra recorded on a Shimadzu IR Affinity- 1 Spectrometer using KBr pellets
- SEM performed on JEOL Model JSM-7600F along with identification of chemical composition of sample using energy dispersive X-ray spectroscopy.
- NMR – Bruker Avance III, 400MHz
- GC-MS –Thermo Fisher Scientific
- TEM analysis done using Jeol/JEM 2100 instrument

#### 4.4 Results and Discussion

The term biogenic synthesis is attributed to the use of biomaterials like plant parts, microorganisms *etc* for the synthesis and stabilization of metal ions to metal nanoparticles. To prepare nanoparticles, we used ripped fruit extract of *Myristica fragrans* which acts as both reducing and stabilizing agent. The genus *Myristica* belongs to the family Myristicaceae. In this genus the commonly found fruit is *Myristica fragrance*. It is commonly known as Nutmeg/ Javitri or Jaiphal, widely used as spice and ingredient in the Unnani, Ayurvedic medicine *etc.*<sup>86,87</sup> The pericarp (fruit covering) is usually thrown away after taking the seed and arils surrounding the seed.

The reducing power of *Myristica fragrans* fruit extract is attributed to the presence of phytoconstituents present in the extract. Polyphenols, proteins *etc* influences the formation of metal nanoparticles.<sup>88,89</sup> Earlier reports suggested the influence of phenolic acids such as caffeic acid, ferulic acid and catechin which is a flavanoid responsible for the formation of nanoparticles.<sup>90,91</sup> Nutmeg contains phenylpropanoid ethers, acyl phenols, fatty acids, their esters, lignane, terpenes, phenolic acid and flavanoids.<sup>92,93</sup> In addition to this, the preicarp of *Myristica fragran* contain phenyl propanoid ethers myristin, eugenol, isoeugenol and methyl eugenol. Among this, eugenol is the most predominant compound present in the pericarp of fruit, which promotes the reduction of metal ions to nanoparticle.<sup>94</sup>



#### 4.4.1 Preparation of *Myristica fragrans* fruit extract

The plant extract was prepared using hydrothermal method. Nutmeg fruit was dried under shade and powdered. Powdered Nutmeg fruit was mixed with distilled water in an autoclave and heated at 110 °C for 2 h. It was then allowed to cool into room temperature. The yellowish colored solution was filtered through Whatman no.1 filter paper and stored at 4 °C.

#### 4.4.2 Visual Inspection

Freshly prepared copper acetate was irradiated under microwave in presence of *Myristica fragrans* fruit extract. The color of the copper acetate solution changes to bluish green and then to a greenish brown suspension indicating the formation of copper oxide (**Fig 1**). Further irradiation results in a black colored residue. The residue was separated by centrifugation and dried in a vacuum oven at 60 °C and used for further analysis.

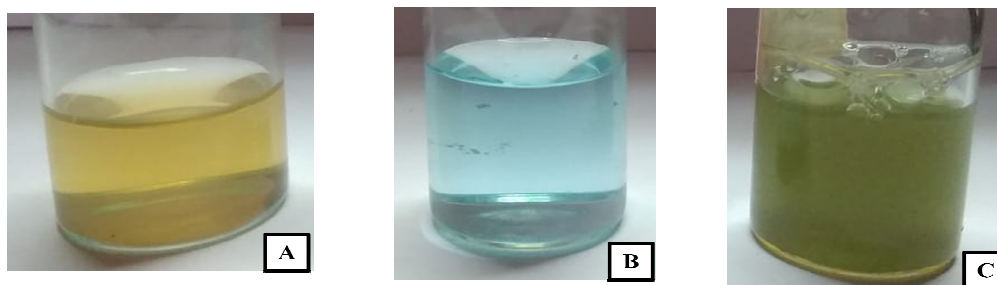


**Fig 1** Photographs of A) *Myristica fragrans* fruit extract B) Copper acetate solution C) Reaction mixture containing CuO nanoparticles obtained after microwave irradiation



#### 4.4.3 UV- Visible spectroscopy Analysis

A gradual color change of copper acetate solution from blue to bluish green then to greenish brown suspension after the addition of *Myristica fragrans* fruit extract is due to the formation of CuO nanoparticle. We observed the characteristic surface plasmon resonance of nano CuO and the corresponding band appears at  $\lambda$  360 nm in the UV-visible spectrum (**Fig.2**)

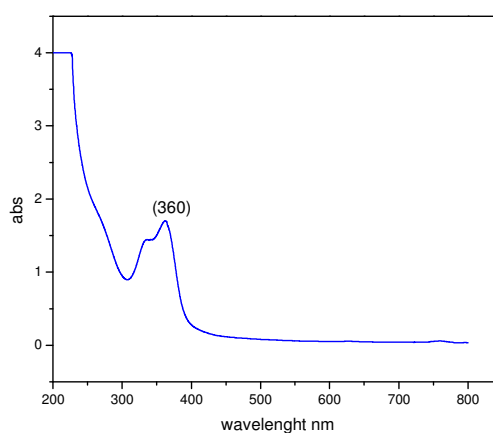


**Fig 2.** UV-Vis absorption spectrum of CuO nanoparticles

#### 4.4.4 Infrared Spectral analysis

Fourier Transform Infrared (FTIR) analysis helps to identify the phytoconstituents present in the plant extract. FT IR of as synthesized CuONPs is shown in **Fig 3**. Characteristic Metal-oxide stretching vibration of CuO was observed at 497, 689 and 868  $\text{cm}^{-1}$  and thereby confirms the presence of CuO in the sample. The presence of eugenol in sample was identified by observing characteristic IR peaks at 713  $\text{cm}^{-1}$  and 1384  $\text{cm}^{-1}$  corresponds to alkanes and alkane  $\text{C-H}_{\text{rocking}}$  vibrations. Peak at 975  $\text{cm}^{-1}$  observed for trans =C-H bond and 3238  $\text{cm}^{-1}$  for phenolic -OH group. Aromatic ring -C=C stretching vibration was observed at 1556  $\text{cm}^{-1}$ . From FT-IR analysis presence of both metal oxide and phytoconstituent which is responsible for the nanoparticle formation was confirmed.

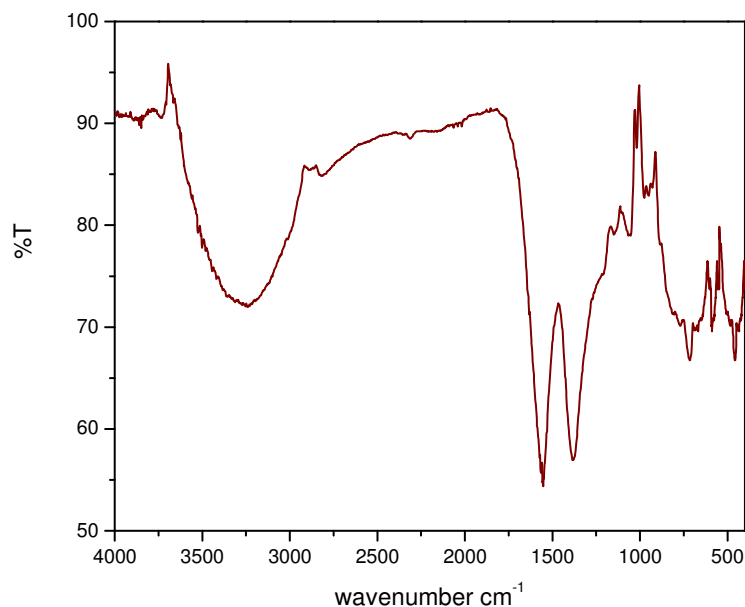


**Fig 3** FT-IR Spectrum of CuO nanoparticle

#### 4.4.5 Powder X-ray Diffraction Analysis

The XRD pattern (**Fig 4**) reveals the presence of CuO as the major component. The peaks at  $2\theta$  values of  $32.5^\circ$ ,  $35.6^\circ$ ,  $38.8^\circ$ ,  $48.7^\circ$ ,  $50.5^\circ$ ,  $58.4^\circ$ ,  $61.5^\circ$ ,  $66.4^\circ$ ,  $67.9^\circ$ ,  $73.7^\circ$  corresponds to (1 1 0) (1 1 -1), (1 1 1), (2 0 -2), (1 1 2), (2 0 2), (1 1 -3), (3 1 0), (1 1 3), (2 2 1) planes of CuO monoclinic phase (JCPDS No:98-009-2367). Those peaks at  $2\theta$  values  $29.7^\circ$ ,  $42.4^\circ$  corresponding to (0 1 1), (0 0 2), planes of  $\text{Cu}_2\text{O}$  (JCPDS No: 96-900-5770).  $43.5^\circ$  are attributed to (1 1 1) plane of Cu respectively ((JCPDS No. 04-0836)). The existence of copper(II)oxide was confirmed by XRD analysis with small amount of copper(I) oxide and copper(0) as impurities as a result of the over reduction of CuO by the plant extract.

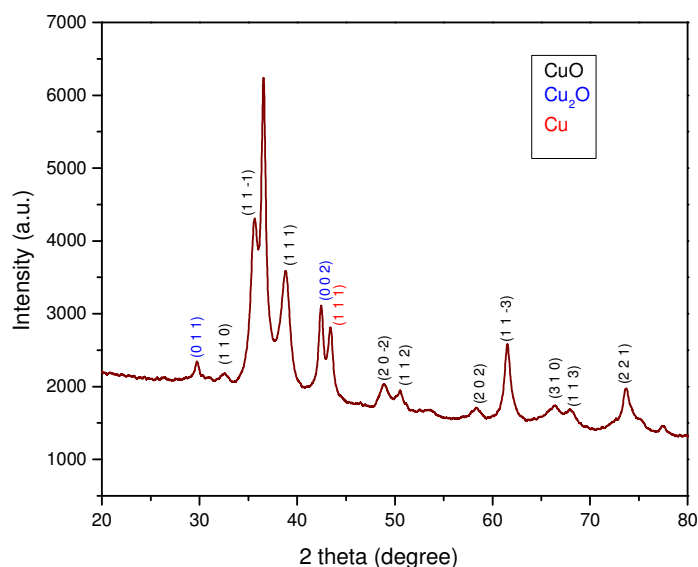


**Fig. 4** XRD pattern of CuO nanoparticle -*Myristica fragrans* fruit extract

In vapor-solid method of nanowire synthesis, it is assumed that initial oxidation of copper acetate leads to the formation of  $\text{Cu}_2\text{O}$  and finally  $\text{CuO}$  was formed.<sup>95</sup> In certain cases complete reduction may occur resulting in metallic copper. The nanoparticle is considered to be an agglomeration of two or more individual crystallites. Using Debye-Scherrer equation the average crystallite size of the synthesized copper oxide nanoparticle was calculated.

$$D = \frac{K\lambda}{\beta \cos \theta}$$

Where

D= Crystallite size of copper oxide nanoparticle

K= The Scherrer constant with value from 0.9 to 1

$\lambda$ = Wavelength of X-ray source used in XRD 0.15406 nm

$\beta$ = full width at half maximum of the diffraction peak

$\theta$ = Bragg's angle

From the Scherrer equation the average crystallite size of copper oxide nanoparticle was found to be 15.7 nm.

#### 4.4.6 Field emission gun scanning electron microscopy (FEG-SEM) Analysis

Typical SEM images of the synthesized CuO nanoparticles are shown in **Fig 5**. The SEM micrograph shows polydispersed spherically shaped particles embedded in the phytoconstituents. Using histogram average estimated particle size was found to be  $13\pm 0.63$  nm (**Fig. 5**)

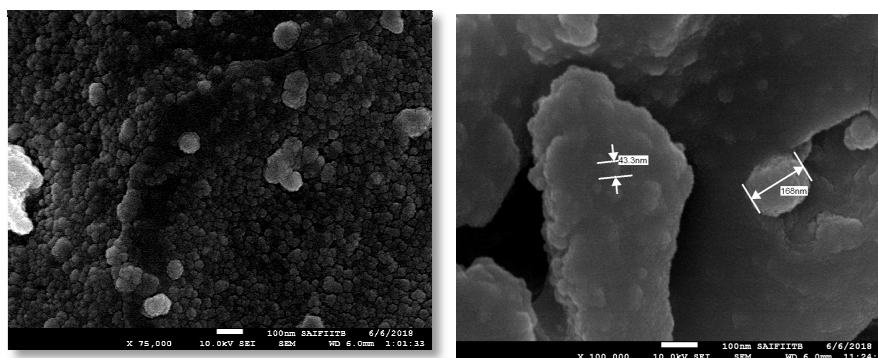


**Fig. 5** Scanning electron microscopy( FEG-SEM) images of CuO nanoparticle synthesized using *Myristica fragrans* fruit extract

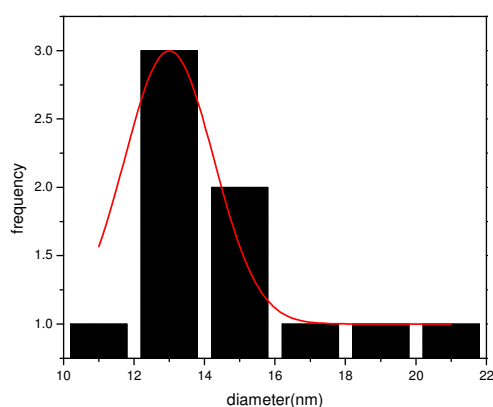


**Fig.6** Particle size distribution histogram of CuO nanoparticles

#### Energy Dispersive X-ray Spectroscopy (EDS) Analysis

The elemental composition of CuO nanoparticle was determined by energy dispersive X-ray spectroscopy (EDS) and shown in **Fig 6**. This spectrum shows a high intense peak at 0.9 and the less intense peak at 8.1 and 8.9 keV represents  $\text{CuL}\alpha$ ,  $\text{CuK}\alpha$  and  $\text{CuK}\beta$  respectively with wt% of 44.11% and a strong peak for elemental oxygen at 0.5keV with wt% of 33.64% which confirms the formation of CuO. Signals obtained

for Na, K, Ca and Zn which can be due to the existence of biomolecules around the nanoparticles.

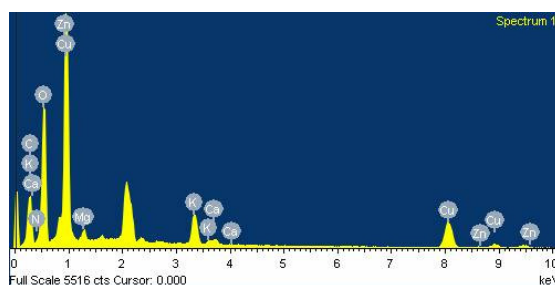


Fig 7 EDS spectrum of CuO NPs-*Myristica fragrans* fruit extract

#### 4.4.7 High resolution transmission electron microscopy (HR-TEM) analysis

The HR-TEM confirms the formation spherical shaped copper oxide nanoparticle which is surrounded by plant biomass. (Fig.7 A,B &C).

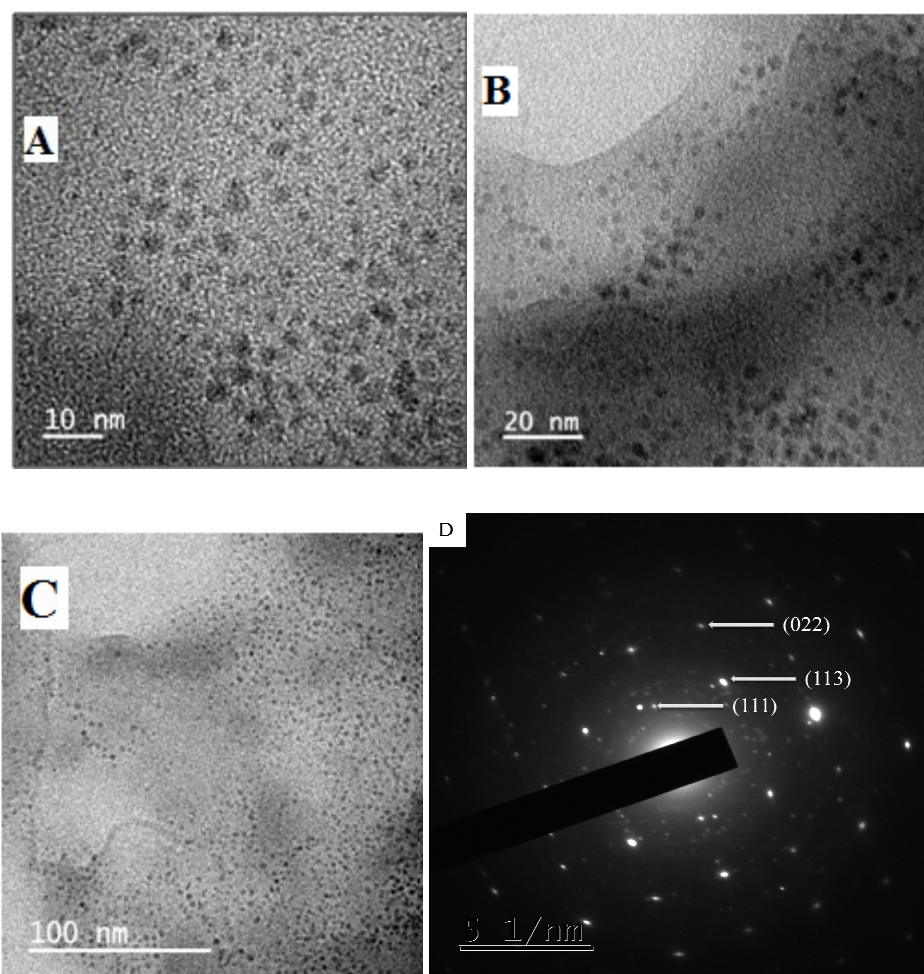
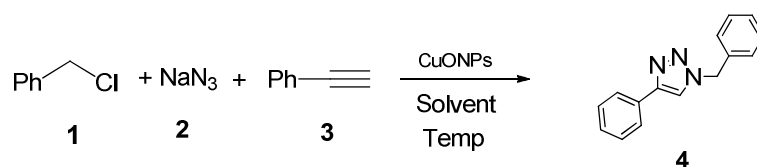


Fig 8 HR-TEM images of CuO NPs at different different magnification (A,B &C) and SAED pattern (D)

The SAED pattern (**Fig 7D**) has the nature of sharp rings with small spots indicating that the compound is nanocrystalline in nature. The “d” spacing was estimated to be 0.21, 0.13, 0.10 nm and that corresponds to “d” spacing of the (111), (113) and (022) orientation of monoclinic structure of metallic CuO nanoparticle.

#### 4.4.8 Catalytic Activity of the Synthesized Copper oxide (CuO) nanoparticle in Azide-Alkyne Cycloaddition reaction

After the successful synthesis and characterization of CuO nanoparticle its catalytic activity was studied for the synthesis of 1,2,3-triazoles using phenyl acetylene, sodium azide and alky/aryl halides. Optimization studies were carried out using benzyl chloride, phenyl acetylene and sodium azide as reactants in terms of solvent, catalyst loading, temperature (**Scheme 1**). The optimization results (**Table 1**) show the effect of solvent on the product yield. Water, ethanol, THF and ethanol/water mixture were tested. Among these solvents water shows a remarkable effect on triazole formation. The best result obtained when 0.01 g of CuO nanoparticle in water at 60 °C (**Table 1, entry 6**). The product was separated by extraction using ethyl acetate and the insoluble catalyst was recovered and dried in vacuum oven at 70 °C. The recyclability of the catalyst was studied using the model reaction and the recovered catalyst was used for a new set of reactions. No significant loss in catalytic activity was observed after the successive first four runs. The CuO nanoparticle could be reused as heterogeneous catalyst. By increasing the catalyst concentration to 0.02 g, the reaction completed within 4 h. Using optimized conditions triazoles with different functional groups have been synthesized from corresponding alkyl/aryl halides and alkynes (**Table 2**).

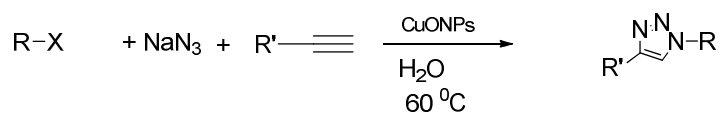


**Scheme 1**

**Table 1** Optimization of the CuAAC reaction in terms of catalyst loading, solvent, temperature and time using benzyl chloride, sodium azide, phenyl acetylene and CuO NPs

Entry	Catalyst loading(g)	Solvent	Temperature	Time(h)	Yield %
1	0.01	H <sub>2</sub> O	rt	12	70
2	0.01	Ethanol	rt	48	65
3	0.01	THF	rt	48	Nil
4	0.01	t-BuOH	rt	20	75
5	0.01	Ethanol/H <sub>2</sub> O	rt	20	50
6	0.01	H <sub>2</sub> O	60°C	5	98
7	0.01	Ethanol	60°C	5	70
8	0.005	H <sub>2</sub> O	60°C	15	90
9	0.02	H <sub>2</sub> O	60°C	4	98

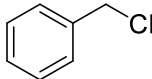
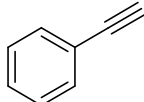
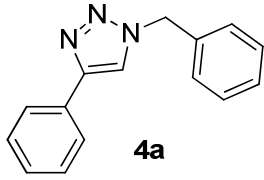
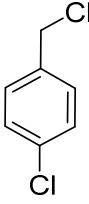
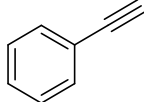
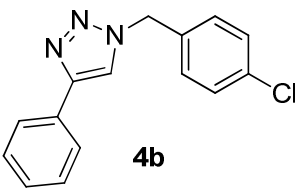
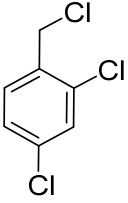
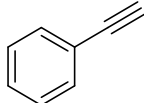
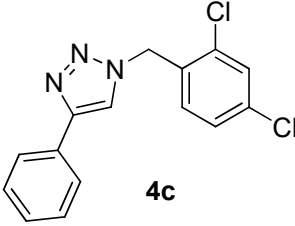
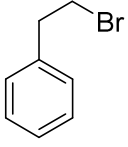
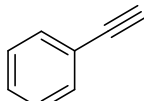
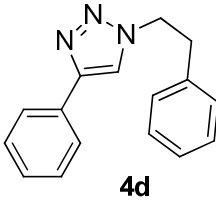
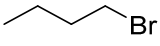
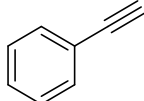
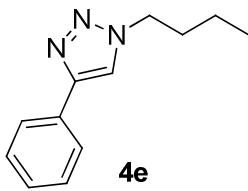
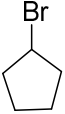
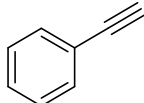
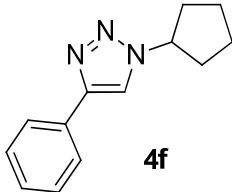
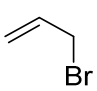
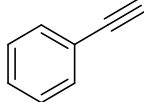
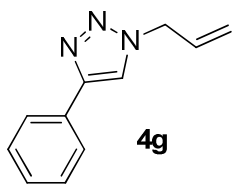
Reaction conditions: benzyl chloride(1 mmol), NaN<sub>3</sub> (1.5 mmol), phenyl acetylene (2 mmol) and solvent (5 ml)

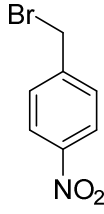
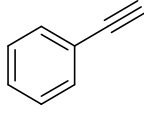
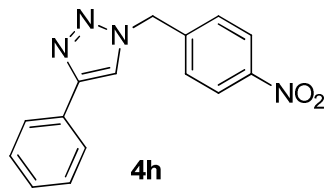
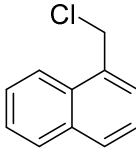
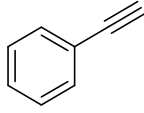
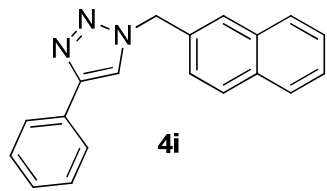
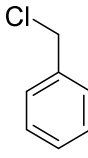
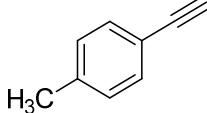
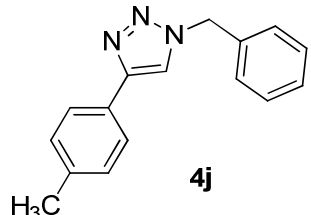
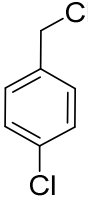
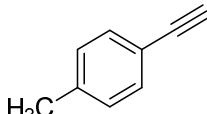
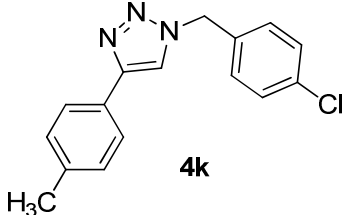
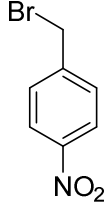
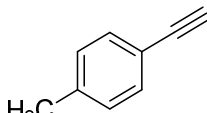
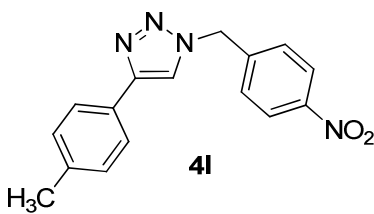
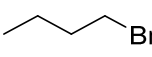
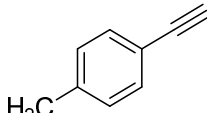
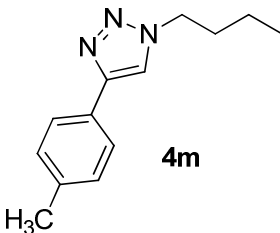


**Scheme 2**



**Table 2** Synthesis of 1,4-disubstituted 1,2,3-triazole using alkyl/aryl halides and alkyne

Sl No.	RX	R'	Product	Yield
1			 <b>4a</b>	98
2			 <b>4b</b>	95
3			 <b>4c</b>	91
4			 <b>4d</b>	98
5			 <b>4e</b>	85
6			 <b>4f</b>	80
7			 <b>4g</b>	90

8			 <b>4h</b>	97
9			 <b>4i</b>	90
10			 <b>4j</b>	92
11			 <b>4k</b>	90
12			 <b>4l</b>	91
13			 <b>4m</b>	84

Reaction conditions: organic halide(1 mmol), NaN<sub>3</sub> (1.5 mmol), alkyne (2 mmol) and CuONPs (10 mg) in water (5 ml) at 60 °C for 5h

Substituents present on both azide and alkyne shows a little effect in the overall yield of products. Among the electron withdrawing substituents Cl<sup>-</sup> and NO<sub>2</sub>, chlorine possess much more effect on decreasing the yield of the reaction (**Table 2, entry 2, 3 & 11**). A drastic decrease in the yield was observed as the azide

changes from aryl to alkyl (Table 2, entry 5, 6 & 11). Presence of substituent on alkyne also influences the reaction. Electron releasing substituent decreases the yield (Table 2, entry 10, 11, 12 & 13).

Reusability of the catalyst was also studied using the same model reaction under same reaction conditions. Insolubility of CuO in water made the easy recovery of the catalyst by simple filtration. Organic impurities which may present in the surface of catalyst were removed by washing with water and acetone followed by drying in vacuum oven at 70 °C for 3 h. Recovered catalyst can be reused four times with slight decrease in the yield (Table 3, Fig 9).

**Table 3** Reusability of CuO NPs

	Yield (%)
Native	98
1	95
2	91
3	90
4	87

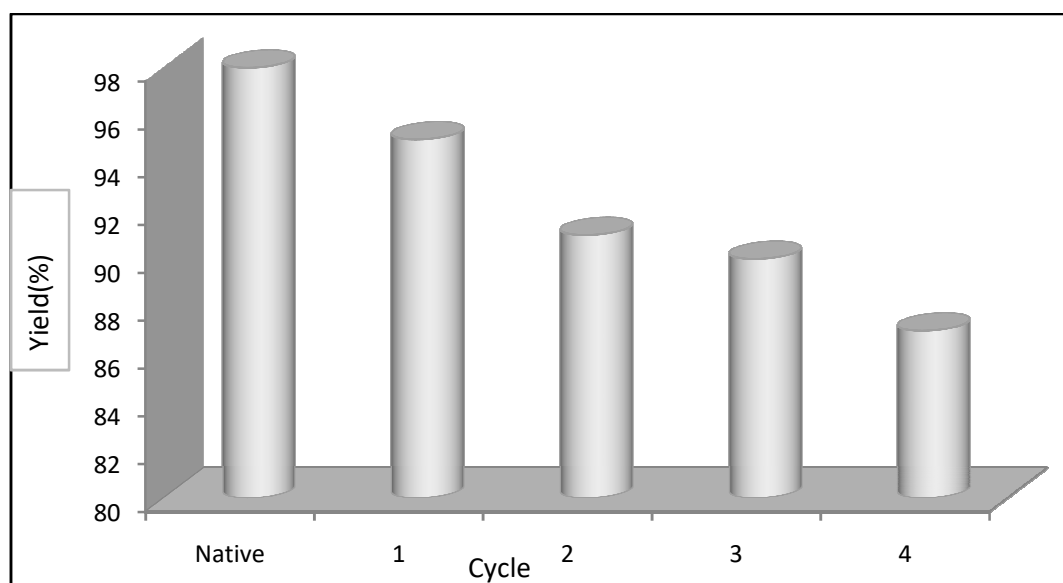
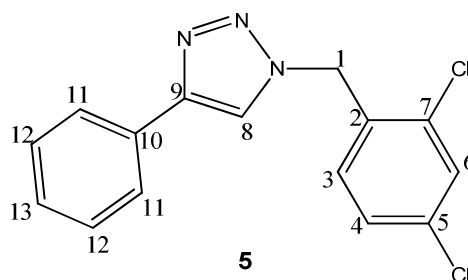


**Fig 9** Reusability of CuO NPs in CuAAC reaction

#### 4.4.9 Characterization of 1,4-disubstituted 1,2,3-triazoles

For the general discussion, the compound 1-(2,4-dichlorobenzyl)-4-phenyl-1H-1,2,3-triazole **5** was taken as a representative molecule.



The FT-IR spectrum (**Fig 10**) of the compound gives major absorptions at 1452, 1209, 839  $\text{cm}^{-1}$  corresponds to  $-\text{CH}_2$ ,  $\text{N}=\text{N}=\text{N}$ - and  $=\text{C}-\text{H}$  stretching of triazole ring.

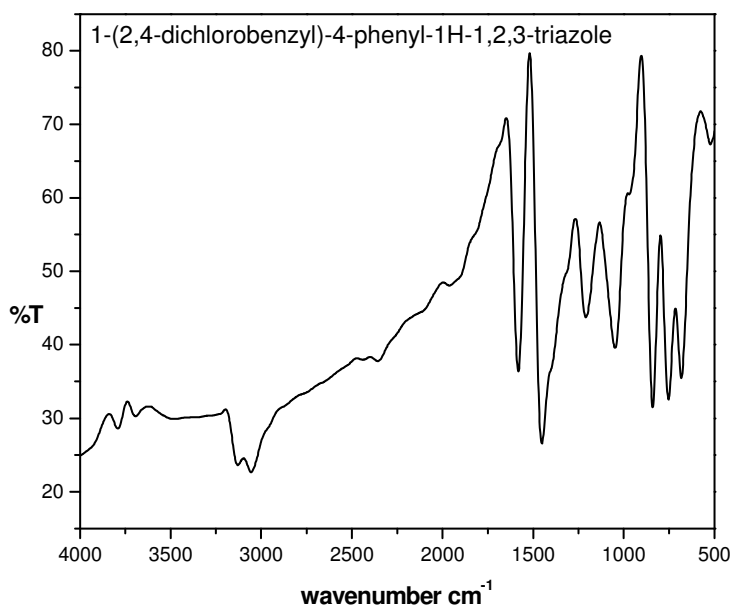


**Fig 10** FTIR spectrum of 1-(2,4-dichlorobenzyl)-4-phenyl-1H-1,2,3-triazole

Structure of the triazole was further confirmed by  $^1\text{H}$  NMR spectrum (**Fig. 11**). The  $-\text{CH}_2$  proton of benzyl is observed as two proton singlet at  $\delta$  5.70. Proton at C3 (3) gives a doublet at  $\delta$  7.49, whereas proton at C4 provide peak at  $\delta$  7.20 and at C6 provides doublet at  $\delta$  7.36. The characteristic  $=\text{C}-\text{H}$  proton at C8 and ortho phenylic

proton at C11 provide triplet at  $\delta$  7.83. Meta protons at C12 of phenyl group gives peak at  $\delta$ 7.43 and the C13 para proton at  $\delta$ 7.28.

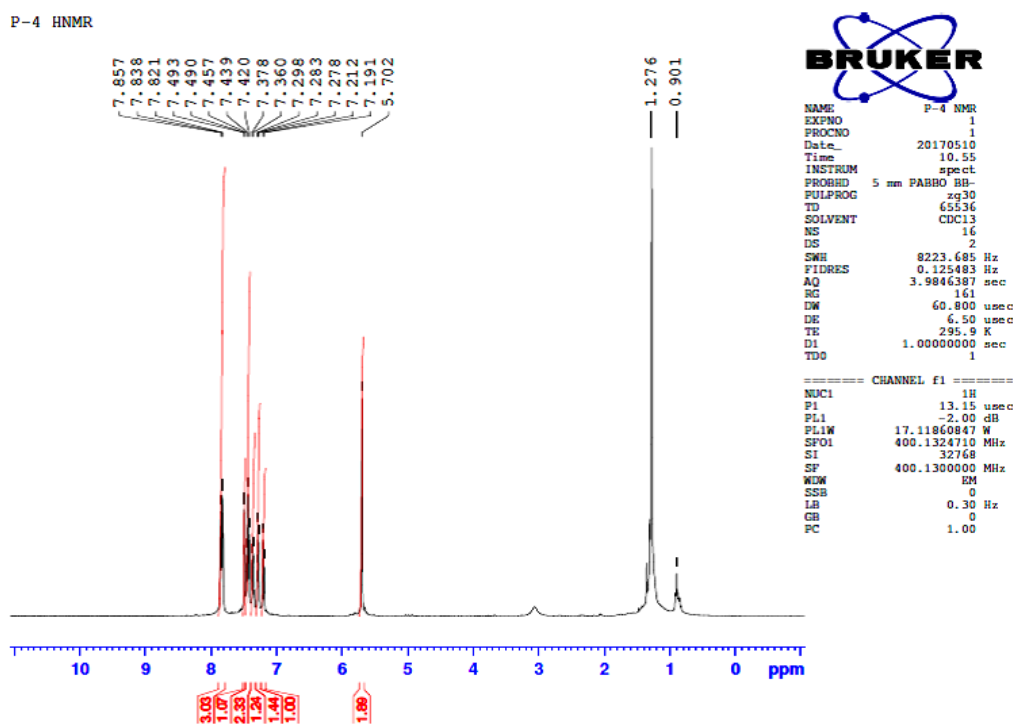


**Fig. 11**  $^1\text{H}$  NMR spectrum of 1-(2,4-dichlorobenzyl)-4-phenyl-1H-1,2,3-triazole

The  $^{13}\text{C}$  NMR spectrum (**Fig 12**) is in agreement with both  $^1\text{H}$  NMR and FT-IR data. The downfield peak at  $\delta$  148.0 is due to the carbon at the position 9. The characteristic peak of triazole carbon (C8) that is directly bonded to hydrogen was observed at  $\delta$ 119.9 confirms the formation 1,4-disubstituted triazoles.<sup>96</sup> The benzylic carbon C1 gives peak at  $\delta$ 51.9 and the values at 135.7, 128.0, 128.5, and 134.1, 134.1 attributed to the phenyl carbons C2, C3, C4, C5 and C7 carbons. Both C6 and C10 show peak at  $\delta$ 129.85. Other peaks at 125.8, 128.7 and 128.9 are respectively the ortho, meta and para carbons of phenyl ring.

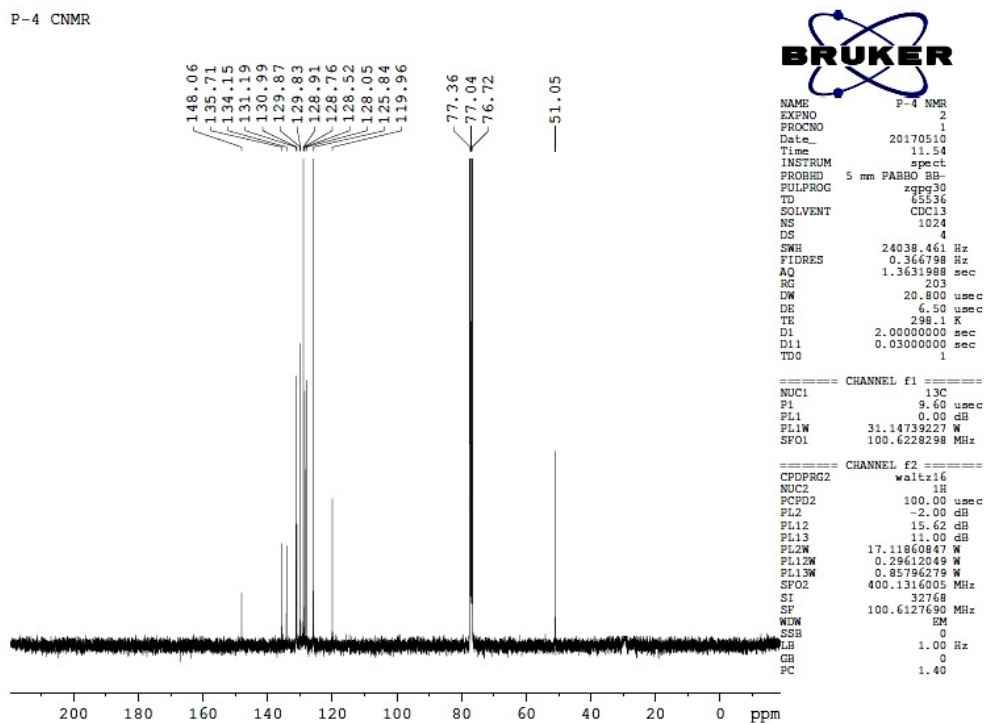


**Fig. 12**  $^{13}\text{C}$  NMR spectrum of 1-(2,4-dichlorobenzyl)-4-phenyl-1H-1,2,3-triazole

The structure of the compound was further confirmed by mass spectral analysis. The molecular ion peak ( $M^+$ ) observed at  $m/z$  303 (10), 307.03 ( $M+4$ ), 116 ( $M-\text{C}_7\text{H}_6\text{Cl}_2\text{N}_2$ ) (**Fig. 13**).

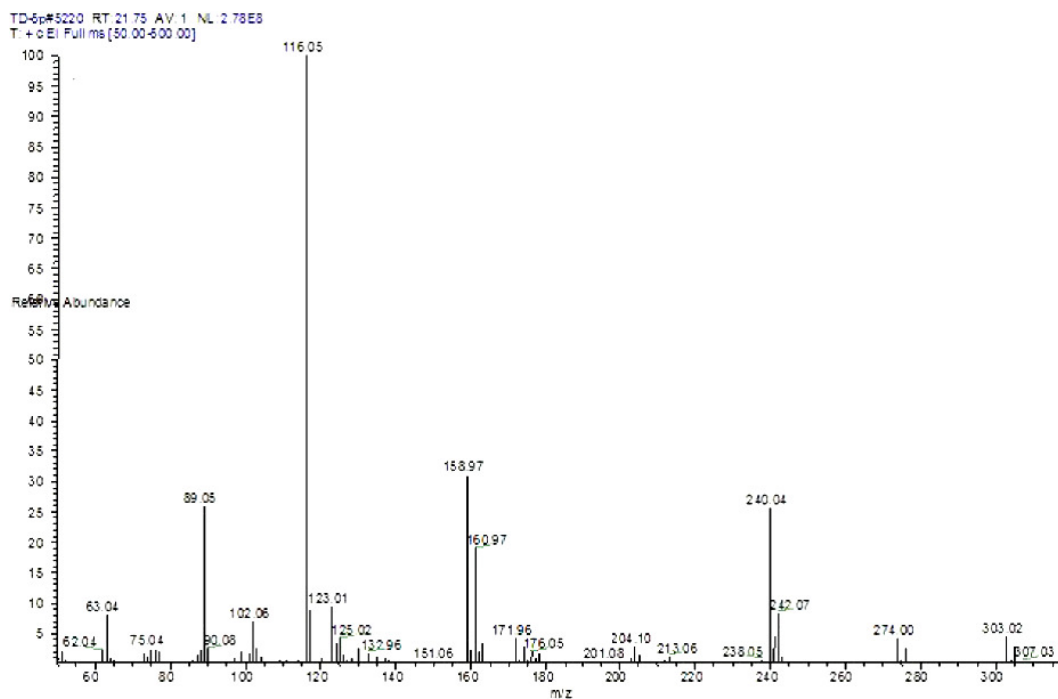
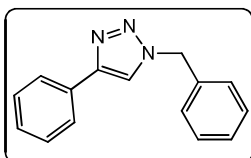


**Fig 13** Mass spectrum of 1-(2,4-dichlorobenzyl)-4-phenyl-1H-1,2,3-triazole

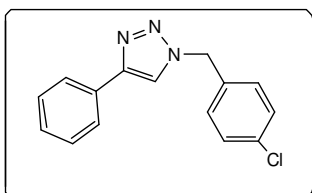
## 4.5 Spectral data of 1,4-disubstituted 1,2,3,-triazoles

### 1. 1-Benzyl-4-phenyl-1*H*-1,2,3-triazole (4a)



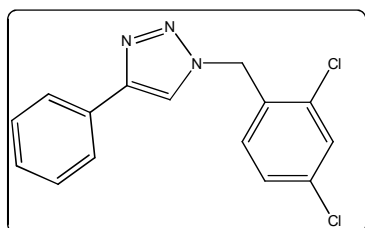
$^1\text{H}$  NMR (400 MHz,  $\text{CDCl}_3$ ):  $\delta$  5.29(s,2H), 7.18(d,2H,  $J=7.2\text{Hz}$ ), 7.30(t,1H), 7.38 (m, 2H), 7.42(t,1H), 7.64(s,1H), 7.66(dd,2H), 7.44(m,2H).  $^{13}\text{C}$  NMR (100.6 MHz,  $\text{CDCl}_3$ ):  $\delta$  52.7, 119.4, 125.7, 127.8, 128.6, 128.7, 128.9, 128.9, 129.1, 135.1, 147.3. Mass  $m/z$  (%): 235.08 ( $\text{M}^+$ ). FTIR (KBr): 3110, 3100, 3052, 3020, 2950, 1492, 1462, 1420, 1343, 1220, 1180, 1070, 1085, 1020, 940, 825, 810, 757, 690, 475  $\text{cm}^{-1}$

### 2. 1-(4-chlorobenzyl)-4-phenyl-1*H*-1,2,3-triazole (4b)



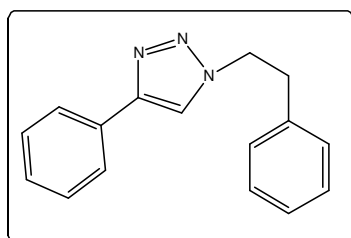
$^1\text{H}$  NMR (400 MHz,  $\text{CDCl}_3$ ):  $\delta$  5.45(s,2H), 7.18(d,3H,  $J=7.2\text{Hz}$ ), 7.36-7.28(m,6H), 7.78(s,1H).  $^{13}\text{C}$  NMR (100.6 MHz,  $\text{CDCl}_3$ ):  $\delta$  51.2, 119.4, 125.2, 128, 128.6, 129.5, 130.9, 132.4, 133.8, 135, 149.2. Mass  $m/z$  (%): 269 ( $\text{M}^+$ , 10), 271 ( $\text{M}^++2$ , 4), 116 (100), 125(44). FTIR (KBr): 3107, 3082, 3064, 3034, 2933, 1492, 1462, 1411, 1350, 1220, 1143, 1091, 1080, 1016, 975, 819, 804, 763, 688, 495  $\text{cm}^{-1}$

### 3. 1-(2,4-dichlorobenzyl)-4-phenyl-1*H*-1,2,3-triazole (4c)



$^1\text{H}$  NMR (400MHz,  $\text{CDCl}_3$ )  $\delta$ : 5.67 (s 2H), 7.16 (s, 1H), 7.25–7.46 (m, 4H), 7.88 (s, 3H).  $^{13}\text{C}$  NMR (100.6MHz,  $\text{CDCl}_3$ )  $\delta$ : 50.8, 119.8, 125.7, 127.9, 128.2, 128.8, 129.7, 130.3, 131, 131.3, 134.1, 135.5, 148.2; Mass  $m/z$  (%): 303 ( $\text{M}^+$ , 5), 305 ( $\text{M}^++2$ , 3), 240, 158, 116 (100).

### 4. 4-phenyl- 1-(2-phenylethyl)-1*H*-1,2,3-triazole (4d)

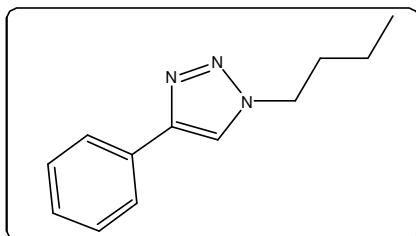


$^1\text{H}$  NMR (400 MHz,  $\text{CDCl}_3$ ):  $\delta$  3.30 (t, 2H,  $J = 7.2\text{Hz}$ ), 4.71 (t, 2H,  $J = 7.6\text{Hz}$ ), 7.20 (d, 1H,  $J=6.8$ ), 7.30–7.36 (m, 3H), 7.42 (t, 2H,  $J = 7.2\text{Hz}$ ), 7.50 (s, 1H), 7.81 (d, 2H,  $J = 6.8\text{Hz}$ ).  $^{13}\text{C}$  NMR (100.6 MHz,  $\text{CDCl}_3$ )  $\delta$ : 52.7, 37.3, 120.1, 122.0, 125.7, 127.5, 128.2, 128.7, 128.8, 131.7, 137.5, 148.2.



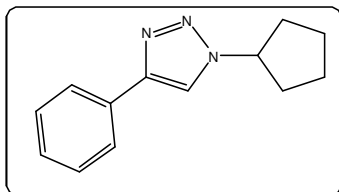
Mass  $m/z$  (%): 249 ( $M^+$ , 35), 220 (18), 193 (13), 179 (8), 130 (34), 118 (71), 105(100), 77 (42), 51 (8). FTIR (KBr): 3107, 3028, 1683, 1483, 1450, 1365, 1220, 1080, 1043, 94, 910, 844, 734, 690  $\text{cm}^{-1}$

### 5. 1-Butyl-4-phenyl-1H-1,2,3-triazole (4e)



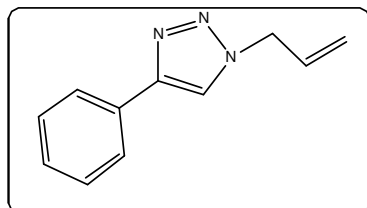
$^1\text{H}$ NMR (400 MHz,  $\text{CDCl}_3$ ):  $\delta$  0.98(t, 3H,  $J = 7.2\text{Hz}$ ), 1.40–1.46 (m, 2H), 1.80–1.85(m, 2H), 4.60(t, 2H,  $J = 7.2\text{Hz}$ ), 7.40(d, 1H,  $J=7.2\text{Hz}$ ) 7.51(t, 2H,  $J=7.2\text{Hz}$ ), 7.80 (s, 1H), 7.89 (d, 2H,  $J=7.2\text{Hz}$ ).  $^{13}\text{C}$  NMR (100.6MHz,  $\text{CDCl}_3$ ):  $\delta$  12.9, 20.2, 31.9, 50.5, 119.6, 125, 128.8, 129.2, 131.2, 148.2. Mass  $m/z$  (%): 201 ( $M^+$ , 33), 145 (16), 117 (100), 90 (24). FTIR (KBr): 3062, 2947, 2870, 1460, 1367, 1215, 1066, 761, 692  $\text{cm}^{-1}$

### 6. 1-cyclopentyl-4-phenyl-1H-1,2,3-triazole (4f)



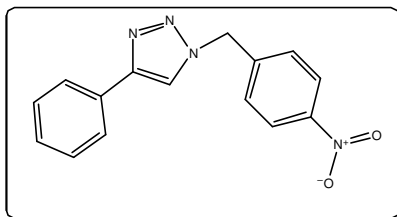
$^1\text{H}$ NMR (400 MHz,  $\text{CDCl}_3$ ):  $\delta$  1.76–1.7 (m, 2H), 1.91–1.95 (m, 2H), 2.05–2.12 (m, 2H), 2.26–2.31 (m, 2H), 4.94–5.01 (m, 1H), 7.31 (t, 1H,  $J = 7.2\text{Hz}$ ), 7.39 (m, 2H), 7.82 (s, 1H), 7.83 (dd, 2H,  $J=7.7, 1.55$ ).  $^{13}\text{C}$  NMR (100.6 MHz,  $\text{CDCl}_3$ ):  $\delta$  23.6, 32.1, 58.8, 119, 125.7, 128.0, 128.7, 129.1, 147.3. Mass  $m/z$  (%): 213 ( $M^+$  33), 184, 156, 117 (100).

### 7. 1-allyl-4-phenyl-1H-1,2,3-triazole (4g)



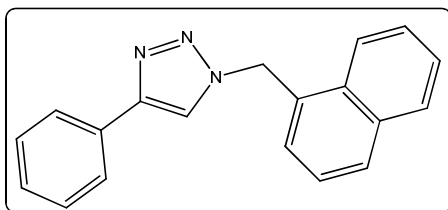
$^1\text{H}$ NMR (400 MHz,  $\text{CDCl}_3$ ):  $\delta$  5.02(dd, 1H,  $J = 16.4\text{Hz}$ ), 5.36(dd, 1H,  $J= 10\text{Hz}$ ), 6.01–6.11 (m, 1H), 7.31–7.44 (m, 3H), 7.76 (s, 1H), 7.83(d, 2H,  $J = 7.6\text{Hz}$ ).  $^{13}\text{C}$  NMR(100.6MHz,  $\text{CDCl}_3$ ):  $\delta$  47.6.7, 117.6, 120.2, 125.7, 128.7, 128.9, 129.1, 131.3, 147.3. Mass  $m/z$ (%): 185( $M^+$ , 19), 116(100). FTIR (KBr): 3120, 3088, 2934, 2854, 1645, 1608, 1460, 1334, 1219, 1166, 1049. 985, 914, 825, 765, 690, 509  $\text{cm}^{-1}$

## 8. 1-(4-Nitrobenzyl)-4-phenyl-1H-1,2,3-triazole (4h)



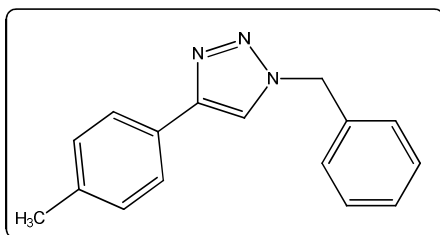
$^1\text{H}$ NMR (400 MHz,  $\text{CDCl}_3$ ):  $\delta$  5.69 (s, 2H), 7.34-7.45(m,5H), 7.76(s, 1H), 7.80(d, 2H,  $J = 7.6\text{Hz}$ ), 8.22(d, 2H,  $J = 8\text{Hz}$ ).  $^{13}\text{C}$  NMR (100.6MHz, $\text{CDCl}_3$ ):  $\delta$  52.7, 119.7, 124.3, 125.7, 128.5, 128.9,129.1, 135, 140.5, 147.3. Mass, $m/z$  (%): 281 ( $\text{M}^+$ , 19), 207 (44), 116 (100), 106 (24), 89 (43). FTIR (KBr): 3118, 3080, 2939, 2857, 1600, 1517, 1429, 1346, 1209, 1107, 1074, 1305, 844, 815, 761, 729, 686  $\text{cm}^{-1}$

## 9. 1-(naphthyl)-4-phenyl-1H-1,2,3-triazole (4i)



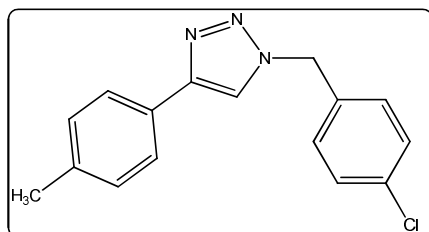
$^1\text{H}$ NMR (400 MHz,  $\text{CDCl}_3$ ):  $\delta$  5.91(s, 2H), 7.37-7.44 (m, 5H), 7.65 (m, 2H),7.81 (m, 2H), 7.90 (m, 3H) 7.91 (s, 1H).  $^{13}\text{C}$  NMR (100.6MHz,  $\text{CDCl}_3$ ):  $\delta$  55.3,119.7, 124.2, 125.6, 125.8, 126.5, 126.9, 127.5, 128.2, 129.3, 129.7, 130.1, 132.6, 133.5, 133.9, 134.0,. Mass  $m/z$  (%): 284 ( $\text{M}^+$ , 5), 253 (10), 207 (98), 115 (90), 84(100). FTIR (KBr); 3115, 2924, 2848, 1454, 1431, 1344, 1307, 1211, 114, 1080, 1037, 974, 912, 842, 771, 688  $\text{cm}^{-1}$

## 10. 1-(benzyl)-4(p-tolyl)-1H-1,2,3-triazole (4j)



$^1\text{H}$ NMR (400 MHz,  $\text{CDCl}_3$ ):  $\delta$  2.38 (s, 3H), 5.58 (s, 2H), 7.22 (d, 2H,  $J = 7.6\text{Hz}$ ), 7.32-7.41(m, 5H), 7.66 (1H, s), 7.71 (d, 2H,  $J = 8.4\text{Hz}$ ).  $^{13}\text{C}$  NMR (100.6MHz,  $\text{CDCl}_3$ ):  $\delta$  148.14, 138.18, 134.62,129.52, 129.17, 128.82, 128.1, 127.41, 125.68, 54.33, 21.33. Mass  $m/z$  (%): 249( $\text{M}^+$ , 15), 220(63), 130(100), 91(72), 77(18) FTIR (KBr): 3138, 3008, 2902, 1446, 1342, 1213, 1122, 1045, 968, 788, 713, 584, 512  $\text{cm}^{-1}$

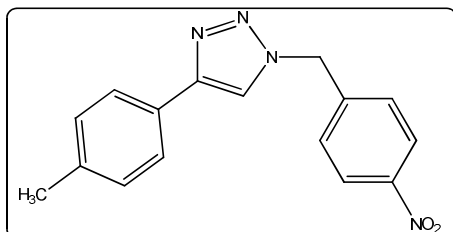
## 11. 1-(4-chlorobenzyl)-4-(p-tolyl)-1H-1,2,3-triazole (4k)



$^1\text{H}$ NMR (400 MHz,  $\text{CDCl}_3$ ):  $\delta$  2.38 (s, 3H), 5.55 (s, 2H), 7.22-7.28(m,3H) 7.37(d,2H,  $J = 8.4\text{Hz}$ ), 7.67 (s, 1H), 7.71 (d, 2H,  $J = 8\text{Hz}$ )  $^{13}\text{C}$

NMR (100.6MHz, CDCl<sub>3</sub>):  $\delta$  24.3, 57.0, 125.6, 127.4, 128.8, 129.6, 130.1, 131.3, 134.4, 138.4, 146.3. Mass  $m/z$  (%): 283 (M<sup>+</sup>, 12), 254 (35), 130(100). FTIR (KBr): 3113, 3012, 2953, 1485, 1436, 1334, 1207, 1080, 1033, 808, 750, 507 cm<sup>-1</sup>

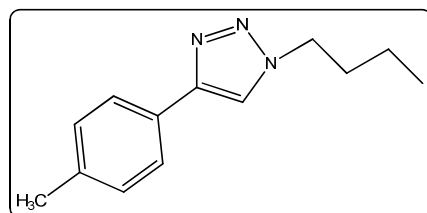
### 12. 1-(4-Nitrobenzyl)-4-(p-tolyl)-1H-1,2,3-triazole (4l)



<sup>1</sup>H NMR (400 MHz, CDCl<sub>3</sub>):  $\delta$  2.39 (s, 3H), 5.71 (s, 2H), 7.24 (d, 2H,  $J = 7.6$ Hz), 7.46 (d, 2H,  $J = 8.4$ Hz), 7.72 (d, 2H,  $J = 8$ Hz), 7.77 (s, 1H) 8.24 (d, 2H,  $J = 8.4$ Hz). <sup>13</sup>C

NMR(100.6MHz, CDCl<sub>3</sub>):  $\delta$  24.3, 57.0, 121.0, 125.7, 127.4, 129.6, 130.1, 138.4, 145.4, 146.3. Mass  $m/z$  (%): 294(M<sup>+</sup> 9), 281 (25), 207 (70), 130 (100). FTIR (KBr): 3088, 3034. 2924, 2856, 1602, 1516, 1444, 1344, 1213, 1101, 1039, 972, 810, 723, 513 cm<sup>-1</sup>

### 13. 1-Butyl-4-(p-tolyl)-1H-1,2,3-triazole (4m)



<sup>1</sup>H NMR (400 MHz, CDCl<sub>3</sub>):  $\delta$  0.89 (t, 3H,  $J = 7.2$ Hz), 1.29-1.34 (m, 2H), 1.87 (m, 2H), 2.30 (t, 3H,  $J = 6.4$ Hz), 4.34 (s, 3H), 7.06-7.18 (m,

3H), 7.33 (m, 2H), 7.73 (s, 1H). <sup>13</sup>C NMR (100.6MHz, CDCl<sub>3</sub>):  $\delta$  13.8, 20.3, 24.3, 30.6, 52.2, 119.7, 125.6, 127.5, 129.2, 130.1, 138.4. Mass  $m/z$  (%): 215 (M<sup>+</sup>, 40), 159(30), 144 (35), 131(100).

## **4.6 Sunlight induced rapid synthesis of silver nanoparticles**

Sunlight is believed to be the largest natural, renewable energy source which is non-toxic and non-polluting. Earlier reports imply that, in nanoparticle synthesis sunlight act as catalyst in presence of reducing agents which is believed to cause photo-excitation process.<sup>97-99</sup>

### **4.6.1 Visual Inspection of silver nanoparticle**

*Myristica fragrans* fruit extract was added to silver nitrate solution. In dark conditions, the color of the solution remains unchanged even after 24h. After the exposure to sunlight the color of the solution changes from yellow to brown within 10 min of incubation due to the formation of silver nanoparticle (**Fig 14**).

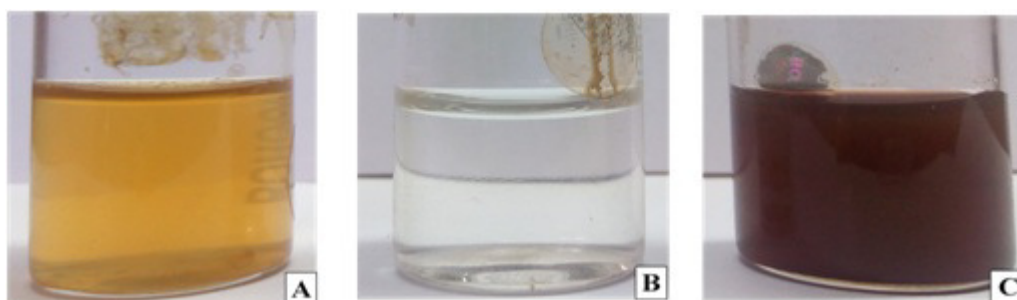


**Fig 14** Photographs of A) *Myristica fragrans* fruit extract B)  $\text{AgNO}_3$  solution C) Reaction mixture containing silver nanoparticle

### **4.6.2 UV-Visible spectral studies of silver nanoparticle**

The gradual color change from yellow to brown is attributed to the reduction of  $\text{Ag}^+$  to  $\text{Ag}^0$ . The final brown color is due to the formation of silver nanoparticle which was due to the surface plasmon vibrations of the synthesized nanoparticle and the SPR band was observed at 478 nm (**Fig 15**). The emergence of surface plasmon resonance can be explained as follows; the metallic silver contains large number of conducting electron and the united oscillation of these conducting electrons results the excitation of local surface plasmon resonances leading to the strong light scattering by the electric field at wavelength of resonance occurred.<sup>66</sup> The difference in the absorption range depends on the size and shape of nanoparticle.

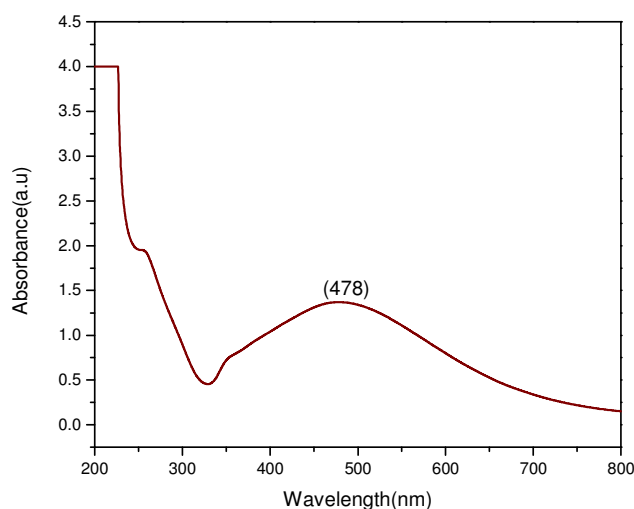


**Fig. 15** UV- Visible spectrum of Ag NPs

#### 4.6.3 Infrared Spectral studies

FT-IR spectrum of silver nanoparticle is given in **Fig 16**. It again confirms the presence of eugenol in the synthesized nanoparticle. Band at 673 and 744  $\text{cm}^{-1}$  corresponds to aromatic-CH out of plane bending vibration. Bending vibration of =C-H was observed at both 906 and 909  $\text{cm}^{-1}$ . C-O-C stretching vibration of ether was observed at 1026  $\text{cm}^{-1}$  and that of  $-\text{CH}_2$  bending observed at 1421  $\text{cm}^{-1}$ .  $-\text{C-H}$  stretching vibration was observed at 2843 and 2920  $\text{cm}^{-1}$  and phenolic  $-\text{OH}$  observed at 3244  $\text{cm}^{-1}$ .

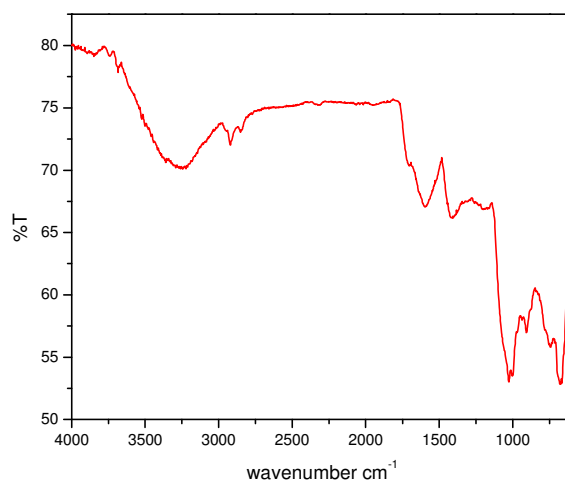


**Fig. 16** FT-IR spectrum of Silver nanoparticle

#### 4.6.4 Powder X-ray Diffraction Analysis

The diffractogram is as shown in **Fig 17**. From this formation of silver nanoparticle was confirmed. The two theta values at  $38.4^\circ$ ,  $44.6^\circ$ ,  $64.8^\circ$ ,  $77.6^\circ$  corresponds to (1 1 1), (0 0 2), (0 2 2) and (1 1 3) reflection of face centered cubic silver crystal (JCPDS No: 00-004-0783). Due to longer exposure to atmospheric oxygen silver nanoparticle gets oxidized to silver oxide with two theta values  $32.5^\circ$ ,  $46.5^\circ$ ,  $55.1^\circ$  and  $57.8^\circ$  indexed as (1 1 1), (1 1 2), (0 2 2) and (1 2 2) planes of silver corresponds to cubic crystal structure (JCPDS No :98-017-4092).

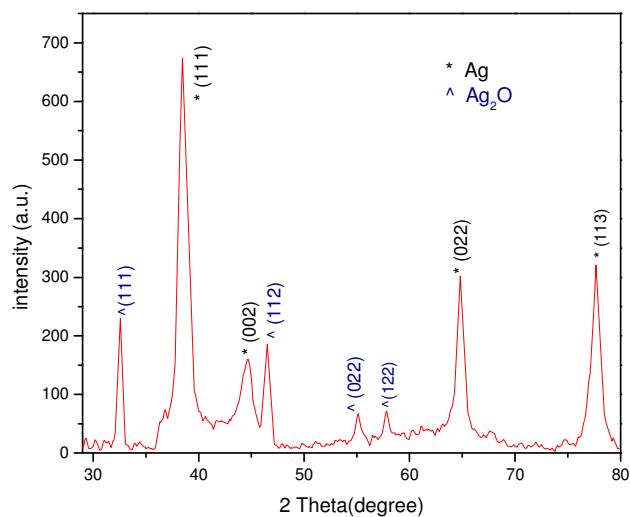


**Fig. 17** XRD pattern of Ag NPs

#### 4.6.5 Energy Dispersive X-ray Spectroscopy (EDS) Analysis

The EDX analysis provides both qualitative and quantitative information about elements involved in the formation of silver nanoparticle (**Fig 18**). The peak at 3keV due to silver with wt% of 32.7% confirms the presence of silver nanoparticle which may be attributed to their surface plasmon resonance<sup>100</sup>. The elemental profile of other elements due to the existence of biomolecules and micronutrients associated with plant extract.

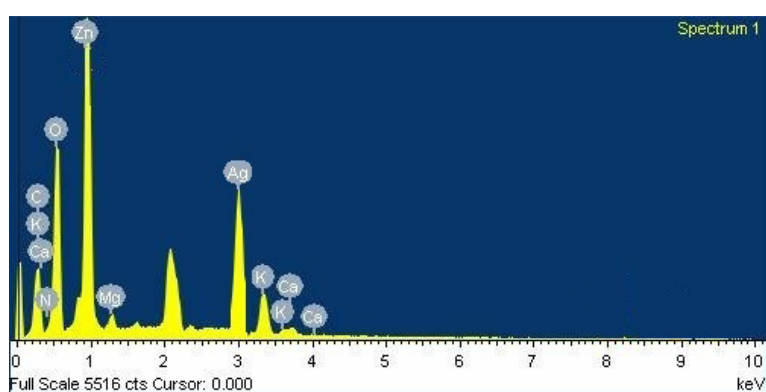


**Fig.18** EDS spectrum of Silver nanoparticle

#### 4.6.6 High resolution transmission electron microscopy (HR-TEM) analysis

The HR-TEM images and SAED pattern (**Fig 19**) clearly indicate the shape and size distribution of silver nanoparticle. The images show that the nanoparticles are capped with phytoconstituents. It was observed that the silver nanoparticle formed with random shapes includes spherical, hexagonal, triangular, rod etc. The average size of spherically shaped nanoparticle was found to be 31.31 nm.

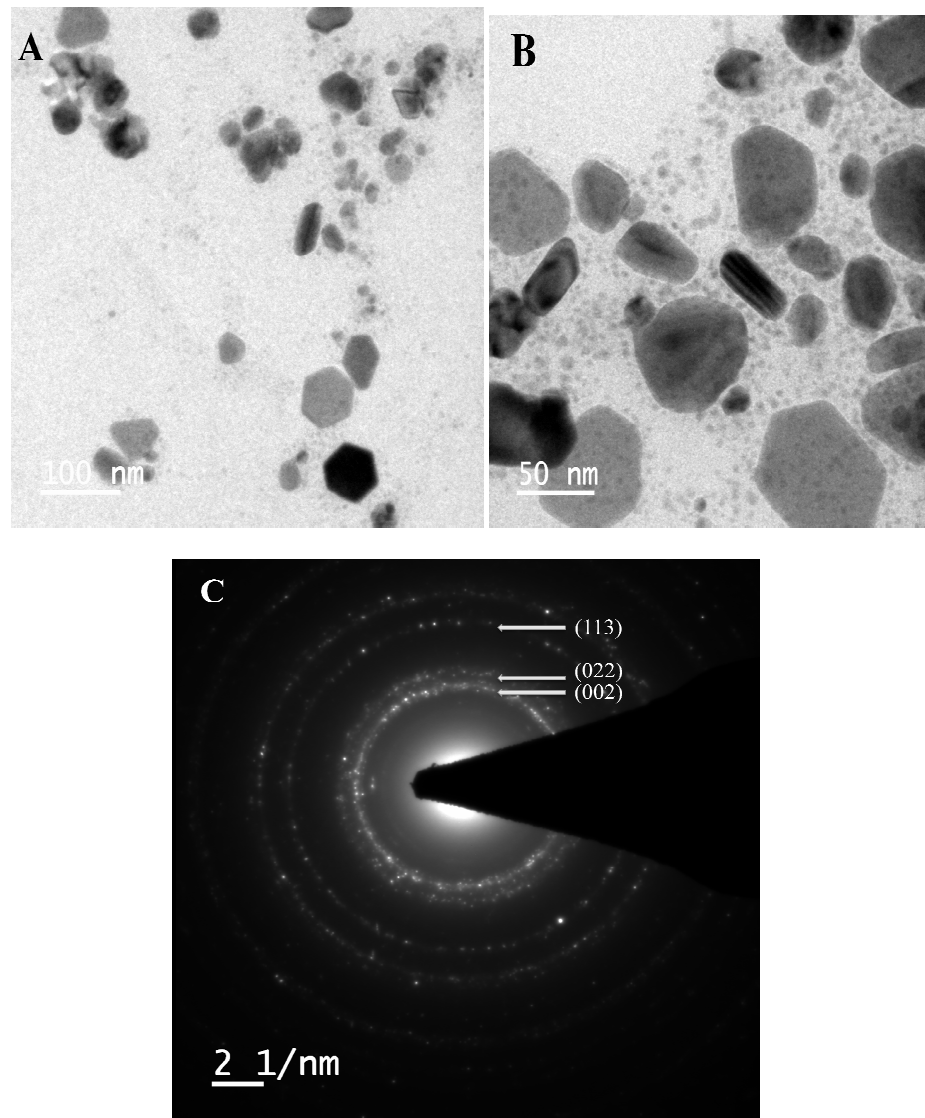


**Fig 19** HR-TEM images of silver nanoparticle at different magnification(A&B), SAED pattern(C)

The SAED pattern had ring with bright spots that indicates the nanocrystalline nature of silver nanoparticle. Each ring corresponds to 'd' value and the SAED patterns of (002), (022) and (113) was observed and thus confirms the formation of silver nanoparticle by this method.



#### 4.6.7 Catalytic activity of silver nanoparticle in Azide-Alkyne cycloaddition

The catalytic activity of silver nanoparticle in azide-alkyne cycloaddition reaction was also studied. In a typical reaction, 10 mmol each of benzyl chloride, sodium azide and phenyl acetylene were mixed with 2 mg of the silver nanoparticle as catalyst and heated at 70 °C for 5 h in water. The reaction was monitored by GCMS which shows a slight excess of 1,4-disubstituted-1,2,3-triazole in the product. Retention time of the copper catalysed reaction product 1-benzyl-4-phenyl-1,2,3-triazole (reported in third chapter of this thesis) was used here to differentiate the regioisomers. Optimization of the reaction with respect to solvent system was carried out by using solvents like water, acetic acid, THF, t-BuOH, DMSO, DMF and their binary mixtures (**Scheme 3**). Better yield of the 1,4-regioisomer was obtained when DMSO was used as the solvent (**Entry 6, Table 4**). Our efforts to synthesize either 1,4 or 1,5 regio isomer of the 1,2,3-triazole were not successful.

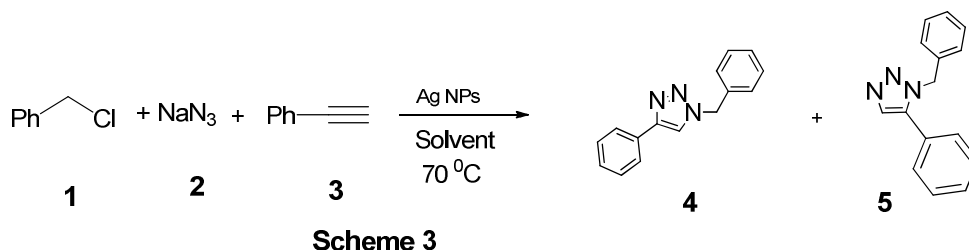


**Table 4** Optimization of solvent system for AgAAC reaction

Entry	Solvent	Conversion (4:5)
1	H <sub>2</sub> O	55:45
2	HAc	60:40
3	t-BuOH/H <sub>2</sub> O	60:40
4	H <sub>2</sub> O:THF	55:45
5	THF	65:35
6	DMSO	80:20
7	DMF	70:30

#### 4.6.8 Antibacterial and Antifungal effect of Silver nanoparticle

The antimicrobial activity of silver nanoparticle was tested using well diffusion method against multidrug resistant human pathogens such as gram negative bacteria *Escherichia coli*, *Pseudomonas aeruginosa* and gram positive bacteria *Staphylococcus aureus* and *Bacillus subtilis*(Fig.20). The bacterial culture spread uniformly over the nutrient agar plate and small discs of 3 mm diameter were cut from the surface. To each disc drugs were induced followed by the incubation at 37 °C for 24 h. Then zone of inhibition (mm) was then calculated. The generalized mechanism of interaction of silver ions with phosphorous moieties in DNA leads to the deactivation of DNA replication.<sup>101,102</sup> Zone of inhibition of silver nanoparticle is given in **Table 5**

**Table 5** Zone of inhibition of silver nanoparticle against bacterial strains

Drug (µl)	Zone of Inhibition(mm)			
	<i>Staphylococcus</i> (1)	<i>Bacillus</i> (2)	<i>Pseudomonas</i> (3)	<i>E.coli</i> (4)
Dist. Water	0	0	0	0
Streptomycin	16	22	14	11
50	13	0	13	14
100	15	0	15	15
150	22	10	16	19
200	24	14	21	22

Silver nanoparticle synthesized by green method was found to have better antibacterial activity against *Staphylococcus* (MTCC 3103) with maximum zone of inhibition of 24 mm for 200 µl whereas its effect was low for *Bacillus subtilis*(MTCC 869). 200 µl produces only 14 mm zone of inhibition. For gram negative bacteria *Escherichia coli* (MTCC 68), *Pseudomonas* (MTCC 2642) silver nanoparticle had almost equal activity in all concentrations. Pericarp extract doesn't shows any antibacterial activity against gram positive bacteria *Staphylococcus* and gram negative bacteria *Escherichia coli*.<sup>103</sup>

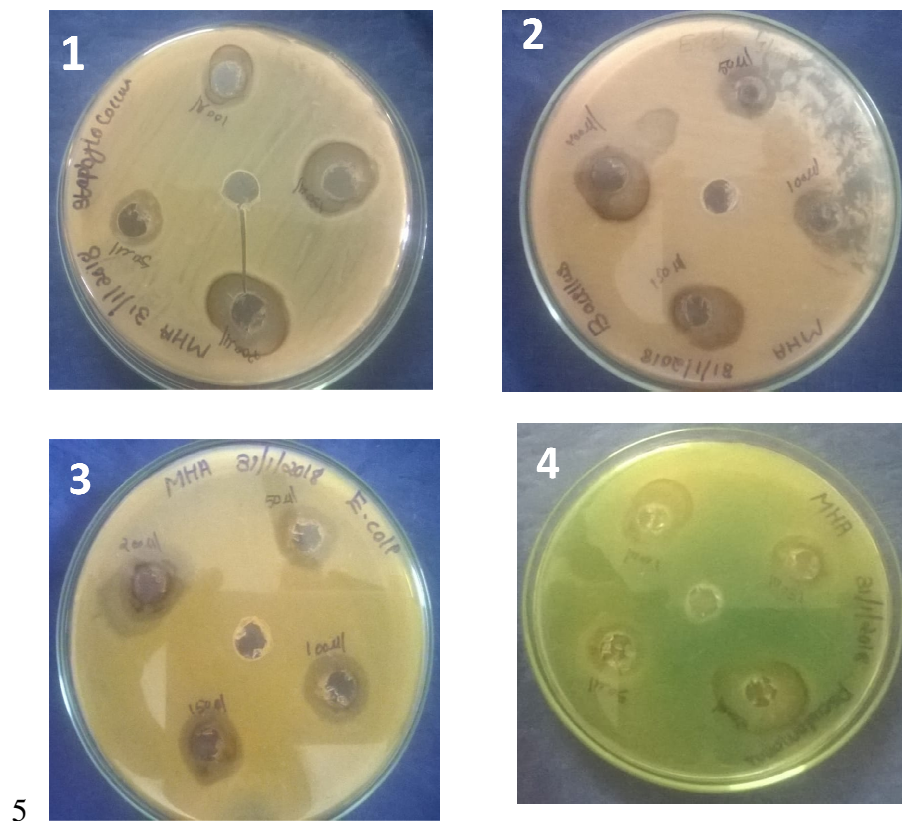


**Fig 20** Antimicrobial activity of AgNPs- *Myrsitca fragrans* against human pathogenic microorganisms using agar well diffusion method 1) *Staphylococcus sp.* 2) *Bacillus* 3) *E. coli* 4) *Pseudomonas*

Both surface Plasmon resonance and the antibacterial activity of silver nanoparticle depend on the size of the nanoparticle. When the size of the particle increases the surface plasmon resonance shifted to longer wavelength and the size of nanoparticle signifies that it had large surface area to interact with the microbes.<sup>104,105</sup> Thus smaller the particle size better will be the interaction. Similarly nanoparticles with different shape do have an effect on antimicrobial activity. Pal reported that for truncated triangular nanoparticle 1  $\mu\text{g}$  quantity show inhibition whereas spherical shaped particle needs a total silver content of 12.5  $\mu\text{g}$  and rod shaped particle needs 50 to 100  $\mu\text{g}$  of silver content.<sup>106</sup>

Antifungal activity of silver nanoparticle was measured using the well diffusion method against *Pencillium*, *Aspergillus*, *Rhizopus* and *Curvularia Sp.* Silver nanoparticle shows its activity only against *Pencillium Sp* with a maximum 24 mm of zone of inhibition.

## **4.7 Experimental details**

### **4.7.1 Preparation of *Myristica fragrans* fruit extract**

Around 500 g of fresh matured nutmeg fruit is collected from Nandipulam, Thrissur, Kerala. The fruit is separated from seed and washed with ordinary water. Then it is washed with deionised water 3 times. Then the fruit cut into small pieces and dried well in sun shade for four days, to remove the moisture completely. Dried nutmeg fruit is grounded to powder using a mortar and pestle.

Powdered Nutmeg (10 g) was mixed with distilled water (50 ml) and autoclaved at 110 °C for

2 h. Then allowed to cool to room temperature and filtered through Whatman no.1 filter paper which was then stored at 4 °C.

### **4.7.2 Green synthesis of CuO nanoparticles**

15 mM solution of copper acetate was prepared and stirred at room temperature for 5min followed by the drop wise addition of *Myristica fragrans* fruit extract (about 75 ml). The sample was divided into three portions, one kept for room temperature stirring, another for sonochemical synthesis and the last portion heated in microwave oven for 3 min. the sample under microwave heating produces a sudden color change from blue to green and then a greenish brown colored suspension further heating for 2 min provides black colored residue. The sample kept at room temperature doesn't produce any color change even after 24 h whereas sonicated sample produce a color change after 2 h but further sonication doesn't produce any brown colored suspension. The CuO nanoparticle obtained by microwave heating was recovered by centrifugation and washed with deionized water in order to remove plant biomass. The residue was dried in a vacuum oven at 70 °C for 6 h.

### **4.7.3 General procedure for azide-alkyne cycloaddition**

To a mixture of azide (1.5 mmol), alkyne (1.5 mmol) halides (1 mmol), CuONPs (0.1 g) and distilled water (1 ml) was added. The reaction was conducted both at room temperature for 24 h and by heating at 60 °C for 1 h. Ethyl acetate (1 ml) was added and the organic layer was separated out using extraction. The solvent was evaporated and purified by recrystallization from ethanol. The catalyst was recovered from aqueous layer and dried in vacuum oven at 70 °C for 3 h.

**4.7.4 Sunlight mediated synthesis of silver nanoparticle**

In a typical procedure, an aqueous solution of silver nitrate (50 ml, 1 mM) was mixed with *Myristica fragrans* (15 ml). The color of the solution remains unchanged when it is kept in dark for 24 h. On exposure to sunlight, the color of the solution changes to yellow and then to reddish brown within 10 min.

**4.7.5 Antibacterial activity by well diffusion method**

The bacterial cultures were maintained in nutrient broth. Each culture was uniformly distributed on nutrient agar plates. Wells of 3 mm diameter were cut on the surface of nutrient agar plates at a distance of 2 cm using sterile borer. Drugs of different concentrations were added in each well with a micropipette. Then these plates were incubated at 37 °C for 24 h.

**4.7.6 Antifungal activity by well diffusion method**

The fungal cultures were maintained in SD broth. Each culture was uniformly distributed on nutrient agar plates. Wells of 3mm diameter were cut on the surface of nutrient agar plates at a distance of 2 cm using sterile borer. Drugs of different concentrations were added in each well with a micropipette. These plates were incubated at room temperature for 6-7 days. The incubation of zone diameter was then measured.

**4.8 Conclusion**

In this chapter, we report eco-friendly and cost effective synthesis of copper oxide and silver nanoparticle using *Myristica fragrans* fruit extract. The CuO nanoparticle showed excellent catalytic activity towards CuAAC reaction and the products obtained in good yield. We have also synthesized silver nanoparticles using the same fruit extract. Silver nanoparticle exhibits better activity against *Staphylococcus*, *Pseudomonas* and *E.Coli* compared to standard Streptomycin

Advantages of using *Myristica fragrans* fruit extract for the synthesis of nanoparticle

- i) Act as stabilizing and reducing agent
- ii) Avoid the use of organic solvents
- iii) Less reaction time

## References

- (1) Choi, O.; Kanjun, K.; Kim, N.; Ross, L.; Surampalli, R. Y.; Hu, Z. The Inhibitory Effects of Silver Nanoparticles , Silver Ions , and Silver Chloride Colloids on Microbial Growth. *Water Res.* **2008**, *42*, 3066–3074.
- (2) Jeong, S. H.; Yeo, S. Y.; Yi, S. C. The Effect of Filler Particle Size on the Antibacterial Properties of Compounded Polymer / Silver Fibers. *J. Mater. Sci.* **2005**, *40*, 5407–5411.
- (3) Gawande, M. B.; Goswami, A.; Felpin, F.-X.; Asefa, T.; Huang, X.; Silva, R.; Zou, X.; Zboril, R.; Varma, R. S. Cu and Cu-Based Nanoparticles : Synthesis and Applications in Catalysis. *Chem. Rev.* **2016**, *116*, 3722–3811.
- (4) Das, D. Multicomponent Reactions in Organic Synthesis Using Copper Based Nanocatalyst. *Chem. Sel.* **2016**, *1*, 1959–1980.
- (5) Ranu, B. C.; Dey, R.; Chatterjee, T.; Ahammed, S. Copper Nanoparticle-Catalyzed Carbon À Carbon and Carbon À Heteroatom Bond Formation with a Greener Perspective. *Chem. Sustain. ChemSusChem Energy Mater.* **2012**, *22*–44.
- (6) Indira, K.; Mudali, U. K.; Rajendran, T. N. N. A Review on TiO<sub>2</sub> Nanotubes : Influence of Anodization Parameters , Formation Mechanism , Properties , Corrosion Behavior , and Biomedical Applications. *J. Bio- Tribo-Corrosion* **2015**, *1* (4), 1–22.
- (7) Fathima, J. B.; Pugazhendhi, A.; Venis, R. Synthesis and Characterization of ZrO<sub>2</sub> Nanoparticles-Antimicrobial Activity and Their Prospective Role in Dental Care. *Microb. Pathog.* **2017**, *110*, 245–251.
- (8) Sisubalan, N.; Ramkumar, V. S.; Pugazhendhi, A. ROS-Mediated Cytotoxic Activity of ZnO and CeO<sub>2</sub> Nanoparticles Synthesized Using the Rubia Cordifolia L . Leaf Extract on MG-63 Human Osteosarcoma Cell Lines. *environmental Sci. Pollut. Res.* **2017**, *25*, 10482–10492.
- (9) Liz-marz, L. M. Nanometals : Formation and Color. *Mater. Today* **2004**, *26*–

- 31.
- (10) LaMer, V. K.; Dinegar, R. H. Theory, Production and Mechanism of Formation of Monodispersed Hydrosols. *J. Am. Chem. Soc.* **1950**, *72*, 4847–4854.
- (11) Al-thabaiti, S. A.; Obaid, A. Y.; Khan, Z. Formation and Characterization of Surfactant Stabilized Silver Nanoparticles : A Kinetic Study. *Colloids Surfaces B Biointerfaces* **2008**, *67*, 230–237.
- (12) Bajpai, S. K.; Bajpai, M.; Gautam, D. In Situ Formation of Silver Nanoparticles in Hydrogels for Antibacterial Application In Situ Formation of Silver Nanoparticles in Regenerated Cellulose-Polyacrylic Acid ( RC-PAAc ) Hydrogels for Antibacterial Application. *Pure J. Macromol. Sci. Part A Pure Appl. Chem.* **2013**, *50*, 46–54.
- (13) Esumi, K.; Isono, R.; Yoshimura, T. Preparation of PAMAM - and PPI - Metal ( Silver , Platinum , and Palladium ) Nanocomposites and Their Catalytic Activities for Reduction of 4-Nitrophenol. *Langmuir* **2004**, *20*, 237–243.
- (14) Yin, B.; Ma, H.; Wang, S.; Chen, S. Electrochemical Synthesis of Silver Nanoparticles under Protection of Poly ( N -Vinylpyrrolidone ). *J. Phys. Chem. B* **2003**, *107*, 8898–8904.
- (15) Mayya, K. S.; Schoeler, B.; Caruso, F. Preparation and Organization of Nanoscale Polyelectrolyte-Coated Gold Nanoparticle. *Adv. Funct. Mater.* **2003**, *13*, 183–188.
- (16) Liu, M.; Lin, M. C.; Tsai, C. Y.; Wang, C. Enhancement of Thermal Conductivity with Cu for Nanofluids Using Chemical Reduction Method. *Int. J. Heat Mass Transf.* **2006**, *49*, 3028–3033.
- (17) Khanna, P. K.; Gaikwad, S.; Adhyapak, P. V; Singh, N.; Marimuthu, R. Synthesis and Characterization of Copper Nanoparticles. *Mater. Lett.* **2007**, *61*, 4711–4714.
- (18) Pillai, Z. S.; Kamat, P. V. What Factors Control the Size and Shape of Silver Nanoparticles in the Citrate Ion Reduction Method ? *J. Phys. Chem. B* **2004**, *108*, 945–951.

- (19) Dong, X.; Ji, X.; Wu, H.; Zhao, L.; Li, J.; Yang, W. Shape Control of Silver Nanoparticles by Stepwise Citrate Reduction. *J. Phys. Chem. C* **2009**, *113*, 6573–6576.
- (20) Ledwith, D. M.; Whelan, A. M.; Kelly, J. M. A Rapid , Straight-Forward Method for Controlling the Morphology of Stable Silver Nanoparticles. *J. Mater. Chem.* **2007**, *17*, 2459–2464.
- (21) Turkevich, J.; Stevenson, P. C.; Hillier, J. A Study of the Nucleation and Growth Processes in the Synthesis of Colloidal Gold. *Discuss. Faraday Soc.* **1951**, *11*, 55–75.
- (22) Xia, H.; Bai, S.; Hartmann, J.; Wang, D. Synthesis of Monodisperse Quasi-Spherical Gold Nanoparticles in Water via Silver ( I ) -Assisted Citrate Reduction. *Langmuir* **2010**, *26*, 3585–3589.
- (23) Stevenson, A. P. Z.; Bea, D. B.; Civit, S.; Contera, S. A.; Cerveto, A. I.; Trigueros, S. Three Strategies to Stabilise Nearly Monodispersed Silver Nanoparticles in Aqueous Solution. *Nanoscale Res. Lett.* **2012**, *7*, 1–8.
- (24) Krutyakov, Y. A.; Kudrinskiy, A. A.; Olenin, A. Y.; Lisichkin, G. V. Synthesis and Properties of Silver Nanoparticles : Advances and Prospects. *Russ. Chem. Rev.* **2008**, *77*, 233–257.
- (25) Qing-ming, L. I. U.; De-bi, Z.; Yamamoto, Y.; Ichino, R.; Okido, M. Preparation of Cu Nanoparticles with NaBH<sub>4</sub> by Aqueous Reduction Method. *Trans. Nonferrous Met. Soc. China* **2012**, *22*, 117–123.
- (26) Samal, A. K.; Sreepasad, Æ. T. S. Investigation of the Role of NaBH<sub>4</sub> in the Chemical Synthesis of Gold Nanorods. *J. Nanoparticle Res.* **2010**, *12*, 1777–1786.
- (27) Sun, Y.; Xia, Y. Large-Scale Synthesis of Uniform Silver Nanowires Through a Soft, Self-Seeding, Polyol Process. *Adv. Mater.* **2002**, *14*, 833–837.
- (28) Kawasaki, H. Surfactant-Free Solution-Based Synthesis of Metallic Nanoparticles toward Efficient Use of the Nanoparticles ' Surfaces and Their Application in Catalysis and Chemo- / Biosensing. *Nanotechnol. Rev.* **2013**, *2*,



5–25.

- (29) Kim, D.; Jeong, S.; Moon, J. Synthesis of Silver Nanoparticles Using the Polyol Process and the Influence of Precursor Injection. *Nanotechnology* **2006**, *17*, 4019–4024.
- (30) Zain, N. M.; Stapley, A. G. F.; Shama, G. Green Synthesis of Silver and Copper Nanoparticles Using Ascorbic Acid and Chitosan for Antimicrobial Applications. *Carbohydr. Polym.* **2014**, 195–202.
- (31) Biçer, M.; İlkay Şişman. Controlled Synthesis of Copper Nano / Microstructures Using Ascorbic Acid in Aqueous CTAB Solution. *Powder Technol.* **2010**, *198*, 279–284.
- (32) Qing-ming, L. I. U.; Yasunami, T.; Kuruda, K.; Okido, M. Preparation of Cu Nanoparticles with Ascorbic Acid by Aqueous Solution Reduction Method. *Trans. Nonferrous Met. Soc. China* **2012**, *22* (9), 2198–2203.
- (33) Xiong, J.; Wang, Y.; Xue, Q.; Wu, X. Synthesis of Highly Stable Dispersions of Nanosized Copper Particles Using L -Ascorbic Acid. *Green Chem.* **2011**, *13*, 900–904.
- (34) Lee, Y.; Choi, J.; Lee, K. J.; Stott, N. E.; Kim, D. Large-Scale Synthesis of Copper Nanoparticles by Chemically Controlled Reduction for Applications of Inkjet-Printed Electronics. *Nanotechnology* **2008**, *415604*, 1–7.
- (35) Dang, T. M. D.; Le, T. T. T.; Fribourg-Blanc, E.; Dang, M. C. The Influence of Solvents and Surfactants on the Preparation of Copper Nanoparticles by a Chemical Reduction Method. *Adv. Nat. Sci. Nanosci. Nanotechnol.* **2011**, *2*.
- (36) Pastoriza-santos, B. I.; Liz-marza, L. M. N , N -Dimethylformamide as a Reaction Medium for Metal Nanoparticle Synthesis. *Adv. Funct. Mater.* **2009**, *19*, 679–688.
- (37) Pastoriza-santos, I.; Liz-marzán, L. M. Reduction of Silver Nanoparticles in DMF . Formation of Monolayers and Stable Colloids. *Pure Appl. Chem.* **2000**, *72*, 83–90.

- (38) Gonz, R.; Del, G.; Rodr, M.; Primera-pedrozo, O. M.; Carlos, R.; Hern, S. P. Improving SERS Detection of *Bacillus Thuringiensis* Using Silver Nanoparticles Reduced with Hydroxylamine and with Citrate Capped Borohydride. *Int. J. Spectroscopy* **2011**, *2011*, 1–9.
- (39) Zhang, W.; Qiao, X.; Chen, J. Synthesis of Silver Nanoparticles — Effects of Concerned Parameters in Water/Oil Microemulsion. *Mater. Sci. Eng. B* **2007**, *142*, 1–15.
- (40) Gutierrez, M.; Henglein, A.; Dohrmann, J. K. Hydrogen Atom Reactions in the Sonolysis of Aqueous Solutions. *J. Phys. Chem.* **1987**, *91*, 6687–6690.
- (41) Dhas, N. A.; Raj, C. P.; Gedanken, A. Synthesis , Characterization , and Properties of Metallic Copper Nanoparticles. *Chem. Mater.* **1998**, *10*, 1446–1452.
- (42) Kumar, R. V.; Mastai, Y.; Diamant, Y.; Gedanken, A. Sonochemical Synthesis of Amorphous Cu and Nanocrystalline Cu<sub>2</sub>O Embedded in Polianiline Matrix. *J. Mater. Chem.* **2001**, *11*, 1209–1213.
- (43) Salkar, R. A.; Jeevanandam, P.; Aruna, S. T.; Koltypin, Y.; Gedanken, A. The Sonochemical Preparation of Amorphous Silver Nanoparticles. *J. Mater. Chem.* **1999**, *9*, 1333–1335.
- (44) Giuffrida, S.; Costanzo, L. L.; Ventimiglia, G.; Bongiorno, C. Photochemical Synthesis of Copper Nanoparticles Incorporated in Poly ( Vinyl Pyrrolidone ). *J. Nanoparticle Res.* **2008**, *10*, 1183–1192.
- (45) Klaus, T.; Joerger, R.; Olsson, E.; Granqvist, C.-G. Silver-Based Crystalline Nanoparticles, Microbially Fabricated. *Proc. Natl. Acad. Sci. United States Am.* **1999**, *96*, 13611–13614.
- (46) Shahverdi, A. R.; Minaeian, S.; Reza, H.; Jamalifar, H.; Nohi, A. Rapid Synthesis of Silver Nanoparticles Using Culture Supernatants of Enterobacteria: A Novel Biological Approach. *Process Biochem.* **2007**, *42*, 919–923.
- (47) Fayaz, A. M.; Girilal, M.; Rahman, M.; Venkatesan, R.; Kalaichelvan, P. T.

- Biosynthesis of Silver and Gold Nanoparticles Using Thermophilic Bacterium *Geobacillus Stearothermophilus*. *Process Biochem.* **2011**, *46*, 1958–1962.
- (48) Kalishwaralal, K.; Deepak, V.; Ram, S.; Pandian, K.; Kottaisamy, M.; Barathmanikant, S.; Kartikeyan, B.; Gurunathan, S. Biosynthesis of Silver and Gold Nanoparticles Using *Brevibacterium Casei*. *Colloids Surfaces B Biointerfaces* **2010**, *77*, 257–262.
- (49) Lakshmi, V.; Roshmi, D.; Varghese, R. T.; Soniya, E. V.; Mathew, J.; Radhakrishnan, E. K. Extracellular Synthesis of Silver Nanoparticles by the *Bacillus* Strain CS 11 Isolated from Industrialized Area. *3Biotech* **2014**, *4*, 121–126.
- (50) Mukherjee, P.; Ahmad, A.; Mandal, D.; Senapati, S.; Sainkar, S. R.; Khan, M. I.; Parishcha, R.; Ajaykumar, P. V.; Alam, M.; Kumar, R.; et al. Fungus-Mediated Synthesis of Silver Nanoparticles and Their Immobilization in the Mycelial Matrix : A Novel Biological Approach to Nanoparticle Synthesis. *Nano Lett.* **2001**, *1*, 515–519.
- (51) Ahmad, A.; Mukherjee, P.; Senapati, S.; Mandal, D.; Khan, M. I.; Sastry, M. Extracellular Biosynthesis of Silver Nanoparticles Using the Fungus *Fusarium Oxysporum*. *Colloids Surfaces B Biointerfaces* **2003**, *28*, 313–318.
- (52) Kumar, S. A.; Abyaneh, M. K.; Gosavi, S. W.; Kulkarni, S. K.; Pasricha, R.; Ahmad, A.; Khan, M. I. Nitrate Reductase-Mediated Synthesis of Silver Nanoparticles from  $AgNO_3$ . *Biotechnol. Lett.* **2007**, *29*, 439–445.
- (53) Kathiresan, K.; Manivannan, S.; Nabeel, M. A.; Dhivya, B. Studies on Silver Nanoparticles Synthesized by a Marine Fungus , *Penicillium Fellutanum* Isolated from Coastal Mangrove Sediment. *Colloids Surfaces B Biointerfaces* **2009**, *71*, 133–137.
- (54) Kasthuri, J.; Kathiravan, K.; Rajendran, N. Phyllanthin-Assisted Biosynthesis of Silver and Gold Nanoparticles : A Novel Biological Approach. *J. Nanoparticle Res.* **2009**, *11*, 1075–1085.
- (55) Iram, F.; Iqbal, M. S.; Athar, M. M.; Saeed, M. Z.; Yasmeen, A.; Ahmad, R.

- Glucosylan-Mediated Green Synthesis of Gold and Silver Nanoparticles and Their Phyto-Toxicity Study. *Carbohydr. Polym.* **2014**, *104*, 29–33.
- (56) Durai, P.; Arulvasu, C.; Gajendran, B.; Ramar, M. Synthesis and Characterization of Silver Nanoparticles Using Crystal Compound of Sodium Para-Hydroxybenzoate Tetrahydrate Isolated from Vitex Negundo . L Leaves and Its Apoptotic Effect on Human Colon Cancer Cell Lines. *Eur. J. Med. Chem.* **2014**, *84*, 90–99.
- (57) Kasthuri, J.; Veerapandian, S.; Rajendiran, N. Biological Synthesis of Silver and Gold Nanoparticles Using Apiin as Reducing Agent. *Colloids Surfaces B Biointerfaces* **2009**, *68*, 55–60.
- (58) Ahmed, K. B. A.; Subramaniam, S.; Veerappan, G.; Hari, N.; Aravind Sivasubramanian, A. V.  $\beta$ -Sitosterol-D-Glucopyranoside Isolated from Desmostachya Bipinnata Mediate Photoinduced Rapid Green Synthesis of Silver Nanoparticles. *RSC Adv.* **2014**, *4*, 59130–59136.
- (59) Basha, S. K.; Govindaraju, K.; Manikandan, R.; Ahn, J. S.; Bae, E. Y.; Singaravelu, G. Phytochemical Mediated Gold Nanoparticles and Their PTP 1B Inhibitory Activity. *Colloids Surfaces B Biointerfaces* **2010**, *75*, 405–409.
- (60) Gardea-torresdey, J. L.; Gomez, E.; Peralta-vidua, J. R.; Parsons, J. G.; Troiani, H.; Jose-yacaman, M. Alfalfa Sprouts : A Natural Source for the Synthesis of Silver Nanoparticles. *Langmuir* **2003**, *19*, 1357–1361.
- (61) Harris, A. T.; Bali, R. On the Formation and Extent of Uptake of Silver Nanoparticles by Live Plants. *J. Nanoparticle Res.* **2008**, *10*, 691–695.
- (62) Sharma, N. C.; Torresdey, J. L. G.-. Synthesis of Plant-Mediated Gold Nanoparticles and Catalytic Role of Biomatrix-Embedded Nanomaterials. *Environ. Sci. Technol.* **2007**, *41*, 5137–5142.
- (63) Rodriguez, J. L. G. Æ. E.; Peralta-vidua, J. G. P. Æ. J. R.; Cruz-jimenez, G. M. Æ. G. Use of ICP and XAS to Determine the Enhancement of Gold Phytoextraction by Chilopsis Linearis Using Thiocyanate as a Complexing Agent. *Anal. Bioanal. Chem.* **2005**, *382*, 347–352.

- (64) Ibrahim, H. M. M. Synthesis and Characterization of Silver Nanoparticles Using Banana Peel Extract and Their Antimicrobial Activity against Representative Microorganisms. *J. Radiat. Res. Appl. Sci.* **2015**, *8*, 265–275.
- (65) Sharma, G.; Sharma, A. R.; Kurian, M.; Bhavesh, R.; Nam, J. S.; Lee, S. S. Green Synthesis of Silver Nanoparticle Using Myristica Fragrans(Nutmeg) Seed Extract and Its Biological Activity. *Dig. J. Nanomater. Biostructures* **2014**, *9*, 325–332.
- (66) Elavazhagan, T.; Arunachalam, K. D. Memecylon Edule Leaf Extract Mediated Green Synthesis of Silver and Gold Nanoparticles. *Int. J. Nanomedicine* **2011**, *6*, 1265–1278.
- (67) Singh, A.; Jain, D.; Upadhyay, M. K.; Khandelwal, N. Green Synthesis of Silver Nanoparticles Using Argemone Mexicana Leaf Extract and Evaluation of Their Antimicrobial Activities. *Dig. J. Nanomater. Biostructures* **2010**, *5*, 483–489.
- (68) Jain, D.; Daima, H. K.; Kachhwaha, S.; Kothari, S. L. Synthesis of Plant Mediated Silver Nanoparticles Using Papaya Fruit Extract and Evaluation of Their Antimicrobial Activities. *Dig. J. Nanomater. Biostructures* **2009**, *4*, 557–563.
- (69) Savithramma, P. Y. N. Biosynthesis , Characterization and Antimicrobial Studies of Green Synthesized Silver Nanoparticles from Fruit Extract of Syzygium Alternifolium ( Wt .) Walp . an Endemic , Endangered Medicinal Tree Taxon. *Appl. Nanosci.* **2016**, *6*, 223–233.
- (70) Rao, Y. S.; Kotakadi, V. S.; Prasad, T. N. V. K. V; Reddy, A. V; Gopal, D. V. R. S. Green Synthesis and Spectral Characterization of Silver Nanoparticles from Lakshmi Tulasi (Ocimum Sanctum ) Leaf Extract. *Spectrochem. Acta PartA Mol. Biomolecular Spectrosc.* **2013**, *103*, 156–159.
- (71) Ahmed, S.; Saifullah; Ahmad, M.; Swami, B. L. Green Synthesis of Silver Nanoparticles Using Azadirachta Indica Aqueous Leaf Extract. *J. Radiat. Res. Appl. Sci.* **2015**, *9*, 1–7.

- (72) Velu, K.; Elumalai, D.; Hemalatha, P.; Janaki, A. Evaluation of Silver Nanoparticles Toxicity of Arachis Hypogaea Peel Extracts and Its Larvicidal Activity against Malaria and Dengue Vectors. *environmental Sci. Pollut. Res.* **2015**, *22*, 17769–17779.
- (73) Zaheer, Z. Biogenic Synthesis, Optical, Catalytic, and in Vitro Antimicrobial Potential of Ag Nanoparticles Prepared Using Palm Date Fruit Extract. *J. Photochem. Photobiol. B Biol.* **2018**, *178*, 584–592.
- (74) Nisha, S. N.; Aysha, O. S.; Nasar, J. S.; Kumar, P. V.; Valli, S.; Nirmala, P.; Reena, A. Lemon Peels Mediated Synthesis of Silver Nanoparticles and Its Antidermatophytic Activity. *Spectrochim. Acta Part A Mol. Biomol. Spectrosc.* **2014**, *124*, 194–198.
- (75) Ahamed, M.; M.A.MajeedKhan; M.K.J.Siddiqui; S.AISalhi, M.; SalmanA.Alrokayan. Green Synthesis , Characterization and Evaluation of Biocompatibility of Silver Nanoparticles. *Phys. E Low-dimensional Syst. Nanostructures* **2011**, *43*, 1266–1271.
- (76) Shende, S.; Ingle, A. P.; Gade, A.; Rai, M. Green Synthesis of Copper Nanoparticles by Citrus Medica Linn.( Idilimbu) Juice and Its Antimicrobial Activity. *World J. Microbiol. Biotechnol.* **2015**, *31*, 865–873.
- (77) Harne, S.; Sharma, A.; Dhaygude, M.; Joglekar, S.; Kodam, K. Novel Route for Rapid Biosynthesis of Copper Nanoparticles Using Aqueous Extract of Calotropis Procera L . Latex and Their Cytotoxicity on Tumor Cells. *Colloids Surfaces B Biointerfaces* **2012**, *95*, 284–288.
- (78) Lee, H.; Song, J. Y.; Kim, B. S. Biological Synthesis of Copper Nanoparticles Using Magnolia Kobus Leaf Extract and Their Antibacterial Activity. *Chem. Technol. Biotechnol.* **2013**, *88*, 1971–1977.
- (79) Nasrollahzadeh, M.; Sajadi, S. M. Green Synthesis of Copper Nanoparticles Using Ginkgo Biloba L . Leaf Extract and Their Catalytic Activity for the Huisgen [ 3 + 2 ] Cycloaddition of Azides and Alkynes at Room Temperature. *J. Colloid Interface Sci.* **2015**, *457*, 141–147.

- (80) Nasrollahzadeh, M.; Sajadi, S. M.; Mehdi Khalaj. Green Synthesis of Copper Nanoparticles Using Aqueous Extract of the Leaves of Euphorbia Esula L and Their Catalytic Activity for Ligand-Free Ullmann-Coupling Reaction and Reduction of 4-Nitrophenol. *RSC Adv.* **2014**, *4*, 47313–47318.
- (81) Mukhopadhyay, R.; Kazi, J.; Debnath, M. C. Synthesis and Characterization of Copper Nanoparticles Stabilized with Quisqualis Indica Extract : Evaluation of Its Cytotoxicity and Apoptosis in B16F10 Melanoma Cells. *Biomed. Pharmacother.* **2018**, *97*, 1373–1385.
- (82) Nazar, N.; Bibi, I.; Kamal, S.; Iqbal, M.; Nouren, S.; Jalani, K.; Umair, M.; Atta, S. Cu Nanoparticles Synthesis Using Biological Molecule of P. Granatum Seeds Extract as Reducing and Capping Agent: Growth Mechanism and Photo-Catalytic Activity. *Int. J. Biol. Macromol.* **2017**, *106*, 1203–1210.
- (83) Ghidan, A. Y.; Al-antary, T. M.; Awwad, A. M. Green Synthesis of Copper Oxide Nanoparticles Using Punica Granatum Peels Extract : Effect on Green Peach Aphid. *Environ. Nanotechnology, Monit. & Manag.* **2016**, *6*, 95–98.
- (84) Sivaraj, R.; Rahman, P. K. S. M.; Rajiv, P.; Abdul, H.; Venckatesh, R. Biogenic Copper Oxide Nanoparticles Synthesis Using Tabernaemontana Divaricate Leaf Extract and Its Antibacterial Activity against Urinary Tract Pathogen. *Spectrochim. Acta Part A Mol. Biomol. Spectrosc.* **2014**, *133*, 178–181.
- (85) Nasrollahzadeh, M.; Momeni, S. S.; Sajadi, S. M. Green Synthesis of Copper Nanoparticles Using Plantago Asiatica Leaf Extract and Their Application for the Cyanation of Aldehydes Using K<sub>4</sub>Fe (CN)<sub>6</sub>. *J. Colloid Interface Sci.* **2017**, *506*, 471–477.
- (86) Abdul, M.; Naikodi, R.; Waheed, M. A.; Shareef, M. A.; Ahmad, M.; Nagaiah, K. Standardization of the Unani Drug – Myristica Fragrans Hoult . ( Javetri ) – with Modern Analytical Techniques. *Pharm. Methods* **2011**, *2*, 76–82.
- (87) Bindu, N. H. S. A. I.; Kumar, S. R. In-Vitro Assimilation of Trimyristin in the Seeds of Myristica Fragrans and in Poly Herbal Ayurvedic Formulation by

- UFLC Method. *Asian J. Pharm. Clin. Res.* **2014**, *6*, 140–145.
- (88) Mittal, A. K.; Chisti, Y.; Banerjee, U. C. Synthesis of Metallic Nanoparticles Using Plant Extracts. *Biotechnol. Adv.* **2013**, *31*, 346–356.
- (89) Thakkar, K. N.; Mhatre, S. S.; Parikh, R. Y. Biological Synthesis of Metallic Nanoparticles. *Nanomedicine Nanotechnology, Biol. Med.* **2010**, *6*, 257–262.
- (90) Nasrollahzadeh, M.; Maham, M.; Sajadi, S. M. Green Synthesis of CuO Nanoparticles by Aqueous Extract of *Gundelia Tournefortii* and Evaluation of Their Catalytic Activity for the Synthesis of N -Monosubstituted Ureas and Reduction of 4-Nitrophenol. *J. Colloid Interface Sci.* **2015**, *455*, 245–253.
- (91) Tamuly, C.; Hazarika, M.; Ch, S.; Das, M. R.; Boruah, M. P. In Situ Biosynthesis of Ag , Au and Bimetallic Nanoparticles Using Piper *Pedicellatum* C . DC : Green Chemistry Approach. *Colloids Surfaces B Biointerfaces* **2013**, *102*, 627–634.
- (92) Pandey, R.; Mahar, R.; Hasanain, M.; Shukla, S. K. Rapid Screening and Quantitative Determination of Bioactive Compounds from Fruit Extracts of *Myristica* Species and Their In-Vitro Antiproliferative Activity. *Food Chem.* **2016**, *211*, 483–493.
- (93) Pandey, R.; Rameshkumar, K. B.; Kumar, B. Ultra High Performance Liquid Chromatography Tandem Mass Spectrometry Method for the Simultaneous Determination of Multiple Bioactive Constituents in Fruit Extracts of *Myristica* Fragrans and Its Marketed Multi-Herbal Formulations Using a Polarity Switchin. *J. Sep. Sci.* **2015**, *38*, 1277–1285.
- (94) Singh, A. K.; Talat, M.; Singh, D. P.; Srivastava, O. N. Biosynthesis of Gold and Silver Nanoparticles by Natural Precursor Clove and Their Functionalization with Amine Group. *J. Nanoparticle Res.* **2010**, *12*, 1667–1675.
- (95) Jiang, X.; Herricks, T.; Xia, Y. CuO Nanowires Can Be Synthesized by Heating Copper Substrates in Air. *Nano Lett.* **2002**, *2*, 1334–1338.
- (96) Creary, X.; Anderson, A.; Brophy, C.; Crowell, F.; Funk, Z. Method for



- Assigning Structure of 1,2,3-Triazoles. *J. Org. Chem.* **2012**, *77*, 8756–8761.
- (97) Ahmed, K. B. A.; Senthilnathan, R.; Megarajan, S.; Anbazhagan, V. Sunlight Mediated Synthesis of Silver Nanoparticles Using Redox Phytoprotein and Their Application in Catalysis and Colorimetric Mercury Sensing. *J. Photochem. Photobiol. B Biol.* **2015**, *151*, 39–45.
- (98) Ulug, B.; Turkdemir, M. H.; Cicek, A.; Mete, A. Role of Irradiation in the Green Synthesis of Silver Nanoparticles Mediated by Fig ( *Ficus Carica* ) Leaf Extract. *Spectrochem. Acta Part A Mol. Biomol. Spectrosc.* **2015**, *135*, 153–161.
- (99) Manikprabhu, D.; Cheng, J.; Chen, W.; Kumar, A.; Mane, S. B.; Kumar, R.; Hozzein, W. N.; Duan, Y.; Li, W. Sunlight Mediated Synthesis of Silver Nanoparticles by a Novel Actinobacterium ( *Sinomonas Mesophila* MPKL 26 ) and Its Antimicrobial Activity against Multi Drug Resistant *Staphylococcus Aureus*. *J. Photochem. Photobiol. B Biol.* **2016**, *158*, 202–205.
- (100) Magudapathy, P.; Gangopadhyay, P.; Panigrahi, B. K.; Nair, K. G. M.; Dhara, S. Electrical Transport Studies of Ag Nanoclusters Embedded in Glass Matrix. *Phys. B* **2001**, *299*, 142–146.
- (101) Lansdown, A. B. G. Silver I: Its Antibacterial Properties and Mechanism of Action. *J. Wound Care* **1970**, *11*, 125–130.
- (102) Castellano, J. J.; Shafii, S. M.; Ko, F.; Donate, G.; Wright, T. E.; Mannari, R. J.; Payne, W. G.; Smith, D. J.; Jj, C.; Sm, S.; et al. Comparative Evaluation of Silver-Containing Antimicrobial Dressings and Drugs. *Int. Wound J.* **2007**, *4*, 114–122.
- (103) Sulaiman, S. F.; Ooi, K. L. Antioxidant and Anti Food-Borne Bacterial Activities of Extracts from Leaf and Different Fruit Parts of *Myristica Fragrans* Houtt. *Food Control* **2012**, *25*, 533–536.
- (104) Mulvaney, P. Surface Plasmon Spectroscopy of Nanosized Metal Particles. *Langmuir* **1996**, No. 12, 788–800.
- (105) Morones, J. R.; Elechiguerra, J. L.; Camacho, A.; Holt, K.; Kouri, J. B.; Ram, J. T.; Yacaman, M. J. The Bactericidal Effect of Silver Nanoparticles.

*Nanotechnology* **2005**, *16*, 2346–2353.

- (106) Pal, S.; Tak, Y. K.; Song, J. M. Does the Antibacterial Activity of Silver Nanoparticles Depend on the Shape of the Nanoparticle? A Study of the Gram-Negative Bacterium *Escherichia Coli*. *Appl. Environmental Microbiol.* **2007**, *73*, 1712–1720.

## Chapter 5

## Synthesis of 1,2,3-triazolyldene palladium complexes: Application as catalyst for Suzuki-Miyaura coupling reaction and cytotoxic studies

### 5.1 Introduction

Carbenes are generally described as compounds having  $sp^2$  hybridized divalent carbon atom with two nonbonding electrons and doesn't carry a formal charge. They can be classified as singlet or triplet depending on whether the nonbonding electrons are either paired (singlet) or unpaired (triplet) (**Fig 1**).

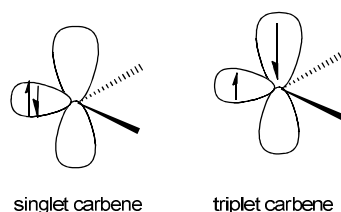


**Fig 1**

Depending on the structure and reactivity of carbenes toward metal ion they can also be classified as Fischer, Schrock and *N*-Heterocyclic Carbene (NHC). In general Fischer carbene forms complexes with metal center at low oxidation state<sup>1</sup> whereas Schrock carbene forms bond with metal centers having high oxidation state.<sup>2</sup> Metal-ligand multiple bond is present in both carbene complexes (**Fig 2**).

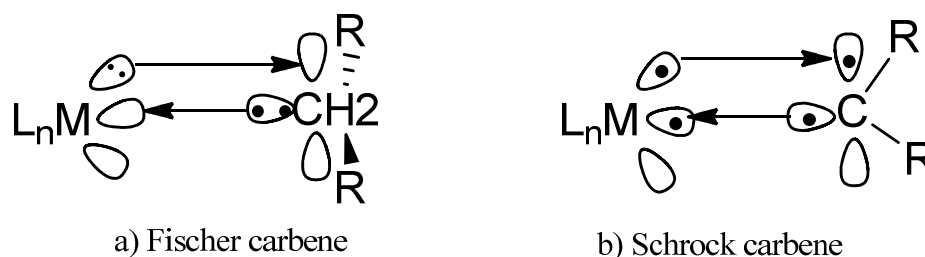


**Fig 2** Bonding in a) Fischer and b) Schrock carbenes

Apart from the above two types, *N*-heterocyclic carbene (NHC) represent a unique type of carbene in which carbene carbon is in a position  $\alpha$  to a heteroatom typically nitrogen. General representation of NHC is shown in (Fig 3).

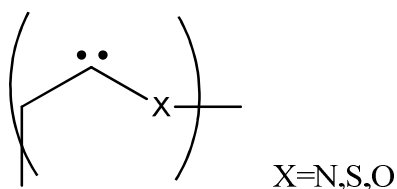


Fig. 3 General representation of NHC

NHC have advantages over the above two carbenes that the nitrogen atom adjacent to carbene carbon stabilize the carbene via  $\sigma$  and  $\pi$  bonding. Stability of NHC acquired by the interaction of  $\pi$  electrons of the substituents with the  $p_\pi$  orbital of carbon give rise to four-electron-three-center  $\pi$  system (Fig.4).

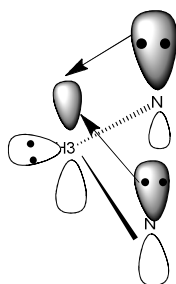
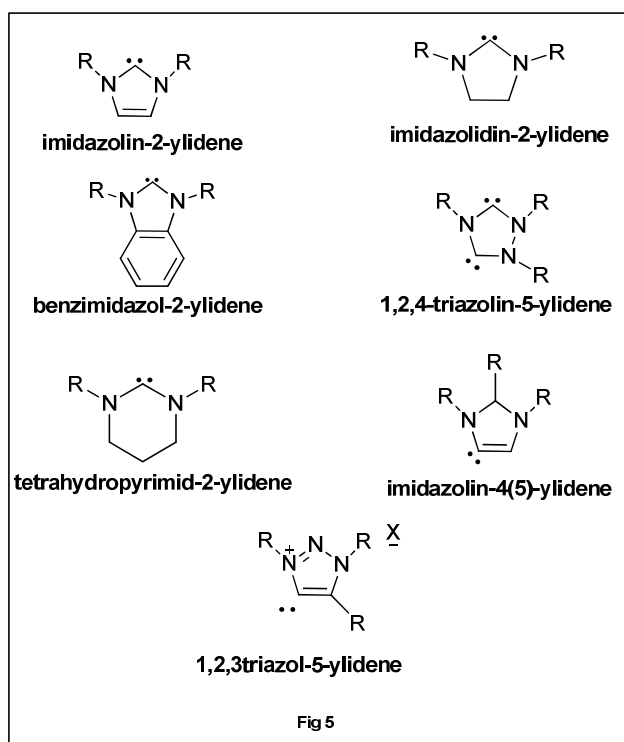
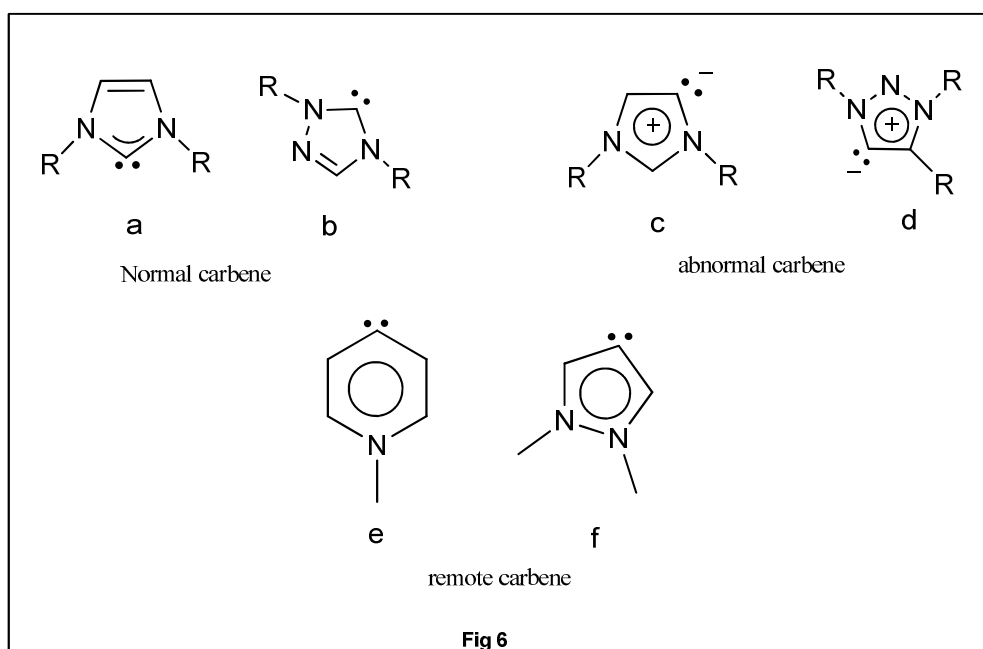


Fig.4

Common subclass of different types of NHCs is shown in Fig 5.



These carbenes are again classified as normal, remote and abnormal or mesoionic carbenes depending on the nature of the carbene species. In remote carbenes (rNHC) there is no heteroatom adjacent to carbene and in abnormal or mesoionic carbene (aNHCs or MICs), no uncharged resonance can be drawn (Fig 6)



Synthesis of biaryls by palladium catalyzed Suzuki-Miyaura cross coupling reactions using organic halides and boronic acid as reactants attained more relevance.<sup>3-5</sup> Traditionally, air and thermal stable phosphine ligands and their complexes have been

employed as catalyst for such coupling reactions.<sup>6</sup> In recent times, nucleophilic N-heterocyclic carbene ligands are used as auxiliary ligands for the coupling reactions<sup>7</sup> and such reactions were usually carried out in organic solvents. However, due to environmental concerns green chemistry protocol demands for such reactions<sup>8,9</sup> which needs proper design of the catalyst to enable the use of water as reaction medium. Such a green protocol involves the use of water soluble ligands, micellar catalysis and hydrophilic ligand precursors.<sup>10,11</sup> Water soluble NHC complexes are used for C-C bond formation reactions such as Suzuki coupling.<sup>12</sup> Generally N-heterocyclic carbenes are neutral, strongly donating and covalently binding ligands and these type of ligands can be tuned for catalytic activity especially those catalysts containing palladium metal.<sup>13</sup>

In 2011, Karimi reported the synthesis of water soluble NHC-Pd catalyst.<sup>14</sup> Then arises a new way for the catalyst design like “throw away” ligand in which a weakly coordinated ligand can leave the complex immediately before an oxidative addition takes place. Such catalytic systems contain imidazolylidene palladium core with N-donor labile ligands like PEPPSI (Pyridine Enhanced Precatalyst Preparation, Stabilization and Initiation), amine, (iso)quinoline, DABCO (1,4-diazabicyclo[2.2.2]octane) etc. There are few reports on triazolylidene palladium complexes bearing throw away ligands that can be used for Suzuki-Miyaura cross coupling reactions.<sup>15-17</sup>

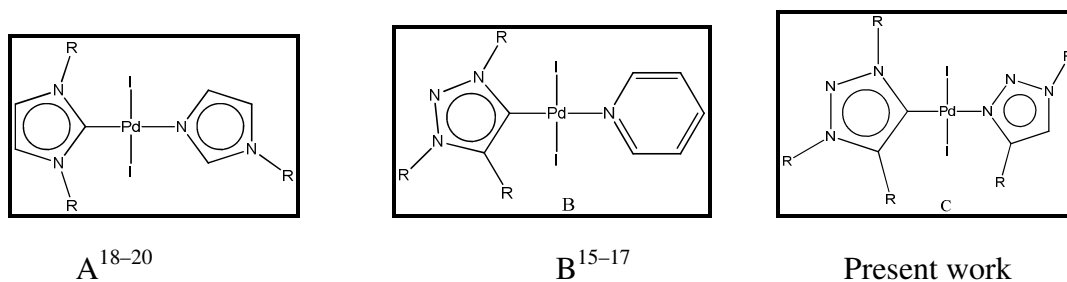
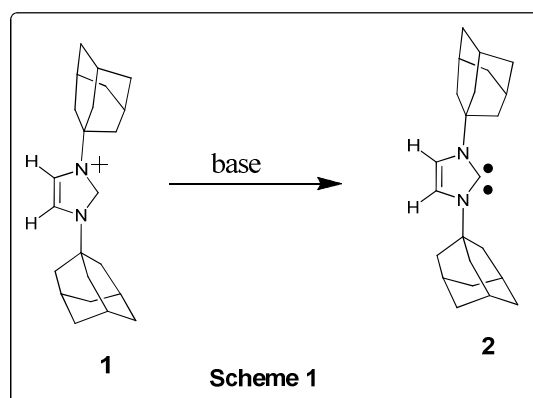


**Fig.7** Development of “throw away” ligand concept in NHC-Pd complexes: C<sub>Im</sub>-Pd(II)-N<sub>Im</sub> complex (A), C<sub>tzi</sub>-Pd(II)-N<sub>PEPPSI</sub> complex (B) and C<sub>tzi</sub>-Pd(II)-N<sub>tzi</sub> complex (C)

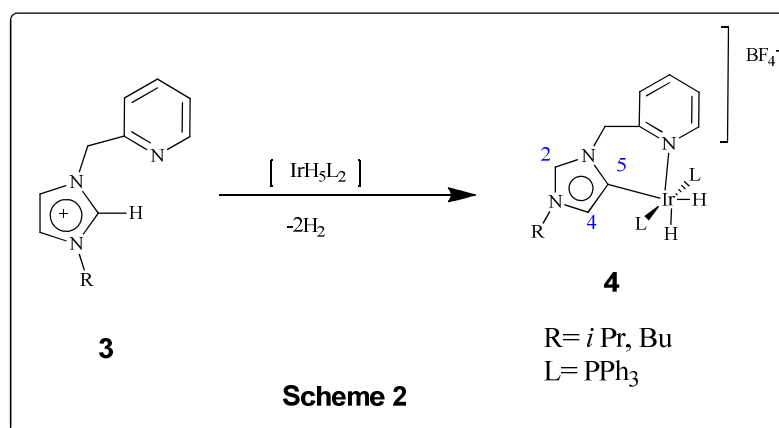
Compared to imidazolylidene counterpart triazolylidene ligands have stronger donor capacity which improves the catalytic activity of such palladium complexes.

## 5.2 Review of Literature

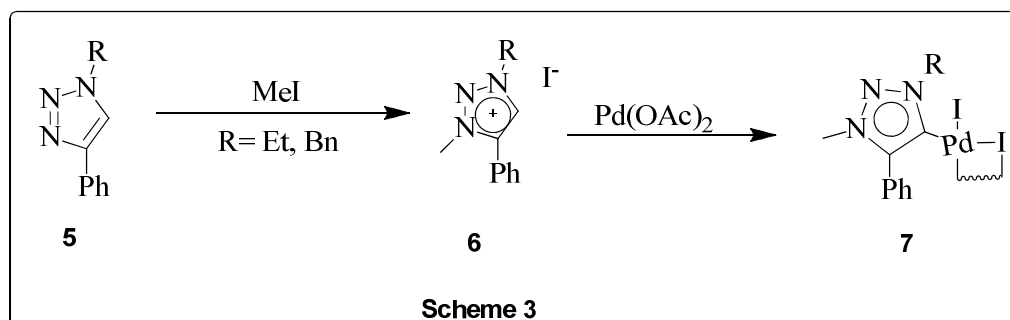
In 1968 Wanzlick synthesized carbene from N,N'-disubstituted imidazolines<sup>21</sup> but it could never be isolated. Arduengo isolated the first stable carbene by the deprotonation of 1,3-bis(adamantyl)imidazolin-2-ylidene using sodium hydride in presence of DMSO<sup>22</sup>(**scheme 1**).



Abnormal imidazol-4-ylidenes with metal attached to C-5 carbon were first reported by Crabtree in 2001<sup>23</sup> (**scheme2**).

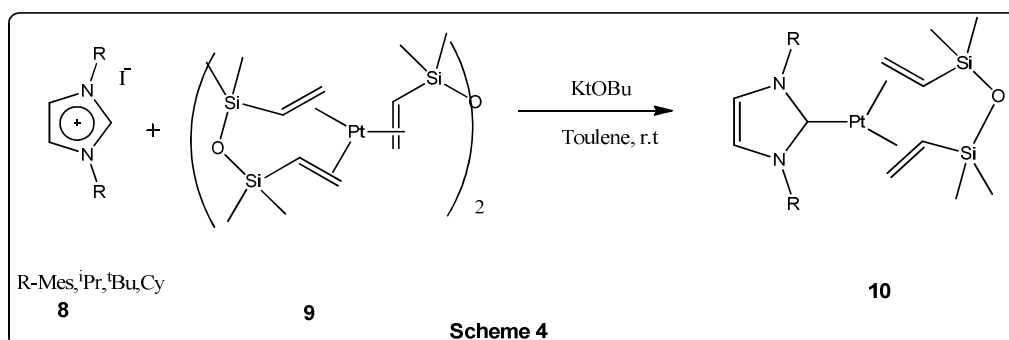


Abnormal binding mode of 1,2,3-triazole ligand at C-5 carbon atom was reported by Albrecht in 2008<sup>24</sup> (**scheme 3**).

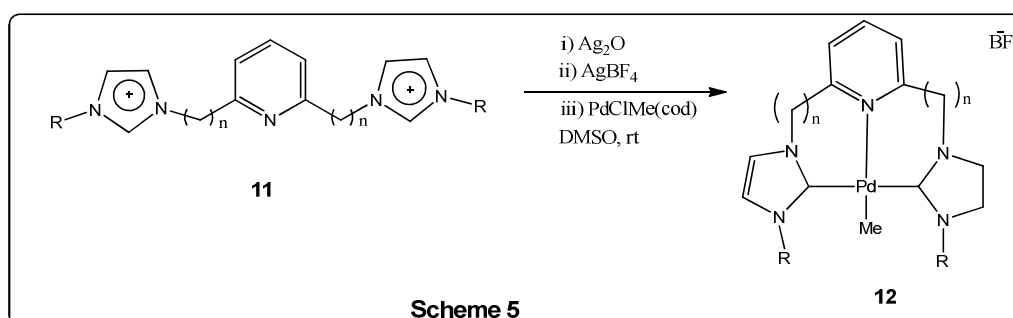


There are various methods for the synthesis of NHC-metal complexes.

A) Proton abstraction: Carbene generated by the deprotonation using a strong base (**Scheme 4**)

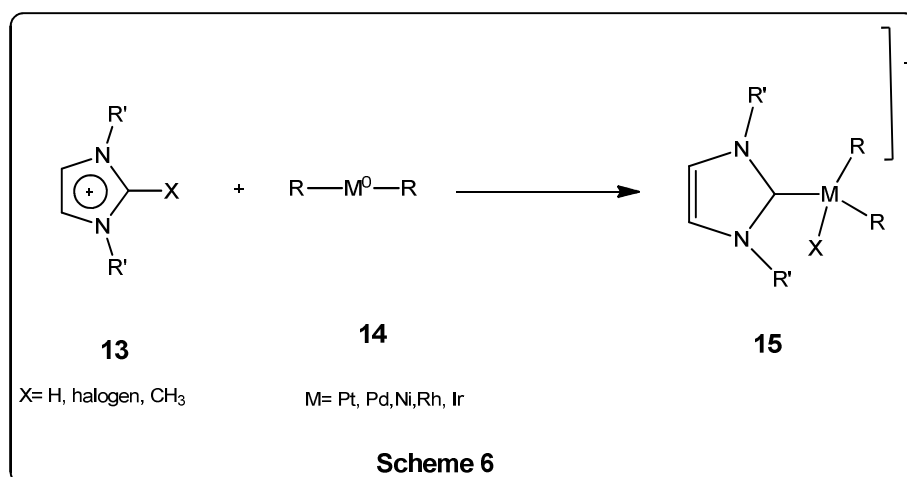


B) Transmetalation from silver: Firstly, a silver complex was prepared using  $\text{Ag}_2\text{O}$  and then NHC transferred from the silver atom to another transition metal atom (**Scheme 5**)

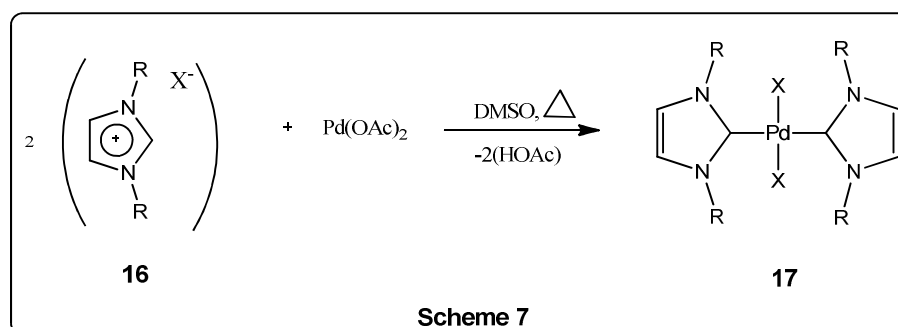


C) Oxidative addition: Oxidative insertion of low valent metal precursor into a C-X bond. (**Scheme 6**)



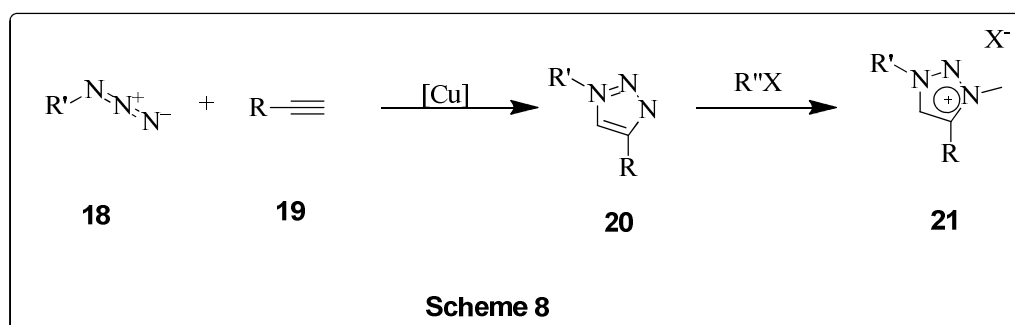


D) Direct metallation: Metallation of ligand using basic ligand of metal precursor such as Pd(OAc)<sub>2</sub> or [Ir(COD)(OEt)]<sub>2</sub> (**Scheme 7**)



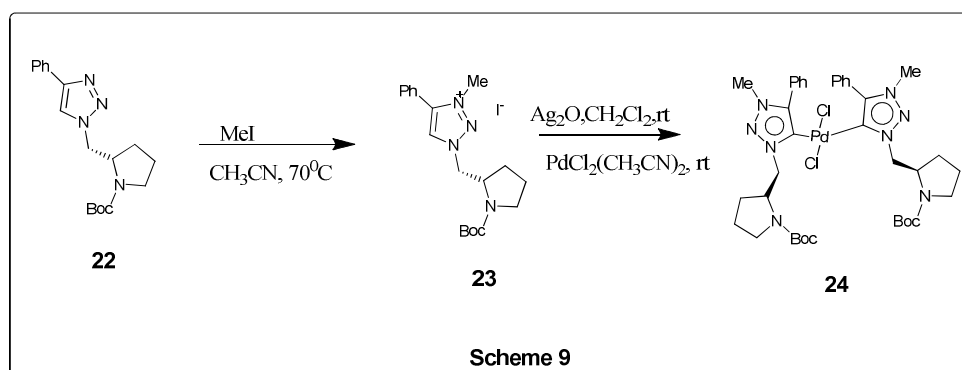
### 5.2.1 Synthesis of palladium N-heterocyclic carbene complexes

Synthesis of triazole by copper (I) catalyzed azide and alkyne click chemistry<sup>25</sup> followed by alkylation with suitable alkylating agent leads to 1,3,4-substituted triazolium salt (**Scheme 8**).

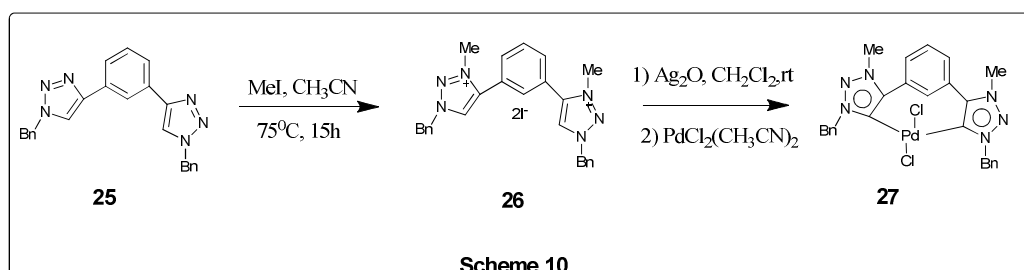


Bertrand and coworkers synthesized 1,2,3-triazol-5-ylidenes and studied its decomposition pathway.<sup>26</sup> Triazole ligand was synthesized from 2,6-diisopropylphenyl azide and phenylacetylene by CuAAC followed by the alkylation using methyl or isopropyl trifluoromethylsulfonate to afford the corresponding triazolium salt. Deprotonation by potassium bases affords the product in moderate yield and the deprotonation is confirmed by the disappearance of triazolium C-H in its <sup>1</sup>H NMR spectrum. They found that the triazolium salt was stable at -30°C for several days. But upon heating in benzene solution at 50°C lead to decomposition into other heterocyclic products. They concluded that the decomposition mainly took place by N3-alkyl bond cleavage.

In 2009 Sankararaman reported abnormal 1,2,3- triazolium palladium complexes and its application in Suzuki coupling reaction.<sup>27</sup> They synthesized the first chiral palladium complex by quarternising the chiral triazole ligand with methyl iodide. Transmetallation reaction of the initially formed silver complex was used to synthesize the palladium NHC complex (**scheme 9**).



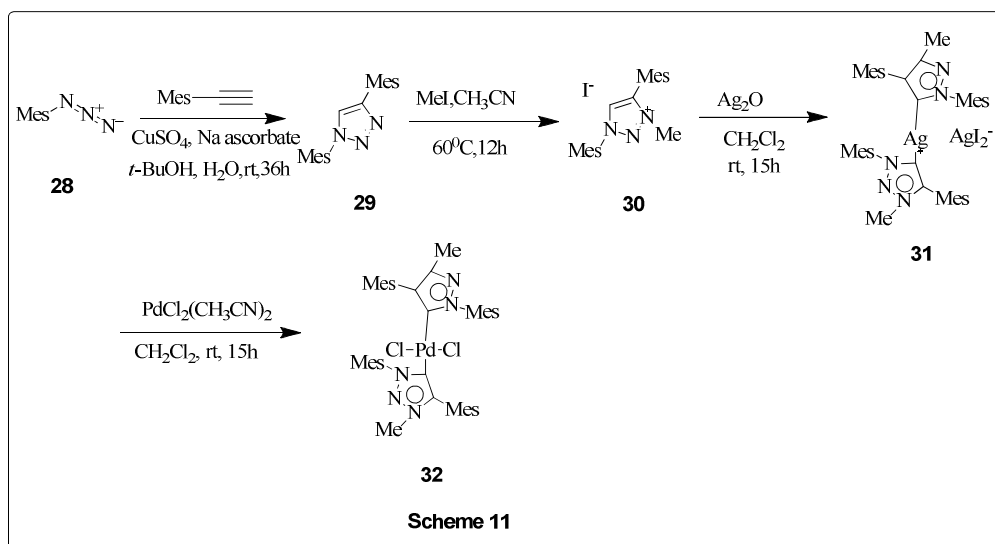
They also synthesized achiral pincer type carbene complex **27** by transmetalation from silver carbene complex using PdCl<sub>2</sub>(CH<sub>3</sub>CN)<sub>2</sub> (**Scheme 10**)



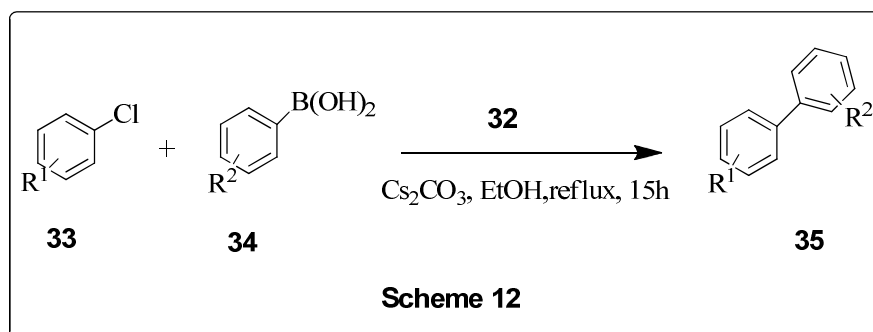
The catalytic activity of **24** was first studied in Suzuki reactions. Substituted aryl bromides were treated with phenylboronic acid or 4-methoxy phenylboronic acid in

THF using different catalyst loading. Depending upon the catalyst loading, time duration and choice of substrates they got moderate to good yield of products. Next, they carried out asymmetric Suzuki coupling reaction to synthesize chiral binaphthalene derivatives. Using the pincer type carbene complex **27**, they failed to conduct the asymmetric Suzuki coupling.

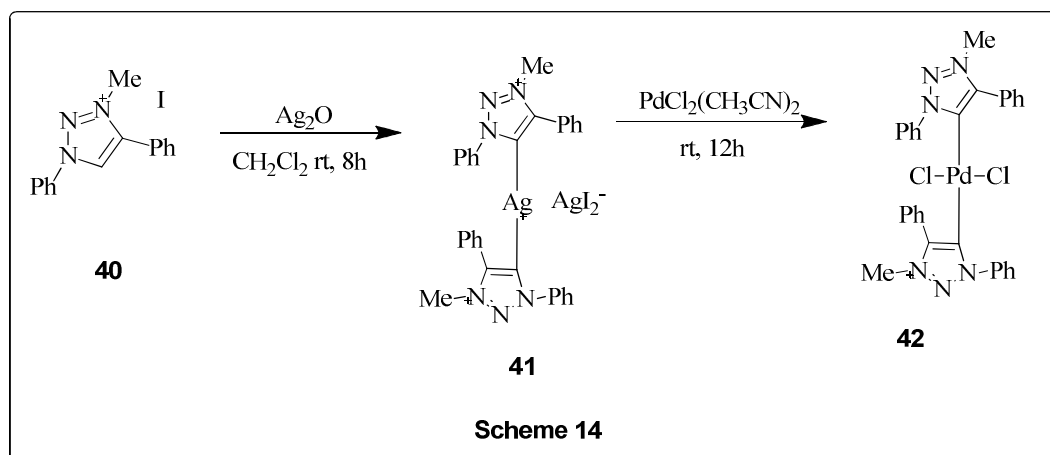
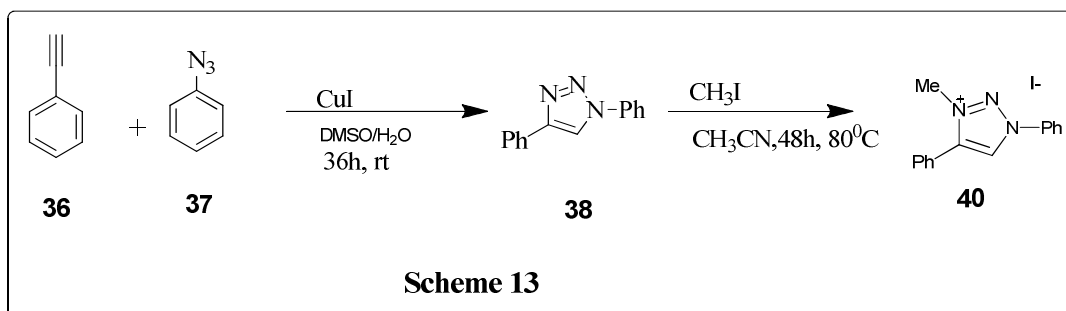
Fukuzawa synthesized triazole NHC Pd complex **32**,<sup>28</sup> starting from CuAAC reaction of mesityl azide and mesitylacetylene in presence of CuSO<sub>4</sub> and sodium ascorbate. Triazolium ion was synthesized by alkylating triazole with methyl iodide. On reaction with Ag<sub>2</sub>O afforded the silver carbene complex **31**. Its formation was confirmed by the disappearance of triazolium proton and this on transmetalation using PdCl<sub>2</sub>(MeCN)<sub>2</sub> in dichloromethane at room temperature afforded dichlorobis(1,2,3-triazol-5-ylidene)palladium complex **32** (Scheme 11).



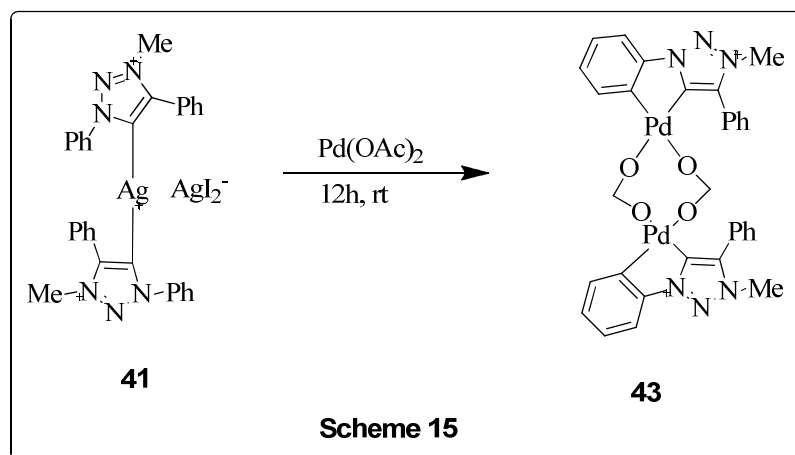
The Suzuki cross coupling reaction of *p*-chloroanisole with phenylboronic acid using 1mol% of **32** in ethanol solution for 15 h in the presence of Cs<sub>2</sub>CO<sub>3</sub> as base gave the desired product in quantitative yield. Efficiency of the catalyst was studied by conducting the coupling reaction in a variety of aryl chlorides with phenylboronic acid or *o*-substituted phenylboronic acid and the product was obtained in good yield (Scheme 12). The catalytic activity of **32** towards Mizoroki-Heck and Sonogashira coupling was also investigated.<sup>29</sup>



Sankararaman *et.al* synthesized 1,4-diphenyl-3-methyl-1,2,3-triazol-5-ylidene palladium complexes **42**.<sup>30</sup> 1,4-diphenyl-1,2,3-triazole **38** was prepared from phenylacetylene and phenyl azide through click reaction which on methylation yielded 1,4-diphenyl-3-methyl-1,2,3-triazolium iodide **40** (**Scheme 13**). Palladium complexes were synthesized from **40** by transmetallation method (**Scheme 14**).

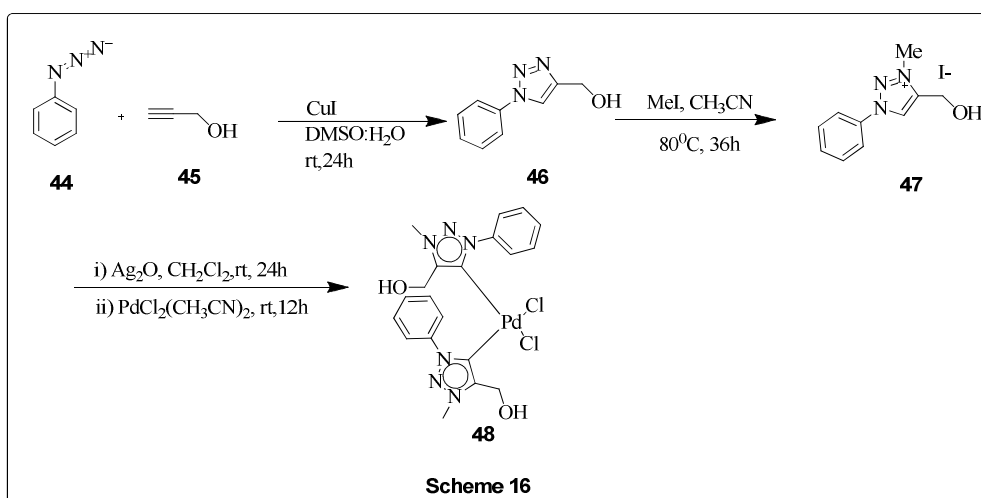


From the silver carbene complex **41**, palladium acetate complex **43** was synthesized using  $\text{Pd}(\text{OAc})_2$  in  $\text{CH}_2\text{Cl}_2$  and stirring for 12h at room temperature for 12 h (**Scheme 15**).

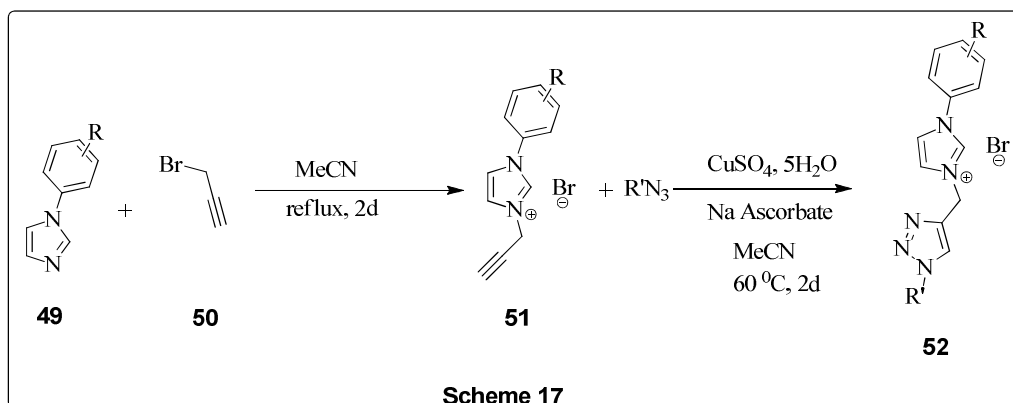


Catalytic efficiency of **43** towards hydroarylation in trifluoroacetic acid at room temperature was investigated and found to be moderate.

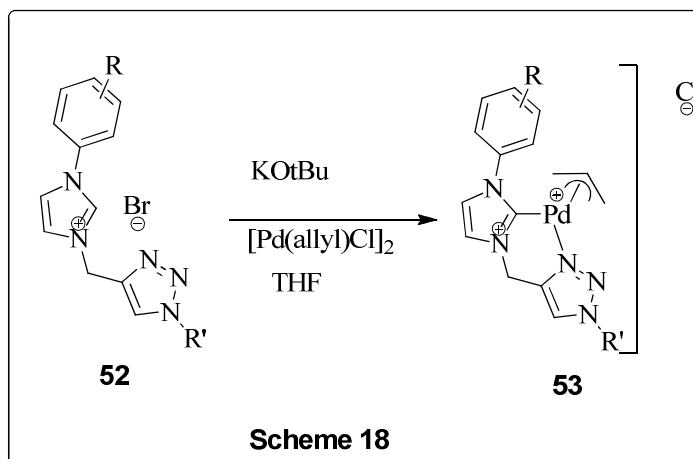
In 2013 Sankararaman and his group reported the synthesis and characterization of palladium complexes of 1,2,3-triazol-5-ylidene ligand.<sup>31</sup> The starting triazole **46** was prepared by CuAAC reaction between phenyl azide and propargyl alcohol in DMSO using CuI as catalyst at room temperature for 24h followed by the methylation using methyl iodide in acetonitrile at 80 °C for 36 h (**scheme 16**). Complex **48** were obtained by transmetalation using Ag<sub>2</sub>O. The reaction was performed at room temperature for 24 h in the absence of light. *In situ* reaction of the generated silver carbene with PdCl<sub>2</sub>(CH<sub>3</sub>CN)<sub>2</sub> for 12h stirring afforded **48**. The complex was characterized spectroscopically and by single crystal XRD data. The XRD data reveals that the 1,2,3-triazoli-5-ylidene adopt *cis* orientation with respect to the palladium metal.



Synthesis of NHC-triazolyl ligand precursors and their palladium complexes were carried out by Chen.<sup>32</sup> Initially they synthesized N-(Prop-2-ynyl)imidazolium salts **51** by refluxing *N*-aryl imidazole<sup>33</sup> and propargyl bromide in acetonitrile (**Scheme 17**). The product was obtained in quantitative yield either by precipitation or by concentration. The propargyl imidazolium salt was then treated with various azides<sup>34</sup> in presence of catalytic amounts of copper(II) sulfate and sodium ascorbate.

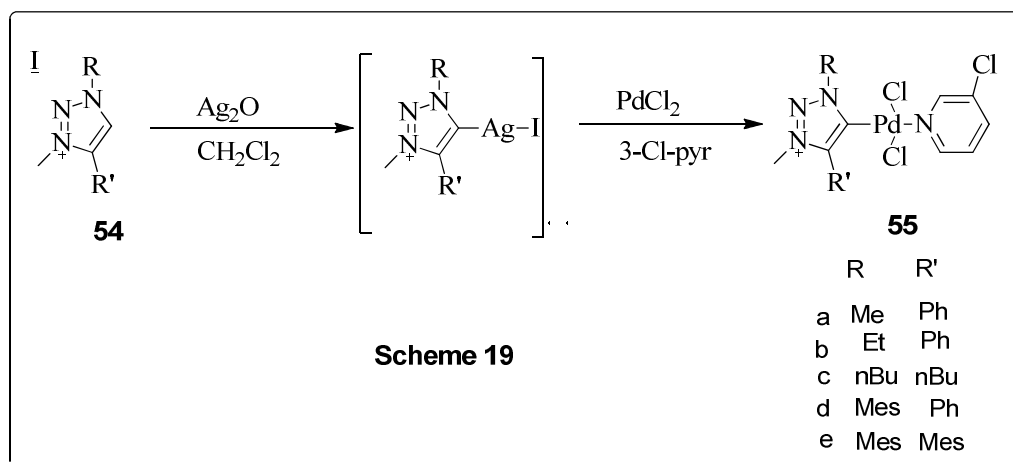


Palladium complex **53** was synthesized by the metalation with  $\eta^3$ -allyl palladium chloride dimer (**Scheme 18**).



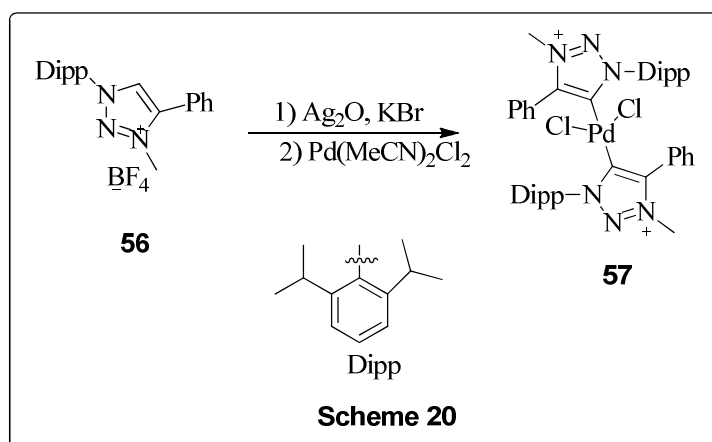
Transfer hydrogenation of alkynes to *Z*-alkenes was carried out in presence of **53**. The catalyst was found to exhibit high *Z*-selectivity with full conversion. Presence of bulky substituent provides 85% conversion.

1,2,3-triazolylidene palladium complexes with 3-chloropyridine ligand was synthesized by Albrecht.<sup>35</sup> Metalation of triazolium salt **54** with Ag<sub>2</sub>O followed by transmetalation with PdCl<sub>2</sub> afforded **55** (**Scheme 19**).

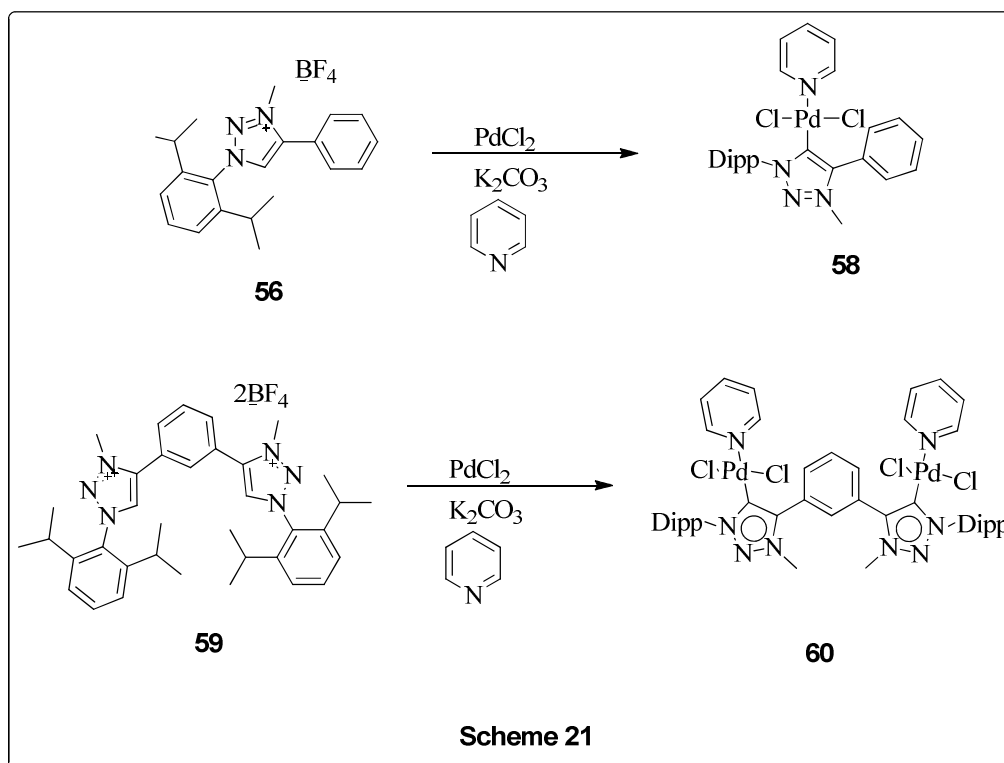


Catalytic activity of **55** was investigated for Suzuki coupling reaction and the complex was found to be heterogeneous in nature which produces palladium nanoparticle in the resting state.

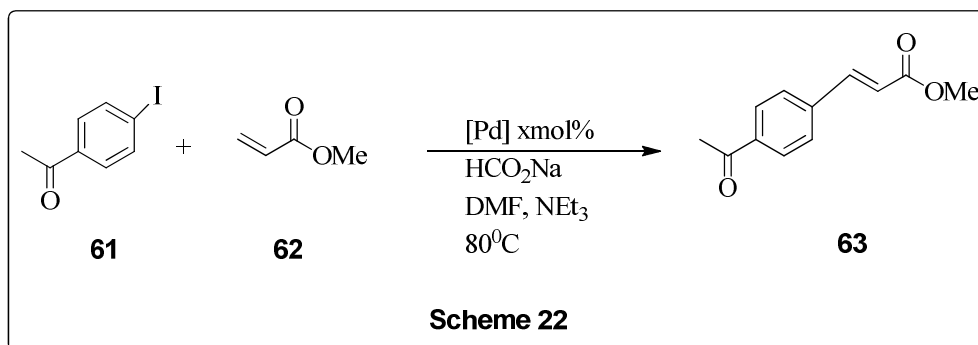
Crudden and coll reported the synthesis of mono- and bimetallic PEPPSI type complexes containing triazole mesoionic carbene ligand.<sup>17</sup> Synthesis of palladium complex **57** was carried out via transmetallation from Ag-MIC (**Scheme 20**)



Without transmetallation they synthesized two palladium complexes **51** and **53** from mesoionic carbene **56** and **59** using PdCl<sub>2</sub> in pyridine and K<sub>2</sub>CO<sub>3</sub> as the base (**Scheme 21**).

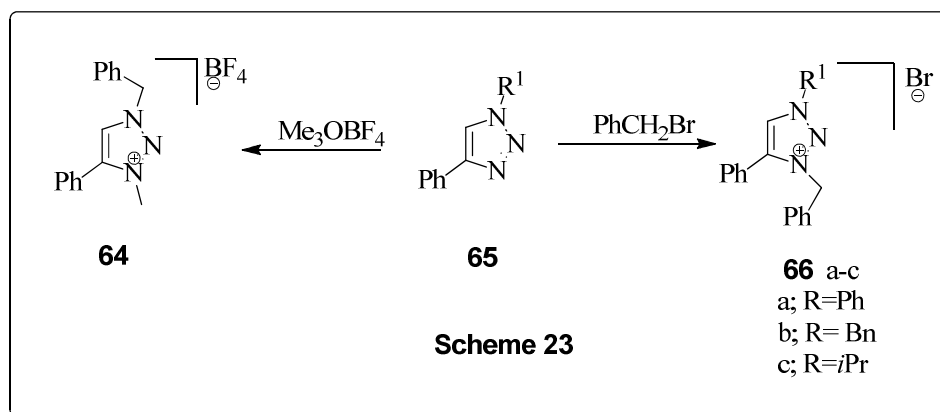


Mizoroki- Heck reaction was studied using **58** and **60** as catalyst for the coupling between *p*-iodo acetophenone and methyl acrylate in presence of sodium formate as reducing agent. Using 2 mol% of catalyst, both complexes provides 99% conversion.

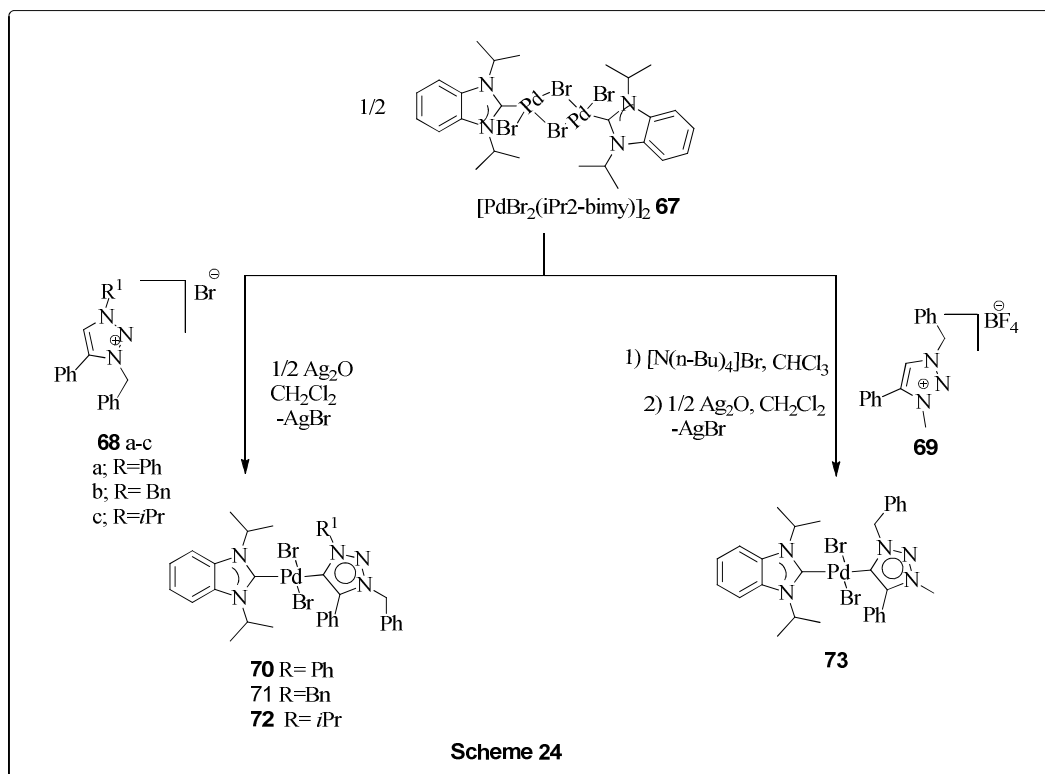


Huynh reported the synthesis of palladium complexes of the type  $\text{trans-[PdBr}_2(\text{}^i\text{Pr}_2\text{-bimy})(\text{trz})]$ .<sup>36</sup> Triazole synthesized via click reaction followed by the alkylation using benzyl bromide or Meerwin salt<sup>37</sup> provided the triazolium salt **66** (**Scheme 23**).





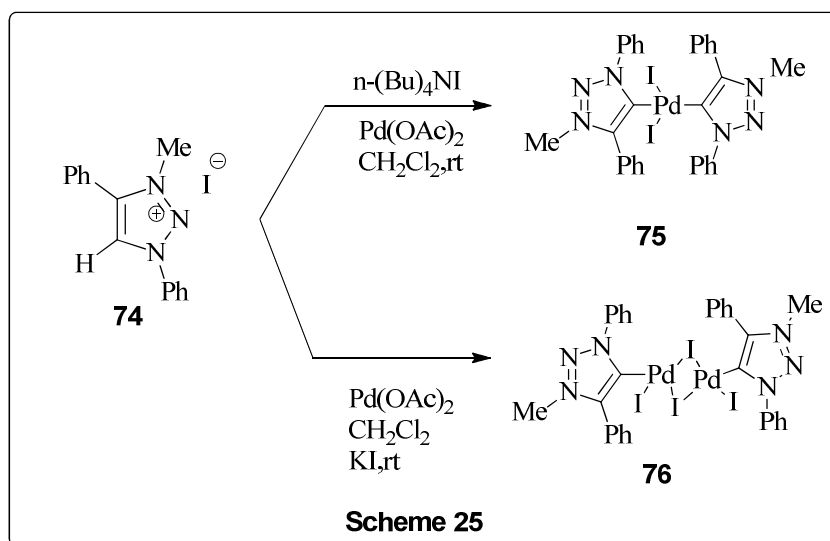
The palladium complexes **70**, **71** & **72** were synthesized by a one-pot bridge cleaving reactions of dimeric  $[\text{PdBr}_2(\text{}^i\text{Pr}_2\text{-bimy})]_2$  **67** with 2 equiv. of ligand precursors **68(a-c)** and 1/2equiv of  $\text{Ag}_2\text{O}$  in dichloromethane. Because of the presence of  $\text{BF}_4^-$  counter ion, the complex **73** from ligand **69** was prepared via reacting tribromido complex generated *in situ* using the reaction of  $[\text{N}(\text{n-Bu})_4]\text{Br}$  to  $[\text{PdBr}_2(\text{}^i\text{Pr}_2\text{-bimy})]_2$  **67**.



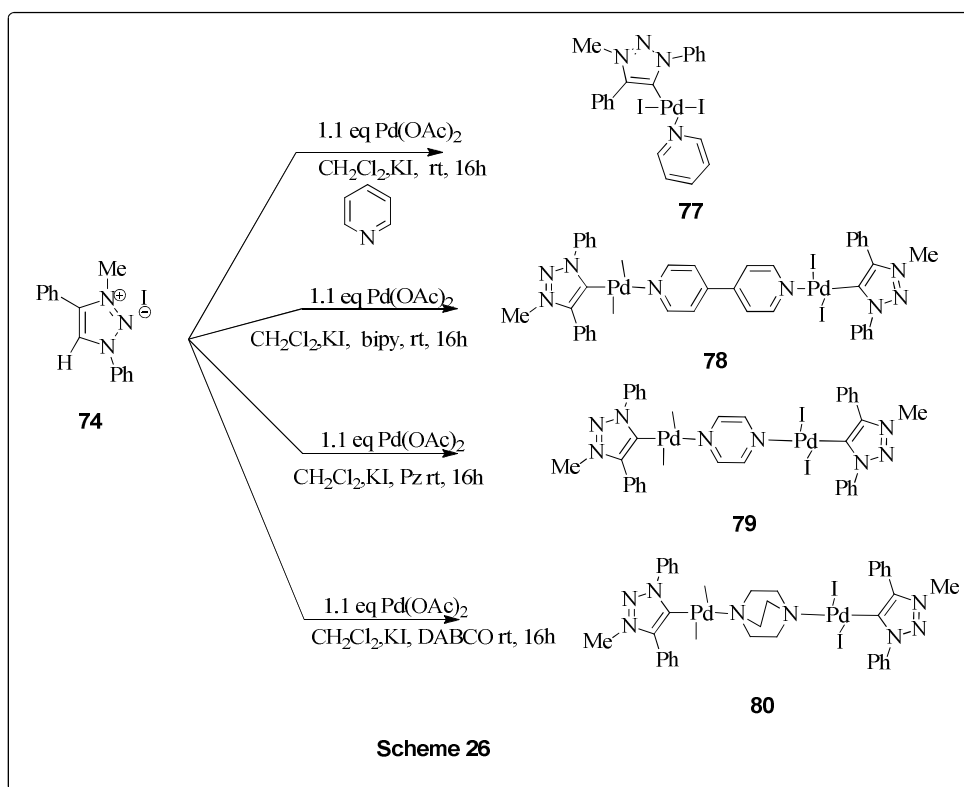
Using 0.5mol% of complexes **70** and **71** each they carried out the arylation of pentafluorobenzene with 4-bromotoluene in the presence of  $\text{K}_2\text{CO}_3$  in DMF at 120° and 140 °C. At 120 °C catalyst **70** provides better yield compared to **71**. But when

temperature was raised to 140 °C formation of Pd black was observed resulting in reduced yield.

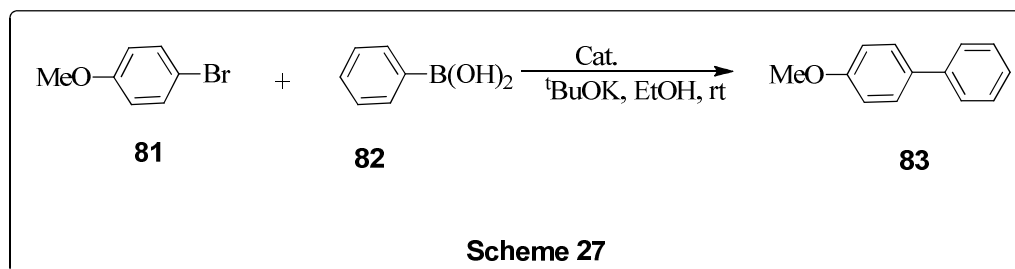
Sankararaman reported the synthesis of mononuclear PEPPSI type complexes and bridged binuclear complexes using 1,4-diphenyl-3-methyl-1,2,3-triazol-5-ylidene.<sup>38</sup> Mononuclear palladium complex **75** was synthesized from triazolium iodide **74**,  $n\text{-}(\text{Bu})_4\text{NI}$  and 0.6eq  $\text{Pd}(\text{OAc})_2$  in dichloromethane at room temperature and bridged binuclear **76** complex was obtained by treating the triazolium **74** salt with  $\text{Pd}(\text{OAc})_2$  and excess KI (Scheme 25).



Treating **74** with 2eq pyridine or its derivatives like 4,4'-bipyridine (bipy), pyrazine (Pz) and 1,4-diazabicyclooctane (DABCO) yielded linearly bridged binuclear complexes **77-80** by one pot procedure (Scheme 26).



Suzuki coupling of aryl bromides with phenyl boronic acid was studied using **75**, **76**, **77** and **79**. Coupling of 4-bromoanisole with phenyl boronic acid was taken as a model reaction. PEPPSI type complex **77** was found to be catalytically more active than **75** and **76**. Complexes other than **77** requires more time to complete the coupling of aryl bromides whereas under similar conditions complex **77** failed to catalyze the coupling of aryl chlorides.

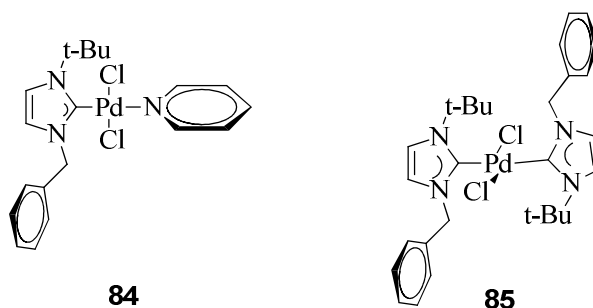


### 5.2.2 Biological activities of palladium N-heterocyclic carbene complexes

Cisplatin, carboplatin and oxaliplatin are widely used drug for anticancer treatment.<sup>39,40</sup> Owing to the side effects arising from the covalent interaction between platinum and DNA,<sup>41–44</sup> high toxicity, limited activity due to lesser aqueous solubility and multidrug resistance of tumor cells, there is a need to develop new drug. Due to

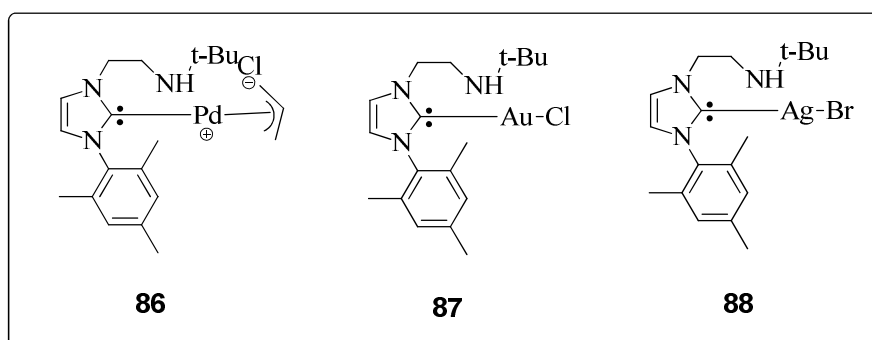
chemical and structural similarities of palladium and platinum, scientists are now considering palladium based drugs as a substitute to platinum. Cell viability and cytotoxicity assay are related to electronic and structural parameters associated with the drugs.

Panda in 2007 designed palladium NHC complexes like (NHC)Pd(pyridine)Cl<sub>2</sub> **84** and (NHC)<sub>2</sub>PdCl<sub>2</sub> **85** with anticancer activity.<sup>45</sup>



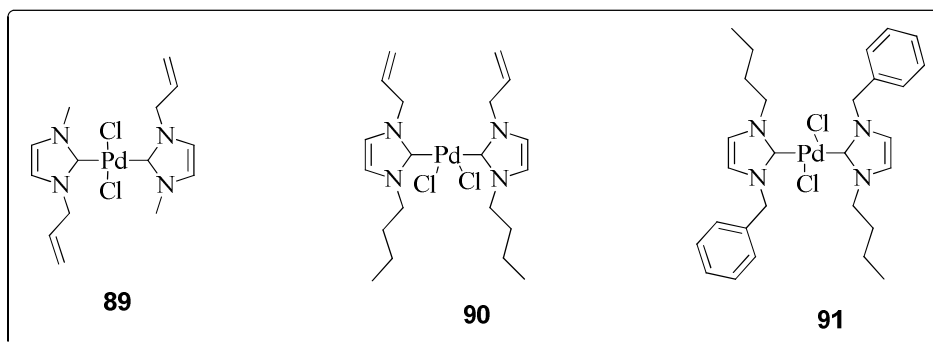
Compared to cisplatin, **85** exhibits significant cytotoxic activity towards three human tumor cells namely cervical cancer (HeLa), breast cancer (MCF-7), and colon adenocarcinoma (HCT 116). The cells were incubated with different concentrations of **85** and cisplatin to find out the inhibition of cell proliferation using sulforhodamine B assay as standard. Halfmaximal inhibitory concentration (IC<sub>50</sub>) values were low at micromolar concentration of **85**.

Cytotoxic activity of amino-NHC complex **86**, **87** and **88** was investigated by Li in 2011.<sup>46</sup> The growth inhibition assays were carried out in three different human cancer cells like breast adenocarcinoma (MCF 7 and MDA-MB-231) and glioblastoma (U-87 MG) using cisplatin as reference drug.



From the results they concluded that compared to silver NHC, palladium and gold NHC complexes exhibit remarkable ant proliferative activities.

Haque *et.al* reported the antimicrobial and anticancer activity of unsymmetrically substituted bis NHC Pd(II) complexes (**89**, **90**, **91**) derived from imidazol-2-ylidenes, having general formula  $[\text{PdCl}_2(\text{NHC})_2]$ .<sup>47</sup> These were synthesized by transmetallation from corresponding silver NHC complexes. Among these, **89** and **91** adopt *trans-anti* arrangement of ligands whereas **90** adopt *cis-syn* arrangement.



**5.3.1 Reagents and Materials**

Phenyl acetylene, palladium (II) acetate, bisacetoneitriledichloropalladium(II), boronic acids from Sigma Aldrich

Sodium sulphate anhydrous, sodium ascorbate, 1,2-dibromoethane, potassium carbonate, dimethyl formamide, acetonitrile, tetrahydrofuran were purchased from Merck

Sodium azide from Nice Chemicals, Kochi

Organic halides from Spectrochem, Mumbai

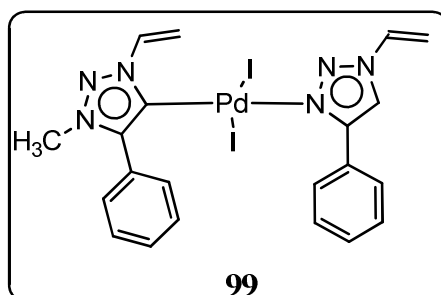
Silica Gel for Thin Layer and Column Chromatography -Merck

**5.3.2 Instruments**

- NMR – Bruker Avance III, 400MHz
- GC-MS –Thermo Fisher Scientific
- Single Crystal X-ray Diffractometer
- C-H-N analyzer- Elementar Vario EL III

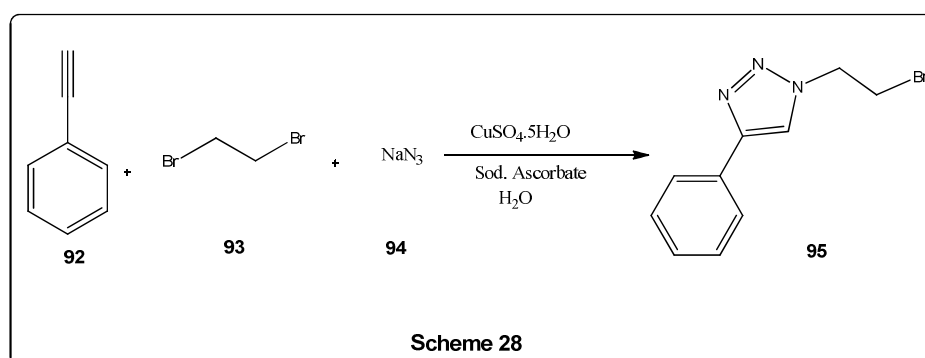
## 5.4 Results and Discussion

In order to effectively utilize the strong donor capacity of triazolylidene ligand and to incorporate the hydrophilicity of the palladium complex, we have designed a novel  $C_{tzi}$ -Pd- $N_{tzi}$  complex **99**. Similar molecules using imidazoles were recently reported by Lu *et.al* and proved to be effective in catalyzing the Suzuki-Miyaura coupling between benzyl chlorides and aryl boronic acids in water<sup>19</sup>.

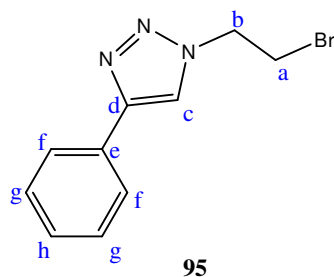


### 5.4.1 Synthesis of compounds 95, 96 & 97

Click reaction between phenyl acetylene and an *in situ* generated monoazide from 1,2-dibromoethane afforded 1,2,3-triazole **95**. Using threefold excess of 1,2-dibromoethane, monoazide formation takes place and 1-(2-bromoethyl)-4-phenyl triazole **95** was obtained as the sole product in good yields (**Scheme 28**). In this new protocol, although the dibromide was used in excess, it could be recovered during work up and be reused after distillation. The structure of the triazole **95** was confirmed from spectral data. Similar triazoles were recently reported by Das *et.al* using copper supported polymer.<sup>48</sup>



**Scheme 28** Synthesis of Compounds **95**



Protons of carbon atom (**a**) that is directly attached to bromine gives triplet at 3.73 ppm, **b** protons which is directly attached to triazole ring system shows peak at 4.74 ppm which is downfield compared to **a**. One proton singlet at 7.84 ppm corresponds to the CH proton of triazole ring system (**c**). Phenylic ortho protons (**f**) appear as doublet at 7.78 ppm, meta protons (**g**) as multiplet at 7.36 ppm and para protons (**h**) 7.28 ppm.

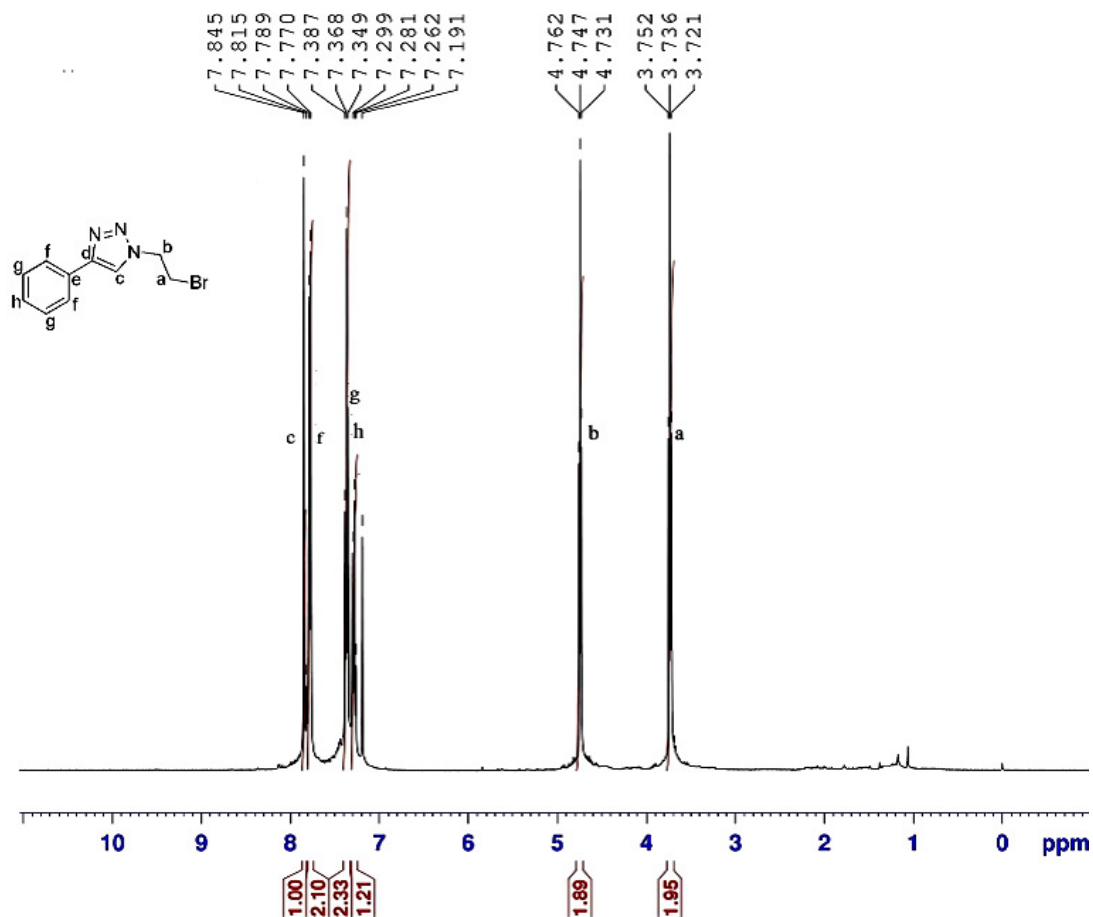


Fig 7.1  $^1\text{H}$  NMR of compound **95**

The peak at 29.3 ppm corresponds to carbon atom (**a**) which is directly attached to bromine and carbon attached to triazole ring system (**b**) shows a peak at 51.7 ppm. Triazole carbon atoms which is directly bonded to hydrogen (**c**) provide a peak at



120.5 ppm and the one which attached to phenyl ring system shows peak at 147.6 ppm. Peaks at 125.8, 128.4, 128.9 and 130.1 ppm corresponds to phenyl carbon atoms (f, h, g & e).

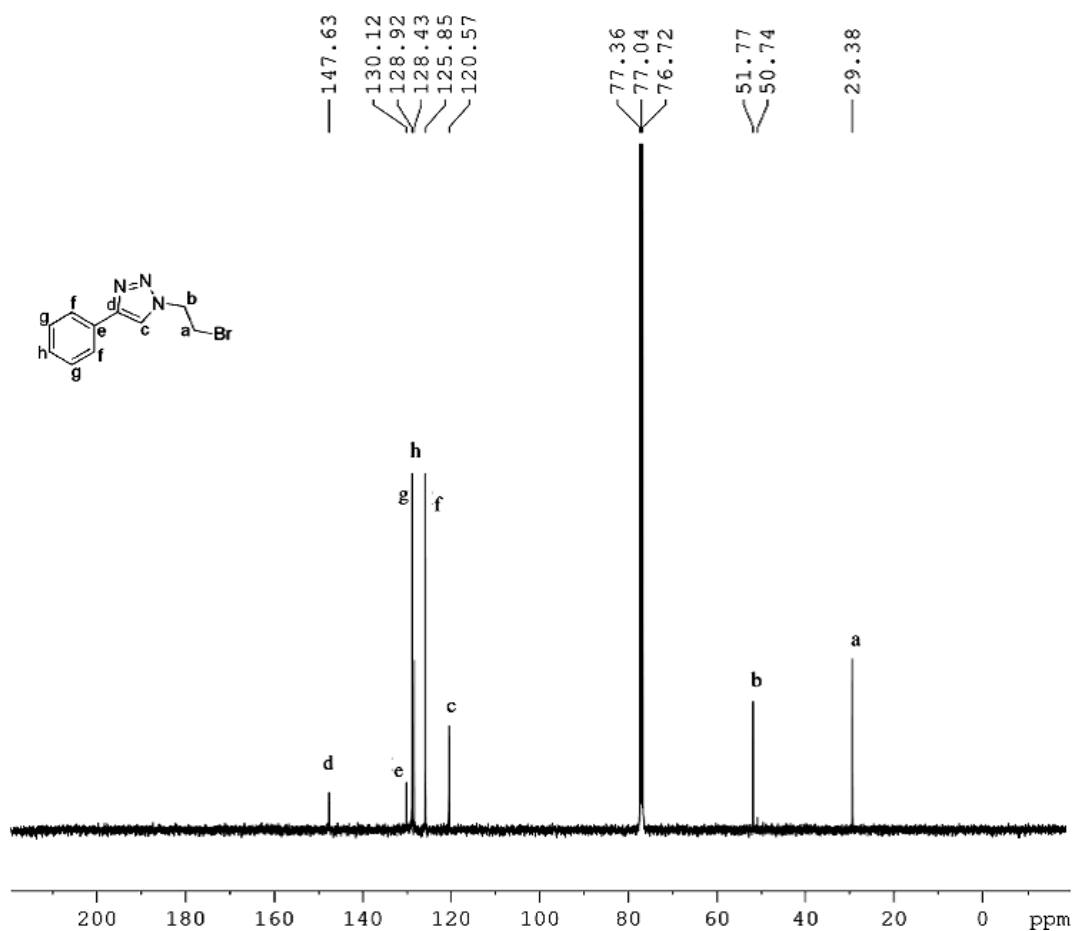
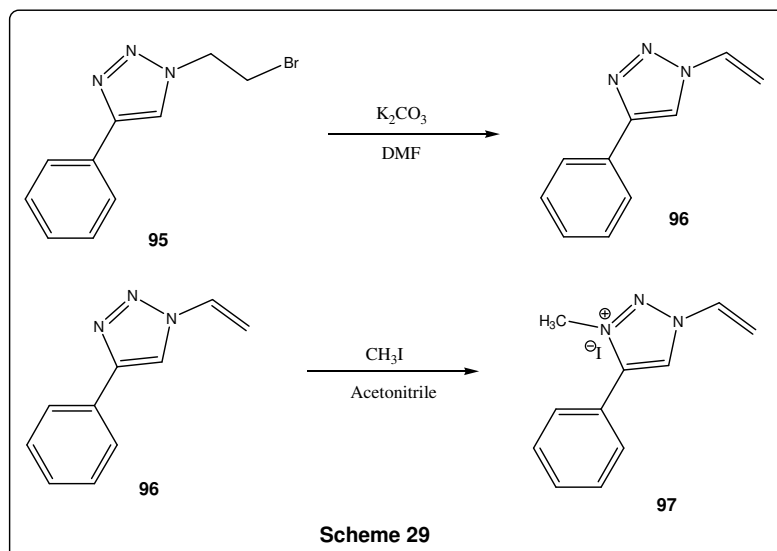
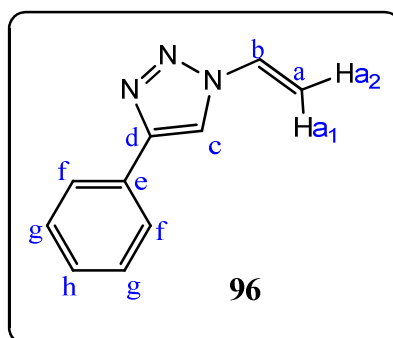


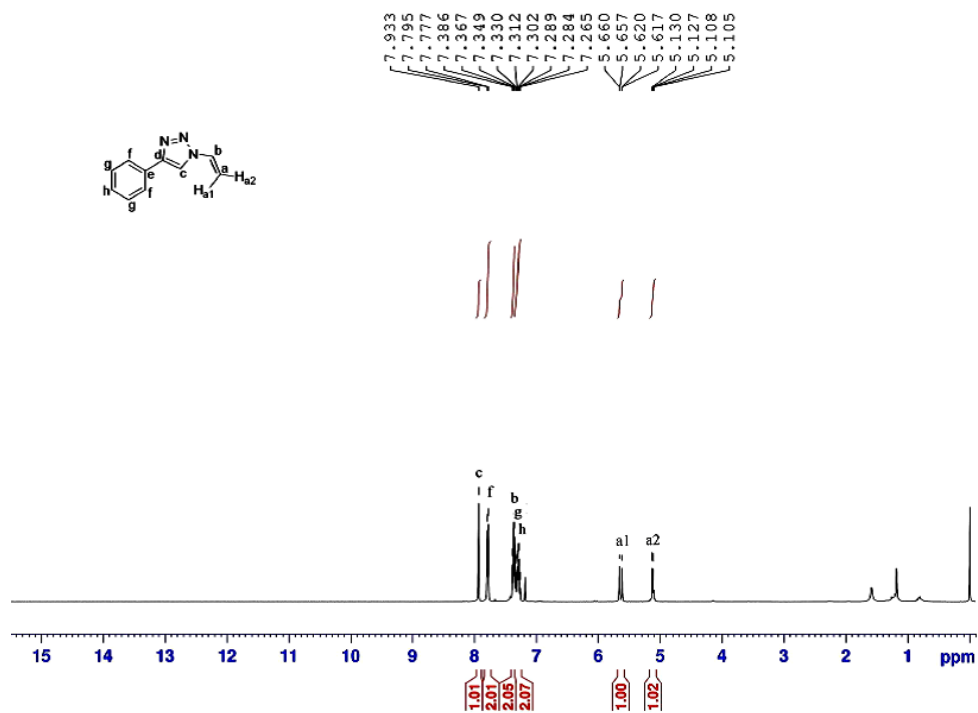
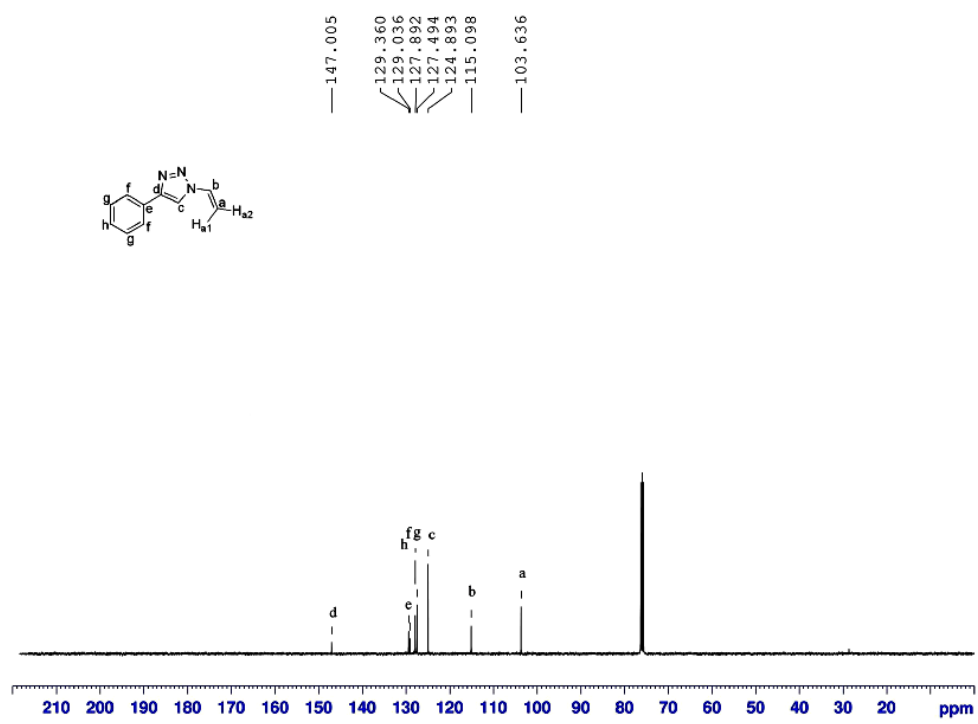
Fig 7.2  $^{13}\text{C}$  NMR of compound 95



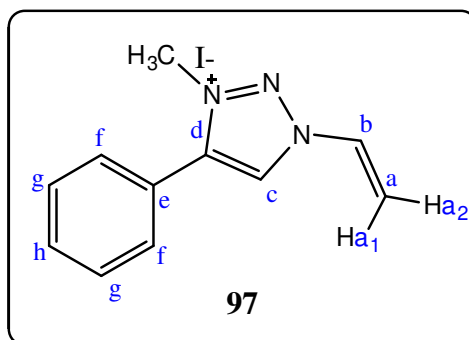
Dehydrobromination of the triazole **95** using  $K_2CO_3$  in DMF afforded the vinyl triazole **96** in 87% yields. Methylation of the vinyl triazole using methyl iodide in acetonitrile as solvent afforded the triazolium salt **3** in quantitative yield and this triazolium salt was used for palladation (**Scheme 29**).



The formation of vinyl triazole obtained by the dehydrohalogenation was confirmed by  $^1H$  NMR and  $^{13}C$  NMR analysis. Vinylic protons ( $a_1$  and  $a_2$ ) appear as doublet of doublet at 5.1 and 5.64 ppm respectively while multiplet at 7.2 ppm corresponds to both meta ( $g$ ), para ( $h$ ) and vinyl ( $b$ ) protons. Peak at 7.79 ppm corresponds to ortho protons of phenyl ring system. Triazole CH proton provide peak at 7.93 ppm

Fig 8.1  $^1\text{H}$  NMR of compound 96Fig. 8.2  $^{13}\text{C}$  NMR of compound 96

$^{13}\text{C}$  NMR provides peak at 103.6 ppm corresponds to  $\text{CH}_2$  (a) and NCH carbon (b) was observed at 115 ppm. Triazole CH peak (c) observed at 124.8 ppm and triazole carbon connected to phenyl ring (d) appeared at 147 ppm. Phenyl carbon peaks were observed at 127.4, 127.8, 129.0 and 129.3 ppm respectively.



The peak at 4.38 ppm corresponds to  $\text{CH}_3$  protons. The vinylic protons ( $\mathbf{a}_1$ ,  $\mathbf{a}_2$  &  $\mathbf{b}$ ) appear at 5.19, 5.70-5.72 and 6.56 ppm. Triazole hydrogen (c) shifted to highly aromatic region after alkylation and observed at 9.74 ppm. The phenyl proton appeared at 7.44, 7.64-770 and 7.79-7.87 ppm.

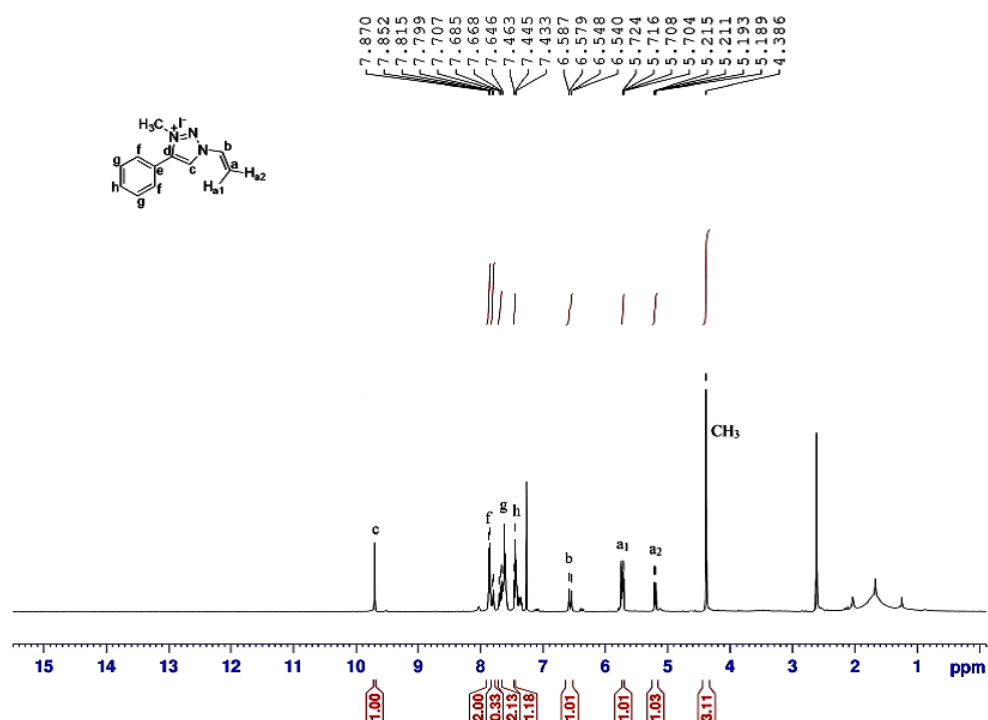


Fig. 9.1  $^1\text{H}$  NMR of compound 97

Peak at 39.68 ppm corresponds to methyl carbon. Vinylic carbons (**a** & **b**) peaks appear at 104.7 and 116.4 ppm. Triazole carbons **c** & **d** appeared at 132.3 and 159.6 ppm. Phenyl carbons observed at 129.8 (**e**), 128.9 (**f**), 127.3 (**h**) and 125.9 (**g**) ppm.

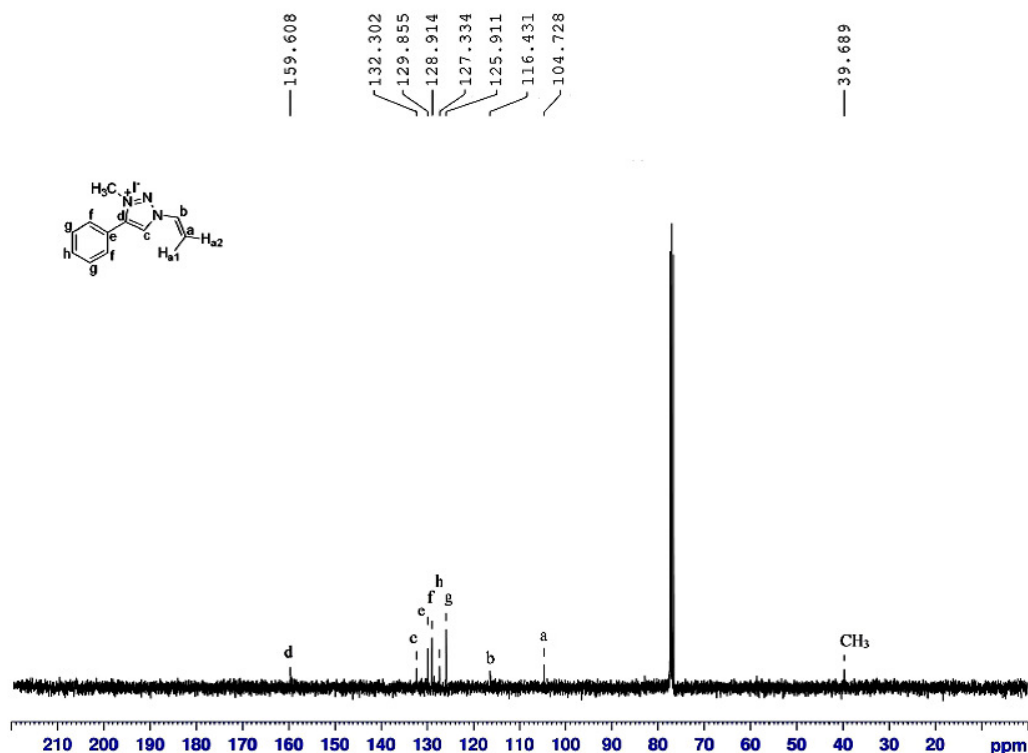
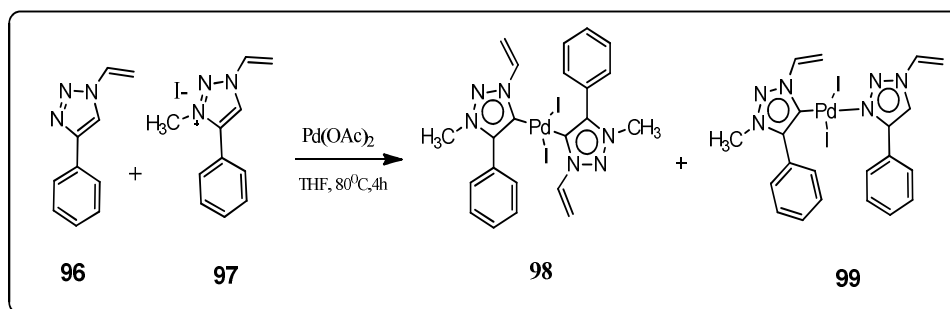


Fig 9.2 <sup>13</sup>C NMR of compound **97**

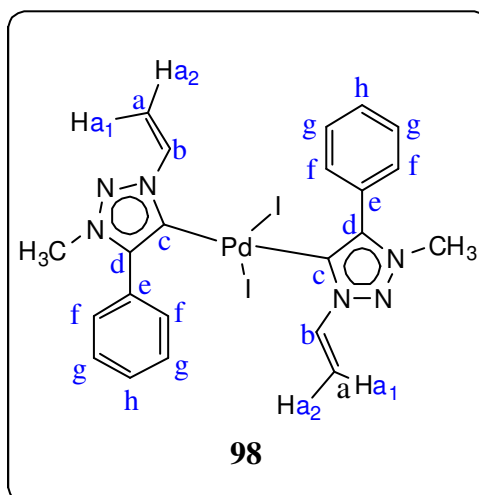
### Synthesis of mixed palladium complexes

In order to synthesize the palladium triazole **99** with labile triazole moiety, equimolar quantities of triazolium salt **97** was mixed with vinyl triazole **96** and palladium acetate in tetrahydrofuran (THF) followed by heating at 80 °C for 4 h. The solvent was removed under reduced pressure to afford a red solid. Thin layer chromatography showed the presence of mixture of products. After column chromatography the complexes **98** and **99** were isolated in 22% and 15% yield respectively (Scheme 30).



**Scheme 30** Synthesis of mixed palladium complexes

When two equivalents of the triazolium salt **97** were treated with palladium acetate in THF, the  $\text{C}_{\text{tzl}}-\text{Pd}-\text{C}_{\text{tzl}}$  complex **98** was obtained as the sole product with 62% yield. The structure of the palladium complex was confirmed by  $^1\text{H}$  NMR,  $^{13}\text{C}$  NMR and elemental analysis.



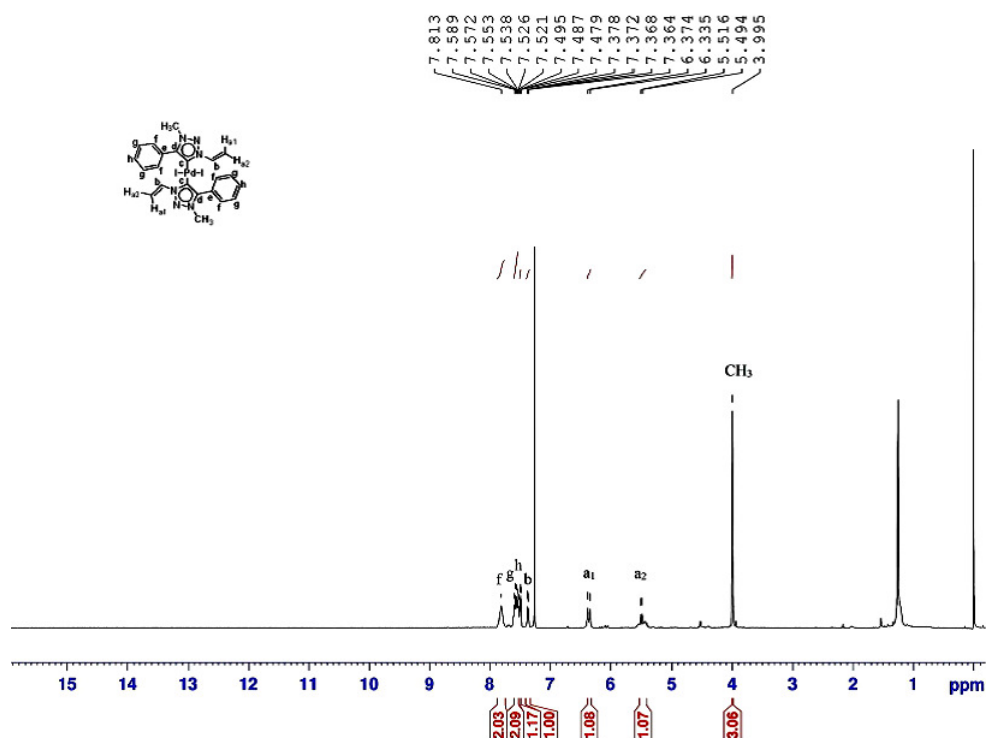


**Fig 10.1**  $^1\text{H}$  NMR of compound **98**

Methyl protons appeared at 3.99 ppm, vinyl protons were observed at 5.50, 6.35 and 7.37 (**a<sub>1</sub>**, **a<sub>2</sub>** & **b**). Phenyl proton (**h**) appear as triplet at 7.48 ppm, multiplet of meta protons (**g**) at 7.52-7.58 ppm and ortho proton at 7.81 ppm. Methyl carbon was observed at 37.9 ppm. Peaks of vinyl carbons (**a<sub>1</sub>** & **a<sub>2</sub>**) observed at 110.1 and 128.8 ppm. Aromatic carbons of phenyl ring were observed at 128.8, 129.1, 129.2, 130.1 whereas triazole carbon (**d**) connected to phenyl ring was observed at 144.8 ppm. Carbon connected to palladium (**c**) shows peak at 130.4 ppm.

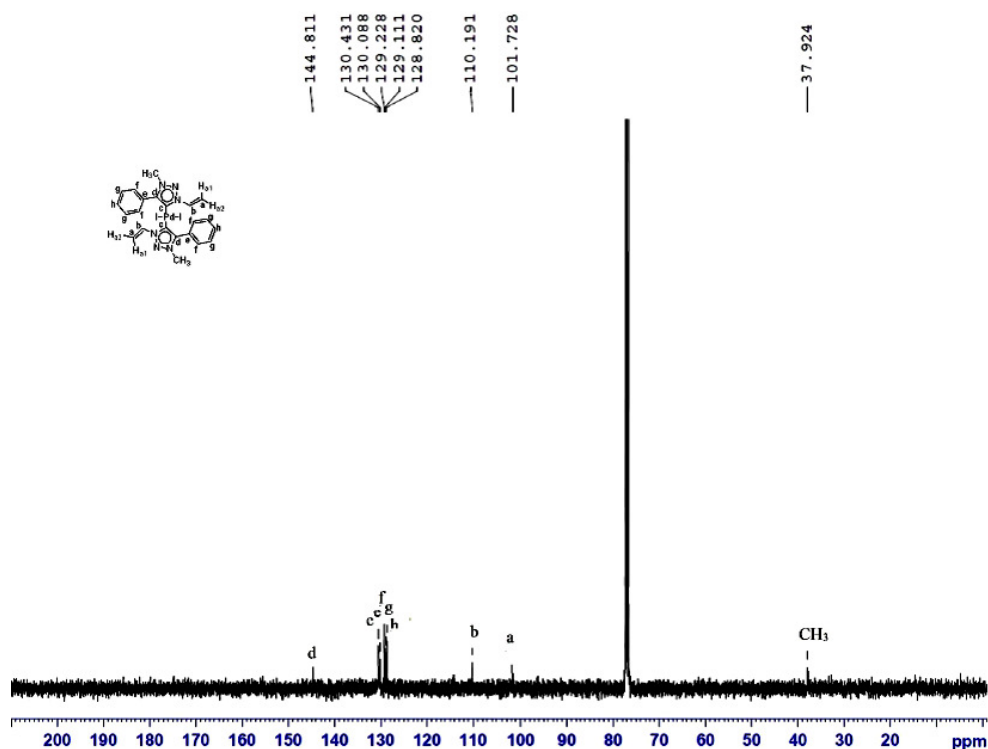
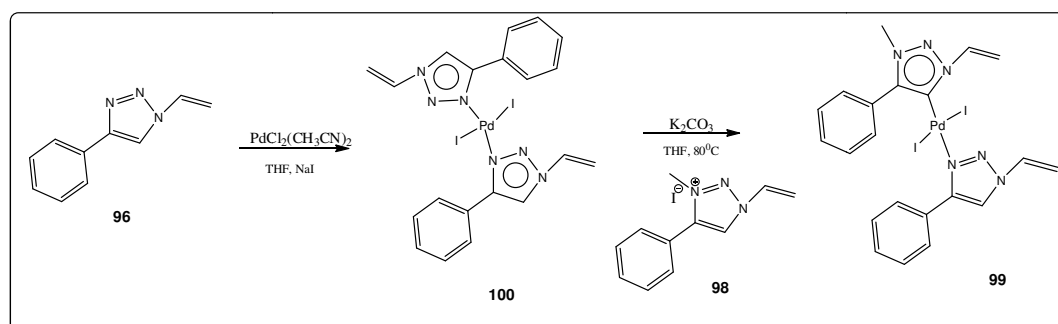


Fig 10.2  $^{13}\text{C}$  NMR of compound **98**

Single palladation of the vinyl triazole **96** using bisacetonitrile dichloropalladium (II) afforded the N-Pd-N complex **100**. Ligand substitution reaction of the complex **100** was then carried out for the synthesis of complex **99**. Complex **100** was allowed to react with the triazolium iodide **97** followed by heating at 80 °C in THF in the presence of base  $\text{K}_2\text{CO}_3$  afforded the air and moisture stable orange colored palladium complex **99** in 70% yield (**Scheme 31**). Here the reaction takes place by substitution of one of the 1,2,3-triazole ligands by an *in situ* generated triazolylidene. It is noteworthy that such a synthetic strategy has not been reported so far for the synthesis of mixed N-heterocyclic carbene complexes.



Scheme 31 Synthesis of complex **99** and **100**



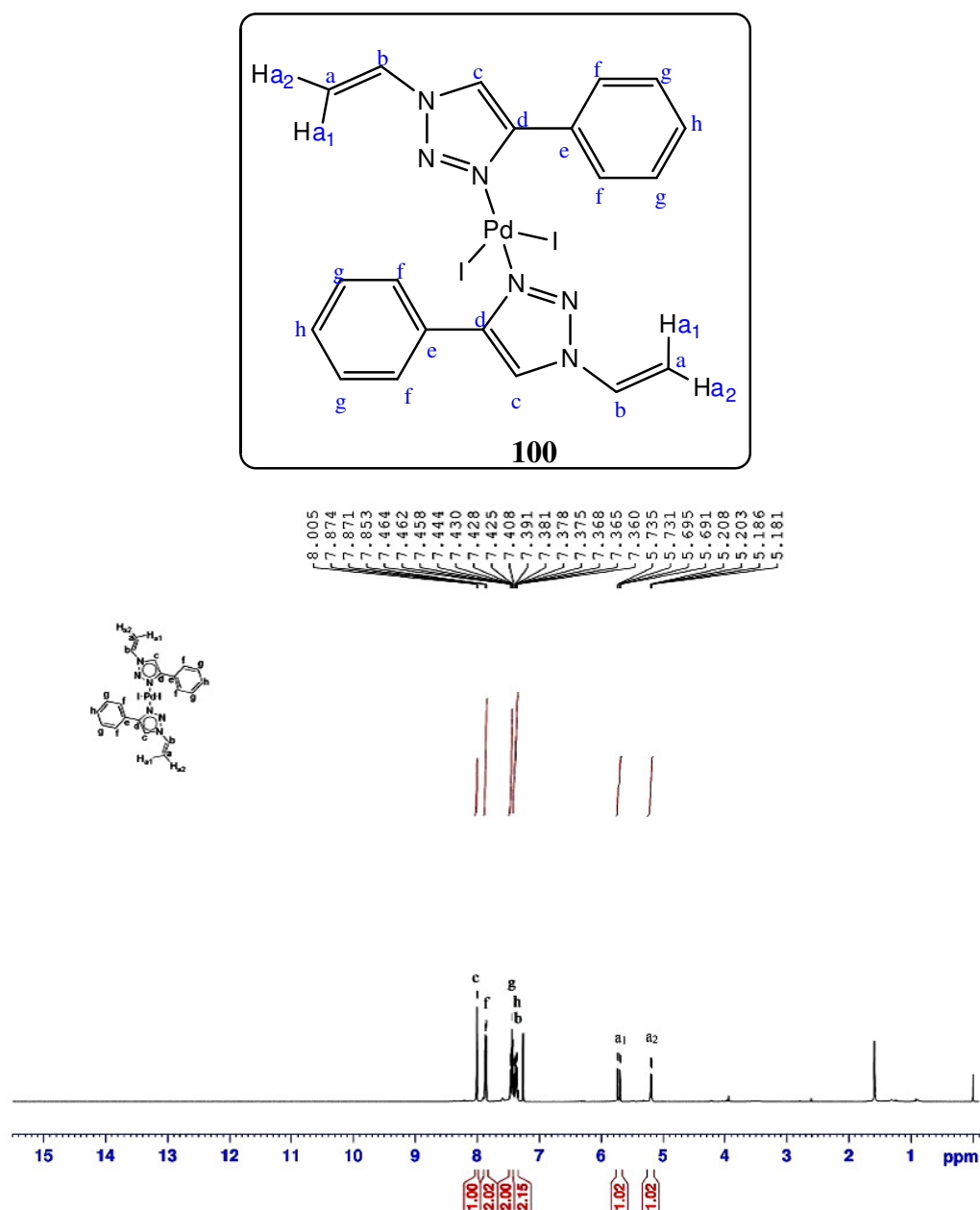


Fig 11.1  $^1\text{H}$  NMR of compound **100**

Protons of vinylic carbons (**a**<sub>1</sub> & **a**<sub>2</sub>) observed at 5.19 and 5.71 ppm. Multiplet at 7.39 ppm corresponds to both vinyl and phenyl para protons (**b** & **h**). Another multiplet at 7.46 ppm for meta protons of phenyl ring. Peak observed at 7.87 ppm corresponds to ortho protons (**f**) and singlet at 8 ppm corresponds to proton of triazole carbon(**c**). In  $^{13}\text{C}$  NMR, vinyl carbons observed at 104.6 and 116.1 ppm while triazole carbon peak was detected at 125.9 ppm. Aromatic carbons were identified at 128.5, 128.9, 130, 130.4 and 148 ppm.

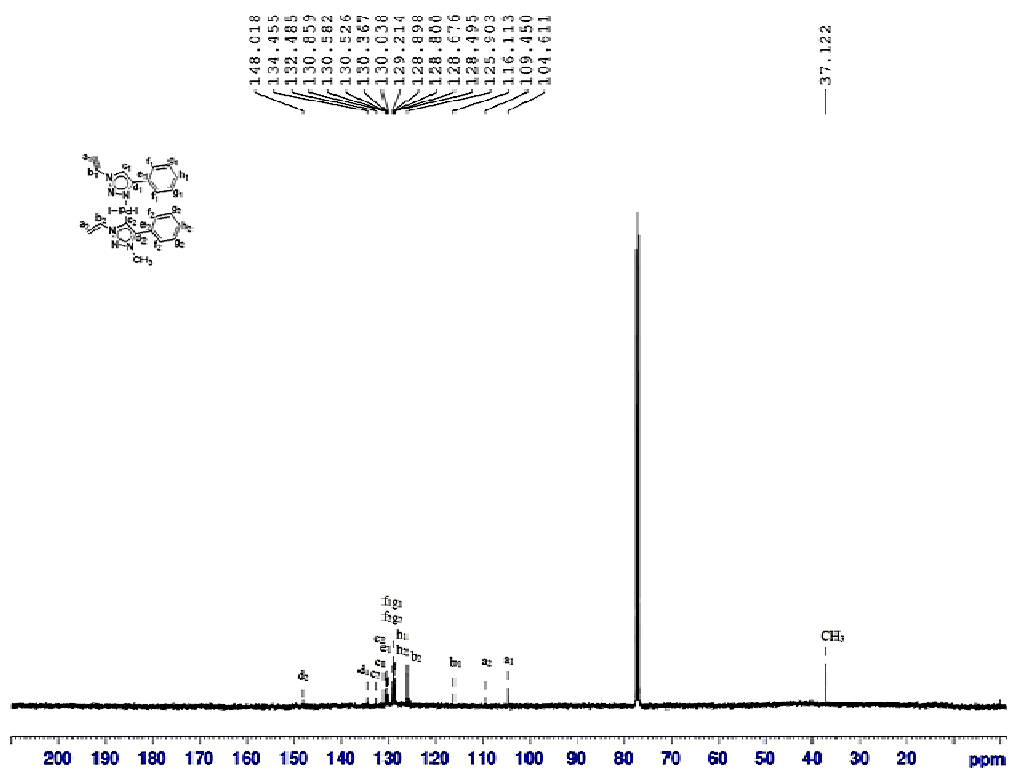
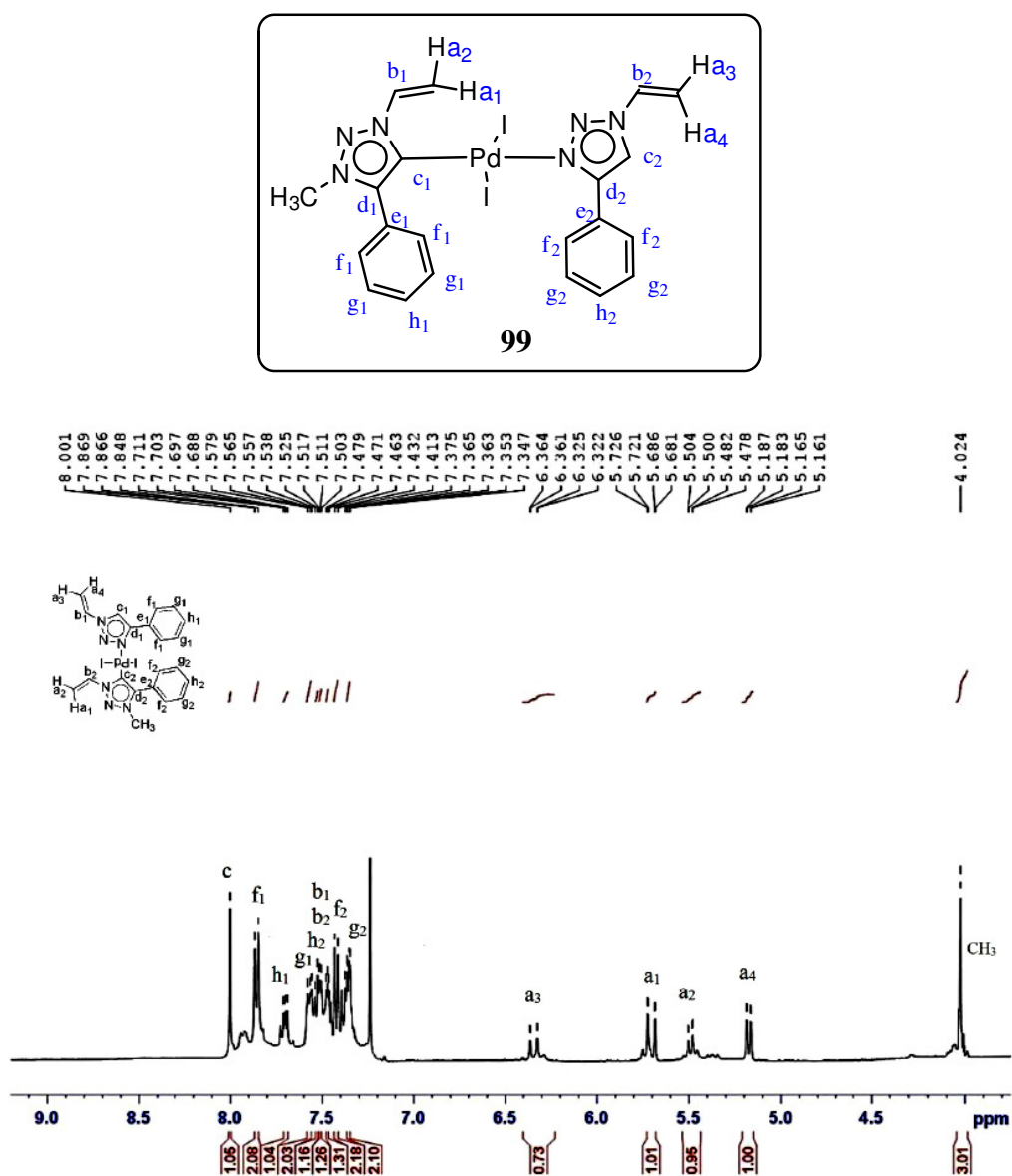


Fig 11.2  $^{13}\text{C}$  NMR of compound 100

Fig 12.1  $^1H$  NMR of compound **99**

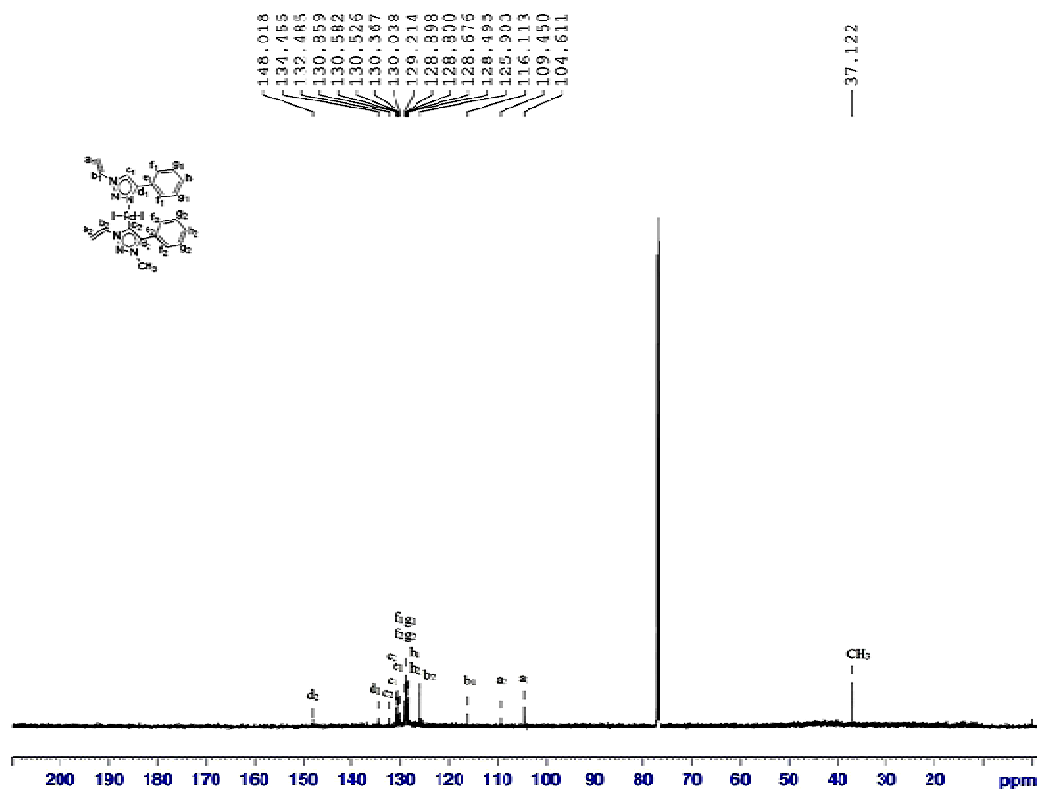
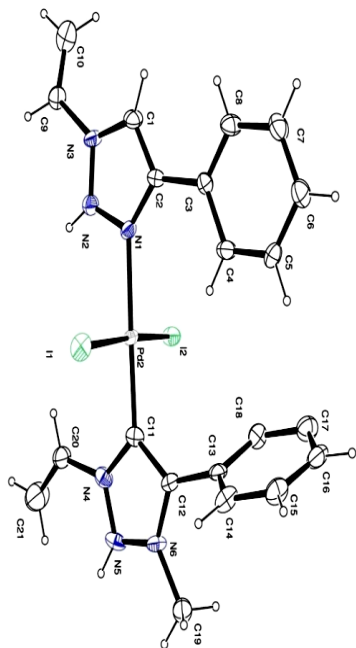


Fig 12.2 <sup>13</sup>C NMR of compound **99**

<sup>1</sup>H NMR spectrum of **99** clearly indicates the presence of both N-bound triazole and C-bound triazolylidene ligands. Methyl group of the triazolylidene moiety appeared as singlet at 4.02 ppm similar to the bistriazolylidene complex **98**. Vinylic protons appeared as doublets at 5.1, 5.5, 5.7, and 6.3 ppm, while the NCH protons of both ligands are shifted downfield to the aromatic region. One proton singlet at 8.0 ppm corresponds to the CH proton of the triazole ring which is consistent with the N-bound bistriazole palladium complex **100**. The <sup>13</sup>C NMR resonance peak also indicates the presence of N and C bound triazole ligands. The peak at 37.1 corresponds to CH<sub>3</sub> carbon. Total number of N-vinyl and aromatic carbons also account for the presence of N-bound triazole and C-bound triazolylidene ligands in the palladium complex.

Table 1 Crystallographic data of compound **99**

Parameters	
<b>Formula</b>	C <sub>12</sub> H <sub>20</sub> I <sub>2</sub> N <sub>6</sub> Pd
<b>Formula weight</b>	716.63
<b>Crystal system</b>	Triclinic
<b>Space group</b>	P-1
<b>a (Å)</b>	9.0794 (5)
<b>b (Å)</b>	12.1285 (7)
<b>c (Å)</b>	13.4377 (8)
<b>α°</b>	94.072(3)
<b>β°</b>	104.798(2)
<b>γ°</b>	93.927(2)
<b>V (Å<sup>3</sup>)</b>	1421.29(14)
<b>T (K)</b>	296(2)
<b>Z</b>	2
<b>Reflections/unique</b>	14906 / 3819
<b>R<sub>int</sub></b>	0.0317
<b>μ mm<sup>-1</sup></b>	2.841
<b>F(000)</b>	680
<b>θ range</b>	1.57 to 23.25
<b>Goodness-of-fit on F<sup>2</sup></b>	1.100
<b>Final R indices</b>	R <sub>1</sub> = 0.0681 wR <sub>2</sub> = 0.1817
<b>R indices</b>	R <sub>1</sub> = 0.0841 wR <sub>2</sub> = 0.1953

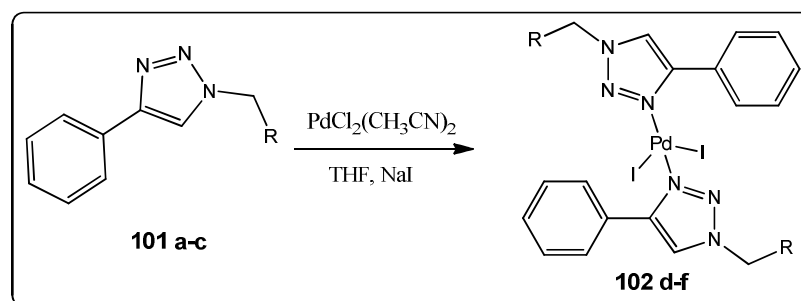
Fig. 13 ORTEP diagram of the palladium complex **99**

Pure crystals of **99** were obtained by slow diffusion of pentane into a solution of **99** in dichloromethane at room temperature. The palladium complex was characterized by single crystal X-ray diffraction (XRD) data (Fig.13). Single crystal XRD shows that the complex **99** adopts a distorted square planar geometry around the palladium centre. In complex **99** the two C,N ligands and the iodide ions respectively adopt *trans* geometry. The phenyl groups are oriented *cis* to each other with respect to C2-axis passing between the triazolylidene ligands, bisecting the N1-Pd-C11 angle. The Pd-C11 and Pd-N1 distances are 1.962 Å and 2.122 Å respectively. The bond lengths are similar to those related Pd C<sub>carbene</sub> complexes derived from triazolylidene and PEPPSI ligands<sup>15</sup> or imidazolylidene stabilized with N-donor ligands such as imidazole,<sup>48</sup> piperazine and DABCO,<sup>49</sup> bezoxazole,<sup>50</sup> dihydrooxazole,<sup>51</sup>

isoquinoline,<sup>52</sup> ethylamine<sup>53</sup> or PEPPSI.<sup>20</sup> Abnormal carbene NHC ligands are considered better  $\sigma$  donors than their normal analogues and this strong *trans* influence of 1,2,3-triazolylidene ligand is reflected in longer Pd-N1 bond length, favoring the “throw away” effect. Bond angle of N1-Pd-C11 was found to be 178.65 Å.

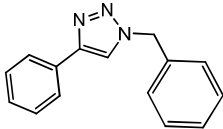
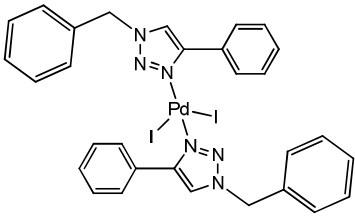
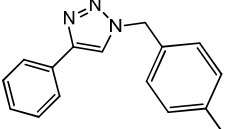
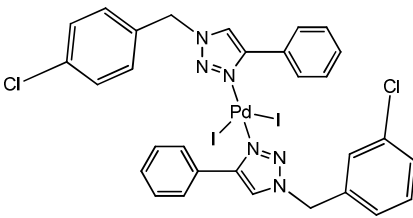
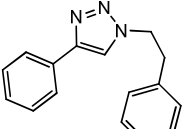
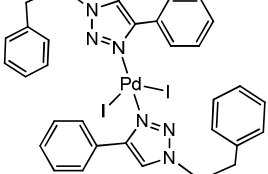
#### Synthesis of N-Pd-N complexes (102 d-f)

Reaction of three different 1,4-disubstituted-1,2,3-triazole (**101 a-c**) with bis(acetonitrile)dichloropalladium (II) in THF and in the presence of NaI at room temperature afforded a yellow colored solids having N-Pd-N bonding pattern (**102 d-f**).

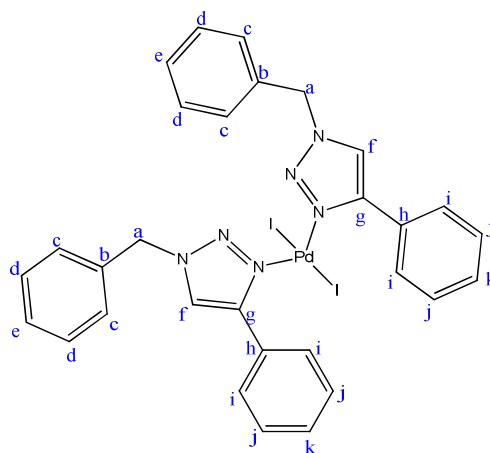


**Scheme 31** General scheme for the synthesis of complexes having N-Pd-N bonding pattern

Table 2 N-Pd-N complexes

Reactant	Product
 <p>1-benzyl-4-phenyl-1H-1,2,3-triazole</p> <p><b>101a</b></p>	 <p><math>N_{benztzl}-Pd-N_{benztzl}</math></p> <p><b>102d</b></p>
 <p>1-(4-chlorobenzyl)-4-phenyl-1H-1,2,3-triazole</p> <p><b>101b</b></p>	 <p><math>N_{Clbenztzl}-Pd-N_{Clbenztzl}</math></p> <p><b>102e</b></p>
 <p>1-phenethyl-4-phenyl-1H-1,2,3-triazole</p> <p><b>101c</b></p>	 <p><math>N_{phenethzl}-Pd-N_{phenethzl}</math></p> <p><b>102f</b></p>

For the general discussion, compound **102d** was taken as representative molecule.

**102d**

$^1\text{H}$  NMR of compound **102d** is given (Fig 14.1). Singlet observed at 5.61 ppm corresponds to benzylic protons (**a**), multiplet at 7.30-7.38 corresponds to ortho and para protons at **c** and **e**. protons at positions **d** and **k** provide multiplet at 7.40-7.48 ppm. 7.49-7.67 ppm corresponds to protons at **j** and peak detected at 7.8 ppm corresponds to proton at **i**. The triazole proton shows singlet at 8.33 ppm.

The  $^{13}\text{C}$  NMR (Fig. 14.2) spectrum is in agreement with  $^1\text{H}$  NMR spectral data. The downfield peak at  $\delta 149.6$  ppm is due to the carbon at the position **g** and the characteristic peak of triazole carbon **f** observed at 119.5 ppm. The benzylic carbon **a** gives peak at 55.8 ppm and the values at 136.2, 128, 128.9 and 129.1 ppm corresponds to **b**, **c**, **d** & **e** carbons of phenyl ring. Peaks at 125.7, 128.1 and 128.8 belong to phenyl carbons attached to triazole carbon.

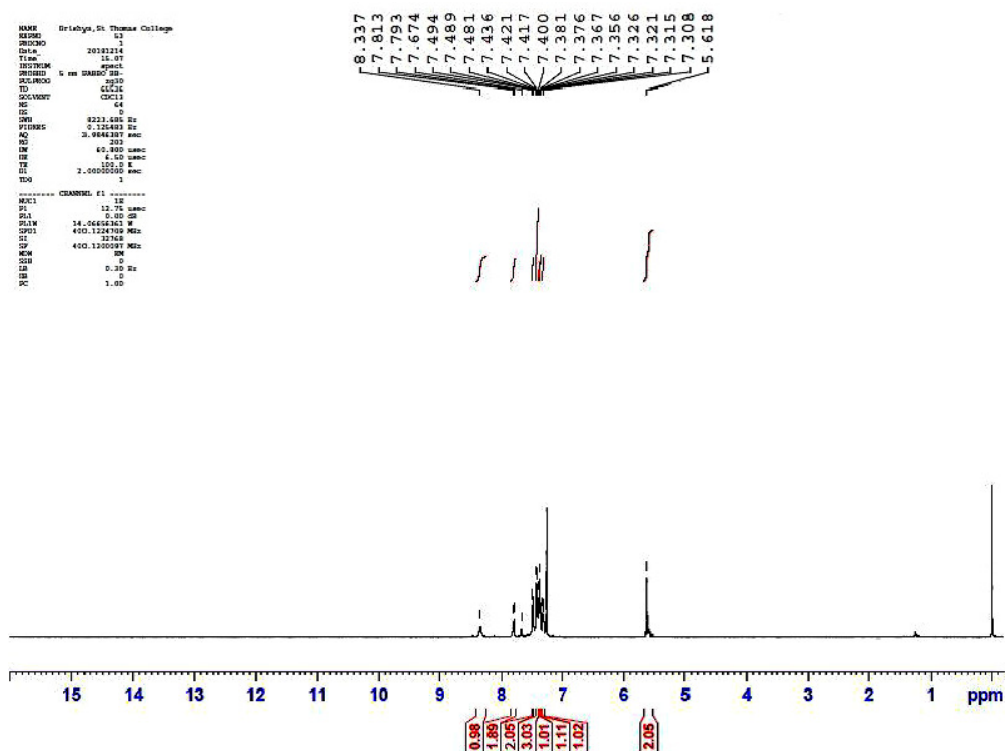
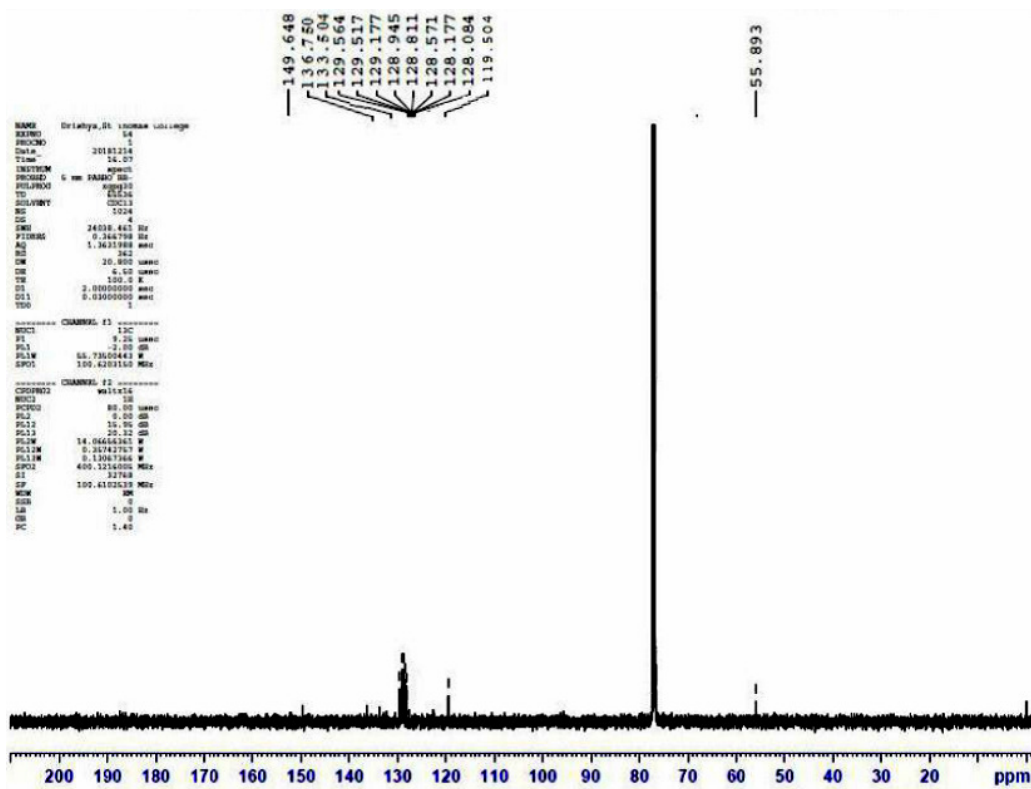


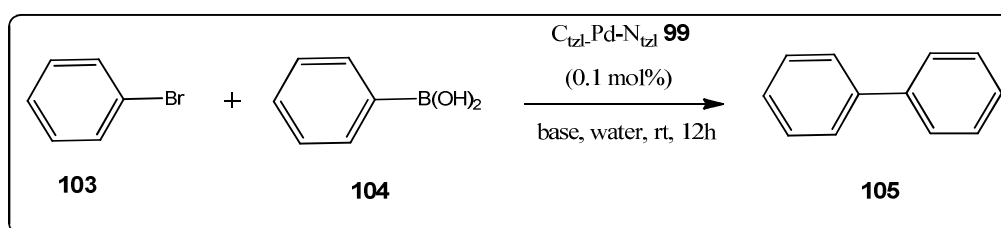
Fig 14.1  $^1\text{H}$  NMR of compound **102d**



Fig 14.2  $^{13}\text{C}$  NMR of compound 102d

### 5.4.2 Catalytic Studies of $C_{tztl}$ -Pd- $N_{tztl}$ complex (**99**)

The palladium complex **99** was screened as catalyst for Suzuki-Miyaura coupling of aryl halides with aryl boronic acids. Bromobenzene and phenyl boronic acid were selected as model substrates and the reaction was carried out under mild conditions using different bases (**Scheme 32 & Table 3**). Among the bases used, potassium *tert*-butoxide ( $KO^tBu$ ) was found to be the most suitable one under our reaction conditions and gives the product biphenyls in excellent yield.  $KOH$ ,  $K_2CO_3$  and  $CS_2CO_3$  etc resulted in slightly lower yields. The aryl halide, phenyl boronic acid, palladium catalyst and  $KO^tBu$  were taken in RB flask containing water and stirred at room temperature for 12 h. The reaction was carried out with very low catalyst loading (0.1 mol%). The better yield was obtained in the case of  $KO^tBu$  compared to  $KOH$  probably due to the difference in the dissociation constants ( $pK_a$ ,  $KOH=15.7$  and  $pK_a$ ,  $KO^tBu=17$ ). Optimum concentration of the hydroxide is important in the formation of hydroxypalladium complex, transmetalation process and to prevent the formation of  $ArB(OH)_3$ .<sup>54-56</sup> Kolmogorov-Smirnov test was used to verify the normality of yields of  $KO^tBu$  and  $KOH$ . *t*-Test was performed to examine whether there is significant difference between the yields obtained using  $KO^tBu$  and  $KOH$ . Since the obtained *p* value (0.025) is less than 0.05 and there is a significant difference in the yields obtained using  $KO^tBu$  and  $KOH$  (5% level of significance)



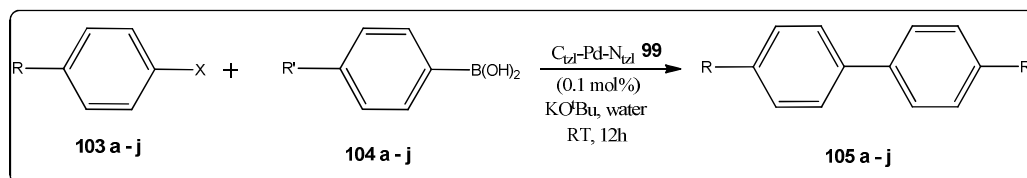
Scheme 32

**Table 3** Optimization of base used for the  $C_{tzl}$ -Pd(II)- $N_{tzl}$  complex **99** catalyzed coupling of bromobenzene **101** with phenyl boronic acid **102**

Entry <sup>a</sup>	Base	Yield <sup>b</sup> (%)
1	K <sub>2</sub> CO <sub>3</sub>	91
2	Na <sub>2</sub> CO <sub>3</sub>	86
3	CS <sub>2</sub> CO <sub>3</sub>	85
4	HCOONa	45
5	NaHCO <sub>3</sub>	72
6	NaOH	83
7	KOH	87
8	KO <sup>t</sup> Bu	94
9	NaO <sup>t</sup> Bu	89

<sup>a</sup>All reactions were carried out using **101** (1.0mmol), **102** (1.0mmol), **99**(0.1 mol%), base(2 equiv.) H<sub>2</sub>O (5ml) at room temperature for 12h. <sup>b</sup> Isolated yield.

Efficiency of other palladium complexes **98** and **100** towards this coupling reaction were also investigated. However they were found to be less reactive than the  $C_{tzl}$ -Pd- $N_{tzl}$  complex **99**. similarly, this catalyst as found to be equally good or even better than other water soluble palladium non-carbene systems.<sup>57-60</sup> The catalyst **99** was very effective in coupling aryl chlorides, bromides or iodides with aryl boronic acids (**Scheme 33**). It was observed that the presence of electron donating or electron withdrawing groups had very little effect on the overall yield of the product (**Table 4**).

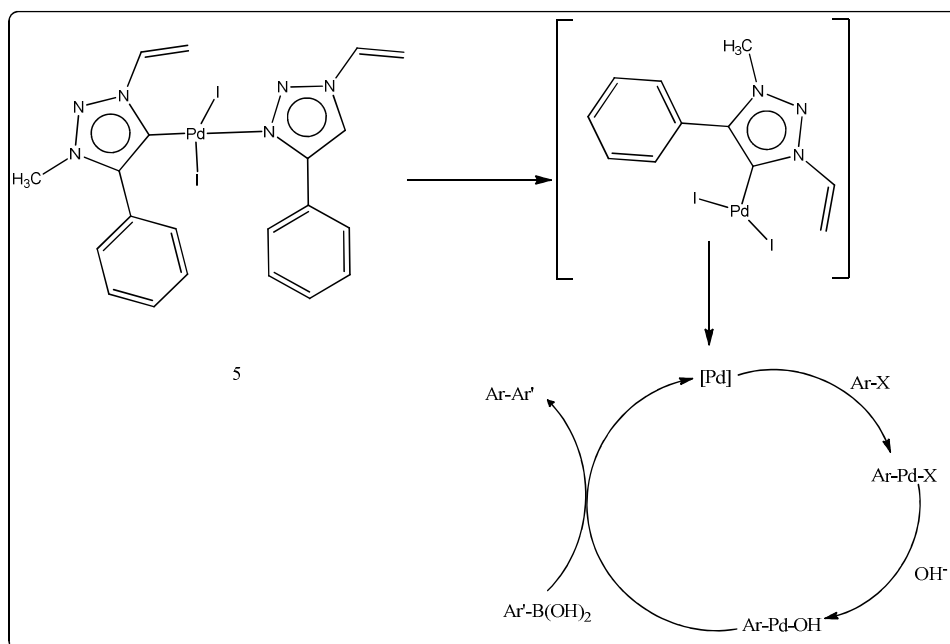
**Scheme 33****Table 4** Suzuki-Miyaura coupling reaction of aryl halides and boronic acids at room temperature

Entry <sup>a</sup>	R ( <b>103 a-j</b> )	R' ( <b>104 a-j</b> )	X	Yield <sup>b</sup> (%) ( <b>105 a-j</b> )
1	H	H	I	94
2	H	OMe	I	92
3	CH <sub>3</sub>	OMe	I	88
4	CH <sub>3</sub>	H	I	90

5	H	2-furyl B(OH) <sub>2</sub>	I	92
6	CH <sub>3</sub>	2-furyl B(OH) <sub>2</sub>	I	90
7	H	H	Br	92
8	COCH <sub>3</sub>	H	Br	94
9	H	H	Cl	92
10	COCH <sub>3</sub>	H	Cl	95

<sup>a</sup>Reactions Conditions: Aryl halide(1mmol), aryl boronic acid (1.1mmol), catalyst **99** (0.1mol%), base (KO<sup>t</sup>Bu, 2mmol), and 5ml water. <sup>b</sup>Isolated yield.

Reusability of the catalyst is of utmost significance with respect to economical and green chemistry perspectives. We have investigated the reusability of the catalyst by performing several catalytic runs in the same reaction vessel. Four catalytic runs were carried out by taking 0.1mol% of the catalyst. After an interval of 12h each, the product formed was extracted using diethyl ether and fresh batch of substrate and base was added into the reaction vessel without adding the catalyst. The substrate consumption was monitored by gas chromatography-mass spectrometry (GC-MS) and even after four successive runs it was observed that the overall yield was about 90%. This indicates that there is no loss of catalytic activity. The catalytic cycle herein involves heterogenization of the pre-catalyst into palladium nanoparticles which are stabilized by the triazolylidene or triazole present in the system. Imidazolium and ammonium salts are known to stabilize palladium nanoparticles generated from palladium NHC complexes.<sup>61,62</sup> Mercury poisoning test was used to study the involvement of palladium nanoparticles. Addition of one drop of Hg(0) to the reaction mixture reduced or decreased the yield of the reaction from 94% to 20% (**Table 10, entry 1**) clearly indicating the heterogenous nature of the catalyst.

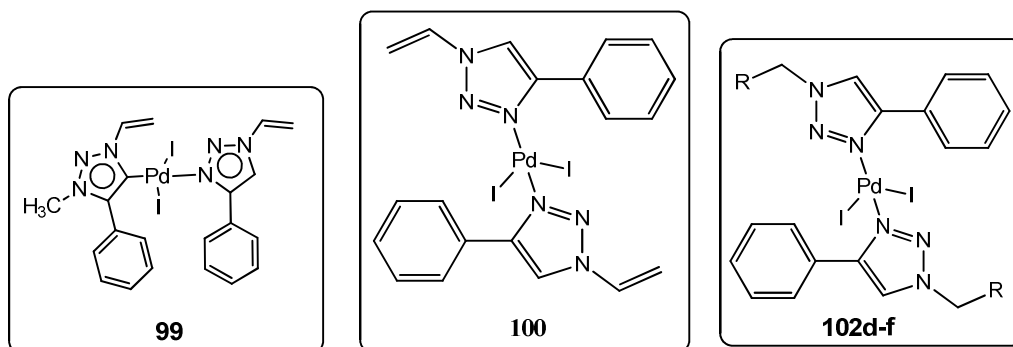


**Scheme 34** Plausible mechanism for Suzuki-Miyaura coupling reaction in water

### 5.4.3 Cytotoxicity studies of complexes

The *in vitro* cytotoxic activity of complexes having different bonding pattern (**99**, **100** and **102 d-f**) were studied using Daltons Lymphoma Ascites (DLA) and Ehrlichs Ascites Carcinoma (EAC) cell lines. Reference drug cyclophosphamide was used for the study.

Surprisingly, all palladium complexes show excellent *in vitro* cytotoxic activity compared to cyclophosphamide against both DLA and EAC cell lines. In DLA cell line with 200 µg of complex **99** produced 70% of cytotoxicity while 100 µg of the same drug produces 55% cell death. At lower concentrations such as 50 µg, 20 µg and 10 µg cytotoxicity was found to be decreased to 40%, 36% and 26% respectively. Complex **99** provides much more cytotoxicity towards DLA cell lines compared to complexes with N-Pd-N bonding pattern. Complex **100**, at 200 µg concentration produces 80% activity. As the concentration decreased to 100 µg, 50 µg, 20 µg and 10 µg the cytotoxicity decreases to 65%, 58% 46% and 35% respectively.



Similar results were obtained with EAC cell line using both complex **100** and **99**. Using 200 µg of complex **100** produce 68% cytotoxicity whereas 85% cytotoxicity was observed in complex **99** with same concentration. 100 µg of both complexes **100** and **99** exhibit 52% and 70% respectively. At lower concentrations like 50 µg, 20 µg and 10 µg complex **100** produce 35%, 30% and 28% respectively whereas complex **99** exhibit 56% 50% and 41% cytotoxicity.

Like complex **99**, complexes **102d-f** produces similar results which indicate that complexes with similar bonding pattern will have similar activity against both DLA and EAC cell lines (Table 5 & 6, Fig 15). For DLA cell line the IC<sub>50</sub> value of the complex **99** is 29 µg and for complex **100** it is about 84 µg. For EAC cell lines IC<sub>50</sub> value of the same complexes is about 20 µg and 94 µg respectively. For DLA cell line

IC<sub>50</sub> value observed at 120 µg, 80 µg and 126 µg for complex **102d**, **102e** and **102f** respectively and that for EAC observed at 100 µg, 92 µg and 95 µg for the complexes **102d**, **102e** and **102f** respectively.

We can conclude that low concentration of complex **99** is enough to produce high cell death compared to other complexes. These results pointed out that complex **99** with C-Pd-N bonding pattern shows better activity at low concentration when compared to complexes with N-Pd-N bonding pattern. Even though both NHC-Pd(II) complexes produce cytotoxicity towards Dalton's lymphoma ascites cell and Ehrlich's ascites carcinoma cell and the cytotoxicity was found to be concentration dependent.

**Table 5** Cytotoxicity results of complexes **99** & **100**

Conc(µg)	Complexes			
	<b>99</b>		<b>100</b>	
	DLA	EAC	DLA	EAC
<b>200µg</b>	80	85	70	68
<b>100 µg</b>	65	70	55	52
<b>50 µg</b>	58	56	40	35
<b>20 µg</b>	46	50	36	30
<b>10 µg</b>	35	40	26	28

**Table 6** Cytotoxicity results of complexes **102d-f**

Conc(µg)	102d		102e		102f	
	DLA	EAC	DLA	EAC	DLA	EAC
<b>200µg</b>	58	56	62	58	56	62
<b>100 µg</b>	48	50	55	52	48	51
<b>50 µg</b>	44	39	42	36	29	32
<b>20 µg</b>	35	23	36	29	23	26
<b>10 µg</b>	23	19	30	25	17	19

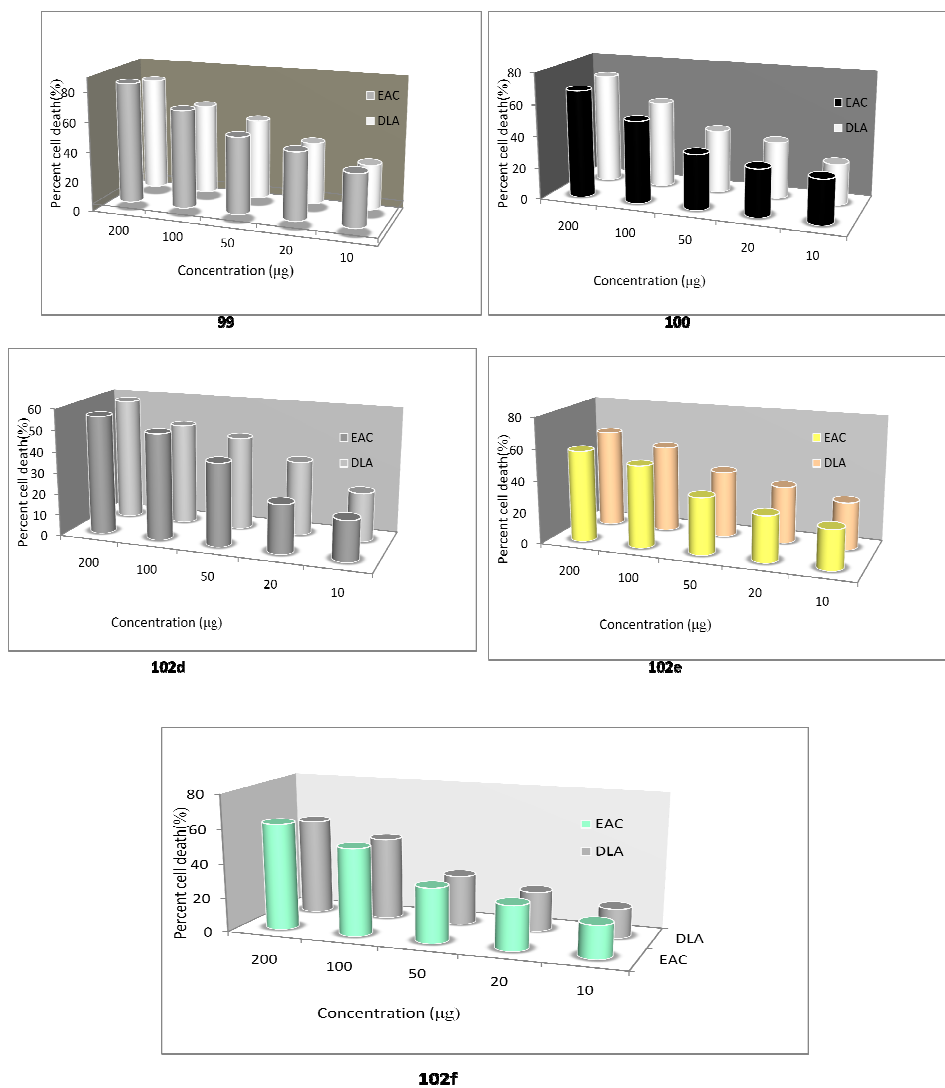
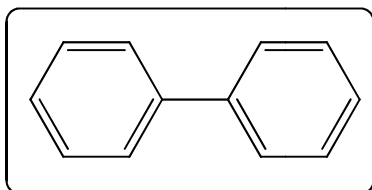


Fig 15. Cytotoxicity activities of complexes 99, 100, 102 d-f



## 5.5 Spectral data of compounds

### 1. 1,1'-biphenyl



$^1\text{H}$  NMR (400 MHz,  $\text{CDCl}_3$ ):  $\delta$  7.59 (d,  $J = 7.2$  Hz, 4H,  $\text{C}_6\text{H}_5$ ), 7.44 (t,  $J = 7.4$  Hz, 4H,  $\text{C}_6\text{H}_5$ ), 7.01 (t,  $J = 6.4$  Hz, 2H, ).  $^{13}\text{C}$  NMR (100.6 MHz,  $\text{CDCl}_3$ ): 137.5,

128.7, 126.7, 126.6

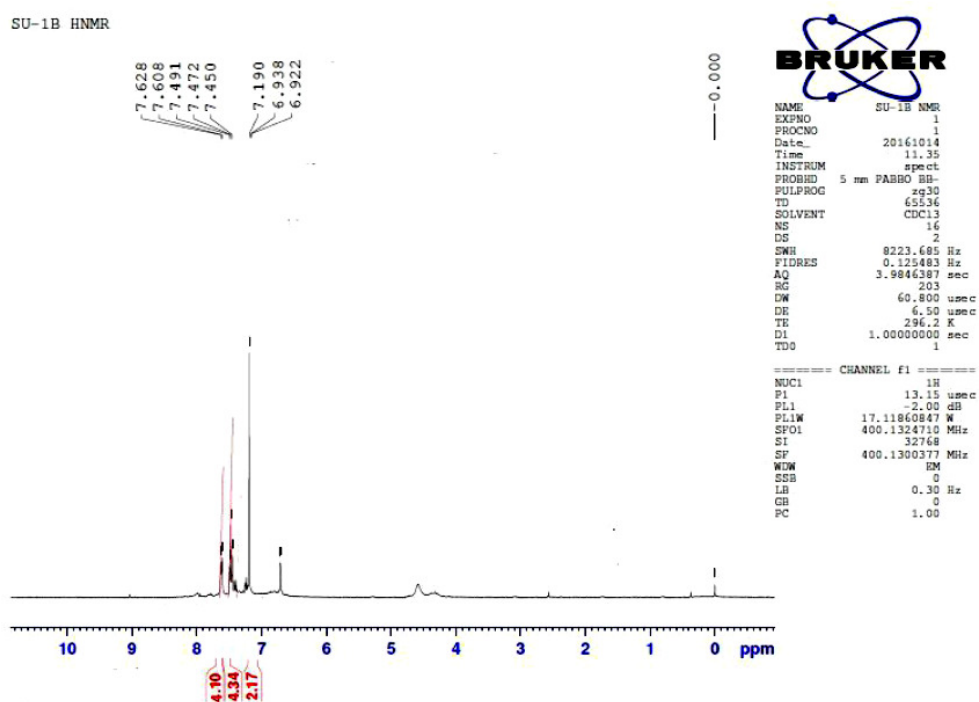
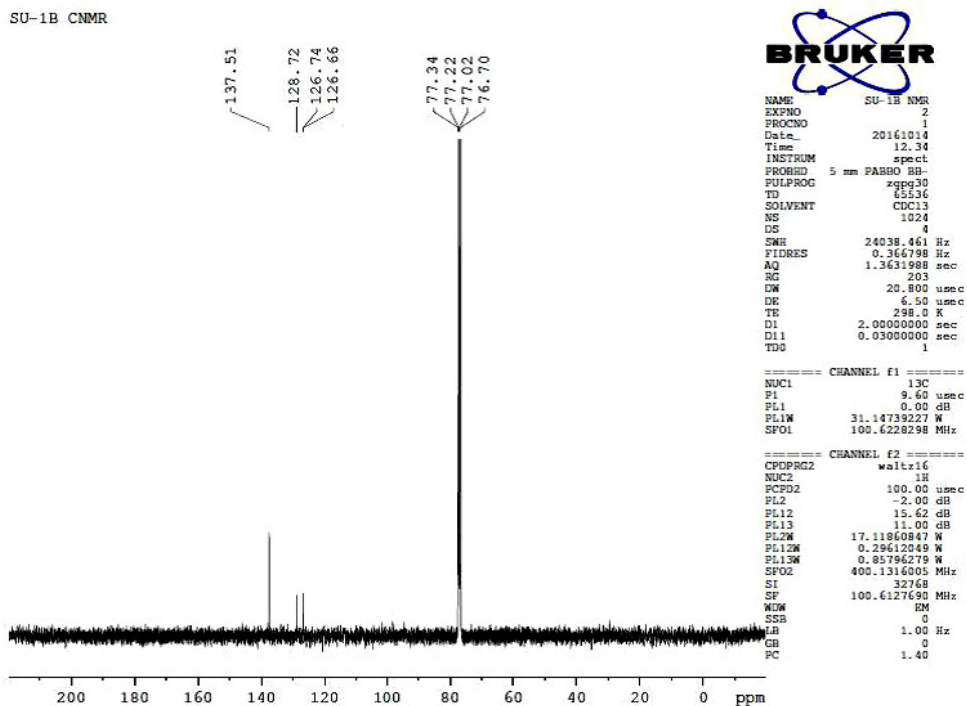
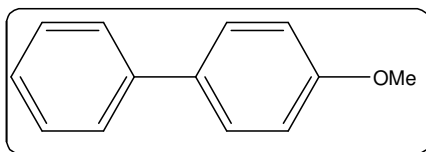


Fig 16.1  $^1\text{H}$  NMR of biphenyl

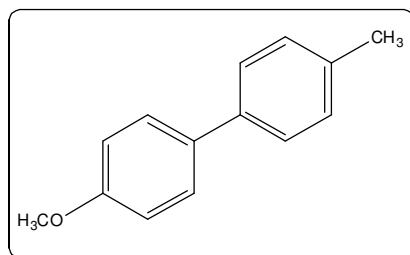
Fig 16.2  $^{13}\text{C}$  NMR of biphenyl

## 2. 4-methoxy-1,1'-biphenyl



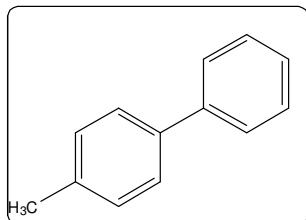
$^1\text{H}$  NMR (400 MHz,  $\text{CDCl}_3$ ) :  $\delta$  7.60 (d,  $J = 1.6$  Hz, 1H) ; 7.57 (d,  $J = 2.0$  Hz, 2H) ; 7.55 (t,  $J = 3.2$  Hz, 1H); 7.44 (m, 2H); 7.33 (t,  $J = 7.2$  Hz, 1H); 7.01 (d,  $J = 8.8$  Hz, 2H), 3.87 (s, 3H);  
 $^{13}\text{C}$  NMR ( $\text{CDCl}_3$ , 100 MHz) : 159.21, 140.88, 132.28, 128.76, 128.19, 126.78, 115.78, 114.27, 55.38.

## 3. 4-methoxy-4'-methyl-1,1'-biphenyl



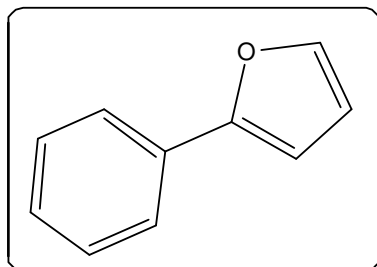
$^1\text{H}$  NMR (400 MHz,  $\text{CDCl}_3$ )  $\delta$  7.56-7.25 (m, 6H), 7.23-6.97 (m 2H), 3.87 (m, 3H), 2.31-2.44 (3H);  
 $^{13}\text{C}$  NMR (100 MHz,  $\text{CDCl}_3$ )  $\delta$  159.12, 158.56, 141.59, 138.30, 135.51, 134.42, 130.33, 130.28, 129.94, 129.48, 128.67, 128.19, 127.98, 127.60, 127.45, 127.01, 126.62, 125.79, 123.89, 116.40, 114.18, 113.53, 55.36, 55.30, 21.59, 20.57.

## 4. 4-methyl-1,1'-biphenyl

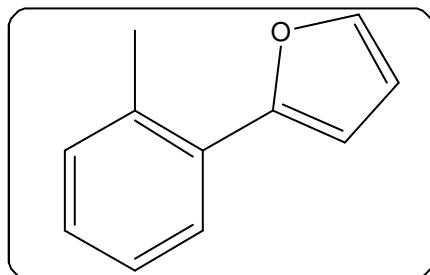


$^1\text{H}$  NMR (400 MHz,  $\text{CDCl}_3$ ):  $\delta$  7.63–7.51 (m, 4H), 7.46–7.40 (m, 2H), 7.35-7.25 (m, 3H), 2.42 (s, 3H);  
 $^{13}\text{C}$  NMR (100 MHz,  $\text{CDCl}_3$ )  $\delta$  141.47, 138.36, 136.88, 128.81, 128.21, 126.85, 21.32.

## 5. 2-Phenylfuran



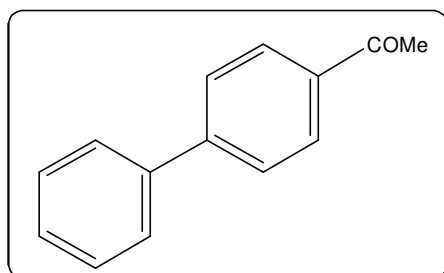
$^1\text{H}$  NMR (400 MHz,  $\text{CDCl}_3$ )  $\delta$  7.9 (dd, 1H) 7.75 (m, 2H,  $J = 7.7$ ), 7.52 (m, 2H), 7.29-7.19 (m, 1H), 6.55 (d, 1H,  $J = 3.3$  Hz), 6.51 (dd, 1H,  $J = 1.8, 3.3$  Hz).  $^{13}\text{C}$  NMR (100 MHz,  $\text{CDCl}_3$ )  $\delta$  153.8, 141.8, 131.3, 127.6, 127.3, 124.1, 111.4, 108.6

6. 2-(*o*-tolyl)furan

122.1, 111.4, 109.8, 20.3

$^1\text{H}$  NMR (400 MHz,  $\text{CDCl}_3$ )  $\delta$  7.6 (dd, 1H), 7.5(d, 1H), 7.3( m,1H), 7.29 (m, 2H), 6.49 (dd, 1H,  $J = 3.3$  Hz), 6.26 (dd, 1H,  $J = 1.8, 3.3$  Hz), 2.3(s, 3H)  $^{13}\text{C}$  NMR (100 MHz,  $\text{CDCl}_3$ )  $\delta$  148.5, 141.8, 136.1, 132.8, 131.3, 130.1, 128.9, 127.6, 127.3,

## 7. 1-([1,1'-biphenyl]-4-yl)ethanone



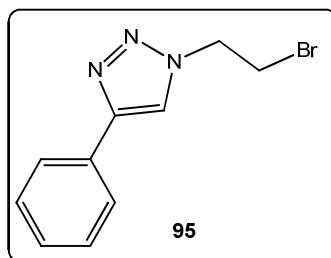
197.65, 145.75, 135.90, 132.68, 128.95, 128.90, 128.23, 127.26, 127.20, 26.60

$^1\text{H}$  NMR (400 MHz,  $\text{CDCl}_3$ )  $\delta$  8.03 (d,  $J = 8.2$  Hz, 2H,  $\text{C}_6\text{H}_4$ ), 7.70 (d,  $J = 8.2$  Hz, 2H,  $\text{C}_6\text{H}_4$ ), 7.63 (d,  $J = 7.4$  Hz, 2H,  $\text{C}_6\text{H}_5$ ), 7.45-7.50 (t,  $J = 7.4$  Hz, 2H,  $\text{C}_6\text{H}_5$ ), 7.37-7.42 (m, 1H,  $\text{C}_6\text{H}_5$ ), 2.64 (s, 3H,  $\text{CH}_3$ ).  $^{13}\text{C}$  NMR (100 MHz,  $\text{CDCl}_3$ ):

## 5.6 Experimental details

### 5.6.1 Synthesis of 1-(2-bromoethyl)-4-phenyl-1,2,3-triazole(95)

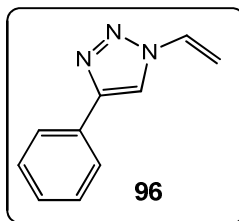
1,2-dibromoethane (5.65 g, 30 mmol), sodium azide (0.65 g, 10 mmol), phenyl acetylene (0.1g, 10mmol), copper acetate monohydrate (0.03g, 0.15 mmol) and sodium ascorbate (0.03 g, 0.15 mmol) were taken in an RB flask containing 20 ml *tert*-butyl alcohol and 10 ml of distilled water. The mixture was then heated at 65 °C for 18 h. It was then cooled to room temperature. Water (50 ml) was again added to it and extracted with ethyl acetate and dried using anhydrous sodium sulphate. The solvent and excess dibromoethane were removed using rotavapor. The product was then purified by passing through a silica gel column using a mixture of hexane and ethyl acetate (3:1) as eluent. The product was obtained as pale yellow needles.



Yield- 2.0g (80%) Mp= 70°C,  $^1\text{H}$  NMR ( $\text{CDCl}_3$ , 400MHz):  $\delta$  3.73 (t,  $J = 6$  Hz, 2H,  $\text{CH}_2\text{Br}$ ), 4.74 (t,  $J = 6$  Hz, 2H,  $\text{NCH}_2$ ), 7.28 (m, 1H,  $\text{H}_{\text{Ar}}$ ), 7.36 (m, 2H,  $\text{H}_{\text{Ar}}$ ), 7.78 (d, 2H,  $J = 7.6$  Hz,  $\text{H}_{\text{Ar}}$ ), 7.84 (s, 1H,  $\text{H}_{\text{trz}}$ ) ppm.  $^{13}\text{C}$  NMR ( $\text{CDCl}_3$  400 MHz):  $\delta$  29.3( $\text{CH}_2\text{Br}$ ), 51.7 ( $\text{NCH}_2$ ), 120.5 ( $\text{CH}_{\text{trz}}$ ), 125.8 ( $\text{C}_{\text{Ar}}$ ), 128.4 ( $\text{C}_{\text{Ar}}$ ), 128.9 ( $\text{C}_{\text{Ar}}$ ), 130.1 ( $\text{C}_{\text{Ar}}$ ), 147.6 ( $\text{C}_{\text{trz}}$ ) ppm. EI-MS [ $\text{M}^+$ ]: 251 (100%). Anal. found: C, 47.59; H, 4.05; Br, 31.65; N, 16.75. Calc. for  $\text{C}_{10}\text{H}_{10}\text{BrN}_3$ : C, 47.64; H, 4.00; Br, 31.69; N, 16.67.

### 5.6.2 Synthesis of 1-ethenyl-4-phenyl-1,2,3-triazole(96)

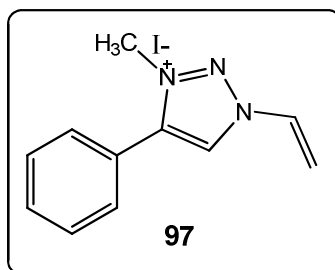
To a solution of 1-(2-bromoethyl)-4-phenyl-1,2,3-triazole **95** (1.0g, 4 mmol) in DMF (10 ml) and  $\text{K}_2\text{CO}_3$  (2.8 g, 20 mmol) was added and stirred at 110 °C for 3 h. It was then cooled to room temperature. Water was added and extracted using ethyl acetate, dried over anhydrous sodium sulphate and concentrated. The product was purified by silica gel column using hexane and ethyl acetate (3:1) as eluent to afford pale yellow crystals.



Yield 0.60g (87%). m.p. 85-86 °C.  $^1\text{H}$  NMR: (400 MHz,  $\text{CDCl}_3$ )  $\delta$  5.12 (dd,  $J = 1.2, 10$  Hz, 1H,  $\text{HCH}_2$ ), 5.64 (dd,  $J = 1.2, 17.2$  Hz, 1H,  $\text{HCH}_2$ ) 7.2 (m, 2H,  $\text{H}_{\text{Ar}} + \text{H}_{\text{NCH}}$ ), 7.3 (t,  $J = 7.6$  Hz, 2H,  $\text{H}_{\text{Ar}}$ ), 7.7 (d,  $J = 7.2$  Hz, 2H,  $\text{H}_{\text{Ar}}$ ), 7.93 (s 1H,  $\text{H}_{\text{tzi}}$ )  $^{13}\text{C}$  NMR: (100 MHz,  $\text{CDCl}_3$ )  $\delta$  103.6 ( $\text{CH}_2$ ), 115 (NCH), 124.8 ( $\text{CH}_{\text{tzi}}$ ), 127.4 ( $\text{CH}_{\text{Ar}}$ ), 127.8 ( $\text{CH}_{\text{Ar}}$ ), 129.0 ( $\text{CH}_{\text{Ar}}$ ), 129.3 ( $\text{C}_{\text{Ar}}$ ), 147.0 ( $\text{C}_{\text{tzi}}$ ) ppm. EI-MS[ $\text{M}^+$ ]: 171 (100%). Anal. found: C, 70.42; H, 5.25; N, 24.84. Calc. for  $\text{C}_{10}\text{H}_{10}\text{BrN}_3$ : C, 70.16; H, 5.30; N, 24.54.

### 5.6.3 Synthesis of 1-ethenyl-3-methyl-4-phenyl-1,2,3-triazolium iodide (97)

1-Ethenyl-4-phenyl-1,2,3-triazole (**96**) (0.31 g, 1 mmol) was taken in acetonitrile (10 ml) to which iodomethane (2.84 g, 2 mmol) was added and heated at 60 °C overnight. After complete consumption of the starting material, the solvent was evaporated under reduced pressure. The solid obtained was washed with dichloromethane: hexane mixture (1:3). The product was obtained as off-white solid.

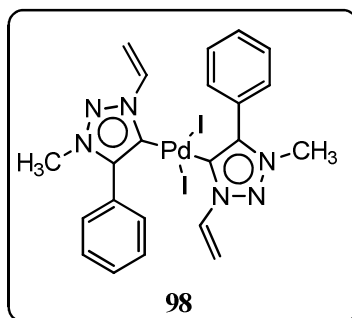


Yield 0.30 g (96%). m.p. 90 °C.  $^1\text{H}$  NMR: (400 MHz,  $\text{CDCl}_3$ )  $\delta$  4.38 (s, 3H,  $\text{CH}_3$ ), 5.19 (dd,  $J = 1.6, 10.4$  Hz, 1H,  $\text{HCH}_2$ ), 5.70–5.72 (m, 1H,  $\text{HCH}_2$ ), 6.56 (dd,  $J = 3.2, 18$  Hz, 1H, NCH), 7.44 (t,  $J = 7.2$  Hz, 1H,  $\text{H}_{\text{Ar}}$ ), 7.64–7.70 (m, 2H,  $\text{H}_{\text{Ar}}$ ), 7.79–7.87 (m, 2H,  $\text{H}_{\text{Ar}}$ ), 9.74 (s, 1H,  $\text{H}_{\text{tzi}}$ ).  $^{13}\text{C}$  NMR: (100 MHz,  $\text{CDCl}_3$ )  $\delta$  39.6 ( $\text{CH}_3$ ), 104.7 ( $=\text{CH}_2$ ), 116.4 (NCH), 125.9 ( $\text{CH}_{\text{Ar}}$ ), 127.3 ( $\text{CH}_{\text{Ar}}$ ), 128.9 ( $\text{CH}_{\text{Ar}}$ ), 129.8 ( $\text{C}_{\text{Ar}}$ ), 132.3 ( $\text{CH}_{\text{tzi}}$ ), 159.6 ( $\text{C}_{\text{tzi}}$ ). Anal. Calc. for  $\text{C}_{11}\text{H}_{11}\text{N}_3$ : C, 42.33; H, 3.55; I, 40.66; N, 13.46. Found: C, 42.52; H, 3.42; I, 40.36; N, 13.63.

### 5.6.4 Synthesis of $\text{C}_{\text{tzi}}\text{-Pd-C}_{\text{tzi}}$ complex (98)

To an oven dried Schlenk flask, 10 ml of dried THF was added followed by 1-ethenyl-3-methyl-4-phenyl-1,2,3-triazolium iodide (**97**) (0.20 g, 0.63 mmol). Nitrogen

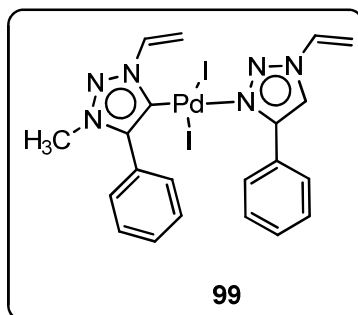
gas was passed through the solution for 10 min and palladium acetate (0.07 g, 0.32 mmol) was added. The reaction mixture was stirred at 80 °C for 4 h. It was then cooled to room temperature and poured into ice water, extracted using ethyl acetate, dried over anhydrous sodium sulphate and concentrated. The product was purified by column chromatography (hexane: ethyl acetate (4:1) over silica gel to get an orange solid.



62% yield (0.14g). m.p. 120°C, <sup>1</sup>H NMR: (400MHz, CDCl<sub>3</sub>) δ 3.99 (s, 3H, CH<sub>3</sub>), 5.50 (d, *J* = 8.8 Hz, 1H, HCH<sub>2</sub>), 6.35 (d, *J* = 15.6 Hz, 1H, HCH<sub>2</sub>), 7.37 (q, *J* = 1.6 Hz, 1H, NCH), 7.48 (t, *J* = 6.4 Hz, 1H, H<sub>Ar</sub>), 7.52–7.58 (m, 2H, H<sub>Ar</sub>), 7.81 (s, 2H, H<sub>Ar</sub>). <sup>13</sup>C NMR: (100 MHz, CDCl<sub>3</sub>) δ 37.9 (CH<sub>3</sub>), 101.7 (=CH<sub>2</sub>), 110.1 (NCH), 128.8 (CH<sub>Ar</sub>), 129.1 (CH<sub>Ar</sub>), 129.2 (HC<sub>Ar</sub>), 130.1 (C<sub>Ar</sub>), 130.4 (C<sub>tzl</sub>-Pd), 144.8 (C<sub>tzl</sub>-Ph). Anal. Calc. for C<sub>22</sub>H<sub>22</sub>I<sub>2</sub>N<sub>6</sub>Pd: C, 36.16; H, 3.03; I, 34.74; N, 11.50. Found: C, 36.46; H, 3.07; I, 34.92; N, 11.42.

### 5.6.5 Synthesis of C<sub>tzl</sub>-Pd-N<sub>tzl</sub> complex (99)

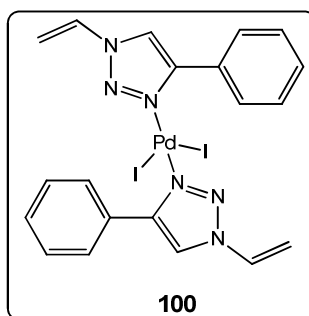
1-Ethenyl-3-methyl-4-phenyl-1,2,3-triazolium iodide (**97**) (0.20 g, 0.64 mmol) was taken in a Schlenk flask containing 10 ml dry THF. Nitrogen gas was purged through the solution for 10min. Bis triazole palladium complex (**100**) (0.45 g, 0.64 mmol) was added to the solution followed by the addition of K<sub>2</sub>CO<sub>3</sub> (0.70 g, 5 mmol). The reaction mixture was then heated at 80 °C for 12 h. It was then cooled to room temperature and solvent removed in vacuum. The residue obtained was filtered through silica column using dichloromethane to afford the product **99** as orange solid. Single crystal was formed by slow diffusion of pentane into dichloromethane.



m.p. 160°C (decomposes).  $^1\text{H}$  NMR: (400 MHz,  $\text{CDCl}_3$ )  $\delta$  4.02 (s, 3H,  $\text{CH}_3$ ), 5.17 (dd,  $J = 1.6, 10.4$  Hz, 1H,  $\text{HCH}_2$ ), 5.59 (dd,  $J = 1.6, 10.4$  Hz, 1H,  $\text{HCH}_2$ ), 5.77 (dd,  $J = 2, 18$  Hz, 1H,  $\text{HCH}_2$ ), 6.34 (dd,  $J = 1.2, 16.8$  Hz, 1H,  $\text{HCH}_2$ ), 7.37 (m, 2H,  $\text{H}_{\text{Ar}}$ ), 7.43 (d, 2H,  $J = 7.6$  Hz,  $\text{H}_{\text{Ar}}$ ), 7.47 (m, 1H, NCH), 7.51 (m, 1H, NCH), 7.55 (m, 1H,  $J = 5.2$  Hz,  $\text{H}_{\text{Ar}}$ ), 7.68 (m, 2H,  $J = 5.6$  Hz,  $\text{H}_{\text{Ar}}$ ), 7.70 (m, 1H,  $\text{H}_{\text{Ar}}$ ), 7.86 (m, 2H,  $\text{H}_{\text{Ar}}$ ), 8.00 (s, 1H,  $\text{H}_{\text{tzl}}$ ).  $^{13}\text{C}$  NMR: (100 MHz,  $\text{CDCl}_3$ )  $\delta$  37.1 ( $\text{CH}_3$ ), 104.6 ( $=\text{CH}_2$ ), 109.4 ( $=\text{CH}_2$ ), 116.1 (NCH), 125.9 (NCH), 128.4 ( $\text{C}_{\text{Ar}}$ ), 128.6 ( $\text{C}_{\text{Ar}}$ ), 128.8 ( $\text{C}_{\text{Ar}}$ ), 129.2 ( $\text{C}_{\text{Ar}}$ ), 130.0 ( $\text{C}_{\text{Ar}}$ ), 130.3, 130.5 ( $\text{C}_{\text{Ar}}$ ), 130.6 ( $\text{C}_{\text{Ar}}$ ), 130.8 ( $\text{C}_{\text{tzl}}$ ), 132.4 ( $\text{C}_{\text{tzl-Pd}}$ ), 134.4 ( $\text{C}_{\text{tzl-Ar}}$ ), 148.0 ( $\text{C}_{\text{tzl-Ar}}$ ). HRMS: Calc. 588.9829, Found; 588.9819 Anal. found: C, 35.12; H, 2.74; I, 35.57; N, 11.63. Calc. for  $\text{C}_{21}\text{H}_{20}\text{I}_2\text{N}_6\text{Pd}$ : C, 35.19; H, 2.81; I, 35.42; N, 11.73; Pd, 14.85.

### 5.6.6 Synthesis of $\text{N}_{\text{tzl}}\text{-Pd-N}_{\text{tzl}}$ complex (100)

To a solution of 1-ethenyl-4-phenyl-1,2,3-triazole **96** (0.170 g, 1 mmol) in THF, (bisacetonitrile) dichloropalladium (0.130 g, 0.5 mmol) and NaI (0.15 g, 1 mmol) were added. The solution was stirred at room temperature for overnight. Yellow solid obtained was filtered and washed with pentane to afford pure product **100**.



Yield: 0.31g, (90%). m.p. 70 °C,  $^1\text{H}$  NMR: (400 MHz,  $\text{CDCl}_3$ )  $\delta$  5.19 (dd,  $J = 2, 10.8$  Hz, 1H,  $\text{HCH}_2$ ), 5.71 (dd,  $J = 1.6, 17.6$  Hz, 1H,  $\text{HCH}_2$ ), 7.39 (m, 2H,  $\text{H}_{\text{NCH}} + \text{H}_{\text{Ar}}$ ), 7.46 (m, 2H,  $\text{H}_{\text{Ar}}$ ), 7.87 (t, 2H,  $J = 8.4$  Hz,  $\text{H}_{\text{Ar}}$ ), 8.0 (s, 1H,  $\text{H}_{\text{tzl}}$ )  $^{13}\text{C}$  NMR: (100 MHz,

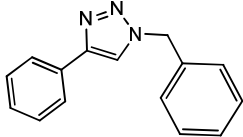
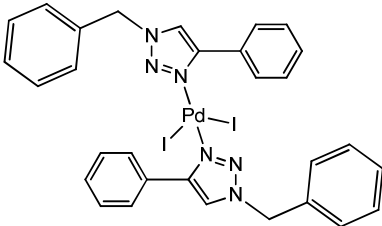
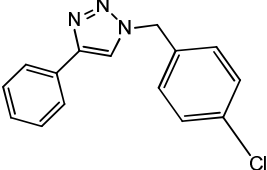
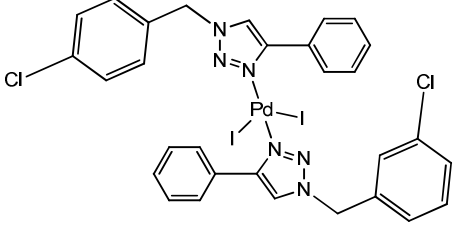
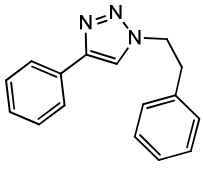
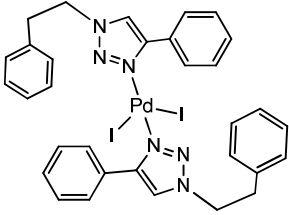


$\text{CDCl}_3$   $\delta$  104.6 ( $\text{C}_{\text{CH}_2}$ ), 116.1 ( $\text{NCH}$ ), 125.9 ( $\text{CH}_{\text{tzl}}$ ), 128.5 ( $\text{CH}_{\text{Ar}}$ ), 128.9 ( $\text{CH}_{\text{Ar}}$ ), 130.0 ( $\text{CH}_{\text{Ar}}$ ), 130.4 ( $\text{C}_{\text{Ar}}$ ), 148.0 ( $\text{C}_{\text{tzl-Ph}}$ ). Anal. found: C, 34.32; H, 2.42; I, 34.18; N, 11.75. Calc. for  $\text{C}_{20}\text{H}_{18}\text{I}_2\text{N}_6\text{Pd}$ : C, 34.19; H, 2.58; I, 36.12; N, 11.96.

### 5.6.7 Synthesis of complexes having N-Pd-N bonding pattern (102d-f)

To a solution of 1,4-disubstituted-1,2,3-triazole (**101 a-c**) (1 mmol) in THF, (bisacetonitrile) dichloropalladium (0.130 g, 0.5 mmol) and NaI (0.15 g, 1 mmol) were added. The solution was stirred at room temperature for overnight. Yellow solid obtained was filtered and washed with pentane to afford pure product (**102 d-f**) (Table 2).

Table 2 N-Pd-N complexes

Reactant	Product
 <p>1-benzyl-4-phenyl-1H-1,2,3-triazole</p> <p><b>101a</b></p>	 <p><math>\text{N}_{\text{benzyl}}\text{-Pd-N}_{\text{benzyl}}</math></p> <p><b>102d</b></p>
 <p>1-(4-chlorobenzyl)-4-phenyl-1H-1,2,3-triazole</p> <p><b>101b</b></p>	 <p><math>\text{N}_{\text{Cibenzyl}}\text{-Pd-N}_{\text{Cibenzyl}}</math></p> <p><b>102e</b></p>
 <p>1-phenethyl-4-phenyl-1H-1,2,3-triazole</p> <p><b>101c</b></p>	 <p><math>\text{N}_{\text{phenethyl}}\text{-Pd-N}_{\text{phenethyl}}</math></p> <p><b>102f</b></p>

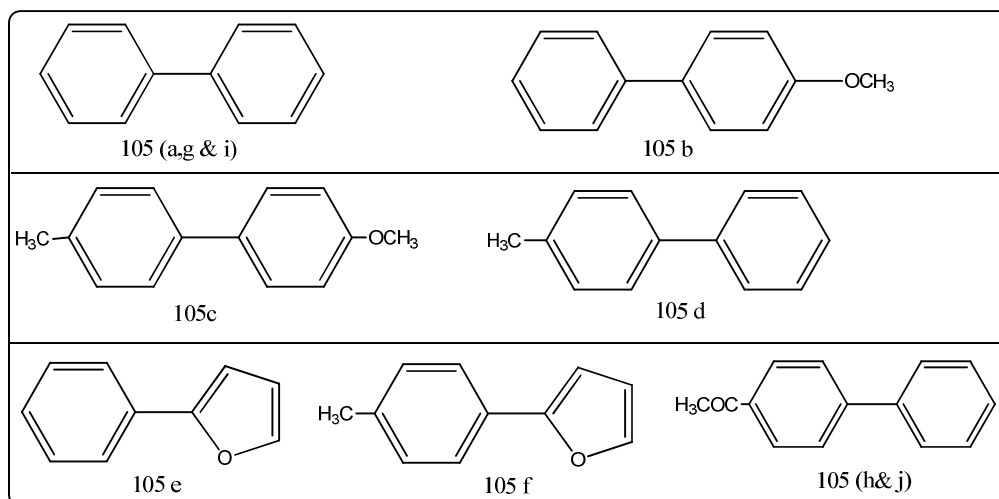
**102d-** Yield: 0.3 g (90%) m.p- 180 °C  $^1\text{H}$  NMR: (400 MHz,  $\text{CDCl}_3$ )  $\delta$  5.61 (s, 2H), 7.30-7.38 (m, 3H), 7.40-7.43(m, 3H), 7.48(t, 2H,  $J= 2, 3.2$ ), 7.81(m, 2H), 8.33(s, 1H).  $^{13}\text{C}$  NMR: (100 MHz,  $\text{CDCl}_3$ )  $\delta$  55.89, 119.5, 125.7, 128.0, 128.1, 128.8, 128.9, 129.1, 133.5, 136.2, 149.6. Anal. Calc. for  $\text{C}_{30}\text{H}_{26}\text{I}_2\text{N}_6\text{Pd}$ : C, 43.37; H, 3.15; I, 30.55; N, 10.12; Pd, 12.81. Anal. Found: C, 43.32; H, 3.07; I, 30.52, N, 10.02.

**102e-** Yield: 0.35 g (92%) m.p- decomposes at 220 °C  $^1\text{H}$  NMR: (400 MHz,  $\text{CDCl}_3$ )  $\delta$  5.55(s, 3H). 7.24 (dd, 2H,  $J= 1.5, 10.8$  Hz ). 7.32 (t,  $J= 7.2$  Hz, 1H), 7.37-7.42(m, 5H), 7.49 (s, 1H), 7.79(dd,  $J=1.3, 10.2$ Hz, 2H)  $^{13}\text{C}$  NMR: (100 MHz,  $\text{CDCl}_3$ )  $\delta$  52.3, 116.9, 127.05, 127.5, 127.85, 128.7, 129.38, 134.59, 136.83, 138.0, 149.51. Anal. Calc. for  $\text{C}_{30}\text{H}_{24}\text{Cl}_2\text{I}_2\text{N}_6\text{Pd}$ : C, 40.05; H, 2.69; Cl, 7.88; I, 28.21; N, 9.34; Pd, 11.83. Anal. Found: C, 40.10; H, 2.64; I, 28.18, N, 9.30.

**102f-** Yield: 0.32 g (90%) m.p- decomposes at 230 °C  $^1\text{H}$  NMR: (400 MHz,  $\text{CDCl}_3$ )  $\delta$  4.64(t, 2H,  $J=7.2, 8.4$ Hz). 3.30( t,  $J=7.2$ Hz, 2H) 7.14(dd, ,  $J= 6.4, 7.8, 1.3$  Hz, 2H) 7.27-7.33 (m, 3H), 7.38-7.46( m, 3H), 7.49 (dd,  $J= 7.7, 1.5$  Hz, 2H) 7.77(s, 1H)  $^{13}\text{C}$  NMR: (100 MHz,  $\text{CDCl}_3$ )  $\delta$  36.8, 51.9, 118.9, 125.7, 128.5, 128.7, 128.8, 128.8, 128.9, 129.0, 137.8, 147.9. Anal. Calc. for  $\text{C}_{32}\text{H}_{30}\text{I}_2\text{N}_6\text{Pd}$ : C, 44.75; H, 3.52; I, 29.55; N, 9.79; Pd, 12.39. Anal. Found: C, 44.69; H, 3.62; I, 29.50, N, 9.89.

### 5.6.7 General procedure for the Suzuki-Miyaura coupling reaction between aryl halide and aryl boronic acid

Nitrogen gas was purged through 5ml water taken in a Schlenk reaction tube for 10 min. Aryl boronic acid (1 mmol), aryl halide (1 mmol),  $\text{KO}^t\text{Bu}$  (1.5 mmol) and the catalyst **99** (0.1 mol%) were successively added to it. The mixture was then stirred at room temperature for 12 h. It was then extracted with diethyl ether and dried over anhydrous sodium sulphate. The solvent was evaporated and the product obtained was purified by filtering through a silica gel column using hexane.



### 5.6.8 Cytotoxic studies of palladium N-heterocyclic carbene Complexes

Both DLA and EAC tumor cells were aspirated from the peritoneal cavity of tumor bearing mice, which was washed three times with phosphate buffered saline. The cell viability was determined using Trypan blue exclusion method. The viable cell suspension was treated with different concentration of complexes **99** and **100**. Total volume of the solution was made up to 1ml using buffer solution followed by incubation for 3h at 37°C. To the above suspension 0.1 ml of 1% trypan blue was added and kept for 2-3 minutes, and loaded to haemocytometer. Cytotoxicity was found out by counting the number of dead cell which in turn was observed by absorbing the blue color of trypan blue.

$$\% \text{ Cytotoxicity} = \frac{\text{No. of dead cells}}{\text{No. of live cells} + \text{No. of dead cells}} \times 100$$

### 5.7 Conclusion

Palladium complexes with different bonding pattern were synthesized. A new palladium complex with  $C_{tzl}-Pd-N_{tzl}$  was characterized by Single XRD. Newly synthesized palladium complex was found to be catalytically active for Suzuki-Miyaura coupling reaction in aqueous medium at room temperature. Coupling reaction performed with very low catalyst loading. Cytotoxicity studies of all synthesized complexes were studied and  $C_{tzl}-Pd-N_{tzl}$  complex shows higher cytotoxicity compared to other complexes.

---

**References**

- (1) Fischer, E. O.; Maasbol, A. Zur Frage Eines Wolfram-Carbonyl-CarbenKomplexes. *Angew. Chem. Int. Ed.* **1964**, *76*, 645.
- (2) Schrock, R. R. An “Alkylcarbene” Complex of Tantalum by Intramolecular Alpha-Hydrogen Abstraction. *J. Am. Chem. Soc.* **1974**, *64*, 6796–6797.
- (3) Miyaura, N.; Suzuki, A.; January, W. Palladium-Catalyzed Cross-Coupling Reactions of Organoboron Compounds. *Chem. Rev.* **1995**, *95*, 2457–2483.
- (4) Das, P.; Linert, W. Schiff Base-Derived Homogeneous and Heterogeneous Palladium Catalysts for the Suzuki–Miyaura Reaction. *Coord. Chem. Rev.* **2015**, *311*, 1–23.
- (5) Lai, Y.; Zong, Z.; Tang, Y.; Mo, W.; Sun, N.; Hu, B.; Shen, Z.; Jin, L.; Sun, W.; Hu, X. Highly Bulky and Stable Geometry-Constrained Iminopyridines : Synthesis , Structure and Application in Pd-Catalyzed Suzuki Coupling of Aryl Chlorides. *Beilstein J. Org. Chem.* **2017**, *13*, 213–221.
- (6) Martin, R.; Buchwald, S. L. Palladium-Catalyzed Suzuki - Miyaura Cross-Coupling Reactions Employing Dialkylbiaryl Phosphine Ligands. *Accounts Chem. Res.* **2008**, *41*, 1461–1473.
- (7) Zhang, C.; Huang, J.; Trudell, M. L.; Nolan, S. P. Palladium - Imidazol-2-Ylidene Complexes as Catalysts for Facile and Efficient Suzuki Cross-Coupling Reactions of Aryl Chlorides with Arylboronic Acids The Palladium-Catalyzed Suzuki Cross-Coupling Reaction of Aryl Bromides , Aryl Iodides , and Pseudohali. *J. Org. Chem.* **1999**, *64*, 3804–3805.
- (8) Kirchhoff, M. M. Origins , Current Status , and Future Challenges of Green. *Acc. Chem. Res.* **2002**, *35*, 686–694.
- (9) Franzén, R.; Xu, Y. Review on Green Chemistry — Suzuki Cross Coupling in Aqueous Media. *Can. J. Chem.* **2005**, *83*, 266–272.

- (10) Shaughnessy, K. H. Hydrophilic Ligands and Their Application in Aqueous-Phase Metal-Catalyzed Reactions. *Chem. Rev.* **2009**, *109*, 643–710.
- (11) Gülcemal, S.; Kahraman, S.; Daran, J.; Çetinkaya, E.; Çetinkaya, B. The Synthesis of Oligoether-Substituted Benzimidazolium Bromides and Their Use as Ligand Precursors for the Pd-Catalyzed Heck Coupling in Water. *J. Organomet. Chem.* **2009**, *694*, 3580–3589.
- (12) Levin, E.; Ivry, E.; Diesendruck, C. E.; Lemco, N. G. Water in N - Heterocyclic Carbene-Assisted Catalysis. *Chem. Rev.* **2013**, *115*, 4607–4692.
- (13) Schuster, O.; Yang, L.; Raubenheimer, G. H.; Albrecht, M. Beyond Conventional N -Heterocyclic Carbenes: Abnormal , Remote , and Other Classes of NHC Ligands with Reduced Heteroatom Stabilization. *Chem. Rev.* **2009**, *109*, 3445–3478.
- (14) Karimi, B.; Akhavan, P. F. A Novel Water-Soluble NHC-Pd Polymer: An Efficient and Recyclable Catalyst for the Suzuki Coupling of Aryl Chlorides in Water at Room Temperature. *Chem. Commun.* **2011**, *47*, 7686–7688.
- (15) Canseco-Gonzalez, D.; Gniewek, A.; Szulmanowicz, M.; Müller-Bunz, H.; Trzeciak, A. M.; Albrecht, M. PEPPSI-Type Palladium Complexes Containing Basic 1,2,3-Triazolylidene Ligands and Their Role in Suzuki-Miyaura Catalysis. *Chem. - A Eur. J.* **2012**, *18*, 6055–6062.
- (16) Mohan, A.; Ramkumar, V.; Sankararaman, S. Synthesis and Structures of ( - ) Menthyl and ( + ) Neomenthyl Substituted Enantio Pure Bis (1,2,3-Triazol-5-Ylidene ) PdI 2 Complexes Comparison of Catalytic Activities for C - C Coupling. *J. Organomet. Chem.* **2015**, *799–800*, 115–121.
- (17) Keske, E. C.; Zenkina, O. V; Wang, R.; Crudden, C. M. Synthesis and Structure of Palladium 1,2,3-Triazol-5-Ylidene Mesoionic Carbene PEPPSI Complexes and Their Catalytic Applications in the Mizoroki – Heck Reaction. *Organometallics* **2012**, *31*, 6215–6221.

- (18) Tang, Y.; Lu, J.; Shao, L. NHC-Pd(II)- Im( NHC= N-Heterocyclic Carbene ; Im = 1-Methylimidazole ) Complexes as Efficient Catalysts for Suzuki-Miyaura Coupling Reactions of Aryl Chlorides. *J. Organomet. Chem.* **2011**, *696*, 3741–3744.
- (19) Zhang, Y.; Feng, M.-T.; Lu, J.-M. N-Heterocyclic Carbene Palladium(II)– 1-Methylimidazole Complex Catalyzed Suzuki–Miyaura Coupling of Benzylic Chlorides with Arylboronic Acids or Potassium Phenyltrifluoroborate in Neat Water. *Org. Biomol. Chem.* **2011**, *11*, 2266–2272.
- (20) Dunsford, J. J.; Cavell, K. J. Pd – PEPPSI-Type Expanded Ring N-Heterocyclic Carbene Complexes: Synthesis, Characterization, and Catalytic Activity in Suzuki – Miyaura Cross Coupling. *Organometallics* **2014**, *33*, 2902–2905.
- (21) Wanzlick, H.W; Schönherr, H.J. Direct Synthesis of a Mercury Salt-Carbene Complex. *Angew. Chemie Int. Ed. English* **1968**, *7*, 141–142.
- (22) Arduengo, A. J.; Harlow, R. L.; Kline, M. A Stable Crystalline Carbene. *J. Am. Chem. Soc.* **1991**, *113*, 361–363.
- (23) Gründemann, S.; Kovacevic, A.; Albrecht, M.; Faller, J. W.; Robert, H. Abnormal Binding in a Carbene Complex Formed from an Imidazolium Salt and a Metal Hydride Complex. *Chem Commun.* **2001**, *0*, 2274–2275.
- (24) Mathew, P.; Neels, A.; Albrecht, M. 1,2,3-Triazolylidenes as Versatile Abnormal Carbene Ligands for Late Transition Metals. *J. Am. Chem. Soc.* **2008**, No. 130, 13534–13535.
- (25) Rostovtsev, V. V.; Green, L. G.; Fokin, V. V.; Sharpless, K. B. “ A Stepwise Huisgen Cycloaddition Process Catalyzed by Copper ( I ): Regioselective Ligation of Azides and Terminal Alkynes .” *Angew. Chem. Int. Ed.* **2002**, *41*, 2596–2599.
- (26) Guisado-barrios, G.; Bouffard, J.; Donnadiou, B.; Bertrand, G. Crystalline 1H-1,2,3-Triazol-5-Yildenes: New Stable Mesoionic Carbenes(MIC). *Angew.*

*Chem. Int. Ed.* **2010**, *49*, 4759–4762.

- (27) Karthikeyan, T.; Sankararaman, S. Palladium Complexes with Abnormal N - Heterocyclic Carbene Ligands Derived from 1,2,3-Triazolium Ions and Their Application in Suzuki Coupling. *Tetrahedron Lett.* **2009**, *50*, 5834–5837.
- (28) Nakamura, T.; Ogata, K.; Fukuzawa, S. Synthesis of Dichlorobis (1,4-d Imesityl -1H-1,2,3-Triazol-5-Ylidene) Palladium [PdCl<sub>2</sub> (TMes)<sub>2</sub>] and Its Application to Suzuki - Miyaura Coupling Reaction. *Chem. Lett.* **2010**, *39*, 920–922.
- (29) Inomata, S.; Hiroki, H.; Terashima, T.; Ogata, K.; Fukuzawa, S. 1,2,3-Triazol-5-Ylidene-Palladium Complex Catalyzed Mizoroki e Heck and Sonogashira Coupling Reactions. *Tetrahedron* **2011**, *67*, 7263–7267.
- (30) Saravanakumar, R.; Ramkumar, V.; Sankararaman, S. Synthesis and Structure of 1,4-Diphenyl-3-Methyl-1,2,3-Triazol5-Ylidene Palladium Complexes and Application in Catalytic Hydroarylation of Alkynes. *Organometallics* **2011**, *30*, 1689–1694.
- (31) Saravanakumar, R.; Ramkumar, V.; Sankararaman, S. Synthesis and Structural Characterization of Cis Isomer of 1 , 2 , 3-Triazol-5-Ylidene Based Palladium Complexes. *J. Organomet. Chem.* **2013**, *736*, 36–41.
- (32) Warsink, S.; Drost, R. M.; Lutz, M.; Spek, A. L.; Elsevier, C. J. Modular Synthesis of Bidentate Triazolyl-Functionalized N-Heterocyclic Carbenes and Their Palladium Complexes. *Organometallics* **2010**, *29*, 3109–3116.
- (33) Chen, J.; Zhao, J.; Zhao, Y.; Li, L.; Zhang, H. A Modified Procedure for the Synthesis of 1-Arylimidazoles. *Synthesis (Stuttg)*. **2003**, *17*, 2661–2666.
- (34) Barral, K.; Moorhouse, A. D.; Moses, J. E. Efficient Conversion of Aromatic Amines into Azides : A One-Pot Synthesis of Triazole Linkages. *Org. Lett.* **2007**, *9*, 1809–1811.
- (35) Canseco-gonzalez, D.; Gniewek, A.; Szulmanowicz, M.; Müller-bunz, H.; Trzeciak, A. M.; Albrecht, M. PEPPSI-Type Palladium Complexes Containing Basic 1,2,3-Triazolylidene Ligands and Their Role in Suzuki–Miyaura

- Catalysis. *Chem. - A Eur. J.* **2012**, *18*, 6055–6062.
- (36) Yuan, D.; Huynh, H. V. 1,2,3-Triazolin-5-Ylidenes: Synthesis of Hetero-Bis(Carbene) Pd(II) Complexes, Determination of Donor Strengths, and Catalysis. *Org. Lett.* **2012**, *31*, 405–412.
- (37) Kilpin, K. J.; Paul, U. S. D.; Lee, A.; Crowley, J. D. Gold(I) “Click” 1,2,3-Triazolyliidenes: Synthesis, Self-Assembly and Catalysis. *Chem. Commun* **2011**, *47*, 328–330.
- (38) Sureshbabu, B.; Ramkumar, V.; Sankararaman, S. A Mild and Efficient Method for the Synthesis of Structurally Diverse 1,2,3-Triazolylidene Palladium ( II ) Diiodo Complexes . Comparison of Catalytic Activities for Suzuki e Miyaura Coupling. *J. Organomet. Chem.* **2015**, *799–800*, 232–238.
- (39) Rixe, O.; Ortuzar, W.; Alvarez, M.; Parker, R.; Reed, E.; Paull, K.; Fojo, T. Carboplatin : Spectrum of Activity in Drug-Resistant Cell Lines and in the Cell Lines of the National Cancer Institute ’ s Anticancer Drug Screen Panel. *Biochem. Pharmacol.* **1996**, *52*, 1855–1865.
- (40) Hato, S. V; Khong, A.; Vries, I. J. M. De; Lesterhuis, W. J. Molecular Pathways : The Immunogenic Effects of Platinum- Based Chemotherapeutics. *Clin. Caner Res.* **2014**, *20*, 2831–2837.
- (41) Todd, R. C.; Lippard, S. J. Inhibition of Transcription by Platinum Antitumor Compounds. *Metallomics* **2009**, *1*, 280–291.
- (42) Muggia, F. Platinum Compounds 30 Years after the Introduction of Cisplatin : Implications for the Treatment of Ovarian Cancer. *Gynecol. Oncol.* **2009**, *112*, 275–281.
- (43) Kelland, L. The Resurgence of Platinum-Based Cancer Chemotherapy. *Nat. Rev. Cancer* **2007**, *7*, 573–584.
- (44) Arnesano, F.; Natile, G. “ Platinum on the Road ”: Interactions of Antitumoral Cisplatin with Proteins \*. *Pure Appl. Chem.* **2008**, *80*, 2715–2725.
- (45) Ray, S.; Mohan, R.; Singh, J. K.; Samantaray, M. K.; Shaikh, M. M.; Panda, D.; Ghosh, P. Anticancer and Antimicrobial Metallopharmaceutical Agents



- Based on Palladium , Gold , and Silver N-Heterocyclic Carbene Complexes. *J. Am. Chem. Soc.* **2007**, *129*, 15042–15053.
- (46) Wang, C.; Shih, W.; Chang, H. C.; Kuo, Y.; Hung, W.; Ong, T.; Li, W. Preparation and Characterization of Amino-Linked Heterocyclic Carbene Palladium , Gold , and Silver Complexes and Their Use as Anticancer Agents That Act by Triggering Apoptotic Cell Death. *J. Med. Chem.* **2011**, *54*, 5245–5249.
- (47) Haque, R. A.; Salman, A. W.; Budagumpi, S.; Abdullah, A. A.-A.; Majid, A. M. S. A. Sterically Tuned Ag(I)- and Pd(II)-N-Heterocyclic Carbene Complexes of Imidazol-2-Ylidenes: Synthesis, Crystal Structures, and in Vitro Antibacterial and Anticancer Studies. *Metallomics* **2013**, *5*, 760–769.
- (48) Shila, A. K.; Kumara, S.; Sharma, S.; Chaudharya, A.; Das, P. Polystyrene Resin Supported Palladium(0) (Pd@PR) Nanocomposite Mediated Regioselective Synthesis of 4-Aryl-1-Alkyl/(2-Haloalkyl)-1H-1,2,3-Triazoles and Their N-Vinyl Triazole Derivatives from Terminal Alkynes. *RSC Adv.* **2015**, *5*, 11506–11514.
- (49) Wang, H.; Yang, J. Piperazine- and DABCO-Bridged Dinuclear N - Heterocyclic Carbene Palladium Complexes: Synthesis , Structure and Application to Hiyama Coupling Reaction. *Appl. Organomet. Chem.* **2016**, *31*, e3543.
- (50) Wang, T.; Xie, H.; Liu, L.; Zhao, W. N-Heterocyclic Carbene-Palladium(II) Complexes with Benzoxazole or Benzothiazole Ligands: Synthesis, Characterization, and Application to Suzuki-Miyaura Cross-Coupling Reaction. *J. Organomet. Chem.* **2016**, *804*, 73–79.
- (51) Huang, P.; Wang, Y.; Yu, H.; Lu, J. N - Heterocyclic Carbene – Palladium(II) – 4,5-Dihydrooxazole Complexes: Synthesis and Catalytic Activity toward Amination of Aryl Chlorides. *Organometallics* **2014**, *33*, 1587–1593.
- (52) Liu, F.; Zhu, Y.-R.; Song, L.-G.; Lu, J.-M. Synthesis of N-Heterocyclic Carbene-PdCl<sub>2</sub>-(Iso)Quinoline Complexes and Their Application in Arylation at Low Catalyst Loadings. *Org. Biomol. Chem.* **2016**, *14*, 2563–

2571.

- (53) Chen, M.; Vicic, D. A.; Turner, M. L.; Navarro, O. ( N-Heterocyclic Carbene ) PdCl<sub>2</sub> (TEA) Complexes : Studies on the Effect of the “ Throw-Away ” Ligand in Catalytic Activity. *Organometallics* **2011**, *30*, 5052–5056.
- (54) Amatore, C.; Jutand, A.; Duc, G. Le. Kinetic Data for the Transmetalation / Reductive Elimination in Palladium- Catalyzed Suzuki – Miyaura Reactions : Unexpected Triple Role of Hydroxide Ions Used as Base. *Chem. - A Eur. J.* **2011**, *17*, 2492–2503.
- (55) Amatore, C.; Duc, G. Le; Jutand, A. Mechanism of Palladium-Catalyzed Suzuki – Miyaura Reactions : Multiple and Antagonistic Roles of Anionic “ Bases ” and Their Counteranions. *Chem. - A Eur. J.* **2013**, *19*, 10082–10093.
- (56) Amatore, C.; Jutand, A.; Duc, G. Le. Mechanistic Origin of Antagonist Effects of Usual Anionic Bases (OH<sup>-</sup>, CO<sub>3</sub><sup>2-</sup>) as Modulated by Their Counteranions (Na<sup>+</sup>, Cs<sup>+</sup>, K<sup>+</sup>) in Palladium-Catalyzed Suzuki – Miyaura Reactions. *Chem. - A Eur. J.* **2012**, *21*, 6616–6625.
- (57) Conelly-espinoza, P.; Morales-morales, D. [Pd(HQS)<sub>2</sub>] (HQS = 8-Hydroxyquinoline-5-Sulfonic Acid ) a Highly Efficient Catalyst for Suzuki – Miyaura Cross Couplings in Water. *Inorganica Chim. Acta* **2010**, *363*, 1311–1315.
- (58) Conelly-espinoza, P.; Toscano, R. A.; Morales-morales, D. Synthesis and Characterization of Hydrophilic Theophylline Base Compounds and Their Use as Ligands in the Microwave Assisted Suzuki-Miyaura Couplings of Halopyridines in Water. *Tetrahedron Lett.* **2014**, *55*, 5841–5845.
- (59) Valdés, H.; Canseco-gonzález, D.; German-acacio, J. M.; Morales-Morales, D. Xanthine Based N-Heterocyclic Carbene (NHC) Complexes. *J. Organomet. Chem.* **2018**, *867*, 51–54.
- (60) Chatterjee, A.; Ward, T. R. Recent Advances in the Palladium Catalyzed Suzuki – Miyaura Cross-Coupling Reaction in Water. *Catal. Letters* **2016**, *146*, 820–840.

- (61) Gniewek, A.; Trzeciak, A. M.; Ziółkowski, J. J.; Kepinski, L.; Wrzyszczyński, J.; Tylus, W. Pd-PVP Colloid as Catalyst for Heck and Carbonylation Reactions: TEM and XPS Studies. *J. Catal.* **2005**, *229*, 332–343.
- (62) Cassol, C. C.; Umpierre, A. P.; Machado, G.; Wolke, S. I.; Dupont, J. The Role of Pd Nanoparticles in Ionic Liquid in the Heck Reaction. *J. Am. Chem. Soc.* **2005**, *127*, 3298–3299.

---

## Chapter 6

### Summary & Conclusions

Synthesis of 1,2,3-triazoles has received wide spread attention over the past decade due to its variety of applications. This scaffold can easily be assembled through regioselective [3+2] cycloaddition of alkyne and azide which provides access to a variety of functional groups on the triazole ring. Developing novel synthetic protocols having high yield, room temperature, short reaction time and use of benign solvent are some of the major objectives in any synthesis. Satisfying these objectives, this thesis describes the design and synthesis of new catalysts for an environmental friendly synthesis of 1,2,3-triazoles. Besides this, it also highlighted the palladation of some of the triazoles or triazolylidene counterpart leading to complexes having different bonding pattern. We have also demonstrated that the palladium complexes have potential applications as catalyst in Suzuki coupling reaction and as antitumor agent.

A comprehensive review on the synthesis and applications of 1,2,3-triazoles has been depicted in chapter 2. Much effort has been made to high light the recent developments in green protocols and use of heterogeneous catalysts in click reaction.

Chapter 3 discusses the use of polymer metal complex as a catalyst and the easiness of using it as a heterogeneous catalyst for click reactions. A mini review on the synthesis, characterization and application of polymer metal complexes as a catalyst has been discussed in the first part of the chapter. It provides a thorough knowledge of the factors affecting the catalyst's performance. However, the micro environment and use of polymer-metal complexes as catalysts in general and copper catalyzed azide-alkyne cycloaddition reaction (CuAAC) has been studied to a lesser extent. The development of such polymer supported metal catalysts for CuAAC reaction would be sensible. The polymer support has been synthesized by suspension polymerization of *N*-vinyl pyrrolidone and *N,N'*-methylenebisacrylamide as monomers and AIBN as initiator. The polymer support was used for the *in situ* generation of Cu<sub>2</sub>O by the reduction of copper sulphate and it protects the copper (I) within in the polymer matrix from further reduction. The

Copper (I) stabilized polymer has been well characterized using FTIR, FEG-SEM, EDS, XRD, XPS analysis. The polymer-metal complex was successfully utilized as a catalyst for 1,3-dipolar cycloaddition between azide and alkyne in water as solvent. Effect of solvent, temperature and catalyst loading were studied as a part of optimization study. The product 1,4-disubstituted 1,2,3-triazole formed was confirmed by  $^1\text{H}$  NMR,  $^{13}\text{C}$  NMR and GCMS analysis. We have also demonstrated that the catalyst can be recovered and recycled for at least five runs. Surface morphology of the catalyst before and after the reactions was examined by SEM and EDS analysis and observed any surface damage or leaching on recycling.

Biosynthesis of nanoparticle and its application in catalysis and biological studies has been discussed in chapter 4. It starts with a mini review on synthesis of nanoparticles using biogenic methods. The use of biomaterials for the synthesis of nanoparticle sounds more effective than other methods because of the easiness in carrying out the process in water as solvent and readily availability of starting materials. Due to these reasons, the biosynthesis of nanoparticels is termed as a “green method”. We explored the effect of *Myristica fragrance* fruit extract for the synthesis of nanoparticles and no previous effort that utilizes the fruit as a biomaterial for nanoparticle synthesis has been reported. Commonly, the pericarp i.e outer layer of fruit is discarded as waste material as it doesn't have any commercial value. For the synthesis of nanoparticles, we used this fruit extract as the biomaterial. The fruit extract was directly used for the synthesis of copper oxide and silver nanoparticles without adding any other stabilizing agents. Among the strategies attempted for the synthesis of copper nanoparticle, microwave irradiation was found to be the fastest route. Nanosize and spherical nature of CuO was identified by HR-TEM analysis. Elemental analysis confirms the presence of copper and oxygen in the sample. The catalytic activity of biosynthesized CuO nanoparticle was screened for CuAAC reaction. Optimization of the reaction conditions in terms of catalyst loading, solvent, temperature and time was studied and the catalyst was found to be effective for the click reaction in water medium. Recovery and reusability of catalyst became easier as it is insoluble in water. The catalyst can be reused for the successive 4 cycles with slight decrease in the yield of each successive step. We have also carried out the synthesis of silver nanoparticles using fruit extract. Here use of sunlight was found to be effective in

the rapid formation of the nanoparticles. Formation of silver nanoparticle can be identified by the color change from yellow to brown within 2 minutes. Silver nanoparticle was found to have lower catalytic activity compared to CuO in Azide-Alkyne cycloaddition reactions. It provided a mixture of both 1,4- and 1,5-disubstituted 1,2,3-triazole. Antibacterial and antifungal activity of silver nanoparticle was also examined and showed promising antibacterial activity but minimum antifungal activity.

A study on the synthesis, characterization and application of palladium complexes with carbene as a labile ligand has been discussed in chapter 5. A brief review on palladium *N*-heterocyclic carbene complexes and its application in both catalysis and anticancer agent has been made in the first part of the chapter. Synthesis of 1,2,3-triazole ligand and its dehydrohalogenation and subsequent alkylation afforded the ligand precursor. Initial attempts to synthesize NHC palladium complex with a labile triazole ligand led to the formation of a mixture of complexes having C-Pd-C and C-Pd-N bonding pattern in very low yields. These complexes were separated by column chromatography and characterized using  $^1\text{H}$  NMR,  $^{13}\text{C}$  NMR and elemental analysis. To synthesis the palladium complex having C-Pd-N bonding pattern, we used ligand substitution reaction on an initially prepared N-Pd-N complex. Palladium compounds are well known catalysts for C-C bond forming cross-coupling reactions. The catalytic activity of C-Pd-N complex towards Suzuki coupling reaction was studied in water. It provided promising results compared to other synthesized complexes with C-Pd-C and N-Pd-N bonding pattern. We have studied the cytotoxic activity of these palladium complexes. Compared to the complexes with N-Pd-N bonding pattern, C-Pd-N complexes show better cytotoxicity.

## Publication

**Drishya Sasidharan**, Aji.C.V and Dr.Paulson Mathew\*, 1,2,3 Triazolylidene palladium complex with triazole ligand: Synthesis, characterization and application in Suzuki-Miyaura coupling reaction in water. *Polyhedron*, vol 157, pp 335-340

## Conference Papers

Drishya Sasidharan, Aji C.V. and Dr. Paulson Mathew\* “Palladium catalyzed Suzuki-Miyaura coupling reaction in water”. Proceedings of Prof. K. V Thomas Endowment International Symposium on New Trends in Applied Chemistry (NTAC-2017) p-108, held at Sacred Heart College, Thevara, Kochi, Kerala, February 09-11, 2017.

Drishya Sasidharan, Namitha T.R. and Dr. Paulson Mathew\*, “Biogenic synthesis of Cu and CuO nanoparticles from *Myristica fragrance* fruit extract: Application in catalysis”. Proceedings of National seminar on Emerging Trends in Chemical Research, held at Christ College, Irinjalakuda, Thrissur, Kerala, 28<sup>th</sup> February and 1<sup>st</sup> March 2017.

Drishya Sasidharan, Dr. Paulson Mathew\*, “Synthesis of NNMBA crosslinked polyvinylpyrrolidone for the *in situ* reduction of Cu(II) to Cu(I)”. Proceedings of International Conference on Chemistry and Physics of Materials (ICCPM-2018), held at St.Thomas’ College, Thrissur, Kerala, December 19-21, 2018.